FINAL TECHNICAL REPORT

Project Title: Engineering Thermotolerant Biocatalysts for Biomass Conversion to Products

Award Number: DE-FG36-04GO14019

Recipient: K. T. Shanmugam, L. O. Ingram & J. A. Maupin-Furlow
Project Location: Department of Microbiology and Cell Science
University of Florida, Gainesville, FL

Reporting Period: April 1, 2004 to September 30, 2009
Date of Report: October 20, 2009 (modified May 20, 2010)
Written by: K. T. Shanmugam

DISCLAIMER

Objective

The main objective of this study is to identify thermotolerant facultative anaerobic bacteria that can ferment all the sugars that can be derived from lignocellulosic biomass to ethanol at 50°C and pH 5.0 that has been reported to be near optimal for the activity of commercial fungal cellulases being developed for simultaneous saccharification and fermentation of cellulose to ethanol. Since such a bacterium has not been described in the literature, we have embarked on isolating a bacterium from nature that can be engineered to ferment the biomass-derived sugars to ethanol. From about 77 environmental samples we have isolated bacteria that can grow both aerobically and anaerobically at 50°C and pH 5.0 in media containing xylose as the primary carbon source. From a total of 380 bacterial isolates we have identified strains 17C5, 36D1 and P4-102B for further study based on their growth and fermentation characteristics. Based on 16S rRNA(DNA) sequence the three bacterial isolates (strains 17C5, 36D1 and P4-102B) were identified as *Bacillus coagulans* that forms a diverse group of sporogenic lactic acid bacteria.

Task A. Physiological characterization of thermotolerant *Bacillus coagulans*

Bacillus coagulans strains 17C5, 36D1 and P4-102B fermented glucose, xylose, cellobiose, sucrose, mannose, arabinose, galactose as well as other minor sugars that are present in lignocellulosic biomass in both rich medium as well as in mineral salts medium supplemented with corn steep liquor (0.5 % w/v). *B. coagulans* strains failed to grow in mineral salts medium without organic supplements that can be met with corn steep liquor. Metabolic information obtained from genome sequence and annotation being developed as a part of this study is expected to provide information on the nutrient requirement based on missing metabolic pathways.

The primary product of fermentation of *B. coagulans* was L(+)-lactic acid and the optical purity of lactic acid was normally higher than 95% in the three isolates. Depending on the growth condition, medium composition, etc., the optical purity of L(+)-lactic acid in the fermentation broth reached 100%. Both strains 36D1 and P4-102B carry a gene that encodes the lactate dehydrogenase (d-LDH) that catalyzes D(-)-lactic acid production. However, this gene (d-*ldh*) appears to be inactive although upon cloning and insertion into *E. coli* this d-LDH from *B. coagulans* catalyzed the production of D(-)-lactic acid suggesting that the d-*ldh* gene is not expressed in *B. coagulans*. In addition to lactic acid, *B. coagulans* also produced small amount of acetate, ethanol, formate and succinate. Presence of formate in the fermentation broth suggests the presence of pyruvate formate-lyase (PFL) activity in the cell. Formate production was higher during xylose fermentation compared to glucose fermentation, as expected due to higher energy demand during anaerobic growth on xylose.

Lactate yield from glucose during fermentation was higher than 85% for all the tested isolates of this study. The lactate yield from the pentose sugar xylose was about 80-85% for these isolates. This higher lactate to xylose ratio is different from the values reported for pentose-fermenting lactic acid bacteria. These non-sporulating lactic acid bacteria, such as *Lactobacillus* and *Lactococcus*, produce lactate and acetate in equimolar amounts

from pentose sugars. This is due to the use of phosphoketolase pathway in pentose metabolism in these bacteria. In contrast, *B. coagulans* utilizes pentose phosphate pathway for pentose metabolism that conserves all the carbon in pentose as lactate (Appendix A). This is important since further engineering of these bacteria to produce ethanol from pentoses requires that all the sugar-carbon be converted to pyruvic acid for further stoichiometric conversion of ethanol and this can be achieved with *B. coagulans* and not with other lactic acid bacteria. The operation of pentose phosphate pathway in pentose metabolism of *B. coagulans* was independently confirmed by isotope tracer methods utilizing ^{13}C-labelled xylose (at C_1 position) and tracing the flow of this ^{13}C in fermentation products by NMR (Appendix A).

During lactate fermentation, the volumetric productivity and specific productivity for strain 36D1 were 0.87 g/L.(h) and 4 g/h.(g cell mass), respectively, for glucose fermentation in rich medium (Appendix B). The specific productivity is comparable to the values reported for yeast, and ethanologenic *E. coli* strain KO11 producing ethanol. The lower volumetric productivity of *B. coagulans* is apparently due to the lower cell yield during lactate fermentation. Although lactic acid is the primary fermentation product of *B. coagulans*, the rate of fermentation of sugars started to decline when the lactic acid concentration in the medium reached about 200-250 mM even when the pH of the medium was maintained at 5.0 or 7.0. Fermentation essentially stopped when the lactic acid concentration in the medium reached about 400-600 mM. It is important to know the potential of *B. coagulans* and its glycolytic flux rate before further metabolic engineering of the bacterium for production of other products. Can the bacterium ferment sugars when they are present at high concentrations, such as 100 g/L or higher? Is the observed lactate ceiling is only to lactate due to toxicity of the organic acid at high concentration or is it a limitation on the fermentation properties of the bacterium? To answer these questions, we attempted to trap the lactic acid produced during fermentation as calcium lactate by adding calcium carbonate to the medium. Results of these fermentations are presented below (Fig. 1).

B. coagulans strain 36D1 failed to ferment 80 g/L glucose to completion even in rich medium (Fig. 1). Lactic acid production was linear up to about 250 mM and the rate of lactic acid production started to decline after 24 hours. Although lactic acid production continued through 120 hours, the rate of production declined considerably. Addition of calcium carbonate increased the rate of lactic acid production, probably due to an increase in cell mass and the added 80 g/L of glucose was completely fermented by about 96 hours with the lactic acid concentration reaching over 0.9 M (81 g/L).

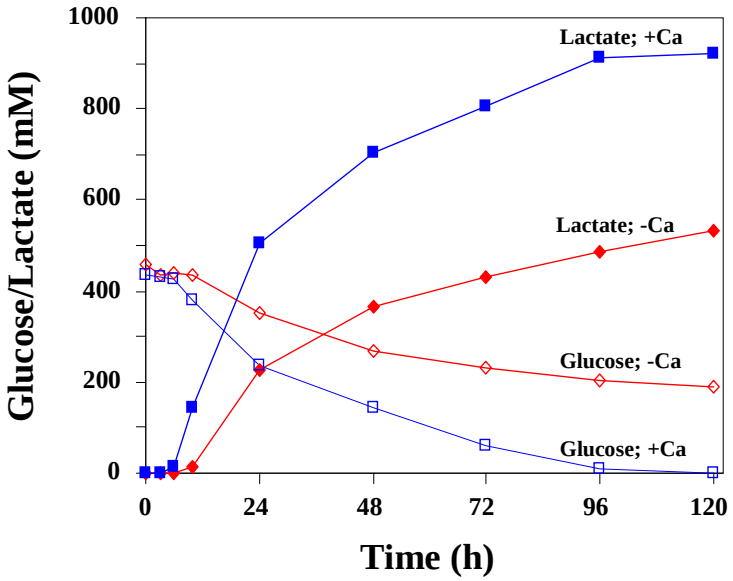

Fig. 1. Fermentation of 80 g/L glucose to L(+)-lactic acid by *B. coagulans* strain 36D1 in rich medium at 50°C and pH 6.0 in a medium supplemented with 0.5 M $CaCO_3$ to trap the lactic acid as calcium lactate.

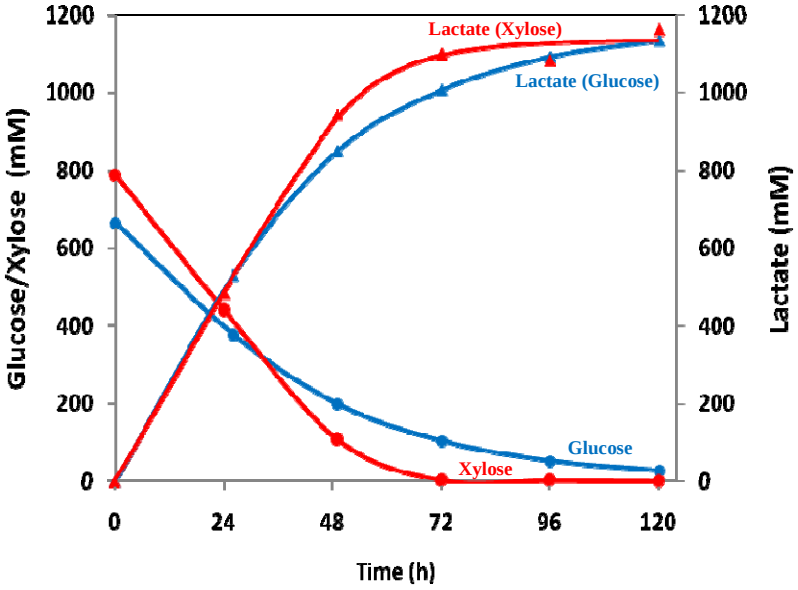

Fig. 2. Fermentation of 120 g/L glucose or xylose to L(+)-lactic acid by *B. coagulans* strain 36D1 in rich medium at 50°C and pH 6.0 in a medium supplemented with 0.75 M $CaCO_3$ to trap the lactic acid as calcium lactate.

B. coagulans strain 36D1 also fermented 120 g/L xylose to completion within 72 hours and produced over 100 g/L of lactic acid (Fig. 2) in the presence of $CaCO_3$. Complete fermentation of 120 g/L glucose took longer than 72 hours and by 120 hours almost all the glucose was fermented to over 100 g/L of lactic acid. These results show that cessation of fermentation around 500 mM of lactic acid (Fig. 1) during normal fermentations is a result of inhibition by accumulating lactic acid. These results also show that *B. coagulans* has the potential to ferment sugars at high concentrations to products provided any potential inhibitory effect of the accumulating product is neutralized.

Fed-batch experiments show that *B. coagulans* strain 36D1 can produce lactic acid at concentrations that are higher than 2 M (180 g/L) as long as the lactic acid is trapped as calcium lactate and does not impose inhibition of growth and fermentation (Fig. 3). The rate of lactic acid production during the first 24 hours was 1.76 g/L.(h) at pH 6.0 and 50°C in this fed-batch experiment. Even after 144 hours of fermentation, this strain still maintained a volumetric productivity that was about 30% of the maximum.

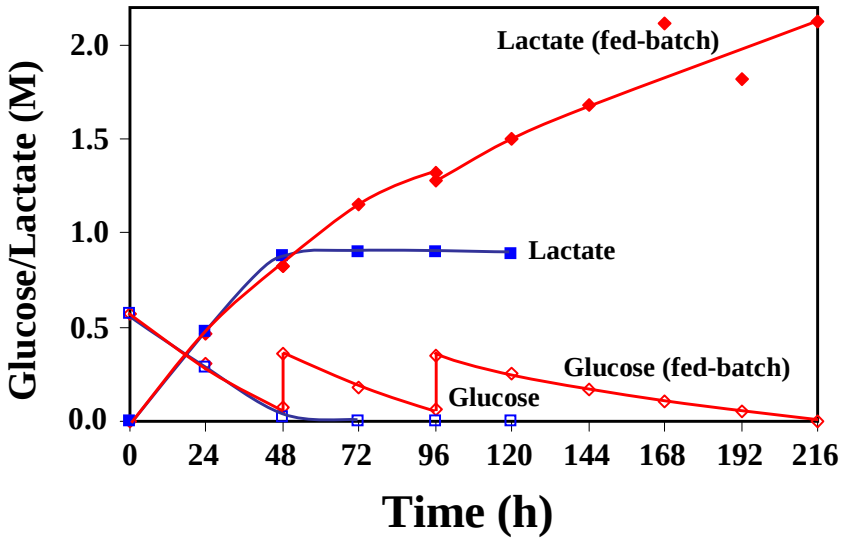

Fig. 3. Fed-batch fermentation of glucose by *B. coagulans* strain 36D1.
In one experiment (blue line), glucose was fed once at time zero at 100 g/L. In another experiment, fermentation was started at 100 g/L and 50 g/L glucose was added at 48 and 96 hours to a cumulative total of 200 g/L. The rich medium used in the fermentation also contained 0.75 M $CaCO_3$. Fermentations were conducted at 50°C and pH 6.0 to minimize $CaCO_3$ loss at low pH.

In a batch fermentation with $CaCO_3$ at pH 6.5 and 50°C, the volumetric productivity averaged over the first 24 hours of fermentation was 2.5 g/L.(h). This is slightly higher than the volumetric productivity of a similar culture at pH 6.0 or 5.5; about 1.8 g/L.(h). This level of volumetric productivity is comparable to that reported for native ethanologenic strains such as *Zymomonas mobilis* (2.0 g/L.(h); Skotnicki, et al. 1981. Appl. Env. Microbiol. 41:889-893) and yeast (about 1.8 g/L.(h); Choi et al., 2009. Appl. Microbiol. Biotechnol. 84:261-269). These results clearly show that *B. coagulans* has the physiological ability to support high rate of glycolytic flux to produce pyruvate and products from pyruvate, with lactic acid as an example.

In mineral salts medium supplemented with 0.5% corn steep liquor, the volumetric productivity of *B. coagulans* declined to about 0.9 g/L.(h) even in the presence of $CaCO_3$. It is possible that the added $CaCO_3$ is precipitating some of the required Mg^{2+} and phosphates leading to a lower growth rate and cell yield. Replacing corn steep liquor with yeast extract increased the volumetric productivity.

Simultaneous Saccharification and Fermentation (SSF) of cellulose

Commercial fungal cellulases function optimally between pH 4.5 and 5.5. Under our experimental conditions, the optimum temperature for cellulase activity is around 60°C or higher with a broad pH optimum between pH 4.5 and 5.5 (cellulases were kindly provided by Genencor and Kerry). *Bacillus coagulans* strain 36D1 has a pH optimum for growth of 5.5 although growth rate was only reduced by less than 10% at pH. 5.0. The temperature optimum for growth of *B. coagulans* strain 36D1 is 55°C. These growth characteristics closely match the optima for activity of fungal cellulases that are being developed for SSF of cellulose to products. This match in the bacterial growth and fermentation optima with that of the fungal cellulase suggests that the amount of cellulases required for SSF at 50-55 °C is less than at the temperature optimum for yeast-based SSF.

Our experimental results show that the amount of fungal cellulases required can be reduced by a factor of 3-4 if the SSF of cellulose is conducted at 55°C and pH 5.0 compared to 35°C that is the optimum for yeast growth and fermentation (Fig. 4) (Appendix B & C).

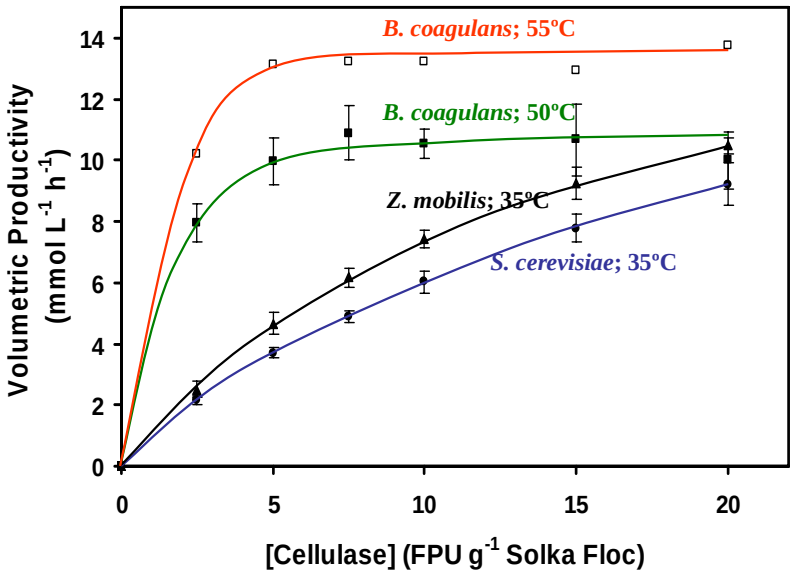

Fig. 4. Cellulase requirement for SSF of crystalline cellulose to products by *B. coagulans* at 50 and 55 °C, yeast and *Z. mobilis* at 35°C.
Cellulase was kindly provided by Genencor. Solka floc (40 g/L) was used as the crystalline cellulose in rich medium at pH 5.0 for *B. coagulans* and *Z. mobilis*. For yeast, the medium pH was 5.5.

B. coagulans fermented sugarcane bagasse dilute acid hydrolysate when the concentration of the hydrolysate in the medium was less than 25%. However, after lime treatment, the hydrolysate concentration in the fermentation can be increased to as high as 75% and all the sugars were completely fermented in 192 hours (51.45 g/L xylose, 8.6 g/L glucose and 0,9 g/L of arabinose) (Appendix D). This longer time interval needed for complete conversion of the sugars is dictated by accumulating lactate that lowered the

volumetric productivity. When sugarcane bagasse dilute acid hydrolysate (lime-treated) (40%) was mixed with crystalline cellulose (20 g/L) and fungal cellulases (15 FPU/g glycan), *B. coagulans* fermented both the sugars in the hydrolysate as well as the glucose and cellobiose released by the cellulases simultaneously (Appendix B).

The physiological characteristics that are critical for the development of *B. coagulans* as a thermotolerant microbial biocatalyst for cost-effective production of fuels and chemicals from lignocellulosic biomass are listed below.

1. *B. coagulans* is a facultative anaerobe that grows at 50-55 °C and pH 5.0, conditions that are also optimal for fungal cellulase activity. Due to the ability of this bacterium to grow at higher temperature than conventional microbial biocatalysts such as yeast, *Z. mobilis* and lactic acid bacteria, the amount of fungal cellulase required for SSF of cellulose with *B. coagulans* is about 3-4-fold lower than corresponding SSF with yeast at its optimum temperature of 35°C. This is expected to reduce the cost of fungal cellulase in lignocellulosic biorefinery by lowering enzyme loading.

2. *B. coagulans* ferments cellobiose in addition to its ability to ferment all the sugars in biomass. This eliminates the need for β–glucosidase in the fungal enzyme cocktail, another cost-saving characteristic.

3. Glycolysis and fermentation rates of *B. coagulans* are comparable to that of yeast and other microbial biocatalysts that are currently in use in the industry.

4. *B. coagulans* produces optically pure L(+)-lactic acid as the primary fermentation product that can serve as the starting material for bioplastics at rates and yields that are comparable to lactic acid bacteria.

5. Fermentation at higher temperature is also expected to minimize contamination in industrial scale fermentations.

Task B. Metabolic engineering of second generation biocatalysts for ethanol production

Fermentation Pathway

During anaerobic growth and fermentation *B. coagulans* produces lactate as the primary fermentation product with small amount of succinate, acetate, ethanol and formate. In addition, when cultured at pH 7.0, *B. coagulans* also produces small amount of acetoin and butanediol. The pathways that lead to these products from pyruvate are listed in Fig. 5. Production of succinate, a minor product, starts with phosphoenol pyruvate, one step above the pyruvate in the glycolysis pathway of sugars to pyruvate.

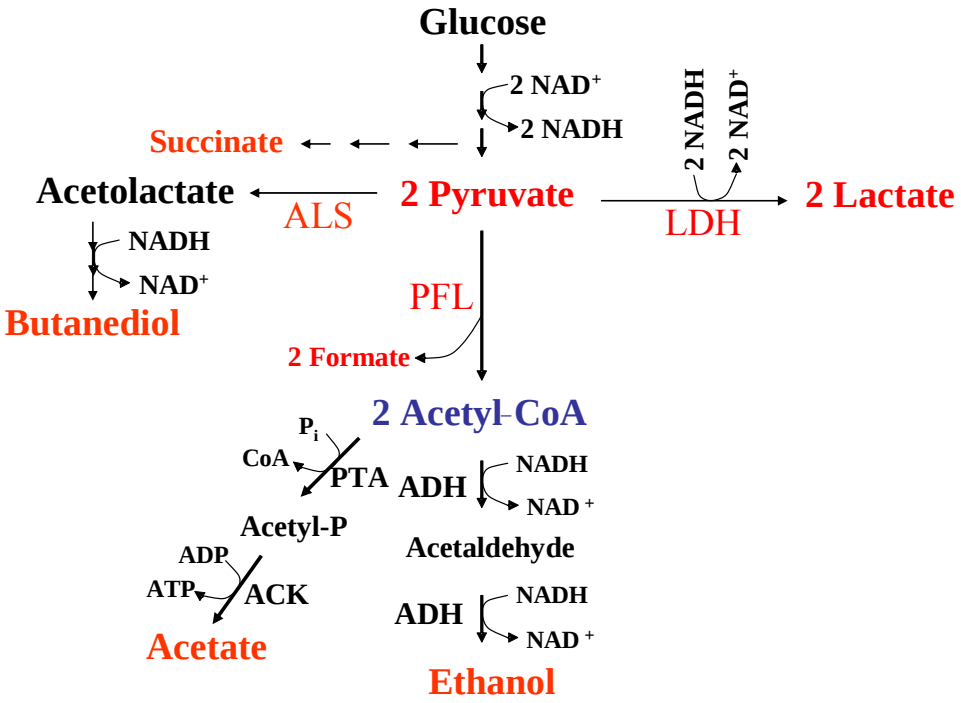

Fig. 5. Fermentation pathways of *B. coagulans*.
ALS, acetolactate synthase; LDH, lactate dehydrogenase; PFL, pyruvate formate-lyase; ADH, alcohol dehydrogenase and aldehyde dehydrogenase; PTA, phosphotransacetylase; ACK, acetate kinase.

Metabolic engineering of *B. coagulans* for production of ethanol as the primary fermentation product requires elimination of competing pathways and introduce a pathway that will lead to ethanol as the fermentation product, as presented in Fig. 6. All naturally occurring ethanologenic microbes decarboxylate pyruvate to acetaldehyde using pyruvate decarboxylase (PDC) and reduce the acetaldehyde to ethanol using alcohol dehydrogenase (ADH). Introduction of this pathway in organisms that are not natural ethanol producers requires introduction of a foreign gene encoding PDC and optimize its expression and activity.

We have constructed a new ethanologenic pathway during this project period using *E. coli* as a model organism that utilizes only native enzymes such as pyruvate dehydrogenase complex (PDH) and ADH for ethanol production (Fig. 6) (Appendix E & F). In this new ethanologenic pathway, PDH generates acetyl-CoA, CO_2 and NADH. The acetyl-CoA is further reduced in a two step process to ethanol. The native PDH is inhibited by NADH, a reduced compound that accumulates to higher concentration in the cytoplasm of an anaerobic cell rendering the enzyme inactive. By introducing a mutation in the specific NADH-sensitive subunit of PDH complex, dihydrolipoamide dehydrogenase (LPD), the altered PDH (PDH*) can be rendered less sensitive to inhibition by NADH. A PDH* with the LPD mutation is active in an anaerobic cell. The combination of PDH* and ADH constitute the new non-recombinant ethanologenic pathway. This non-recombinant ethanologenic pathway can be constructed using existing enzymes in all facultative anaerobes, including *B. coagulans*.

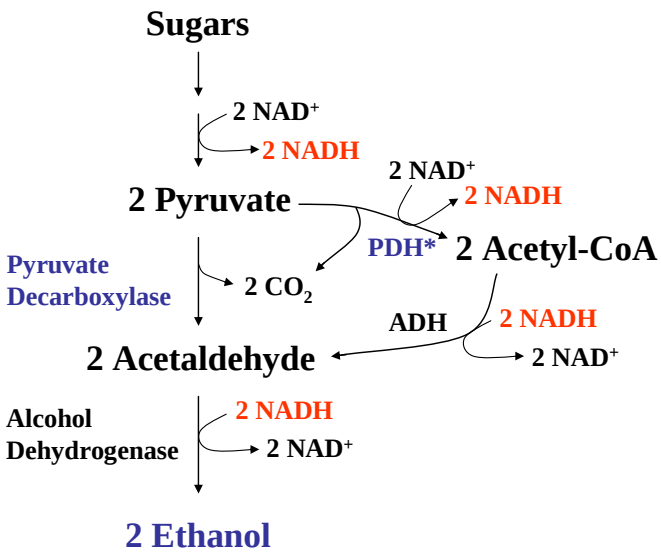

Fig. 6. Fermentation pathways that can lead to ethanol as the primary product.
PDH*, pyruvate dehydrogenase with a mutation in its dihydrolipoamide dehydrogenase component that makes the PDH complex less sensitive to NADH inhibition; ADH, aldehyde/alcohol dehydrogenase.

Gene Transfer in *B. coagulans*

To construct an ethanologenic *B. coagulans* we have attempted to eliminate the competing pathways leading to lactate, 2,3-butanediol and acetate and feed all the pyruvate to ethanol production. This can be accomplished by deleting the corresponding genes encoding enzymes catalyzing the competing pathways (Fig. 5) and then elevate the level of PDH*-dependent ethanol pathway. This requires genetic manipulation of *B. coagulans* that has not been accomplished and reported in the literature. The first step is to develop gene transfer tools for the genetically recalcitrant *B. coagulans* that can be used for modification of individual genes.

We evaluated about 10 selected isolates for their ability to be transformed with a plasmid and found only strain P4-102B was transformable by electroporation. Strain P4-102B is the only one among the 24 independent isolates tested that carried two native plasmids (6.8 kbp and 15 kbp). The DNA sequence of the smaller plasmid was determined and the DNA needed for plasmid replication from this plasmid was used to construct a shuttle vector between *E. coli* and Gram-positive bacteria. Transformation of strain P4-102B was optimized using this plasmid and another shuttle vector constructed for plasmid transfer in *B. stearothermophilus* (Appendix G). We also adapted a *Lactococcus* plasmid, pGK12, as a temperature-sensitive plasmid (in *B. coagulans*) to help with integration of DNA into the chromosome of *B. coagulans*. The plasmid transfer rate into *B. coagulans* was comparable to the rate of plasmid transfer by electroporation into *B. subtilis*, a well-studied Gram-positive bacterium. Gene transfer into *B. coagulans* strain P4-102B was not significantly influenced by the source of plasmid DNA; derived

from *B. coagulans* strain P4-102B, DNA modification defective *E. coli*, or plasmid DNA methylated in vitro by *B. coagulans* strain P4-102B modification system.

Isolation of mutants with altered fermentation properties

Using the genetic tools we have developed, two types of *ldh* mutants in two different *B. coagulans* strains were constructed. In strain P4-102B, a part of the *ldh* gene was deleted since this strain is amenable to genetic transformation. A point mutation in *ldh* gene was introduced in strain 36D1 that is not found to be transformable by plasmids or linear DNA. Aerobic growth rates of the *ldh* mutants were comparable to the corresponding parent strains. Anaerobic growth of the *ldh* mutants in a medium at pH 7.0 was comparable to the parent strains. However, at pH 5.0, anaerobic growth of the mutants was minimal. This growth defect at pH 5.0 was traced to low level of expression of the *pfl* gene at pH 5.0.

Since the Δ*ldh* (deletion) strain (#20) grew very poorly at pH 5.0, pH-controlled fermentations were started with air in the gas phase. As the culture grow and reach a cell density of about 0.5 optical density (OD) at 420nm, the cultures generally become O_2-limited and fermentation of the sugars commence. Using this method, the fermentation profile of the Δ*ldh* strain #20 in a culture medium that was maintained at pH 5.0 or 7.0 was determined (Fig. 7 & 8). These results show that at pH 7.0, the primary product of fermentation is ethanol with 2,3-butanediol, acetate, formate and succinate as other products. Although not presented in the figure, at the end of fermentation of 30 g/L glucose at pH 7.0, the concentrations of formate, acetate and ethanol were 66, 47 and 172 mM, respectively. If PFL is the only enzyme contributing to ethanol production, the molar ratio of acetate to ethanol is expected to be 1:1 and formate concentration is expected to be the sum of acetate and ethanol concentrations (Fig. 5). The disproportionately high ethanol concentration among the fermentation products suggests that the PDH also contributed to ethanol production in this strain (Fig. 6).

Strain #20 with Δ*ldh*, produced 2,3-butanediol as the primary fermentation product when cultured at pH 5.0 (Fig. 8). Presence of air in the gas phase supported early growth of the culture and the growth stopped when the culture was O_2-limited at an OD of 1.8. Growth resumed at a very low rate after about 48 hours and the 30g/L glucose added to the medium at the beginning of the experiment was not completely consumed even after 186 hours. Formate production, an indication of the PFL activity, was very low and at the end of 186 h, the amount of formate in the medium was only 16 mM suggesting that the PFL activity of the pH 5.0 culture was very low. It is possible that the very low level of PFL in the culture contributed to the observed poor growth. Although the ethanol yield is low in this pH 5.0 culture (40 mM), both PDH and PFL appear to contribute to this ethanol based on the ethanol to formate ratio. The ratio of ethanol to formate in the fermentation broth of the pH 7.0 and pH 5.0 cultures was 3.0 and 2.5, respectively. These results suggest that the level of PFL and PDH activities of *B. coagulans* growing under anaerobic conditions at pH 5.0 are significantly lower compared to the cultures growing at pH 7.0. To evaluate the potential difference in these enzyme activities of the cultures grown at the two pH, we determined the level of expression of the various genes encoding the enzymes at the pyruvate branch point, *pfl*, *ldh*, *als* and *pdh* (Fig. 5 & 6) to

understand the regulation of these genes and pyruvate flux through the different pathways. Since in bacteria, gene transcription is coupled to translation of the mRNA, transcript level is an acceptable measure of the protein and enzyme production.

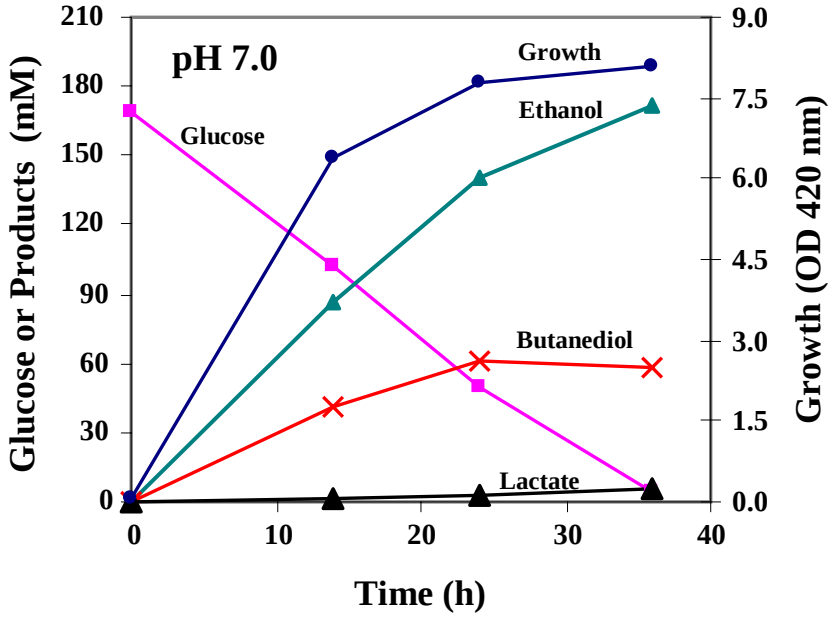

Fig. 7. pH controlled fermentation of 30 g/L glucose by an *l-ldh* deletion mutant (#20) of *B. coagulans* at pH 7.0.

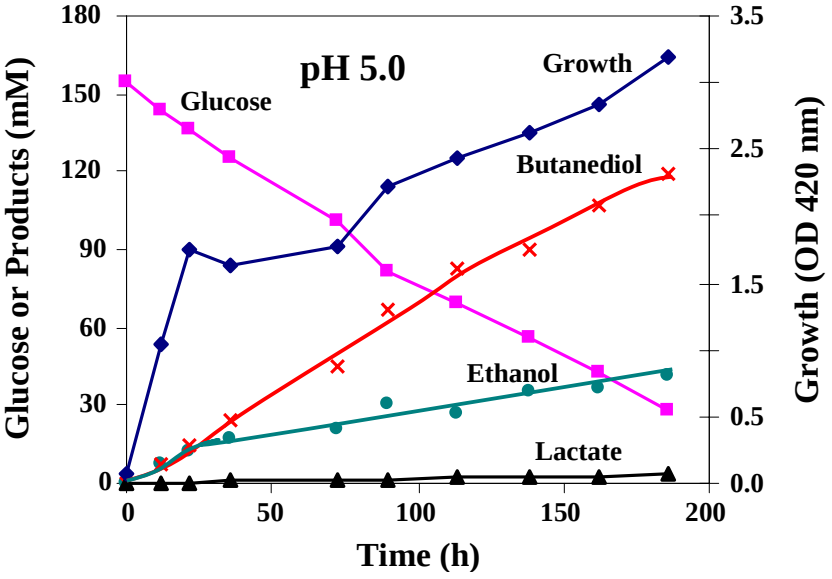

Fig. 8. pH controlled fermentation of 30 g/L glucose by an *l-ldh* deletion mutant (#20) of *B. coagulans* at pH 5.0.

When the wild type *B. coagulans* was cultured at pH 5.0 and pH 7.0, the final cell density of the pH 7.0 cultures was about twice that of the pH 5.0 cultures. The primary mRNA of these fermenting cultures was the one encoding l-LDH and the level of this

mRNA in the cell did not change significantly during the growth phase or pH of the culture medium (Table 1). The, level of *pfl* mRNA increased by 45-fold during late-exponential phase of growth at pH 7.0 while this increase in mRNA level was only about 16-fold during growth at pH 5.0. The mRNA encoding the α-subunit of E1 component of the PDH complex also increased during the late-exponential phase of growth but by only 2-3 fold irrespective of the culture pH. The *als* mRNA also increased during late exponential phase by about 40-fold at pH 7.0 but only by about 6-fold during growth at pH 5.0.

Table 1. Ratio of mRNA levels in *B. coagulans* grown in LB + glucose (30 g/L)) at pH 5.0 or pH 7.0

	Time (h)	OD420 nm	Relative mRNA level			
			pfl	*pdh*	*ldh*	*als*
pH 5.0	2.00	0.48	1.00 (1.03)	1.00 (0.58)	1.00 (92.03)	1.00 (0.07)
	3.50	2.24	0.49	0.21	0.95	2.34
	5.75	3.98	16.81	2.28	0.76	6.30
pH 7.0	2.00	0.33	1.82 (1.65)	1.12 (0.65)	1.00 (80.70)	1.28 (0.09)
	4.50	3.01	2.32	0.53	1.33	4.63
	6.75	6.38	83.3	3.76	1.06	50.55

The first sample (2 h) of both cultures was from early exponential phase of growth and the second sample was from mid-exponential phase of growth and the third sample was from an early stationary phase culture. Values in parenthesis are the concentration of specific mRNA (pg/µl of RNA preparation). The *pdh* represents the mRNA level of the gene encoding E1α subunit of the PDH complex.

Although the *pdh* mRNA was present in the anaerobically grown *B. coagulans*, this mRNA level did not correlate with enzyme activity in cell extracts. In batch fermentations starting with air in the gas phase, PDH activity was detected in the crude extracts during the aerobic growth phase but not during the anaerobic fermentation phase. This is unexpected since the mRNA is expected to be translated to active protein. It is possible that the PDH is inhibited in vivo by high NADH concentration during the anaerobic phase. However, upon breaking the cells, the NADH concentration in the extract is expected to decrease to a level that is no longer inhibitory to the enzyme activity. Also, during the assay of the enzyme activity, NAD^+ to NADH ratio would significantly favor NAD^+, the substrate added to the reaction, and overcome any inhibition of the PDH activity by residual NADH. The absence of enzyme activity in the cell extract suggests a potential unknown modification (or degradation) of the PDH to inactive form that is similar to that observed with PDH from eukaryotes but only during

anaerobiosis or high in vivo NADH concentration. A potential uncoupling of transcription and translation is unlikely since unique DNA sequence that may contribute to such an uncoupling was not detected in the *pdh* operon.

In order to improve the ethanol yield, we introduced a second mutation, either in the *pflB* gene or the *alsS* gene, in the Δ*ldhA* strain #20. These double mutants had the following phenotypes; the first one (strain 20-B2) (*ldhA, pflB*) lacks lactate dehydrogenase (LDH) and pyruvate formate-lyase (PFL) activities and the second (*ldhA, alsS*) lost lactate dehydrogenase and acetolactate synthase (ALS) activities. Mutant strain 20-B2 still has the intact 2,3-butanediol pathway and produced 2,3-butanediol as the fermentation product during fermentation under O_2-limitation condition. However, production of one 2,3-butanediol from one glucose by *B. coagulans* is expected to utilize only one NADH in this bacterium (based on pathway construction from the genome sequence) while the production of two pyruvates (from one glucose) releases 2 NADHs (Fig. 5). Because of this difference in NADH production and consumption, this *ldhA, pflB* double mutant failed to grow anaerobically. Anaerobic growth of this double mutant requires activation of the PDH-based ethanol fermentation.

Further mutagenesis of the *ldh* point mutant, strain Suy27 (strain Suy27-13), supported anaerobic growth at pH 5.0 by increasing expression of the genes encoding pyruvate dehydrogenase complex and produced ethanol as the main fermentation product. This is similar to the non-recombinant homo-ethanologenic *E. coli* strain we have constructed (Appendix E). The only problem we encountered with strain Suy27-13 is the high reversion rate of the *ldhA* mutation to LDH-positive phenotype during long-term fermentations. Based on this information, it is expected that the anaerobic growth of the double mutant, strain 20-B2, can be restored upon increasing the pyruvate dehydrogenase activity of the culture. Current experiments are focused on increasing the PDH activity of this mutant strain by further mutagenesis and selection as colonies that will grow anaerobically at pH 7.0.

The second mutant with mutations in the genes encoding LDH and ALS produced acetate, ethanol and formate. This mutant also had anaerobic growth defect due to the low level of expression of *pflB* gene during the growth phase. This double mutant did produce ethanol as the primary fermentation product under oxygen-limitation condition but the cell yield was lower than the parent strain. The level of PDH activity needs to be increased in this mutant also to support anaerobic growth with ethanol as the fermentation product.

Pyruvate decarboxylase

An alternate way of overcoming the anaerobic growth defect of the *ldh* mutants at pH 5.0 is to introduce pyruvate decarboxylase into these mutants and convert glucose to ethanol using the classical ethanol pathway (Fig. 6). Towards this objective, we have cloned *pdc* gene from various bacteria that are known to encode the *pdc* gene and the proteins were purified and biochemically characterized. Among these PDCs, only the ones from *Zymomonas mobilis* and *Zymobacter palmae* had detectable activity at 50-55 °C. However, the genes encoding these specific enzymes, although transcribed in *B.*

coagulans failed to produce an active protein. Even with the change of codon of the *Z. palmae* PDC to that of the *B. coagulans* l-LDH, PDC activity was not detected in recombinant clones carrying the modified *Z. palmae* PDC. These results suggest a limitation in PDC activation with appropriate cofactors in *B. coagulans*. This limitation needs to be removed before the PDC-based ethanol pathway can be functional in *B. coagulans*.

Genome Sequence of *B. coagulans*

Genome sequence and derived enzyme composition of the bacterium is expected to help understand and overcome the limitations in gene transfer as well as provide the physiological and biochemical potential of the bacterium. DOE-JGI has attempted to sequence the entire genome of *B. coagulans* strain 36D1 and has sequenced about 3.5 Mbp of the genome as four non-overlapping fragments (Contigs). Due to difficulty in closing the gaps, after about 3.5 years DOE-JGI concluded that the genome sequence will be left as a permanent draft genome. Although the genome sequence is not complete, the sequence information is very valuable providing critical information for our understanding of the bacterium and developing tools for construction of deletion mutants described above. More recently, we have constructed a circular restriction map of the genome of *B. coagulans* (Fig. 9) and identified the location of the gaps in the genome sequence. Using the information from the genome sequence and the circular restriction map, we are in the process of closing the gaps and complete the genome sequence of *B. coagulans* strain 36D1.

The genome sequence information led to identification of seven genes that could encode alcohol dehydrogenase and only one of the seven is similar to the *E. coli* ADH-E that has both alcohol dehydrogenase and aldehyde dehydrogenase activity that is needed for reduction of acetyl-CoA to ethanol in the two step process (Fig. 6). All seven potential *adh* genes were cloned and expressed in *E. coli* and only three of the seven including the *adhE* produced an active protein. The *adhE* gene is currently tested for its ability to increase anaerobic growth of *ldh* mutants at pH 5.0.

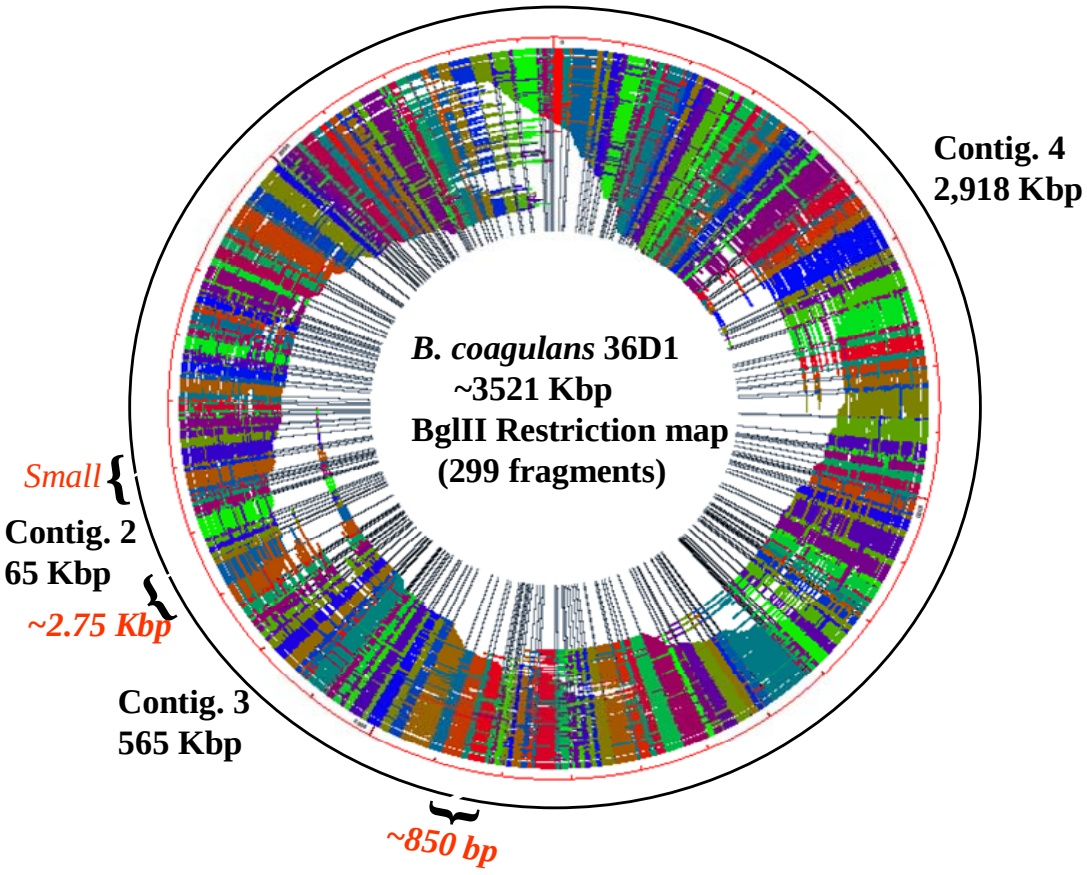

Fig. 9. Circular BglII restriction map of *B. coagulans* strain 36D1. Vertical lines represent the location of the BglII recognition sequence (AGATCT). The outer circle (black lines) represents the known genome sequence aligned to the BglII restriction map. The three Contigs (2, 3 and 4) and the gaps between the three are labeled. The location of Contig. 1 (2.7 kbp) is too small to be identified by this method.

During the course of this study we have accomplished the following.

1. Identified a facultative anaerobic thermotolerant bacterial platform for production of chemicals and ethanol using lignocellulosic biomass as feedstock. This select bacterium, *Bacillus coagulans,* grows and ferments at 50-55 °C and pH 5.0 conditions that are also optimal for fungal cellulase activity. With this match in optima, the amount of cellulase required for SSF of crystalline cellulose is about 3-4 times lower than with yeast or other natural ethanologenic microbial biocatalysts.
2. *Bacillus coagulans* ferments all the sugars in the biomass including cellobiose to L(+)-lactic acid.
3. The lactic acid concentration in the broth of *B. coagulans* can be increased to higher than 150 g/L under appropriate fermentation conditions.
4. Glycolytic flux rate of *B. coagulans* is comparable to yeast and other microbial biocatalysts.

5. Developed a genetic system for this genetically recalcitrant bacterium for genetic engineering for production of fuels and chemicals.
6. Constructed stable mutant strains that are deleted for lactate dehydrogenase and established the physiological and fermentation characteristics of the mutant.
7. Constructed double mutants that carry in addition to the Δ*ldh* a mutation in *pfl* or *als* removing pyruvate formate-lyase or acetolactate synthase (starting point of the 2,3-butanediol pathway). Construction of these mutants is insignificant if the bacterium is *E. coli* or *B. subtilis*. But for the genetically recalcitrant *B. coagulans* these are very important stepping points in our ability to manipulate the organism for production of a specific product.
8. Identified the rate-limiting steps in ethanol production in these single and double mutants. This yielded unique insight into the physiology of *B. coagulans*, information that is critical as we advance towards developing this bacterial platform for cost-effective conversion of biomass derived sugars to products.
9. With the help of DOE-JGI developed a partial draft genome sequence.
10. Developed a new ethanologenic pathway for engineering *B. coagulans* for production of ethanol as a major product.
11. Physiological studies with the mutants revealed that neither the PDH/ADH, PFL/ADH nor the butanediol pathway is operating at a high enough rate in an *ldh* mutant to support high glucose flux through glycolysis, especially at pH 5.0 to support anaerobic growth. These results point to the focus of the next phase of research in developing *B. coagulans* as the thermophilic bacterial biocatalyst for production of fuels and chemicals.

Although this DOE-funded project has concluded, genetic engineering of the thermotolerant *B. coagulans* as a microbial platform is continuing with support from the State of Florida and University of Florida. These studies are focused towards the following.

1. Experiments to overcome the rate-limiting steps in ethanologenic pathway in the Δ*ldh*, *pfl* double mutants of *B. coagulans* are in progress.
2. A *B. coagulans* derivative that produces D(-)-lactic acid as the primary product is under construction. The D(-)-lactic acid is a source of polylactide for biopolymers with varying physical characteristics.
3. Experiments to complete the genome sequence of *B. coagulans* are in progress.

Task C: **Fermentation characteristics of ethanologenic strains**

Specific accomplishments in fulfilling this task are listed under Task B since it was found to be difficult to separate these two tasks.

Appendix A.
Patel, M. A., M. S. Ou, R. Harbrucker, H. C. Aldrich, M. L. Buszko, L. O. Ingram and K. T. Shanmugam. 2006. Isolation and characterization of acid-tolerant, thermophilic bacteria for effective fermentation of biomass-derived sugars to lactic Acid. Appl. Environ. Microbiol. 72:3228-3235.
http://www.ncbi.nlm.nih.gov/pmc/articles/PMC1472308/pdf/3064-05.pdf

Appendix B
Patel, M. A., M. Ou, L. O. Ingram and K. T. Shanmugam. 2005. Simultaneous saccharification and fermentation of crystalline cellulose and sugar cane bagasse hemicellulose hydrolysate to lactate by a thermotolerant acidophilic *Bacillus* sp. Biotechnol. Prog. 21:1453-1460.
http://www3.interscience.wiley.com/cgi-bin/fulltext/121399220/PDFSTART

Appendix C
Ou, M. S., N. Mohammed, L. O. Ingram and K. T. Shanmugam. 2009. Thermophilic *Bacillus coagulans* requires less cellulases for simultaneous saccharification and fermentation of cellulose to products than mesophilic microbial biocatalysts. Appl. Biochem. Biotechnol. 155:379-385.
http://www.springerlink.com/content/062g325187155747/fulltext.pdf

Appendix D
Patel, M., M. Ou, L. O. Ingram and K. T. Shanmugam. 2004. Fermentation of sugar cane bagasse hemicellulose hydrolysate to L(+)- lactic acid by a thermotolerant acidophilic *Bacillus* sp. Biotech. Letters 26:865-868.
http://www.springerlink.com/content/l57102r70x402386/fulltext.pdf

Appendix E
Kim, Y., L. O. Ingram and K. T. Shanmugam. 2007. Construction of an *Escherichia coli* K-12 mutant for homo-ethanol fermentation of glucose or xylose without foreign genes. Appl. Environ. Microbiol. 73:1766-1771.
http://www.ncbi.nlm.nih.gov/pmc/articles/PMC1828829/pdf/2456-06.pdf

Appendix F
Kim, Y., L. O. Ingram and K. T. Shanmugam. 2008. Dihydrolipoamide dehydrogenase mutation alters the NADH sensitivity of pyruvate dehydrogenase complex of *Escherichia coli* K-12. J. Bacteriol. 190:3851-3858.
http://www.ncbi.nlm.nih.gov/pmc/articles/PMC2395023/pdf/0104-08.pdf

Appendix G
Rhee, M. S., J. W. Kim, Y. Qian, L. O. Ingram and K. T. Shanmugam. 2007. Development of plasmid vector and electroporation condition for gene transfer in sporogenic lactic acid bacterium, *Bacillus coagulans*. Plasmid 58:13-22.
http://www.sciencedirect.com/science?_ob=MImg&_imagekey=B6WPF-4MSHTBN-1-B&_cdi=6989&_user=2139813&_orig=search&_coverDate=07%2F31%2F2007&_sk=999419998&view=c&wchp=dGLbVlb-zSkzS&md5=abd473d448ccace3b19b4927613da1d8&ie=/sdarticle.pdf

Appendix H

Wang, Q., M. S. Ou, Y. Kim, L. O. Ingram and K. T. Shanmugam. 2010. Metabolic flux control at the pyruvate node in an anaerobic *Escherichia coli* strain with an active pyruvate dehydrogenase. Appl. Environ. Microbiol. 76:2107-2114.
http://aem.asm.org/cgi/reprint/76/7/2107

Appendix I

Ou, M. S., N. Mohammed, L. O. Ingram and K. T. Shanmugam. 2009. Thermophilic *Bacillus coagulans* requires less cellulases for simultaneous saccharification and fermentation of cellulose to products than mesophilic microbial biocatalysts. Appl. Biochem. Biotechnol. 155:379-385.
http://www.springerlink.com/content/062g325187155747/fulltext.pdf

Appendix J

Do, P. M., A. Angerhofer, I.Hrdy, L. Bardonova, L. O. Ingram and K. T. Shanmugam. 2009. Engineering *Escherichia coli* for fermentative dihydrogen production: potential role of NADH-ferredoxin oxidoreductase from the hydrogenosome of anaerobic protozoa. Appl. Biochem. Biotechnol. 153:21-33.
http://www.springerlink.com/content/0u76731787347382/fulltext.pdf

Final Technical Report

Project Title: Engineering Thermotolerant Biocatalysts for Biomass Conversion to Products

Award Number: DE-FG36-04GO14019

Recipient: K. T. Shanmugam, L. O. Ingram & J. A. Maupin-Furlow
Project Location: Department of Microbiology and Cell Science
University of Florida, Gainesville, FL

Reporting Period: April 1, 2004 to September 30, 2009
Date of Report: October 20, 2009
Written by: K. T. Shanmugam

Appendices

Appendix A

Applied and Environmental Microbiology, May 2006, p. 3228–3235 Vol. 72, No. 5
0099-2240/06/$08.00+0 doi:10.1128/AEM.72.5.3228–3235.2006

Isolation and Characterization of Acid-Tolerant, Thermophilic Bacteria for Effective Fermentation of Biomass-Derived Sugars to Lactic Acid

Milind A. Patel,† Mark S. Ou, Roberta Harbrucker, Henry C. Aldrich, Marian L. Buszko, Lonnie O. Ingram, and K. T. Shanmugam*

Department of Microbiology and Cell Science, University of Florida, Gainesville, Florida 32611

Received 29 December 2005/Accepted 16 February 2006

Biomass-derived sugars, such as glucose, xylose, and other minor sugars, can be readily fermented to fuel ethanol and commodity chemicals by the appropriate microbes. Due to the differences in the optimum conditions for the activity of the fungal cellulases that are required for depolymerization of cellulose to fermentable sugars and the growth and fermentation characteristics of the current industrial microbes, simultaneous saccharification and fermentation (SSF) of cellulose is envisioned at conditions that are not optimal for the fungal cellulase activity, leading to a higher-than-required cost of cellulase in SSF. We have isolated bacterial strains that grew and fermented both glucose and xylose, major components of cellulose and hemicellulose, respectively, to L(+)-lactic acid at 50°C and pH 5.0, conditions that are also optimal for fungal cellulase activity. Xylose was metabolized by these new isolates through the pentose-phosphate pathway. As expected for the metabolism of xylose by the pentose-phosphate pathway, [^{13}C]lactate accounted for more than 90% of the total ^{13}C-labeled products from [^{13}C]xylose. Based on fatty acid profile and 16S rRNA sequence, these isolates cluster with *Bacillus coagulans*, although the *B. coagulans* type strain, ATCC 7050, failed to utilize xylose as a carbon source. These new *B. coagulans* isolates have the potential to reduce the cost of SSF by minimizing the amount of fungal cellulases, a significant cost component in the use of biomass as a renewable resource, for the production of fuels and chemicals.

Rising costs and the finite nature of fossil fuels have led to renewed interest in lignocellulosic biomass as a renewable feedstock for the production of ethanol and other chemicals (5, 11, 17, 25). For this feedstock to be competitive, efficient technologies must be developed to extract and ferment the sugars from both the cellulosic and hemicellulosic portions of fibrous plants, comprising ca. 70% of the dry weight (1, 15). The most efficient process for the utilization of cellulose as a feedstock is yet to be defined but may represent either a two-step process with complete conversion to sugar prior to fermentation (sugar platform) or a one-step process in which saccharification of cellulose by cellulases occurs concurrently with fermentation (simultaneous saccharification and fermentation [SSF]) (24).

Yeast is the preferred organism for glucose conversion to ethanol and lactic acid bacteria serve as the primary organisms for the production of lactic acid (10, 26). Neither organism effectively ferments pentose (hemicellulose) sugars to high levels of products (1, 10). Although pentose-utilizing lactic acid bacteria are available, the phosphoketolase pathway used by these organisms converts two of the five carbons in pentoses to acetic acid, limiting yields and increasing the cost of product purification (7, 22). In addition, optimal growth and fermentation conditions for these traditional microbes are far removed from the optimum conditions for the fungal cellulases (50°C and pH 5.0) required for SSF of cellulose (24). Ethanologenic enteric bacteria have been developed that reduce the requirement for fungal cellulases by functionally expressing integrated cellulase genes from *Erwinia chrysanthemi* and ferment effectively at pH 5.0 (27). Although these strains efficiently ferment both hexose and pentose sugars, the lack of thermal tolerance precludes their use at temperatures above 43°C. The mismatch of optima for growth of and fermentation by microbes and activity of fungal cellulases increases the enzyme level required for an effective SSF process, arguably a major cost component in lignocellulose conversion to fuels and chemicals (24).

New gram-positive bacterial strains were recently reported that can grow and ferment at pH 5.0 and at temperatures up to 60°C, conditions that are optimal for cellulose hydrolysis by fungal enzymes (18, 19). These new isolates produced L(+)-lactic acid as the major fermentation product during SSF processes with low levels of cellulase (7.5 filter paper units [FPU]/g of glucan). Glucose and xylose were fermented efficiently with yields exceeding 90% by weight, an impossibly high yield for lactic acid bacteria which typically ferment pentoses using the phosphoketolase pathway (10).

We describe here the isolation and physiological characterization of three new gram-positive bacterial isolates with growth optima that match those for fungal cellulases. These strains, producing lactic acid from glucose and xylose, were identified as *Bacillus coagulans* based on a comparison of 16S rRNA sequences, fatty acid profiles, and physiological properties. Analyses of fermentation products revealed that these bacteria utilize the pentose-phosphate pathway for xylose fermentation, in contrast to the phosphoketolase pathway used by most other lactic acid bacteria (14).

* Corresponding author. Mailing address: Department of Microbiology and Cell Science, Box 110700, University of Florida, Gainesville, FL 32611. Phone: (352) 392-2490. Fax: (352) 392-5922. E-mail: shan@ufl.edu.

† Present address: Argonne National Laboratory, Argonne, IL 60439.

MATERIALS AND METHODS

Culture media. The mineral salts solution used for initial isolation of bacteria contained, per liter, 1.36 g of KH_2PO_4, 2.0 g of NaCl, 0.2 g of $MgSO_4 \cdot 7H_2O$,

1.0 g of $(NH_4)_2SO_4$, and 10 mg of $FeSO_4 \cdot 7H_2O$. Initial pH of the mineral salts solution, as well as the complete media, was 5.0 and was adjusted with HCl. For Xylose-YE medium, this mineral solution was supplemented with 0.1% (wt/vol) yeast extract and 1% (wt/vol) xylose. In some experiments, xylose was replaced with other sugars at the same concentration. Yeast extract was replaced by corn steep liquor (CSL; 0.5% dry weight/vol) in pH-controlled fermentations. L broth (per liter, 10 g of Trypticase peptone, 5 g of yeast extract, and 5 g of NaCl; LB) supplemented with 1% sugar (wt/vol) served as rich medium (12). Agar was added (1.5% [wt/vol]) for the preparation of the solid medium. Aerobic cultures were grown in 10 ml of medium in 125-ml flasks in a shaker at 200 rpm at 50°C starting with an overnight-grown aerobic culture as inoculum at 1% (vol/vol). Cells from the aerobic cultures were used as needed either at 6 to 8 h of growth (early stationary phase) or after 16 to 18 h. *Lactococcus lactis* subsp. *lactis* strain NRRL B-4449 obtained from the U.S. Department of Agriculture was cultured in M17 broth (Difco) supplemented with either glucose or xylose (1% [wt/vol]).

Isolation of thermotolerant, acidophilic bacteria. Environmental samples were collected from various sources. Approximately 3.5 g of each was suspended in 50 ml of mineral salts solution with the aid of 2-g glass beads (125-ml flask, 200 rpm, 3 h, 50°C), and a sample of the suspension was plated on Xylose-YE medium. After 16 h of incubation at 50°C, representative colonies were selected and stored in 20% glycerol at −75°C for further physiological analysis.

For enrichment of xylose-utilizing bacteria, 44 ml of the suspension described above was supplemented with yeast extract (0.05%) and xylose (1%). After incubation (200 rpm) for 24 h at 50°C, a sample from this enrichment was plated on Xylose-YE medium and incubated at 50°C for 16 h. Individual colonies with distinct morphological characteristics were selected and stored for further analysis.

Fermentations. Batch fermentations without pH control were conducted in 13-by-100-mm screw cap tubes filled to the top with appropriate medium. Inoculum (1% [vol/vol]) was an overnight aerobic culture grown in the same medium. Growth and fermentation profile of the isolates were determined after 24 h of growth at 50°C. In these fermentations, growth was restricted to the first 6 to 8 h, and the cell yield was limited by decreasing pH due to lactic acid accumulation. pH-controlled fermentations were performed in 500-ml vessels with 250 or 300 ml of medium in a custom-designed pH-stat (18, 19). The mineral salts solution described above supplemented with CSL (0.5% [wt/vol]) and glucose or xylose (3% [wt/vol]) served as the growth medium. The gas phase above the culture was air. The inoculum (1% [vol/vol]) was derived from a 3- to 4-h-old culture (mid-exponential phase of growth) grown aerobically at 50°C and pH 5.0 in L broth with glucose (1% [wt/vol]). The automatic addition of 2 N KOH maintained the pH at 5.0. Samples were removed at various times for determination of cell density and fermentation products. Sugars and fermentation products were determined by using a Hewlett-Packard HPLC chromatograph (HP1090) equipped with a filter photometric detector and a refractive index detector in series (23). An Aminex HPX-87H column (Bio-Rad laboratories, Hercules, CA) was used to separate fermentation products with 4 mM H_2SO_4 as the eluent.

SSF of cellulose. SSF of crystalline cellulose was carried out in pH-controlled fermentations as described previously (19). The medium contained mineral salts, CSL (0.5% [wt/vol]), Solka Floc as crystalline cellulose (2% [wt/vol]; International Fiber Corp., North Tonawanda, NY), and different amounts of cellulase (GC220; Genencor International, Palo Alto, CA). The inoculum was derived from a pH-stat culture grown in mineral salts medium with glucose (1% [wt/vol]) and CSL (50°C, pH 5). Cells were collected by centrifugation at room temperature and resuspended in mineral salts solution at 1/10 of the original volume. These concentrated cells were used to inoculate the SSF medium at 1% (vol/vol). Fermentations were at 50°C and pH 5.0. Samples were removed at various times for determination of sugars and fermentation products by high-pressure liquid chromatography (HPLC).

^{13}C-NMR experiments. For evaluation of the metabolic pathway utilized by the three bacterial isolates during xylose fermentation, cultures were grown in LB plus xylose to mid-exponential phase in a pH-stat at pH 5.0 and 50°C. For the experiment with nongrowing cells, 40 ml of culture was centrifuged, and the cells were washed with 5.0 ml of LB at room temperature. The cells were resuspended in 4.75 ml of LB-xylose (1%) (pH 5.0). Sufficient D-[1-^{13}C]xylose (99% enrichment; Cambridge Isotope Laboratories, Andover, MA) was added to the culture to bring the xylose concentration to 1.2%, a ^{13}C enrichment of 20.8% at the xylose C-1 position. For the experiment with growing cells, cells from 0.5 ml of the mid-exponential-phase culture were removed from the pH-stat, washed with an equal volume of LB at room temperature, and resuspended in 4.75 ml of LB-xylose medium (pH 5.0). Both fermentations were carried out at 50°C with the manual addition of 1.0 N KOH to maintain the pH between 6.0 and 7.0. When acid production stopped, cells were removed by centrifugation, and the supernatant was analyzed by HPLC and ^{13}C nuclear magnetic resonance (NMR). NMR spectra were obtained by using a modified Nicolet NT300 spectrometer (2) operating in the Fourier transform mode as follows: 75.46 MHz; excitation pulse width, 25 μs; pulse repetition delay, 9 s; spectral width, 18 kHz; and 1,000 scans. [1-^{13}C]propionate (50 mM) served as an internal reference. Fermentation products were identified by comparison with known standards. *L. lactis* was grown in M17 broth with xylose (1% [wt/vol]) at pH 7.0 and 37°C in a pH-stat and fermentations were carried out in M17 broth. [1-^{13}C]xylose fermentations by *L. lactis* were at 37°C and the pH was maintained between 6.0 and 7.0 by manual addition of 1.0 N KOH.

Phylogenetic characterization. Physiological characteristics of select isolates were determined by using API 20E and 50CH test kits (bioMérieux, Inc., Durham, NC) as described by the manufacturer. Inoculated tests were incubated at 50°C and read after 24 and 48 h. Fatty acid methyl ester profile and 16S rRNA (DNA) sequences of the isolates were determined by Midi Labs (Newark, DE) according to their standard protocol. The 16S rRNA (DNA) sequence of strain P4-102B was determined as described by Suzuki and Yamasato (21) using appropriate primers. The PCR amplified product was cloned into pUC19 and sequenced by using Licor automated DNA sequencer at the Department of Microbiology and Cell Science (University of Florida) DNA sequencing facility. The 16S rRNA sequences of the three isolates were compared to *B. coagulans* sequences from the GenBank and the database at the Ribosomal Database Project (3). A phylogram was drawn with the help of Treeview (16).

Materials. Components for microbiological media were from either BBL or Difco and purchased through Fisher Scientific (Pittsburgh, PA). Analytical grade inorganic chemicals and organic chemicals were from Fisher Scientific or Sigma Chemical Co. (St. Louis, MO).

Nucleotide sequence accession numbers. The 16S rRNA (DNA) sequences were deposited in GenBank under the accession numbers DQ297925 (strain 17C5), DQ297926 (strain 36D1), DQ297927 (strain P4-102B), and DQ297928 (*B. coagulans* strain ATCC 7050).

RESULTS AND DISCUSSION

Isolation of bacteria for optimum SSF and SSCF. Using the procedures described in Materials and Methods, 380 bacterial isolates that grew in xylose mineral salts medium with 0.1% (wt/vol) yeast extract at pH 5.0 and 50°C were isolated from 77 environmental samples. A total of 270 of these isolates grew in filled tubes, suggesting anaerobic growth. This subsample of facultative anaerobes was tested for the following properties: (i) growth and cell yield in rich and mineral salts medium with either glucose or xylose at pH 5.0 and 6.8 under both aerobic and anaerobic conditions; (ii) fermentation profile; (iii) ability to grow and ferment the sugars in sugar cane bagasse hemicellulose acid hydrolysate (50% [vol/vol], with or without overliming with $Ca[OH]_2$) with CSL; (iv) ethanol tolerance (≥4% [wt/wt]); cellulolytic activity (CM-cellulose hydrolysis); (v) fermentation of cellobiose; and (vi) xylanolytic activity (RBB-xylan hydrolysis). Based on the results of these experiments, pH-controlled fermentations of glucose and xylose in mineral salts medium with CSL, as well as fermentation of overlimed sugar cane bagasse hemicellulose acid hydrolysate (50%), two isolates, strains 17C5 and 36D1, that performed better than other isolates in lactate yield from both glucose and xylose, were selected for detailed study. Although the lactate yield of strain P4-102B in hemicellulose acid hydrolysate fermentations was only ca. 65% of the other two strains, this strain was found to be transformable with plasmid DNA by electroporation and was also selected in the present study. Strain 17C5 was isolated from a soil sample adjacent to Georgia Highway 121 about a mile north of the Florida border. Strain 36D1 was isolated from a mud sample in the effluent stream of Old Faithful Geyser 1, Calistoga, CA. Strain P4-102B was obtained from a mixed soil enrichment for isolates that can grow and ferment at

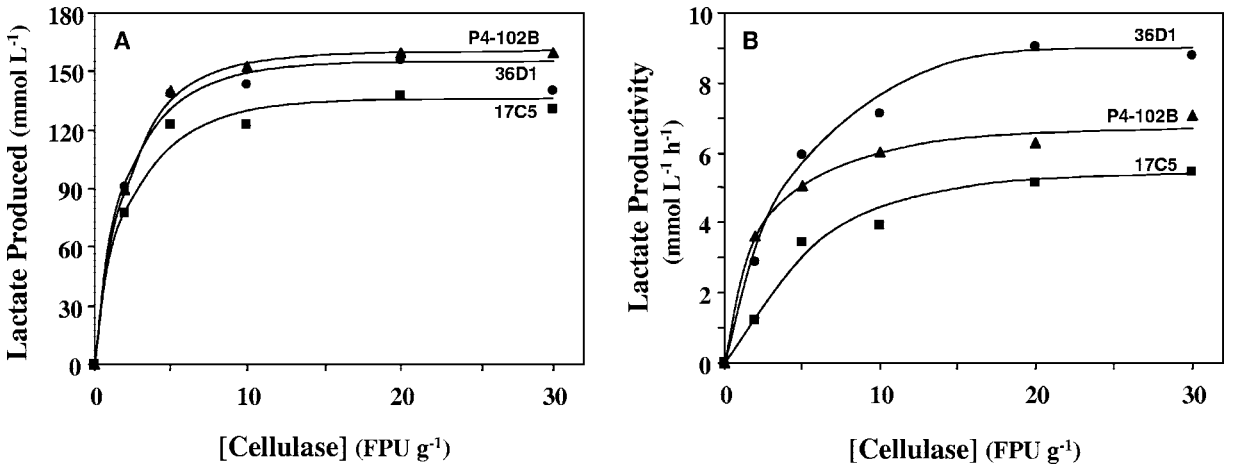

FIG. 1. SSF of crystalline cellulose (Solka Floc) by selected isolates. Crystalline cellulose (20 g/liter) was saccharified by the addition of indicated amount of cellulase (GC220; Genencor) and simultaneously fermented to lactic acid by the specific bacterial isolate (strain 17C5, 36D1, or P4-102B) at 50°C and pH 5.0. Samples were withdrawn at different times, and the amount of lactate present in the broth was determined by HPLC. From these data, the total amount of lactate produced (A) and the volumetric productivity of lactate (B) were determined. For other details, see the text.

pH 4.0 in xylose-yeast extract medium. Under aerobic conditions, the three isolates produced acetate as the primary product and, under anaerobic conditions, lactate was the primary fermentation product with small amounts of acetate, ethanol, formate, and succinate.

SSF of cellulose. Since the main objective was to isolate bacterial strains that can ferment both glucose and xylose under conditions that are optimal for fungal cellulases, the three selected isolates were evaluated for a cellulase requirement in the SSF of the crystalline cellulose, Solka Floc (Fig. 1). In a typical SSF, all three strains fermented the glucose released by cellulases to lactic acid as the major product with small amounts of acetate and ethanol. Based on total lactic acid produced (Fig. 1A), the minimal amount of cellulase required for optimum SSF was about 10 FPU per g of cellulose. Strains 36D1 and P4-102B fermented ca. 85% of glucose equivalents in cellulose in about 72 h with 10 FPU per g of cellulose, whereas strain 17C5 required about 96 h to reach a similar level. Based on the volumetric productivity (Fig. 1B), the minimal amount of cellulase required was about 15 FPU per g of cellulose. This optimum for cellulase matches the minimal requirement for cost-effective cellulose conversion (24). Strain 36D1 was the most efficient strain in SSF, while strain 17C5 was the least efficient, probably due to its low rate of glucose fermentation (Fig. 2A). This lower lactic acid productivity of strain 17C5 can be accounted for by the higher-than-expected acetate and ethanol in the broth.

Fermentation characteristics. The three selected isolates—strains 17C5, 36D1, and P4-102B—produced L(+)-lactic acid as the major fermentation product from both glucose and xylose (Fig. 2). Of these, strain 36D1 was the most efficient in converting glucose and xylose to lactic acid, with xylose being fermented more rapidly. Strain 17C5 fermented xylose at a higher rate than glucose, while the reverse was true for strain P4-102B. The primary product of glucose fermentation in all three strains was L(+)-lactic acid (ca. 95% of the fermentation products) with small amounts of acetate, ethanol, and succinate. With xylose as the carbon source, lactic acid represented 80 to 93% of the total fermentation products among the different strains. The presence of formate in the medium, as well as the higher fraction of lactic acid (>60%) in the products, suggests that the pentose phosphate pathway is the main pathway of xylose metabolism in these strains (Fig. 3) in contrast to the phosphoketolase pathway observed in other pentose utilizing lactic acid bacteria such as *Lactobacillus pentosus* and *L. lactis* (7, 22). If xylose was metabolized through the phosphoketolase pathway, the yield of lactate is not expected to be higher than 60% (Fig. 3).

The small amount of acetate and ethanol produced by the three isolates during xylose fermentation is in agreement with the presence of pyruvate formate-lyase activity.

Xylose is utilized by the pentose-phosphate pathway. In pentose-fermenting lactic acid bacteria, phosphoketolase cleaves xylulose-5-phosphate to glyceraldehyde-3-phosphate and acetylphosphate (7, 10, 22). These two intermediates are converted to 1 mol each of lactic acid and acetic acid as end products of fermentation (Fig. 3). In other organisms, such as *Escherichia coli*, the xylulose-5-phosphate enters the pentose-phosphate pathway, yielding fructose-6-phosphate and glyceraldehyde-3-phosphate (13). These compounds can be further metabolized to homolactic acid by appropriate bacteria. To establish the primary pathway for xylose metabolism in these new bacterial isolates, [^{13}C]xylose labeled at the C-1 position was used as a substrate (8, 20). [1-^{13}C]xylose metabolism by the phosphoketolase pathway is expected to yield [2-^{13}C]acetate and unlabeled lactate (Fig. 3) (8, 14). In contrast, [^{13}C]xylose metabolism by the pentose phosphate pathway would label both the C-1 and C-3 of lactate. Lactate labeled at both the C-1 and C-3 positions is expected to account for one-fifth of the total lactate, with C-3-labeled lactate accounting for another one-fifth of total lactate. The remaining three-fifths of the lactate is not expected to carry the 1-^{13}C label of xylose except for a small amount produced by the cycling of carbon through the pentose phosphate pathway (Fig. 3). Carbon cycling through the pentose-phosphate pathway would also ac-

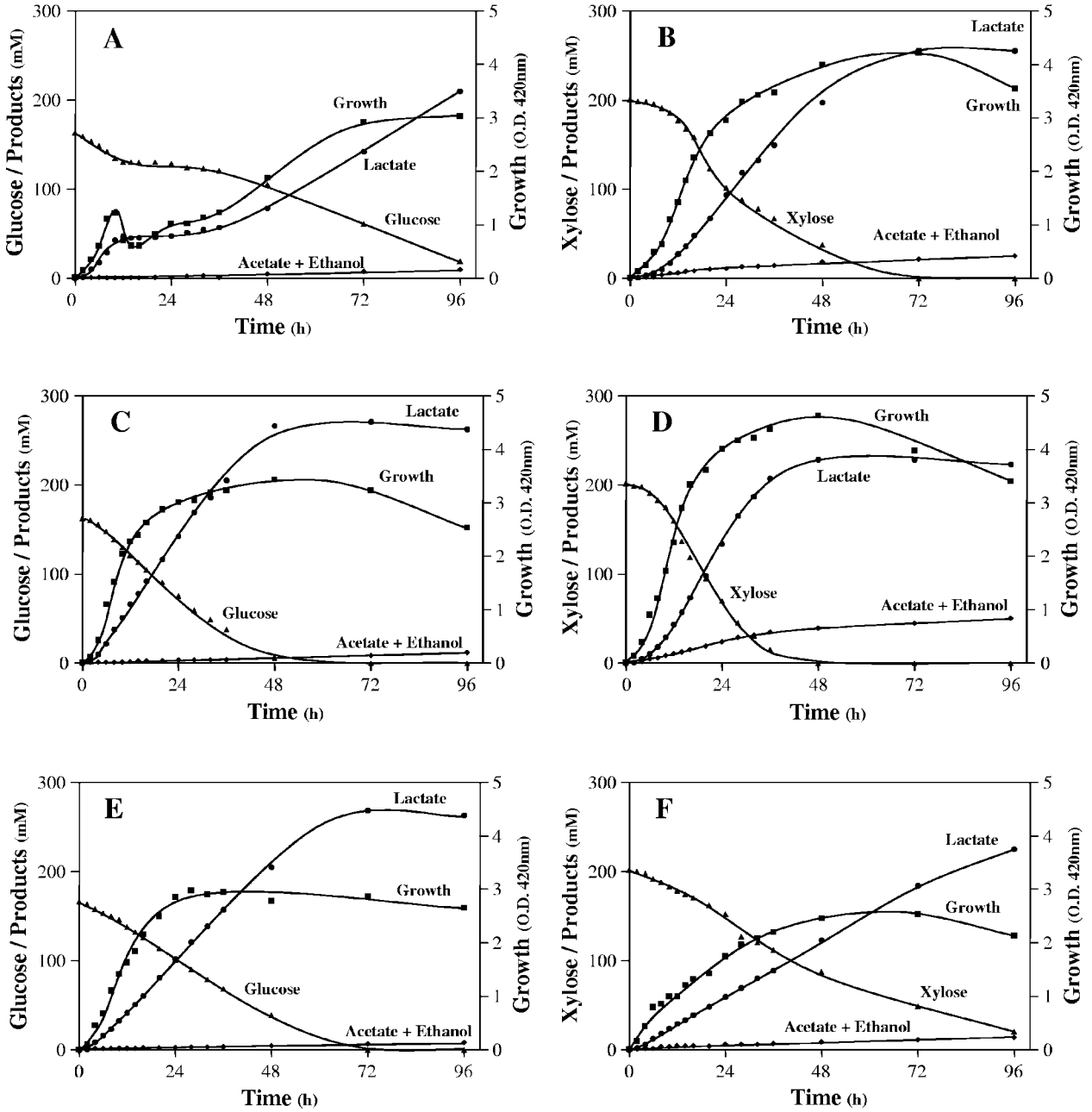

FIG. 2. Glucose and xylose fermentation by selected isolates in mineral salts medium with 3% sugar (wt/vol) and 0.5% CSL (dry wt/vol) in a pH-stat at pH 5.0 and 50°C. (A and B) Strain 17C5; (C and D) strain 36D1; (E and F) strain P4-102B. A, C, and E, glucose; B, D, and F, xylose.

count for any label in the C-2 of lactate. Enrichment of the ^{13}C label in lactate and acetate would differentiate between the two pentose utilization pathways and provide information on the primary pathway from xylose to lactic acid in this group of lactic acid bacteria.

Pyruvate formate-lyase is expected to yield [2-^{13}C]acetate from both 3-^{13}C- and 1,3-^{13}C-labeled pyruvate. Although this acetate is indistinguishable from the [2-^{13}C]acetate produced by the phosphoketolase pathway, the concentration of labeled acetate is expected to be very low in comparison with [^{13}C]lactate in an organism with pentose phosphate pathway.

Integration of the peaks in the ^{13}C-NMR spectrum of the spent medium from [1-^{13}C]xylose fermentation by strain 36D1 and comparison of the peaks to known standards revealed that 91% of the ^{13}C label from [1-^{13}C]xylose was present in lactate (Fig. 4). Acetate and ethanol accounted for the remainder. This distribution of label among the products was comparable to the product ratio as determined by HPLC. In the lactate fraction, 74% of the label was in the C-3 position. Label at the C-1 and C-2 positions of lactate was about 21 and 5%, respectively. The unexpected label at the C-2 position is apparently a result of a small amount of carbon cycling through the pentose phosphate pathway that randomized the 1-^{13}C label of xylose. In both acetate and ethanol, almost all of the label was found

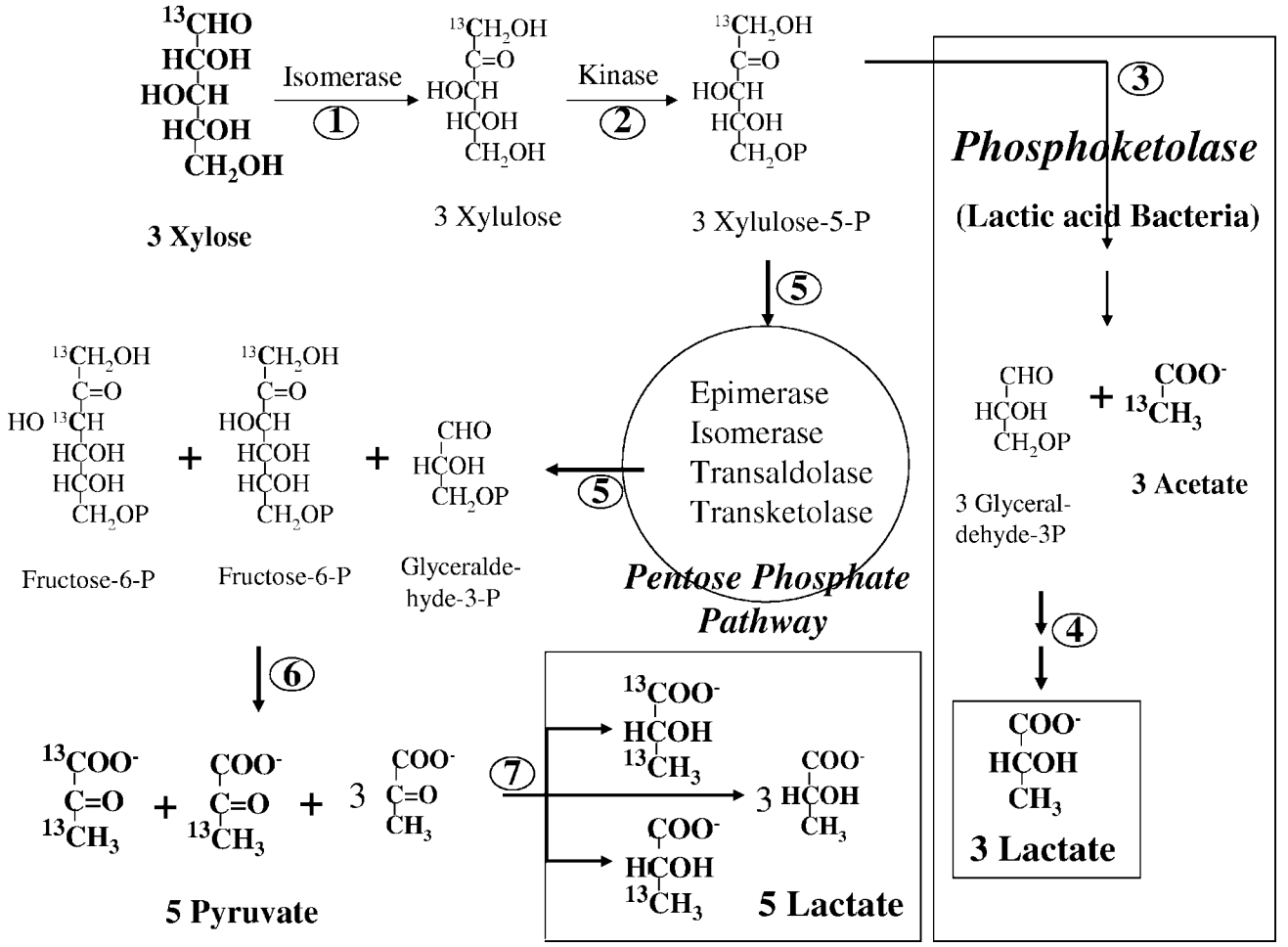

FIG. 3. Predicted flow of [1-^{13}C]xylose tracer into the metabolic products of xylose fermentation either by the pentose-phosphate pathway or phosphoketolase pathway. Numbers represent the corresponding enzymes that catalyze the particular step as follows: 1, xylose isomerase; 2, xylulose kinase; 3, phosphoketolase (phosphoketolase produces glyceraldehyde-3-phosphate and acetyl phosphate that is converted to acetate and ATP by acetate kinase with ADP); 4, enzymes of glycolysis (glyceraldehyde-3-phosphate dehydrogenase, phosphoglycerokinase, enolase, pyruvate kinase, and lactate dehydrogenase); 5, enzymes of the pentose phosphate pathway (phosphopentose epimerase, phosphopentose isomerase, transketolase, and transaldolase); 6, same enzymes as step 4 with phosphofructokinase, aldolase, and triose phosphate isomerase; 7, lactate dehydrogenase.

at the C-2 position, as expected. Although the presence of label in acetate may suggest that a fraction of the xylose is metabolized by the phosphoketolase pathway, it is unlikely due to the presence of formate and ethanol among the fermentation products.

Taking the amount of label in the C-2 of lactate as 1 to account for the randomization of carbon due to cycling, an enrichment at the other two positions was calculated (Table 1). The enrichment ratio at C-1 of lactate was about 5.0 for all three strains (17C5, 36D1, and P4-102B). Enrichment at the C-3 position was about 15 for the three strains.

L. lactis subsp. *lactis* NRRL B-4449 is a xylose-utilizing lactic acid bacterium and, as with other lactic acid bacteria, utilizes the phosphoketolase pathway for xylose metabolism (6). In the [1-^{13}C]xylose fermentation, ^{13}C label enrichment at the C-2 position of acetate was about 230 (compared to C-1 of acetate) in contrast to less than 15 at C-2 of acetate in the three *Bacillus* strains (Fig. 4 and Table 1). The *E. coli* W3110 xylose fermentation profile is also included in this table for comparison since this bacterium, lacking phosphoketolase, ferments xylose through the pentose phosphate pathway.

These results show that the pentose phosphate pathway is the main metabolic pathway for xylose utilization in these new isolates. This is in agreement with the xylose fermentation profile of these bacteria (Fig. 2). Since these bacteria are effective in SSF of cellulose to lactate in mineral salts medium with 0.5% (wt/vol) of CSL (Fig. 1), as well as in hemicellulose acid hydrolysate medium (18, 19), the taxonomic positions of these isolates were determined by using the fatty acid profile and 16S rRNA (DNA) sequence.

Taxonomic characterization. Strains 36D1 and P4-102B had similar fatty acid methyl ester (FAME) profiles that were comparable, with minor variations, to that of *Bacillus coagulans* strain 7050 (4), an ATCC type strain. Strain 17C5 differed from the other two by the presence of higher iso-$C_{15:0}$ and lower anteiso-$C_{15:0}$, iso-$C_{16:0}$, $C_{16:0}$, and anteios-$C_{17:0}$. Fatty acid lev-

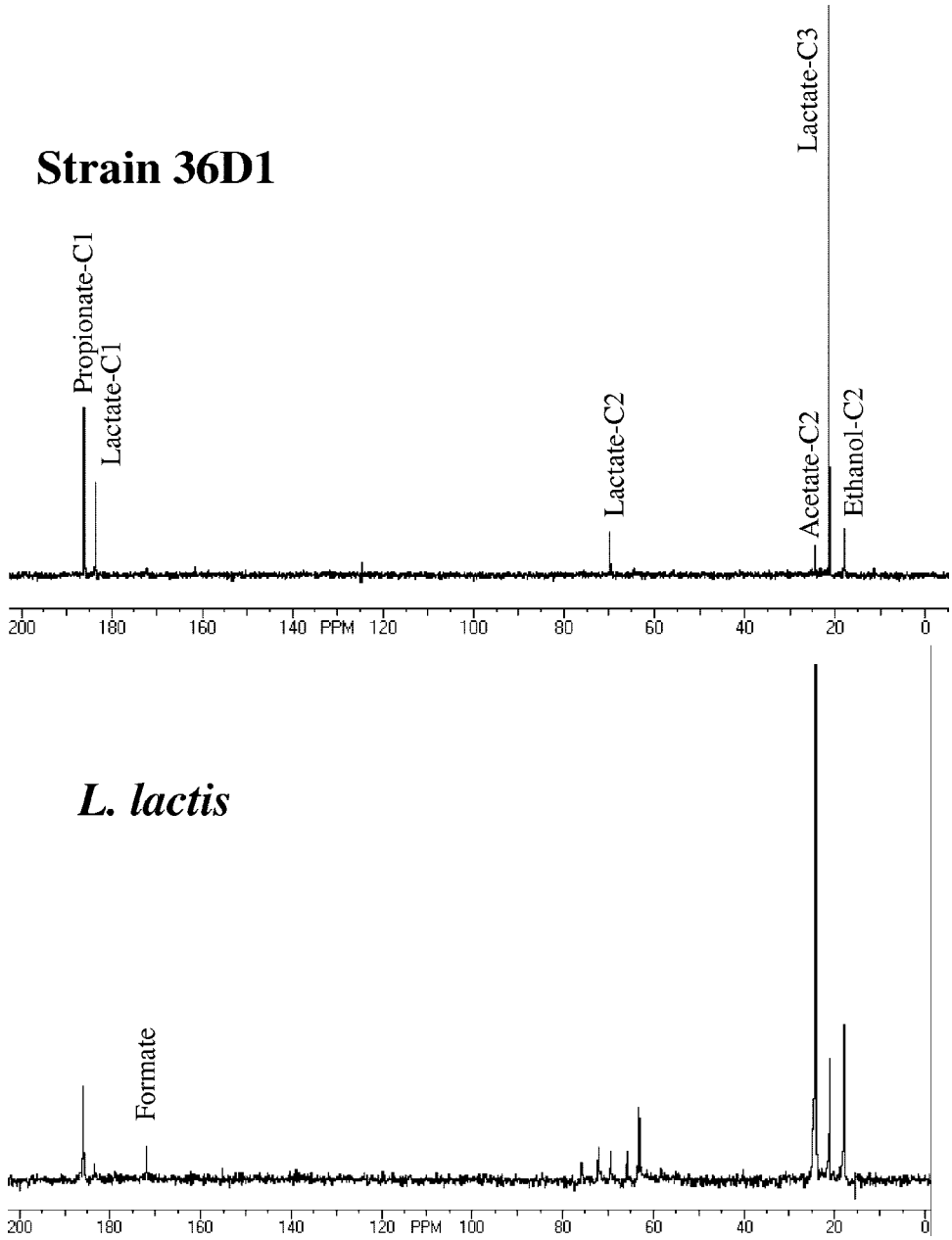

FIG. 4. ^{13}C-NMR spectrum of spent medium of strain 36D1 and *L. lactis* NRRL B-4449. Strain 36D1 was grown in LB plus [1-^{13}C]xylose at 50°C. *L. lactis* was grown in M17 broth with [1-^{13}C]xylose at 37°C. [1-^{13}C]propionate (50 mM) served as a standard and reference. See Materials and Methods for details.

els of strain 17C5 also differed from the observed composition of strains 36D1, P4-102B, and *B. coagulans* 7050 (data not presented). Based on the fatty acid profiles, isolates 36D1 and P4-102B can be grouped with *B. coagulans*. Since *B. coagulans* is a very diverse group (4, 21), strain 17C5 is also included in this group.

Identification of the three isolates as *B. coagulans* is also supported by the 16S rRNA (DNA) sequence-based phylogenetic analysis. In the phylogram (Fig. 5), the three strains (17C5, 36D1, and P4-102B) cluster together, indicating the closeness of the isolates to each other. The three isolates also comprise a larger group that includes a *B. coagulans* ATCC type strain, 7050, and two other strains identified as *B. coagulans* strains IDSp and LMG12346. Based on the comparison of the 16S rRNA (DNA) sequence, *B. coagulans* type strain ATCC 7050 from three different culture collections—IAM12463, JCM2257, and NCDO1761—clusters away from the present isolates, as well as from the sequence of strain ATCC 7050 obtained recently. Although strains 17C5, 36D1, and P4-102B are separated from other type strains and other bacilli identified as *B. coagulans*, a continuum exists among the various *B. coagulans* strains analyzed in the present study. This diversity within *B. coagulans* has been recognized by others (4, 21). Due to the heterogeneity of this species, as well as in the same isolate

TABLE 1. ^{13}C enrichment ratios of fermentation products produced from [1-^{13}C]xylose[a]

Product	Carbon position	Isotope enrichment ratio				
		17C5	36D1	P4-102B	*L. lactis*	*E. coli* W3110
Lactate	C-1	5.5	4.6	5.7	2.5	11.0
	C-2	1.0	1.0	1.0	1.0	1.0
	C-3	15.1	15.8	12.6	7.7	11.1
Acetate	C-1	1.0	1.0	1.0	1.0	1.0
	C-2	15.0*	10.7*	5.5*	234.7*	4.6
Ethanol	C-1	1.0	1.0	1.0	1.0	1.0
	C-2	32.3*	36.7*	13.6	17.0	5.8

[a] Distribution of [1-^{13}C]xylose label in fermentation products of various bacteria was determined as described in the text. All enrichment ratios were based on the abundance of ^{13}C at the indicated positions with C-2 of lactate or C-1 of acetate and ethanol as reference. An asterisk indicates that the C-1 carbons of acetic acid and ethanol were not labeled or the amount of label at the C-1 position was below the detection limit. The presented values were computed using 0.5 mM at these positions as the minimal sensitivity of the instrument for ^{13}C.

from different culture collections, we have identified all of the three strains isolated in the present study as *B. coagulans*.

B. coagulans is a facultative, slightly acidophilic, moderately thermophilic bacterium originally isolated from spoiled milk (9), and the members of this species constitute a very heterogeneous group (4). Although strains 17C5, 36D1, and P4-102B are closely related to *B. coagulans* strain 7050 based on their FAME profiles and 16S rRNA (DNA) sequence analyses, significant differences in the physiological properties of the three isolates and that of the ATCC type strain 7050 can be detected. The most striking and relevant difference between strain 7050 and the three present isolates is the inability of strain 7050 to utilize xylose either aerobically or anaerobically. Although De Clerck et al. (4) reported that xylose utilization by strain 7050 is variable, in several attempts in our laboratory xylose failed to support growth of or fermentation by strain 7050. Since xylose is one of two major components of biomass, its utilization by the three new isolates elevates them to potential use as organisms for biomass conversion to products. Minor differences among the three isolates and the emended description of *B. coagulans* (4) are also readily identifiable. For example, De Clerck et al. described that the optimum pH for growth of *B. coagulans* as 7.0 (4). The three isolates described in here had a very broad optimum pH for growth, between 4.5 and 6.0, and growth at pH 7.0 was poor (19).

Summary. Three unique members of *B. coagulans* have been described that can ferment both hexoses and pentoses to lactic acid at pH 5.0 and 50°C, conditions that are also optimal for fungal cellulases during SSF processes. These strains utilize the pentose-phosphate pathway for the fermentation of pentose sugars, facilitating the near-complete conversion of the pentose sugars such as xylose and arabinose (in addition to glucose) into optically pure L(+)-lactic acid.

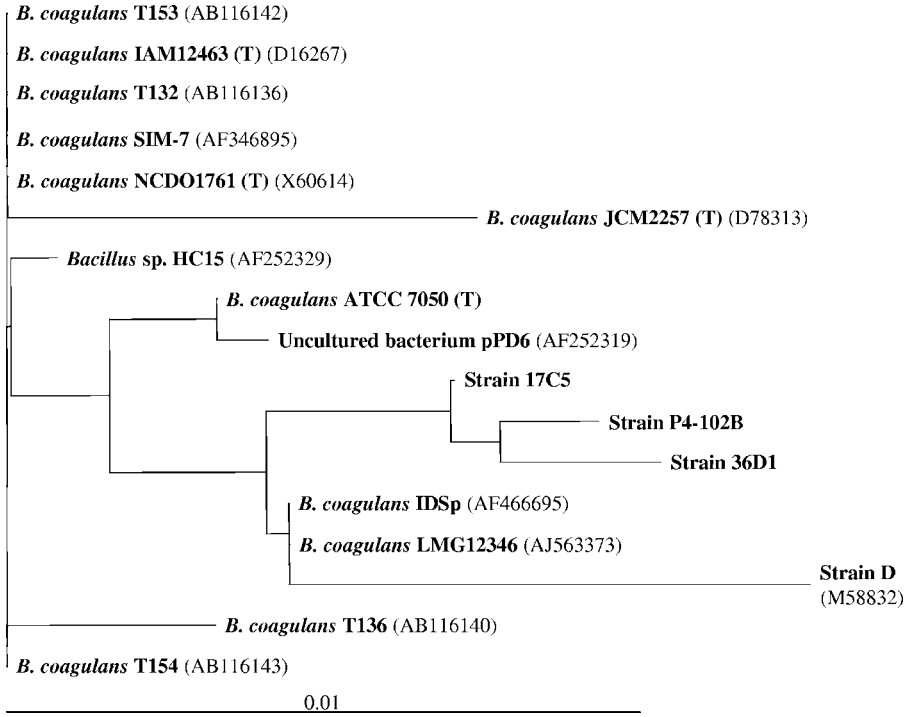

FIG. 5. Phylogenetic relationship of various isolates from the present study and other known *B. coagulans* strains based on their 16S rRNA sequence. Numbers in parentheses represent the GenBank accession numbers for the respective sequences. Strains marked with "(T)" represent a type strain in that specific collection, and all are equivalent to ATCC 7050 originally isolated by Hammer (9). Strain collections: IAM, Institute of Applied Microbiology, Japan; NCDO, National Collection of Dairy Organisms, now incorporated into National Collection of Industrial Food and Marine Bacteria, Scotland, United Kingdom; JCM, Japan Collection of Microorganisms, Japan; ATCC, American Type Culture Collection. The scale represents 1% divergence between sequences.

ACKNOWLEDGMENTS

We thank A. P. Rooney, USDA-ARS, for providing the *L. lactis* strain and M. Moniruzzaman, Genencor, for the cellulase preparation used in this study.

This study was supported by funds from the U.S. Department of Energy (DE-FC36-01GO11073, DE-FG36-04GO14019, and DEFG02-96ER20222), the U.S. Department of Agriculture (00-52104-9704 and 01-35504-10669), and the State of Florida, University of Florida Agricultural Experiment Station.

REFERENCES

1. **Aden, A., M. Ruth, K. Ibsen, J. Jechura, K. Neeves, J. Sheehan, B. Wallace, L. Montague, A. Slayton, and J. Lukas.** 2002. Lignocellulosic biomass to ethanol process design and economics utilizing co-current dilute acid prehydrolysis and enzymatic hydrolysis for corn stover. NREL/TP-510-32438. National Renewable Energy Laboratory, Golden, Colo. [Online.] http://www.nrel.gov/docs/fy02osti/32438.pdf.
2. **Buszko, M. L., D. Buszko, and D. C. Wang.** 1998. Internet technology in magnetic resonance: a common gateway interface program for the world-wide web NMR spectrometer. J. Magn. Reson. **131:**362–366.
3. **Cole, J. R., B. Chai, T. L. Marsh, R. J. Farris, Q. Wang, S. A. Kulam, S. Chandra, D. M. McGarrell, T. M. Schmidt, G. M. Garrity, and J. M. Tiedje.** 2003. The Ribosomal Database Project (RDP-II): previewing a new autoaligner that allows regular updates and the new prokaryotic taxonomy. Nucleic Acids Res. **31:**442–443.
4. **De Clerck, E., M. Rodriguez-Diaz, G. Forsyth, L. Lebbe, N. A. Logan, and P. DeVos.** 2004. Polyphasic characterization of *Bacillus coagulans* strains, illustrating heterogeneity within this species, and emended description of the species. Syst. Appl. Microbiol. **27:**50–60.
5. **Duff, S. J. B., and W. D. Murray.** 1996. Bioconversion of forest products industry waste cellulosics to fuel ethanol: a review. Bioresource Technol. **55:**1–33.
6. **Erlandson, K. A., J. H. Park, W. E. Khal, H. H. Kao, P. Basaran, S. Brydges, and C. A. Batt.** 2002. Dissolution of xylose metabolism in *Lactococcus lactis.* Appl. Environ. Microbiol. **66:**3974–3980.
7. **Garde, A., G. Jonsson, A. S. Schmidt, and B. K. Ahring.** 2002. Lactic acid production from wheat straw hemicellulose hydrolysate by *Lactobacillus pentosus* and *Lactobacillus brevis.* Bioresource Technol. **81:**217–223.
8. **Gunsalus, I. C., B. L. Horecker, and W. A. Wood.** 1955. Pathways of carbohydrate metabolism in microorganisms. Bacteriol. Rev. **19:**79–128.
9. **Hammer, B. W.** 1915. Bacteriological studies on the coagulation of evaporated milk. Iowa Agric. Exp. Station Res. Bull. **19:**119–131.
10. **Hofvendahl, K., and B. Hans-Hagerdal.** 2000. Factors affecting the fermentative lactic acid production from renewable resources. Enz. Microb. Technol. **26:**87–107.
11. **Kheshgi, H. S., R. C. Prince, and G. Marland.** 2000. The potential of biomass fuels in the context of global climate change: focus on transportation fuels. Annu. Rev. Energy Environ. **25:**199–244.
12. **Lee, J. H., P. Patel, P. Sankar, and K. T. Shanmugam.** 1985. Isolation and characterization of mutant strains of *Escherichia coli* altered in H_2 metabolism. J. Bacteriol. **162:**344–352.
13. **Lin, E. C. C.** 1996. Dissimilatory pathways for sugars, polyols, and carboxylates, p. 307–342. *In* F. C. Neidhardt, R. Curtiss III, J. L. Ingraham, E. C. C. Lin, K. B. Low, B. Magasanik, W. S. Reznikoff, M. Riley, M. Schaechter, and H. E. Umbarger (ed.), *Escherichia coli* and *Salmonella*: cellular and molecular biology, 2nd ed. ASM Press, Washington, D.C.
14. **Lokman, B. C., P. van Santen, J. C. Verdoes, J. Kruse, R. J. Leer, M. Posno, and P. H. Pouwels.** 1991. Organization and characterization of three genes involved in D-xylose catabolism in *Lactobacillus pentosus.* Mol. Gen. Genet. **230:**161–169.
15. **Lynd, L. R., C. E. Wyman, and T. U. Gerngross.** 1999. Biocommodity engineering. Biotechnol. Prog. **15:**777–793.
16. **Page, R. D. M.** 1996. TREEVIEW: an application to display phylogenetic trees on personal computers. Comput. Appl. Biosci. **12:**357–358.
17. **Parajo, J. C., J. L. Alonso, and V. Santos.** 1996. Lactic acid from wood. Process Biochem. **31:**271–280.
18. **Patel, M., M. Ou, L. O. Ingram, and K. T. Shanmugam.** 2004. Fermentation of sugar cane bagasse hemicellulose hydrolysate to L(+)-lactic acid by a thermotolerant acidophilic *Bacillus* sp. Biotechnol. Lett. **26:**865–868.
19. **Patel, M. A., M. Ou, L. O. Ingram, and K. T. Shanmugam.** 2005. Simultaneous saccharification and co-fermentation of crystalline cellulose and sugar cane bagasse hemicellulose hydrolysate to lactate by a thermotolerant acidophilic *Bacillus* sp. Biotechnol. Prog. **21:**1453–1460.
20. **Scott, A. I., and R. L. Baxter.** 1981. Applications of ^{13}C NMR to metabolic studies. Annu. Rev. Biophys. Bioeng. **10:**151–174.
21. **Suzuki, T., and K. Yamasato.** 1994. Phylogeny of spore-forming lactic acid bacteria based on 16S rRNA gene sequences. FEMS Microbiol. Lett. **115:**13–18.
22. **Tanaka, K., A. Komiyama, K. Sonomoto, A. Ishizaki, S. J. Hall, and P. E. Stanbury.** 2002. Two different pathways for D-xylose metabolism and the effect of xylose concentration on the yield coefficient of L-lactate in mixed-acid fermentation by the lactic acid bacterium *Lactococcus lactis* IO-1. Appl. Microbiol. Biotechnol. **60:**160–167.
23. **Underwood, S. A., S. Zhou, T. B. Causey, L. P. Yomano, K. T. Shanmugam, and L. O. Ingram.** 2002. Genetic changes to optimize carbon partitioning between ethanol and biosynthesis in ethanologenic *Escherichia coli.* Appl. Environ. Microbiol. **68:**6263–6272.
24. **Wooley, R., M. Ruth, D. Glassner, and J. Sheehan.** 1999. Process design and costing of bioethanol technology: a tool for determining the status and direction of research and development. Biotechnol. Prog. **15:**794–803.
25. **Wyman, C. E.** 2003. Potential synergies and challenges in refining cellulosic biomass to fuels, chemicals, and power. Biotechnol. Prog. **19:**254–262.
26. **Zaldivar, J., J. Nielsen, and L. Olsson.** 2001. Fuel ethanol production from lignocellulose: a challenge for metabolic engineering and process integration. Appl. Microbiol. Biotechnol. **56:**17–34.
27. **Zhou, S., F. C. Davis, and L. O. Ingram.** 2001. Gene integration and expression and extracellular secretion of *Erwinia chrysanthemi* endoglucanase CelY (*celY*) and CelZ (*celZ*) in ethanologenic *Klebsiella oxytoca* P2. Appl. Environ. Microbiol. **67:**6–14.

Appendix B

Simultaneous Saccharification and Co-Fermentation of Crystalline Cellulose and Sugar Cane Bagasse Hemicellulose Hydrolysate to Lactate by a Thermotolerant Acidophilic *Bacillus* sp.†

Milind A. Patel,‡ Mark S. Ou, Lonnie O. Ingram, and K. T. Shanmugam*

Department of Microbiology and Cell Science, University of Florida, Gainesville, Florida 32611

Polylactides produced from renewable feedstocks, such as corn starch, are being developed as alternatives to plastics derived from petroleum. In addition to corn, other less expensive biomass resources can be readily converted to component sugars (glucose, xylose, etc.) by enzyme and/or chemical treatment for fermentation to optically pure lactic acid to reduce the cost of lactic acid. Lactic acid bacteria used by the industry lack the ability to ferment pentoses (hemicellulose-derived xylose and arabinose), and their growth and fermentation optima also differ from the optimal conditions for the activity of fungal cellulases required for depolymerization of cellulose. To reduce the overall cost of simultaneous saccharification and fermentation (SSF) of cellulose, we have isolated bacterial biocatalysts that can grow and ferment all sugars in the biomass at conditions that are also optimal for fungal cellulases. SSF of Solka Floc cellulose by one such isolate, *Bacillus* sp. strain 36D1, yielded L(+)-lactic acid at an optical purity higher than 95% with cellulase (Spezyme CE; Genencor International) added at about 10 FPU/g cellulose, with a product yield of about 90% of the expected maximum. Volumetric productivity of SSF to lactic acid was optimal between culture pH values of 4.5 and 5.5 at 50 °C. At a constant pH of 5.0, volumetric productivity of lactic acid was maximal at 55 °C. Strain 36D1 also co-fermented cellulose-derived glucose and sugar cane bagasse hemicellulose-derived xylose simultaneously (SSCF). In a batch SSCF of 40% acid-treated hemicellulose hydrolysate (over-limed) and 20 g/L Solka Floc cellulose, strain 36D1 produced about 35 g/L lactic acid in about 144 h with 15 FPU of Spezyme CE/g cellulose. The maximum volumetric productivity of lactic acid in this SSCF was 6.7 mmol/L (h). Cellulose-derived lactic acid contributed to about 30% of this total lactic acid. These results show that *Bacillus* sp. strain 36D1 is well-suited for simultaneous saccharification and co-fermentation of all of the biomass-derived sugars to lactic acid.

Introduction

The finite nature of fossil resources has focused attention on expanding bioplastics production using renewable resources. Approximately 107 billion pounds of plastics were produced from petroleum in North America during 2003 (*1*). Worldwide, less than 1% of this amount was produced from renewable, biobased feedstocks. Optically pure lactic acid can be readily produced from starch (glucose) by lactic acid bacteria and subsequently converted into biodegradable, polylactide plastics (*2*−*6*). However, large-scale production of polylactides from starch as a primary replacement for petroleum-based plastics will compete with existing food and feed uses, potentially increasing the cost of raw materials. Other carbohydrate sources such as lignocellulosic biomass (cellulose and hemicellulose) offer the potential to replace starch as a renewable feedstock with minimal impact on other markets (*7*−*9*).

Pretreatment of biomass at low acid concentrations can be used to hydrolyze hemicellulose into monomeric sugars while yielding cellulose-rich residual solids that are readily hydrolyzed by fungal cellulases (*10*−*12*). With appropriate biocatalysts, cellulose can be simultaneously fermented to lactate during enzymatic saccharification, the SSF process (*9*, *13*). For an effective SSF process, both the biocatalyst and the fungal cellulases should function optimally under the same conditions. Since fungal cellulases are one of the significant cost factors in fermentation of biomass-derived cellulose (*12*, *14*−*16*), biocatalysts are needed that grow and ferment optimally in inexpensive media under conditions that are optimal for cellulase activity.

Lactic acid bacteria currently used by industry for lactic acid production require complex media and also lack the ability to grow and ferment at pH 5.0 and 50 °C (*9*, *17*−*19*), conditions that are optimal for fungal cellulase activity. Few if any of these biocatalysts are able to efficiently ferment pentose sugars, a main constituent of hemicelluloses. Recently, we have described *E. coli* strains that produce either D(−)- or L(+)-lactate as the sole fermentation product in mineral salts medium and are able to utilize all hexose and pentose sugars in biomass at a pH close to the optimum for fungal cellulase

* To whom correspondence should be addressed. Ph: 352-392-2490. Fax: 352-392-5922. E-mail: shan@ufl.edu.

† Florida Agricultural Experiment Station Journal Series No. R-10967.

‡ Present address: Argonne National Laboratory, Argonne, IL 60439.

10.1021/bp0400339 CCC: $30.25
Published on Web 08/12/2005

Table 1. Fermentation Profile of *Bacillus* sp. Strain 36D1 at pH 5.0 and 50°C[a]

medium	cell mass[b] (g/L)	sugar utilized (mM)	fermentation products (mM)					sugar consumption (mmol/ h·L)	specifiic sugar consumption rate (mmol/ h·g)	volumetric productivity (mmol/ h·L) (lactate)	specific productivity (mmol/ h·g) (lactate)	yield (%)[c]	
			lactate	acetate	ethanol	formate	succinate					lactate	total[d]
glucose													
LB	1.4	169.3	278.6	4.9	5.1	0.0	0.5	5.9	27.1	9.6	44.5	82.3	85.4
MM	1.3	162.5	271.1	5.9	6.4	0.0	0.4	3.8	18.0	6.2	29.8	83.4	87.3
xylose													
LB	1.5	203.1	240.8	11.2	24.2	4.6	0.8	4.9	14.5	5.6	16.6	71.1	81.8
MM	1.8	201.8	228.7	16.6	34.9	4.3	4.3	6.2	11.9	6.8	13.0	68.0	84.6

[a] Cultures were grown in a pH-stat in either rich medium (LB) or mineral salts medium with corn steep liquor (0.5%) (MM) and 30 g/L glucose or xylose. Values are from the end of experiments at 96 h. Reported rates are the highest values determined. [b] Cell mass represents the final dry cell density of the culture. [c] Yield was calculated on an expected molar basis (glucose to 2 pyruvates; xylose to 1.67 pyruvates based on the pentose phosphate pathway). [d] Since all fermentation products are derived from pyruvate or phosphoenol pyruvate and acetate/ethanol represent the amount of pyruvate converted to these products with formate as a byproduct, total molar product yield was calculated by dividing the sum of lactate, ethanol, acetate, and succinate by the amount of sugar consumed.

(*20*, *21*). However, these strains grow poorly above 42 °C. More recently, we have isolated thermotolerant strains of *Bacillus* from nature that grow well at pH 5 and 50 °C and have a homolactate pathway for both hexose and pentose sugars. One of these strains was very effective for converting hemicellulose syrups from sugar cane bagasse into lactate in a mineral salts medium supplemented with small amounts of corn steep liquor (CSL) (*22*).

In this paper, we describe the use of *Bacillus* sp. strain 36D1 as a biocatalyst for lactic acid production via SSF in which sugars derived from both hemicellulose and cellulose are fermented in a single vessel.

Materials and Methods

Organism, Media, and Culture Conditions. *Bacillus* sp. strain 36D1 was isolated from Old Faithful Geyser, Calistoga, CA. Details of isolation, physiological properties, and taxonomy of strain 36D1 will be presented elsewhere. Strain 36D1 was routinely cultured in L broth (*23*) with 1.0% glucose. Mineral salts medium supplemented with 0.5% dry weight CSL (Grain Processing Corp., Muscatine, IA) (MS-CSL) was used in all fermentations as described previously (*22*).

Fermentations. Fermentations were carried out in custom-made fermenters with pH and temperature control as described previously (*22*, *24*). Fermentation culture volume was 250 mL in a 500-mL vessel; pH was maintained by addition of 2.0 N KOH. Inocula for fermentations were grown in glucose (1.5%)−MS-CSL medium (pH of 5.0, 50 °C, approximately 14 h). Cells were harvested at a cell density of 1 g/L dry weight, washed once with minimal medium, and used to inoculate SSF at an initial cell density of 50 mg/L dry weight. Samples were removed periodically for measurements of growth, sugars, and fermentation products.

Sugar cane acid hydrolysate was prepared using dilute acid hydrolysis by BC International (Dedham, MA) and treated with lime as described previously (*25*). The sugar content of the lime-treated hydrolysate was 81.3 g/L (xylose, 68.6 g/L; glucose, 11.5 g/L; arabinose, 1.2 g/L). Lime-treated hydrolysate was adjusted to pH 5.0 and used in the fermentations with Solka Floc (20 g/L) in mineral salts medium supplemented with 0.25% CSL (dry weight).

Analytical Methods. Sugars and fermentation products were measured by HPLC using a HP1090 liquid chromatograph (Hewlett-Packard) equipped with a Bio-Rad Aminex HPX87-H column (Bio-Rad Laboratories, Hercules, CA) and dual detectors (filter photometric and refractive index detectors in series) as described previously (*26*). Optical purity of lactic acid was determined as described previously (*22*).

Cellulase (Spezyme CE) activity at different temperature and pH was determined in the same mineral salts medium used for fermentations but without corn steep liquor. Tubes containing 0.2 g Solka Floc (5 mL total reaction volume) were incubated for 10 min at the indicated temperature before the addition 10 FPU of Spezyme CE. Samples (1 mL) were removed at different times (0−30 min) and immediately acidified with 4 μL of 1.0 M H_2SO_4 to stop the reaction. After centrifugation (12,000 × *g*; room temperature), samples were filtered through a 0.2-μm filter (Fisher Scientific, Pittsburgh, PA) and analyzed for cellobiose and glucose by HPLC (*26*). Under these conditions, glucose and cellobiose production was linear during the first 20 min. Activity was calculated from the linear phase between 5 and 15 min. The specific hydrolytic activity of Spezyme was expressed as μmol/min (mg protein) of combined glucose and cellobiose.

Materials. Solka Floc (International Fiber Corporation, N. Tonawanda, NY) and sugar cane bagasse hemicellulose acid hydrolysate were generously provided by BC International (Dedham, MA). The moisture content of Solka Floc was determined to be 7.4%. Spezyme CE was kindly provided by Genencor Intl. (Palo Alto, CA). Organic and inorganic chemicals were obtained from Fisher Scientific.

Results and Discussion

Isolation of New Biocatalysts. Optimum conditions for the activity of cellulases from *Trichoderma reesei* and other fungi were reported to be near pH 5.0 and 50 °C (*14*, *27*, *28*). Under these conditions, *Bacillus* sp. strain 36D1 grew well in both rich medium and mineral salts medium supplemented only with 0.5% CSL (dry weight) (MS-CSL). During fermentation, glucose was converted into L(+)-lactate with small amounts of acetate, ethanol, and succinate as coproducts in both media (Table 1). Lactate accounted for over 95% of the total fermentation products from glucose. In contrast to many other lactic acid bacteria (*18*), strain 36D1 also fermented xylose, the predominant sugar in hemicellulose from most plants. Again, L(+)-lactate was the main product (80−87% of total fermentation products) with smaller amounts of acetate, ethanol, formate, and succinate. Xylose-grown cultures produced 2-fold higher levels of acetate and about 5-fold higher amount of ethanol (and formate) than glucose-grown cultures. The presence of formate suggests that pyruvate formate lyase activity is responsible for some of the acetate and ethanol produced from xylose.

The specific and volumetric rates of glucose utilization by strain 36D1 were higher during growth in rich

medium (L broth) than in MS-CSL medium (Table 1). The difference between results in L broth and MS-CSL medium was also reflected in the specific productivity of lactate by the glucose-grown cultures. The specific productivity of lactate was higher in glucose fermentation compared to xylose fermentation, irrespective of the growth medium. Apparently, glucose flux during glycolysis is higher than xylose flux in strain 36D1. Xylose flux is also lower than glucose flux in ethanologenic *E. coli* (*29*, *30*). In *E. coli* and other related bacteria, xylose is transported by an ATP-dependent ABC-type transporter or a xylose/H^+ symport and further metabolized through the pentose-phosphate pathway to fructose-6-phosphate and glyceraldehyde-3-phosphate (*31*, *32*). In Gram-positive bacteria, such as *Bacillus megaterium* and pentose-utilizing *Lactobacillus*, genes encoding xylose/H^+ symport as well as xylose isomerase and xylulose kinase are linked (*33*, *34*). It is possible that xylose/H^+ symport, xylose isomerase, and xylulose kinase all contribute to flux control for xylose metabolism in *Bacillus* sp. strain 36D1.

Although the xylose flux in strain 36D1 was lower than the glucose flux, the final cell density of strain 36D1 was slightly higher in xylose-minimal medium compared to glucose-minimal medium (Table 1). This slight increase in cell mass apparently compensated for the lower xylose flux, and the volumetric productivity of lactate in xylose-minimal medium was comparable to that in glucose-minimal medium. Production of formate as a fermentation product along with acetate and ethanol suggests that growth on xylose in MS-CSL medium is accompanied by induction of pyruvate formate-lyase (PFL) as seen with other Gram-positive bacteria, *Lactococcus lactis* and *Enterococcus* grown in limiting C-sources or poor C-sources, such as galactose (*35*, *36*). Conversion of pyruvate to acetate and ethanol by the coupled action of PFL, phosphotransacetylase, and acetate kinase is expected to yield an additional ATP, supporting the higher growth rate, higher cell yield, and the corresponding higher volumetric productivity.

Simultaneous Saccharification and Fermentation. *Trichoderma reesei* cellulases are being commercially developed for cost-effective saccharification of cellulose as a feedstock for fermentation into fuels and chemicals (*16*, *37*, *38*). Because the fungal cellulases are inhibited by both cellobiose and glucose (*39*), products of cellulase activity, the SSF process was proposed in order to rapidly remove these sugars and maintain high rates of enzymatic activity (*40*, *41*).

Addition of 15 FPU Spezyme CE per gram of Solka Floc to a freshly inoculated culture of strain 36D1 in a medium containing cellulose, mineral salts, and CSL (0.5% dry weight) at pH 5.0 and 50 °C led to rapid accumulation of lactate (Figure 1). At 2 h of SSF, when the cell density is expected to be low, 3.2 mM cellobiose and 5.5 mM glucose were detected in the broth (data not presented). After about 6 h, the concentrations of both sugars in the medium started to decline and by about 10−12 h, when the bacterial culture was expected to reach the stationary phase of growth, neither sugar was detected in the culture medium. About 90% of the sugar equivalents in 20 g/L Solka Floc were fermented within 48 h while lactate production reached a maximum of 140 mM by about 72 h (Figure 1). Lactate (140 mM; 12.6 g/L) represented 80% of the total products with lesser amounts of acetate (14 mM), ethanol (22 mM), formate (15 mM), and succinate (2 mM). The lactate produced was the L-(+) isomer, with an optical purity of 96%. About 10% of the cellulose originally present was recalcitrant to hydrolysis by Spezyme CE during the 96-h SSF process despite the retention of cellulase activity (not shown).

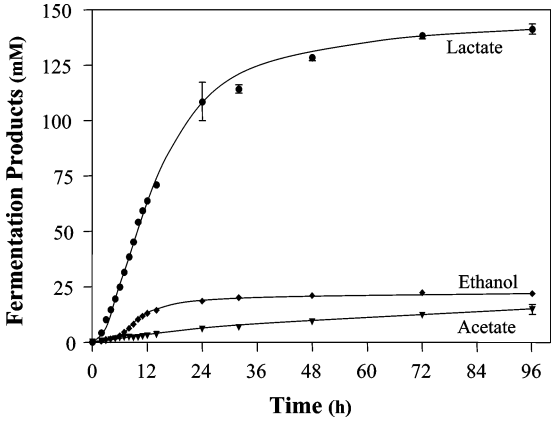

Figure 1. Simultaneous saccharification and fermentation of cellulose by *Bacillus* sp. strain 36D1. The SSF contained 20 g/L Solka Floc in MS-CSL medium and Spezyme CE (15 FPU/g cellulose) added at the beginning of fermentation at 50 °C and pH 5.0. The results are the average of three experiments.

Accumulation of cellobiose during the early stages of SSF when the cell density of the growing culture is low is in agreement with the observation that *T. reesei* cellulases are low in β-glucosidase activity (*14*). Removal of cellobiose along with glucose with increasing cell number suggests that strain 36D1 readily utilized cellobiose as a carbon source. This was subsequently confirmed in small-scale fermentations where cellobiose was supplied as the sole sugar source (data not shown).

Bacillus spp. are well-known producers of extracellular proteases, and the new biocatalysts also produced proteases as seen by casein and gelatin hydrolysis tests. This raises the possibility that the added cellulases are hydrolyzed by the native proteases, leading to loss of cellulase activity. In addition, fungal cellulases were reported to be inactivated by heat with a half-life at 50 °C and pH 4.8 of about 24 h (*14*, *15*). Proteolytic activity of the bacterial biocatalyst and temperature inactivation of Spezyme CE could limit SSF of cellulose to lactate and account for the observed reduction in the rate of lactate production after about 12 h of SSF (Figure 1).

To evaluate this potential limitation, SSF was started with 20 g/L Solka Floc and different concentrations of Spezyme CE (2−10 FPU/g cellulose) (Figure 2). After 72 h of SSF, when the lactate production reached a plateau, an additional 20 g/L cellulose was added to each of the SSF and lactate production was monitored until 168 h. The amount of lactate produced (as a measure of cellulose hydrolysis) during the 24 h period after the second addition of Solka Floc was about 80−100% of the yield during the first 24 h of fermentation (Figure 2). Especially at the lower Spezyme CE concentration of 4 FPU/g cellulose, the lactate yield during the 24 h after the second cellulose addition was close to 100% of the lactate yield during the initial 24 h of SSF. These results show that at least 80% of the hydrolytic activity of cellulases was still present and available even after 72 h of incubation at pH 5.0 and 50 °C.

Spezyme CE Concentration on SSF. Based on volumetric productivity of lactate (Figure 3), the minimal amount of Spezyme CE required for SSF with 20 g/L Solka Floc (pH 5.0 and 50 °C) was about 10 FPU/g cellulose. Below this threshold level of Spezyme CE, the volumetric productivity of lactate was significantly lower than the maximum observed value. On the basis of the product yield after 96 h, 7.5 FPU/(g cellulose) appears to

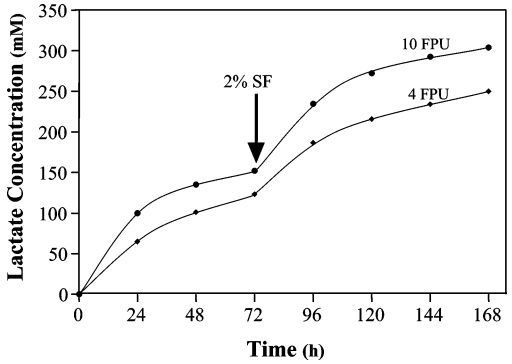

Figure 2. SSF of Solka Floc by *Bacillus* sp. strain 36D1. SSF was started with 20 g/L Solka Floc and either 4 or 10 FPU/g cellulose Spezyme CE. At 72 h, an additional 20 g/L Solka Floc (SF) was added to both fermentations and lactate production was determined. Batch fermentations were at 50 °C and pH 5.0.

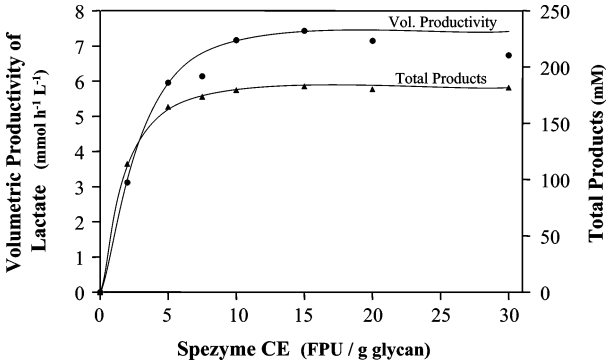

Figure 3. Effect of Spezyme CE concentration on SSF by *Bacillus* sp. strain 36D1. Total products include mostly lactate and small amounts of acetate, ethanol, and succinate. SSF conditions were 20 g/L Solka Floc at 50 °C and pH 5.0 in a batch mode. The reported values were the highest amount of each product produced in a 96 h SSF.

be sufficient. Small amounts of free cellobiose and glucose were detected during the first 12 h of growth at all Spezyme concentrations, indicating that the rate of saccharification during early phases of SSF exceeds that of fermentation, presumably as a result of low starting cell density (inoculum of 50 mg/L). At 2 FPU/g cellulose, the highest level of glucose detected in the medium was about 0.5 mM, whereas at 30 FPU/g cellulose, the level of glucose in the culture medium was as high as 10 mM (data not presented). The absence of free sugars after 10−12 h of SSF, even with 30 FPU/g cellulose, indicates that the rate of cellulase-mediated sugar release was the limiting factor determining the rate of fermentation at maximal cell density. It has been suggested that even crystalline cellulose contains localized regions with increased digestibility (*10*). Such regions in Solka Floc may also contribute to the release and accumulation of cellobiose and glucose during early stages of SSF. Apparently, the inoculum size of the biocatalyst (50 mg dry weight/L) was insufficient to metabolize the high rate of cellobiose and glucose production during the early stages of SSF. Irrespective of the Spezyme CE level, total product yield was between 86% and 91% of the theoretical yield of the amount of cellulose removed from the medium.

Effect of Cellulose Concentration on SSF. Increasing the cellulose concentration in the SSF with 10 FPU/g cellulose of Spezyme CE increased the rate of lactate production up to about 60 g/L cellulose (Figure 4). The highest concentration of lactate produced under these conditions was 0.45 M (approximately 40 g/L). These results show that at pH 5.0 and 50 °C, 10 FPU Spezyme/g

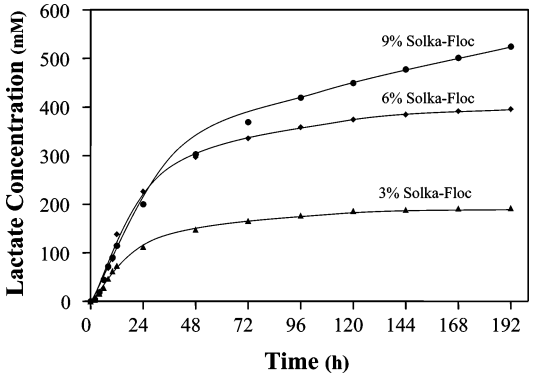

Figure 4. Effect of cellulose concentration on SSF. The cellulase concentration was 10 FPU/g cellulose of Spezyme CE.

cellulose can optimally support SSF of about 60 g/L of Solka Floc by *Bacillus* sp. strain 36D1.

Effect of Fermentation pH on SSF. The results reported in Table 1 and Figures 1−4 were from experiments conducted at pH 5 and 50 °C, the reported optima for fungal cellulases (*14*, *15*). At 50 °C, this pH optimum was confirmed for SSF with strain 36D1 in our fermentation medium by conducting a series of fermentations under more basic and more acidic conditions (Figure 5A). Based on both volumetric productivity of lactate and total products at the end of 96 h (a measure of cellulose depolymerization), the optimum pH for SSF with this strain was between 4.5 and 5.5. Because of poor growth of strain 36D1 at pH 4.5, SSF tests were not conducted at pH lower than 4.5. At pH 4.5, lactate represented 89% of the total products; 98% of the expected cellulose-derived glucose was recovered as fermentation products (Table 2). With increasing culture pH, the lactate fraction of the products declined with an increase in all the other products. These results emphasize the importance of pH for successful SSF processes.

It is interesting to note that almost 90 mM formate, higher than that of lactate or acetate and ethanol combined, was detected in the fermentation broth of SSF at pH 6.0 and 50 °C. The identity of formate and other products in the broth was confirmed by ^{1}H NMR. Pyruvate formate-lyase is the predicted enzyme catalyzing the production of acetyl-CoA and formate. Since acetyl-CoA is the precursor for both acetate and ethanol, the sum of the concentrations of acetate and ethanol is expected to equal that of formate. This is indeed the case at only one growth condition: pH 5.5 and 55 °C (Table 2). Under all other conditions, the formate concentration in the broth was either lower than predicted or as seen with the fermentation at pH 6.0 and 50 °C, significantly higher than expected. It is possible that at pH 6.0, acetyl-CoA is also converted to a product(s) undetectable under the present experimental condition by either HPLC or ^{1}H NMR.

In several bacteria, including *E. coli*, formate is dissimilated by formate hydrogen-lyase (FHL) to H_2 and CO_2 (*23*). The lower than expected level of formate in most of the fermentations would suggest the presence and activity of FHL in strain 36D1. Since the fermentations were not closed systems, volatile gases produced by the cultures would have been lost. However, in closed batch fermentations, H_2 was not detected in the gas phase of the cultures (by GC) grown at pH 5.0 and 50 °C. An alternate possibility is that strain 36D1 produced an active pyruvate dehydrogenase in a pH-dependent manner that is contributing to the observed differences in the acetate, ethanol, and formate levels in the broth. In this

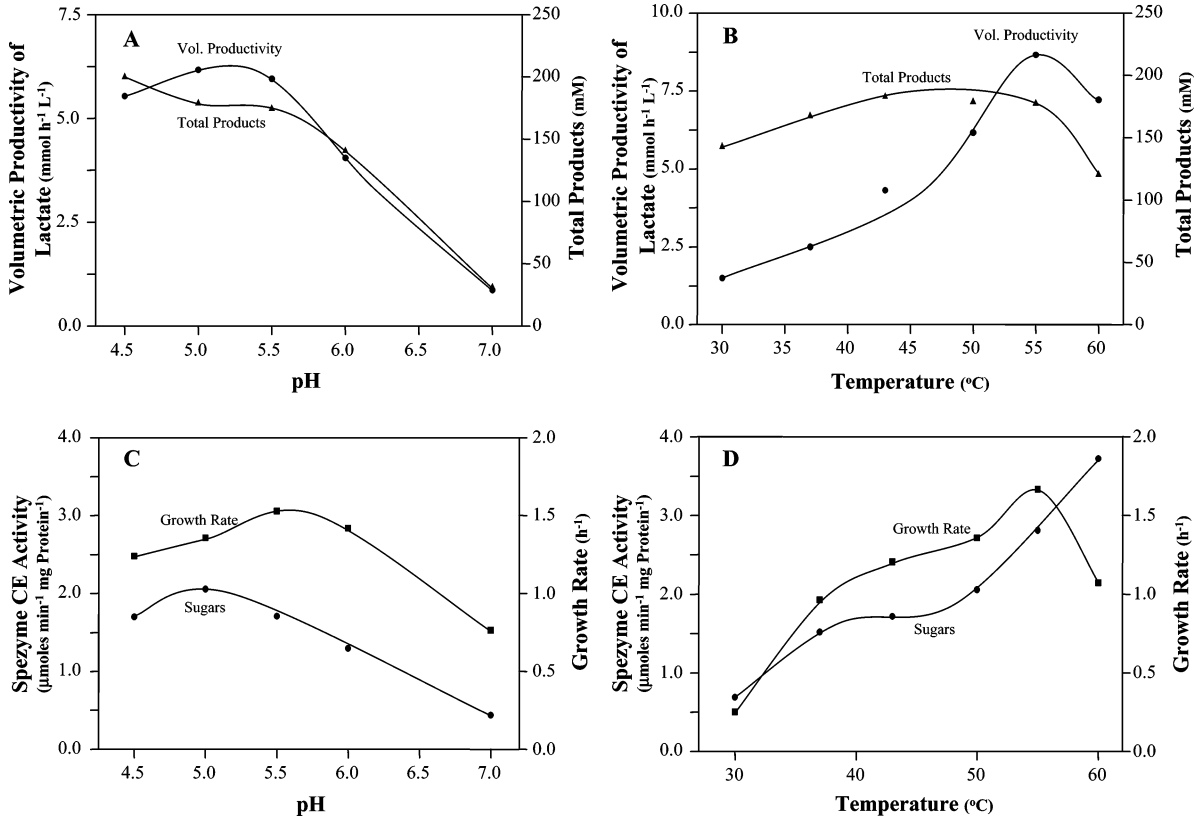

Figure 5. Effect of pH and temperature on the growth, cellulase activity, and SSF by *Bacillus* sp. strain 36D1. Batch SSF contained 20 g/L Solka Floc and 15 FPU/g cellulase Spezyme CE. Total products represent mostly lactate and varying amounts of acetate, ethanol, and succinate (Table 2). (A) Effect of pH on SSF. Growth temperature was 50 °C. (B) Effect of temperature on SSF. pH of the cultures was 5.0. (C) Effect of pH on Spezyme activity (10 FPU/g cellulose) and growth of *Bacillus* sp. strain 36D1. Spezyme activity is the initial rate of release of both cellobiose and glucose in the same medium used in SSF (Figure 5A) but without CSL and cells at 50 °C. Growth rate of the biocatalyst was determined in glucose−MS-CSL medium at the indicated pH values at 50 °C. (D) Effect of temperature on Spezyme activity (10 FPU/g cellulose) and growth of *Bacillus* sp. Strain 36D1 at pH 5.0. Conditions were similar to the experiments presented in B and C. See Figure 3 legend for other details.

Table 2. SSF Profile of *Bacillus* sp. Strain 36D1 in Mineral Salts Medium at Different pH and Temperature [a]

		fermentation products (mM)					lactate	yield (%)[b]	
pH	temp (°C)	lactate	acetate	ethanol	formate	succinate	fraction (%)	lactate	total
4.5	50	182.8	7.6	9.0	0.0	1.5	92	89.0	97.7
5.0	50	141.3	14.6	22.0	15.3	1.8	79	68.8	87.5
5.5	50	113.9	27.6	29.5	58.2	4.2	65	55.5	85.3
6.0	50	66.7	36.6	34.8	90.7	3.5	47	32.5	68.9
7.0	50	4.9	19.6	7.1	17.4	0.4	16	2.4	15.6
temp (°C)	pH								
30	5.0	122.2	12.2	7.7	0.0	1.6	85	59.5	70.0
37	5.0	138.0	9.1	19.7	0.0	1.7	82	67.2	82.0
43	5.0	146.0	11.5	24.8	12.0	1.5	79	71.1	89.5
50	5.0	141.3	14.6	22.0	15.3	1.8	79	68.8	87.5
55	5.0	152.9	12.0	12.2	0.0	1.3	86	75.5	86.9
60	5.0	105.9	12.4	2.4	0.0	0.6	87	51.6	59.0

[a] Batch fermentations were carried out for 96 h, at the indicated pH and temperature in a pH-stat in medium containing Solka-Floc (2%), mineral salts, corn steep liquor (0.5%) and Spezyme CE (10 FPU/g cellulose). [b] % yield is that of the expected maximum. See Table 1 for other details.

context, it should be noted that strain 36D1 cultured at pH 4.5 and 50 °C produced no detectable formate (Table 2). Further oxidation of acetyl-CoA by the culture to CO_2 with the aid of small amount of O_2 entering the fermentation would also alter the composition of fermentation products.

To differentiate between the role of Spezyme and the biocatalyst in the lower than expected product yield at nonoptimal pH, growth rate of the biocatalyst (using glucose as a carbon source) and cellulase activity were independently determined in the same medium used for SSF (Figure 5C). The highest rate of hydrolytic activity of Spezyme CE was at pH 5.0, and the activity progressively declined with increasing pH. At pH 6.0, the Spezyme CE activity decreased by about 40% from the maximum activity at pH 5.0. At pH 7.0, the Spezyme activity was only about 20% of the activity found at pH 5.0. This is in agreement with previous observations that the *T. reesei* and other fungal cellulases optimally hydrolyzed crystalline celluloses at pH 4.5−5.0 (*14*, *15*, *28*).

The highest growth rate for strain 36D1 was at pH 5.5, and the growth rates between pH 4.5 and 6.0 were comparable (Figure 5C). Growth rate of strain 36D1 was

the lowest when the pH was raised to 7.0. These results show that the decrease in volumetric productivity and product yield at pH 6.0 is solely attributable to lower cellulase activity and at pH values higher than 6.0 is due to both lower cellulase activity and poor growth and metabolism of the biocatalyst.

Effect of Temperature on SSF. Within the temperature range of the SSF (30−60 °C), Spezyme CE activity was highest at 60 °C and lowest at 30 °C (Figure 5D). Cellulase activity more than doubled between 30 and 37 °C with a modest further increase between 37 and 50 °C. Total cellulase activity almost doubled again between 50 and 60 °C. This second increase in activity between 50 and 60 °C was unexpected since the optimum temperature for fungal cellulases has been reported to be around 50 and 55 °C (*10*). This observed difference could be a result of variations in the assay methods (initial rate of Solka Floc hydrolysis vs filter paper assay), buffer conditions, etc. The growth rate of strain 36D1 also increased with increasing temperature with the optimum at 55 °C. At 60 °C, growth rate of the biocatalyst declined and the value was similar to that at 37 °C.

Volumetric productivity of lactate in SSF of Solka Floc was highest at 55 °C (Figure 5B). The slight decline at 60 °C is probably due to lower activity of the biocatalyst, strain 36D1, at this temperature. Total product yield after 96 h was comparable in SSF experiments carried out between 43 and 55 °C. These results show that on the basis of the combination of Spezyme CE activity and biocatalyst performance the optimum for SSF of Solka Floc by strain 36D1 to lactate is pH 4.5−5.0 and 55 °C with Spezyme CE. At this SSF condition, 87% of the products was lactate, with acetate accounting for about 10% of the total. Ethanol and succinate accounted for the rest.

Product Profile at Different pH and Temperature. It is interesting to note that at pH 4.5 and 50 °C, lactate yield from the SSF experiment was about 92% of the theoretical maximum product yield (Table 2). With increasing pH, the lactate fraction of the total decreased, with acetate, ethanol, and formate accounting for the rest. At pH 6.0, although the total product yield was about 70% of the expected maximum, the lactate fraction was only about 50% of the total. This difference in the lactate fraction of the total products was not observed during fermentation of 30 g/L glucose in mineral salts medium at these different pH values.

Pyruvate formate-lyase cleaves pyruvate to 1 mol of acetyl CoA and formate. To maintain cellular redox balance, one acetyl CoA is converted to acetate and the other to ethanol. Under these conditions, the sum of acetate and ethanol in the medium is expected to equal that of formate, as seen with the SSF at pH 5.5 and 50 °C (Table 2). Deviation from this expected ratio at other pH values suggests a yet to be identified alteration in fermentation pathways. These results show that SSF at the pH values that are far removed from the optimum for cellulase activity leads to sugar limitation of the growing culture and the biocatalyst compensates for this limitation by inducing pyruvate formate-lyase for additional ATP associated with acetate production. Such an induction of pyruvate formate-lyase in sugar-limited or growth-limited cultures of *Lactococcus lactis* and *Enterococcus* has been reported (*35*, *36*), and the present observation with *Bacillus* sp. strain 36D1 is in agreement with these studies.

Simultaneous Saccharification and Co-Fermentation with Hemicellulose Acid Hydrolysate (SSCF). The two major fermentable components of biomass are

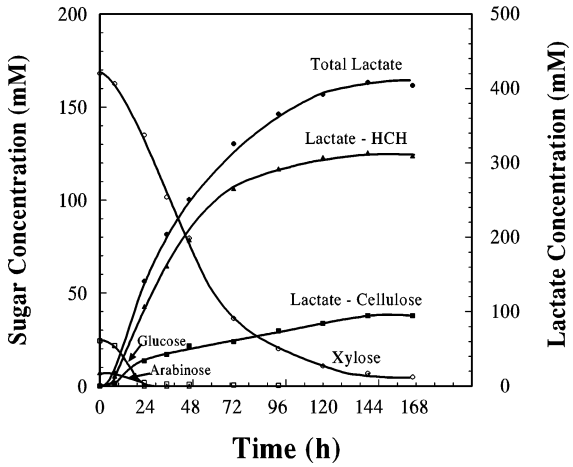

Figure 6. Simultaneous saccharification and co-fermentation of cellulose and sugar cane hemicellulose acid hydrolysate. The medium contained 40% hemicellulose hydrolysate over-limed and adjusted to pH 5.0, 20 g/L Solka Floc and Spezyme CE (15 FPU/g cellulose) in addition to mineral salts and CSL (0.25%, dry weight). Contribution of hemicellulose hydrolysate to total lactate was calculated on the basis of the hydrolysate fermentation profile (*22*), and the difference was deemed to be from cellulose.

cellulose and hemicellulose. Dilute acid hydrolysis of biomass releases most of the sugars in the hemicellulose fraction that can be readily fermented by appropriate biocatalyst, leaving intact the cellulose fraction. Fermentation of the hemicellulose-derived sugars simultaneously with cellulose in a single fermentation could significantly reduce the cost of production compared to separate fermentation by eliminating a solid separation and a duplication of vessels. Since the newly isolated biocatalysts fermented hemicellulose hydrolysate effectively to L(+)-lactate (*22*), simultaneous co-fermentation of both cellulose and hemicellulose hydrolysate by strain 36D1 was evaluated (Figure 6). In this experiment, the hemicellulose hydrolysate contained 168 mM xylose, 25 mM glucose, and 8 mM arabinose. Glucose, arabinose, and xylose were simultaneously utilized by strain 36D1, with lactate as the main product. Both glucose and arabinose were completely fermented within the first 24 h, whereas xylose fermentation continued until 144 h. Total lactate production in this batch fermentation reached about 0.4 M (36 g/L) with highest volumetric productivity of 6.7 mmol lactate/L (h). On the basis of the fermentation profile of sugar cane bagasse acid hydrolysate alone (*22*), the fraction of lactate derived from the hemicellulose hydrolysate was calculated and the difference from the total was computed to be from cellulose. The fraction of lactate derived from cellulose was about 25% of the total amounting to a yield of 46% of cellulose carbon to lactate. Between 8 and 24 h, the rate of cellulose-derived lactate production of 2.4 mmol/L (h) was about 40% of the highest rates observed in SSF alone (Figure 5). This difference could be due to inhibition of cellulases by the glucose present in the hemicellulose hydrolysate, as well as the utilization of the free sugars present in the medium by the biocatalyst. After 24 h, the rate of cellulose-derived lactate production declined to a constant value of 0.52 mmol/L (h). This lower calculated rate of lactate production from cellulose persisted until about 144 h. This lower than expected rate of lactate production from cellulose is likely due to competition between a higher concentration of xylose in the medium and the lower concentration of enzyme-generated glucose for the biocatalyst. These results show that both cellulose and

hemicellulose acid hydrolysate can be simultaneously fermented to lactate by the biocatalyst *Bacillus* sp. strain 36D1.

Conclusion

Although lactic acid bacteria such as *L. delbrueckii* and *L. acidophilus* employed by the industry can produce lactic acid from corn starch derived glucose at concentrations higher than 1 M in about 24 h, these bacteria lack the ability to ferment pentoses. These fermentations also start at pH values between 5.5 and 6.5 and at temperatures not higher than 42 °C, conditions that are not optimal for hydrolysis of cellulose by fungal cellulases. *Bacillus* sp. strain 36D1, described in this study, can effectively ferment cellulose (depolymerized by Spezyme CE) under conditions that are optimal for cellulase activity and cell growth (55 °C and pH 5.0). The main product was L(+)-lactate with an optical purity of about 96%. At the optimal SSF condition with about 10 FPU/g cellulose of cellulases, about 85−90% of the cellulose was metabolized to products. Strain 36D1 also served as a biocatalyst for lactate production during the SSF of cellulose and co-fermentation of sugar cane bagasse hemicellulose acid hydrolysate. In batch fermentations, both the xylose from the hemicellulose fraction and glucose from cellulose were simultaneously fermented at a maximum volumetric productivity of 6.7 mM lactate/L (h), in which the calculated contribution from cellulose was 2.4 mM/L (h). In these batch fermentations, both SSF and SSCF, the biocatalyst produced about 45 g/L of L-(+)-lactate. These results show that a biocatalyst such as *Bacillus* sp. strain 36D1 with optimal growth conditions near those of fungal cellulases can convert lignocellulosic biomass into lactate with relatively high product yield.

Acknowledgment

We thank Dr. G. Luli, BC International, for providing Solka Floc and sugar cane bagasse hemicellulose acid hydrolysate and Genencor Intl. for Spezyme CE. This study was supported in part by grants from the Department of Energy (DE-FG36-04GO14019, DE-FC36-01GO11073 and FG02-96ER20222) and the U.S. Department of Agriculture (00-52104-9704 and 01-35504-10669).

References and Notes

(1) American Plastics Council; APC year-end statistics for 2003. www.americanplasticscouncil.org; 2004.
(2) Brown, S. F. Bioplastic fantastic. *Fortune* **2003**, *148*, 92−94.
(3) Biobased PLA polymers grow new markets for American corn products; Department of Energy Publication 6980; DOE: Washington, DC, 2003.
(4) Datta, R.; Tsai, S.; Bonsignore, P.; Moon, S.; Frank, J. R. Technological and economic potential of poly(lactic acid) and lactic acid derivatives. *FEMS Microbiol. Rev.* **1995**, *16*, 221−231.
(5) Kulkarni, R. K.; Moore, E. G.; Hegyeli, A. F.; Leonard, F. Biodegradable poly(lactic acid) polymers. *J. Biomed. Mater. Res.* **1971**, *5*, 169−181.
(6) Mecking, S. Nature or petrochemistry? Biologically degradable materials. *Angew. Chem., Int. Ed.* **2004**, *43*, 1078−1085.
(7) Parajo, J. C.; Alonso, J. L.; Santos, V. Lactic acid from wood. *Process Biochem.* **1996**, *31*, 271−280.
(8) Schmidt, S.; Padukone, N. Production of lactic acid from wastepaper as a cellulosic feedstock. *J. Ind. Microbiol. Biotechnol.* **1997**, *18*, 10−14.
(9) Yanez, R.; Moldes, A. B.; Alonso, J. L.; Parajo, J. C. Production of D(−)-lactic acid from cellulose by simultaneous saccharification and fermentation using *Lactobacillus coryniformis* subsp. *torquens*. *Biotechnol. Lett.* **2003**, *25*, 1161−1164.
(10) Lynd, L. R.; Weimer, P. J.; van Zyl, W. H.; Pretorius, I. S. Microbial cellulose utilization: fundamentals and biotechnology. *Microbiol. Mol. Biol. Rev.* **2002**, *66*, 506−577.
(11) Duff, S. J. B.; Murray, W. D. Bioconversion of forest products industry waste cellulosics to fuel ethanol: a review. *Bioresour. Technol.* **1996**, *55*, 1−33.
(12) Wooley, R.; Ruth, M.; Glassner, D.; Sheehan, J. Process design and costing of bioethanol technology: a tool for determining the status and direction of research and development. *Biotechnol. Prog.* **1999**, *15*, 794−803.
(13) Abe, S.; Takagi, M. Simultaneous saccharification and fermentation of cellulose to lactic acid. *Biotechnol. Bioeng.* **1991**, *37*, 93−96.
(14) Castellanos, O. F.; Sinitsyn, A. P.; Vlasenko, E. Y. Comparative evaluation of hydrolytic efficiency toward microcrystalline cellulose of *Penicillium* and *Trichoderma* cellulases. *Bioresour. Technol.* **1995**, *52*, 119−124.
(15) Jana, S. K.; Ghosh, V. K.; Singh, A. Production and hydrolytic potential of cellulase enzymes from a mutant strain of *Trichoderma reesei*. *Biotechnol. Appl. Biochem.* **1994**, *20*, 233−239.
(16) Wyman, C. E. Potential synergies and challenges in refining cellulosic biomass to fuels, chemicals, and power. *Biotechnol. Prog.* **2003**, *19*, 254−262.
(17) Carr, F. J.; Chill, D.; Maida, N. The lactic acid bacteria: A literature survey. *Crit. Rev. Microbiol.* **2002**, *28*, 281−370.
(18) Hofvendahl, K.; Hans-Hagerdal, B. Factors affecting the fermentative lactic acid production from renewable resources. *Enzyme Microb. Technol.* **2000**, *26*, 87−107.
(19) Martin, A. M. Fermentation processes for the production of lactic acid. In *Lactic Acid Bacteria: Current Advances in Metabolism*, *Genetics and Applications*; Bozoglu, T. F., Ray, B., Eds.; Springer-Verlag: New York, 1996; Nato ASI Series Vol. H98, pp 269−301.
(20) Zhou, S.; Causey, T. B.; Hasona, A.; Shanmugam, K. T.; Ingram, L. O. Production of optically pure D-lactic acid in mineral salts medium by metabolically engineered *Escherichia coli* W3110. *Appl. Environ. Microbiol.* **2003**, *69*, 399−407.
(21) Zhou, S.; Shanmugam, K. T.; Ingram, L. O. Functional replacement of the *Escherichia coli* D-(−)-lactate dehydrogenase gene (*ldhA*) with the L-(+)-lactate dehydrogenase gene (*ldhL*) from *Pediococcus acidilactici*. *Appl. Environ. Microbiol.* **2003**, *69*, 2237−2244.
(22) Patel, M.; Ou, M.; Ingram, L. O.; Shanmugam, K. T. Fermentation of sugar cane bagasse hemicellulose hydrolysate to L(+)-lactic acid by a thermotolerant acidophilic *Bacillus* sp. *Biotechnol. Lett.* **2004**, *26*, 865−868.
(23) Lee, J. H.; Patel, P.; Sankar, P.; Shanmugam, K. T. Isolation and characterization of mutant strains of *Escherichia coli* altered in H_2 metabolism. *J. Bacteriol.* **1985**, *162*, 344−352.
(24) Beall, D. S.; Ohta, K.; Ingram, L. O. Parametric studies of ethanol production from xylose and other sugars by recombinant *Escherichia coli*. *Biotechnol. Bioeng.* **1991**, *38*, 296−303.
(25) Martinez, A.; Rodriguez, M. E.; Wells, M. L.; York, S. W.; Preston, J. F.; Ingram, L. O. Detoxification of dilute acid hydrolysates of lignocellulose with lime. *Biotechnol. Prog.* **2001**, *17*, 287−293.
(26) Underwood, S. A.; Zhou, S.; Causey, T. B.; Yomano, L. P.; Shanmugam, K. T.; Ingram, L. O. Genetic changes to optimize carbon partitioning between ethanol and biosynthesis in ethanologenic *Escherichia coli*. *Appl. Environ. Microbiol.* **2002**, *68*, 6263−6272.
(27) Coward-Kelly, G.; Aiello-Mazzari, A.; Kim, S.; Granda, C.; Holtzapple, M. Suggested improvements to the standard filter paper assay used to measure cellulase activity. *Biotechnol. Bioeng.* **2003**, *82*, 745−749.
(28) Mandels, M. Application of cellulases. *Biochem. Soc. Trans.* **1985**, *13*, 414−416.
(29) Gonzalez, R.; Tao, H.; Shanmugam, K. T.; York, S. W.; Ingram, L. O. Global gene expression differences associated with changes in glycolytic flux and growth rate in *Escherichia*

coli during fermentation of glucose and xylose. *Biotechnol. Prog.* **2002**, *18*, 6−20.
(30) Lawford, H. G.; Rousseau, J. D. Comparative energetics of glucose and xylose metabolism in ethanologenic recombinant *Escherichia coli* B. *Appl. Biochem. Biotechnol.* **1995**, *51*−*52*, 179−195.
(31) Henderson, P. J. F.; Maiden, M. C. J. Homologous sugar transport proteins in *Escherichia coli* and their relatives in both prokaryotes and eukaryotes. *Philos. Trans. R. Soc. London, Ser. B* **1990**, *326*, 391−410.
(32) Lin, E. C. C. Dissimilatory pathways for sugars, polyols, and carboxylates. In *Escherichia coli and Salmonella. Cellular and Molecular Biology*; Neidhardt, F. C. et al., Eds.; ASM Press: Washington, DC, 1996; pp 307−342.
(33) Chaillou, S.; Bor, Y. C.; Batt, C. A.; Postma, P. W.; Pouwels, P. H. Molecular cloning and functional expression in *Lactobacillus plantarum* 80 of *xylT*, encoding the D-xylose-H+ symporter of *Lactobacillus brevis*. *Appl. Environ. Microbiol.* **1998**, *64*, 4720−4728.
(34) Schmiedel, D.; Kintrup, M.; Küster, E.; Hillen, W. Regulation of expression, genetic organization and substrate specificity of xylose uptake in *Bacillus megaterium*. *Mol. Microbiol.* **1997**, *23*, 1053−1062.
(35) Yun, J.-S.; Wee, Y.-J.; Ryu, H.-W. Production of optically pure L(+)-lactic acid from various carbohydrates by batch fermentation of *Enterococcus faecalis* RKY1. *Enzyme Microb. Technol.* **2003**, *33*, 416−423.
(36) Tanaka, K.; Komiyama, A.; Sonomoto, K.; Ishizaki, A.; Hall, S. J.; Stanbury, P. E. Two different pathways for D-xylose metabolism and the effect of xylose concentration on the yield coefficient of L-lactate in mixed-acid fermentation by the lactic acid bacterium *Lactococcus lactis* IO-1. *Appl. Microbiol. Biotechnol.* **2002**, *60*, 160−167.
(37) Aden, A.; Ruth, M.; Ibsen, K.; Jechura, J.; Neeves, K.; Sheehan, J.; Wallace, B.; Montague, L.; Slayton, A.; Lukas, J. Lignocellulosic biomass to ethanol process design and economics utilizing co-current dilute acid prehydrolysis and enzymatic hydrolysis for corn stover. National Renewable Energy Laboratory/TP-510-32438, 2002.
(38) Nieves, R. A.; Ehrman, C. I.; Adney, W. S.; Elander, R. T.; Himmel, M. E. Survey and analysis of commercial cellulase preparations suitable for biomass conversion to ethanol. *World J. Microbiol. Biotechnol.* **1998**, *14*, 301−304.
(39) Holtzapple, M.; Cognata, M.; Shu, Y.; Hendrickson, C. Inhibition of *Trichoderma reesei* cellulase by sugars and solvents. *Biotechnol. Bioeng.* **1990**, *36*, 275−287.
(40) Pemberton, M. S.; Crawford, S. D. Method for ethanol fermentation. U.S. Patent 4,224,410, 1980.
(41) Gauss, W. F.; Suzuki, S.; Takagi, M. Manufacture of alcohol from cellulosic materials using plural ferments. U.S. Patent 3,990,944, 1976.

Accepted for publication July 7, 2005.

BP0400339

Appendix C

Appl Biochem Biotechnol (2009) 155:379–385
DOI 10.1007/s12010-008-8509-4

Thermophilic *Bacillus coagulans* Requires Less Cellulases for Simultaneous Saccharification and Fermentation of Cellulose to Products than Mesophilic Microbial Biocatalysts

Mark S. Ou · Nazimuddin Mohammed · L. O. Ingram · K. T. Shanmugam

Received: 21 May 2008 / Accepted: 22 December 2008 /
Published online: 21 January 2009

Abstract Ethanol production from lignocellulosic biomass depends on simultaneous saccharification of cellulose to glucose by fungal cellulases and fermentation of glucose to ethanol by microbial biocatalysts (SSF). The cost of cellulase enzymes represents a significant challenge for the commercial conversion of lignocellulosic biomass into renewable chemicals such as ethanol and monomers for plastics. The cellulase concentration for optimum SSF of crystalline cellulose with fungal enzymes and a moderate thermophile, *Bacillus coagulans*, was determined to be about 7.5 FPU g^{-1} cellulose. This is about three times lower than the amount of cellulase required for SSF with *Saccharomyces cerevisiae*, *Zymomonas mobilis*, or *Lactococcus lactis* subsp. *lactis* whose growth and fermentation temperature optimum is significantly lower than that of the fungal cellulase activity. In addition, *B. coagulans* also converted about 80% of the theoretical yield of products from 40 g/L of crystalline cellulose in about 48 h of SSF with 10 FPU g^{-1} cellulose while yeast, during the same period, only produced about 50% of the highest yield produced at end of 7 days of SSF. These results show that a match in the temperature optima for cellulase activity and fermentation is essential for decreasing the cost of cellulase in cellulosic ethanol production.

Keywords Cellulase · Cellulose SSF · *Bacillus coagulans* · *Saccharomyces* · *Zymomonas* · Lactic acid bacteria

Introduction

The limited nature and rising costs of fossil fuels have provided the needed impetus to the use of sustainable and renewable sources of fuels and chemicals. Lignocellulosic biomass from plants is the only promising sustainable feedstock that can be converted to both fuels

M. S. Ou · N. Mohammed · L. O. Ingram · K. T. Shanmugam (✉)
Department of Microbiology and Cell Science, University of Florida, Box 110700,
Gainesville, FL 32611, USA
e-mail: shan@ufl.edu

and chemicals without increasing greenhouse gas emissions [1]. Although the hemicellulose in the biomass can be readily hydrolyzed to fermentable sugars by mild acid treatment, bioconversion of cellulose in the biomass to glucose requires hydrolysis by cellulases before fermentation by microbial biocatalysts [2–7].

Fungal cellulases, such as those from *Trichoderma reesei*, dominate the industrial applications of cellulases and are one of the significant cost components of deriving sugars from cellulose for fermentation to ethanol and other chemicals [5–7]. One processing strategy in the production of cellulose-based fuels and chemicals involves separate hydrolysis of cellulose by enzymes followed by fermentation by microbial biocatalysts (SHF) [8]. Due to the low yield of glucose in the SHF process, a result of inhibition of cellulases by the hydrolysis products cellobiose and glucose [9], combined with inherent low specific activity of the fungal cellulases [10], the amount of cellulases required for optimal conversion of cellulose to ethanol is higher than desired for economical production of ethanol and other commodity chemicals. To overcome the product inhibition of cellulases, a strategy of simultaneous saccharification and fermentation (SSF) has been developed in which hydrolysis of cellulose is coupled with fermentation of the released sugars in the same reaction vessel [11]. In the SSF process, the fungal enzymes hydrolyzed the cellulose to sugars that were immediately fermented by the microbial biocatalyst to ethanol and/or chemicals. Because of this combination, hydrolysis of cellulose by the enzymes could not be optimized separately and the growth and fermentation optimum of the microbial biocatalyst also need to be considered in selecting an optimum temperature and pH for SSF of cellulose to products.

Although the SSF process minimized the product inhibition of cellulase activity, the relatively low specific activity of fungal cellulases in relation to bacterial-cell-associated cellulases is yet to be overcome [1, 8]. This is further magnified by the SSF process at a lower-than-optimum temperature for the enzyme activity (optimum of 50 °C and pH 5.0) [10, 12] due to the need for a lower temperature (30–35 °C) that is the growth and fermentation optimum for the current industrial biocatalysts, such as *Saccharomyces cerevisiae* [13] and *Zymomonas mobilis*. Lactic acid bacteria used by the industry for production of optically pure lactic acid, a potential renewable source of plastics, also suffers from the low temperature optimum (35–40 °C) for growth and fermentation compared to that of the fungal cellulase activity optimum [10, 12, 14–16]. Using these microbial biocatalysts in SSF of cellulose to products is expected to result in a mismatch in optima leading to either a higher requirement of fungal cellulases or an increase in the time required for SSF, both of which significantly increase the cost of bioconversion of cellulose to fuels and chemicals.

Our laboratory has described Gram-positive bacterial isolates that have growth and fermentation temperature optima which closely match those of fungal cellulases being developed for use in SSF of cellulose [12, 17]. These isolates, such as *Bacillus coagulans* strain 36D1, grow and ferment hexoses and pentoses at 50–55 °C and pH 5.0 producing L (+)-lactic acid as the primary fermentation product. Use of *B. coagulans* for optically pure lactic acid production for plastics industry or an engineered *B. coagulans* derivative for ethanol production at 50–55 °C is expected to reduce the amount of fungal cellulases required for optimum conversion of cellulose to products in the SSF process. However, no comparative experimental evidence exists establishing this possibility. In this communication, evidence is presented that coupling the microbial biocatalyst in the SSF process to the optimum temperature for fungal cellulases significantly reduces the amount of enzyme required for conversion of cellulose to products in comparison with yeast or lactic acid bacteria currently used by the industry as microbial biocatalysts. This reduction in the

amount of cellulase in SSF of cellulose to products is expected to reduce the cost of the process and final product.

Materials and Methods

Organisms, Media, and Growth Conditions

B. coagulans strain 36D1 was described previously [12, 17]. Media used in experiments with *B. coagulans* strain 36D1 contained, per liter: 6.25 g Na_2HPO_4, 0.75 g KH_2PO_4, 2 g NaCl, 0.2 g $MgSO_4 \cdot 7H_2O$, 1 g $(NH_4)_2SO_4$, 10 mg $FeSO_4 \cdot 7H_2O$, 10 mg $Na_2MoO_4 \cdot H_2O$, 1 ml trace mineral solution [18], and 5 ml corn steep liquor (50% dry solids; Grain Processing Corp., Muscatine, IO), adjusted to pH 5.0 with H_2SO_4. Media used for *Lactococcus lactis* subsp. *lactis* (NRRL B-4449) SSF contained, per liter: 10 g yeast extract, 2 g K_2HPO_4, 0.2 g $MgSO_4 \cdot 7H_2O$, 0.05 g $MnSO_4 \cdot H_2O$, 2 g $(NH_4)_2SO_4$, adjusted to pH 5.5 with H_2SO_4. Media used for *S. cerevisiae* (NRRL Y-12632) SSF contained, per liter: 10 g yeast extract, 2 g KH_2PO_4, 1 g $MgSO_4 \cdot 7H_2O$, 1 g $(NH_4)_2SO_4$, adjusted to pH 5.5 with H_2SO_4. Media used for *Z. mobilis* (ATCC 1050) SSF contained, per liter: 10 g yeast extract and 0.3 g KH_2PO_4, adjusted to pH 5 with H_2SO_4. These media were supplemented with glucose at 1% (*w*/*v*) for growth and fermentation without pH control and with 2% (*w*/*v*) in fermentations with pH control for preparation of inoculum for SSF experiments. Optimum temperature and pH for the growth of organisms were determined in batch fermentations without pH control as described previously [17], at various temperatures and initial culture pH.

SSF of Cellulose

SSF of crystalline cellulose (Solka Floc) was carried out in the media described above containing 40 g L^{-1} Solka Floc (International Fiber Corp., North Tonawanda, NY) and varying amounts of cellulase (GC220; Genencor International, Palo Alto, CA). Specific activity of the cellulase preparation as FPU/ml was determined before use as described previously [12]. SSF of crystalline cellulose was carried out at the temperature and pH that were found to be optimal for growth of the specific microbial biocatalyst (*B. coagulans* strain 36D1 at 50 °C and pH 5.0; *L. lactis* at 40 °C and pH 5.5; *S. cerevisiae* at 35 °C and pH 5.5; *Z. mobilis* at 35 °C and pH 5.0). Fermentation pH was maintained by automatic addition of 2 N KOH for strain 36D1 and *L. lactis* or 0.5 N KOH for *S. cerevisiae* and *Z. mobilis*. Sugar and fermentation products were determined using HPLC as described previously [19]. Inoculum for SSF experiments with crystalline cellulose was derived from pH-controlled fermentations in the same media but with 2% (*w*/*v*) glucose. Cells were collected by centrifugation at room temperature and resuspended in appropriate growth media before inoculation in the SSF medium at an initial O.D. at 420 nm of 0.2.

Results and Discussion

In order to obtain the highest volumetric productivity for each organism, optimal temperature and pH for anaerobic growth and fermentation of glucose was determined for each of the four microbial biocatalysts in batch fermentations without pH control. Based on the results of these experiments, the optimal conditions for *B. coagulans* strain 36D1, *L.*

lactis, *S. cerevisiae*, and *Z. mobilis* were determined to be 50 °C and pH 5.0, 40 °C and pH 5.5, 35 °C and pH 5.5, 35 °C and pH 5.0, respectively. These conditions were subsequently used for SSF of cellulose by each organism such that growth and fermentation conditions of the microbial biocatalyst would not be limiting the rate of conversion of cellulose-derived glucose to products. Although industrial yeast fermentations of corn starch to ethanol are conducted at temperatures below 35 °C, this temperature was used in this study since the growth rate of *S. cerevisiae* NRRL Y-12632 at 35 °C was slightly higher than at 30 °C.

SSF of crystalline cellulose was carried out with varying concentrations of cellulase. For each organism, the fermentation profile was dominated by one major fermentation product: lactate produced by *B. coagulans* and *L. lactis* or ethanol produced by *S. cerevisiae* and *Z. mobilis*. The rate of product formation was linear with time and also the highest during the first 18 h; after this period, the rate of product formation continually declined, irrespective of the microbial biocatalyst or the cellulase concentration. Representative SSF profiles for *B. coagulans* and yeast are presented in Fig. 1. With *B. coagulans* as the microbial biocatalyst and the SSF at 50 °C, the initial rate of product formation was not significantly altered by increasing the cellulase concentration from 5 FPU to 20 FPU g^{-1} of cellulose (Fig. 1a). Contrasting this observation, with yeast as the biocatalyst and SSF at 35 °C, the initial rate of ethanol production doubled with every twofold increase in cellulase concentration from 5–20 FPU g^{-1} cellulose (Fig. 1b).

Using the initial high rate of product formation, maximum volumetric productivity for each cellulase concentration and microbial biocatalyst was calculated and presented in

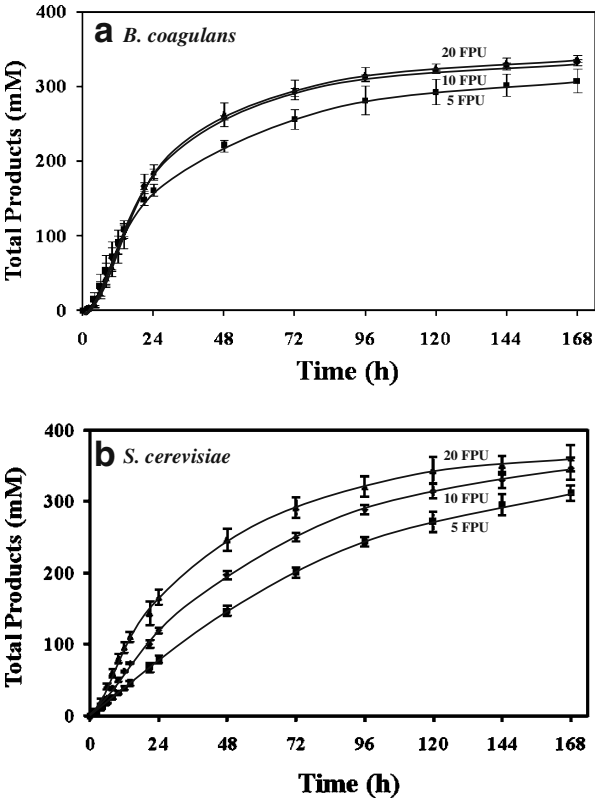

Fig. 1 Time course of SSF of 40 g L^{-1} crystalline cellulose (Solka Floc) with different concentrations of fungal cellulase (GC220; Genencor) **a** *B. coagulans* strain 36D1 at 50 °C and pH 5.0; **b** *S. cerevisiae* at 35 °C and pH 5.5

Fig. 2. Except for *L. lactis*, the volumetric productivity of the other three organisms increased with increasing cellulase concentration until the maximum value was reached. For *B. coagulans*, SSF at 50 °C, the cellulase concentration required for the highest volumetric productivity was between 5 and 7.5 FPU g^{-1} cellulose. With yeast or *Z. mobilis* as the microbial biocatalyst, volumetric productivity continued to increase up to a cellulase concentration of 30 FPU g^{-1} cellulose and, at this concentration of cellulase, the volumetric productivities of the ethanologens and *B. coagulans* at 50 °C were about the same. These results show that SSF at 50 °C can reduce the cellulase requirement by at least threefold without affecting volumetric productivity.

Increasing the SSF temperature to 55 °C with *B. coagulans* as the microbial biocatalyst, increased the volumetric productivity by about 40% without affecting the cellulase requirement (Fig. 2). *L. lactis*-based SSF also reached the same high volumetric productivity observed with *B. coagulans* at 55 °C but this required higher than 20 FPU g^{-1} cellulose in contrast to *B. coagulans* at 55 °C that required only about 5 to 7.5 FPU g^{-1} cellulose, a three- to fourfold reduction in cellulase requirement. At a cellulase concentration of 5 FPU g^{-1} cellulose, the volumetric productivity with *B. coagulans* SSF at 55 °C was at least 2.5-fold higher than that of any of the other three microbial biocatalysts. This difference is apparently due to the higher activity of the enzyme at 55 °C [12] compared to by the optimum temperature for growth of the microbial biocatalysts.

Although the maximum volumetric productivity of yeast and *Z. mobilis* was lower in the presence of lower cellulase concentrations (7.5 FPU g^{-1} cellulose) as compared to *B. coagulans*, all three fermentations produced about the same final yield of products at the end of 168 h of SSF (Table 1). At the end of 168 h of SSF and with 20 FPU g^{-1} cellulose, all three microbial biocatalysts (except *L. lactis*) converted about 90–95% of the glucose equivalents of cellulose. For *B. coagulans*, the time required to reach this product yield was about 96 h while the other three microbial biocatalysts required at least 168 h to reach the same product yield. These results are in agreement that SSF with *B. coagulans* at 50 °C is more effective in converting cellulose to products than with yeast as the microbial biocatalyst even at its optimal growth and fermentation temperature.

The amount of product produced by the various microbial biocatalysts in the SSF of cellulose at the end of 48 h was determined to further evaluate the efficiency of the process. The results presented in Fig. 3 are the fraction of the major product of fermentation at 48 h as compared to the maximum yield obtained at the end of fermentation at 168 h. In an SSF

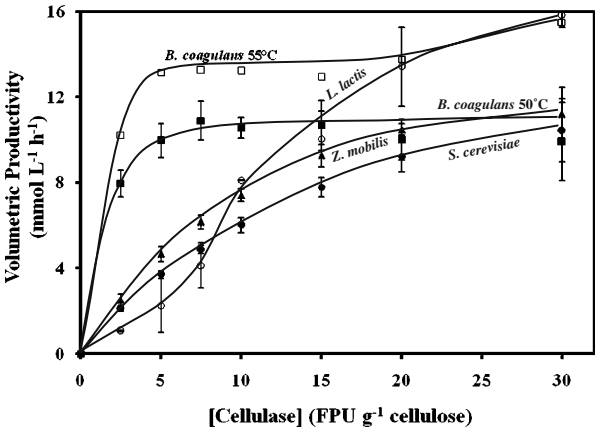

Fig. 2 Maximum volumetric productivity of SSF of 40 g L^{-1} cellulose (Solka Floc) by *B. coagulans* strain 36D1 (50 or 55 °C; pH 5.0), *L. lactis* (40 °C; pH 5.5), *S. cerevisiae* (35 °C; pH 5.5), and *Z. mobilis* (35 °C; pH 5.0) as a function of fungal cellulase concentration. Volumetric productivity was calculated as lactate produced by *B. coagulans* strain 36D1 and *L. lactis* and as ethanol produced by *S. cerevisiae* and *Z. mobilis*. See text for other details

Table 1 Profile of SSF of crystalline cellulose by *B. coagulans*, *L. lactis*, *S. cerevisiae*, and *Z. mobilis*.

Organism	Net production (mM)					Total product	Major product
	Lactate	Ethanol	Acetate	Succinate	Glycerol	Yield (%)[a]	Fraction (%)[b]
B. coagulans	299.9±0.8	17.6±2.4	17.9±1.0	2.2±1.9	0.0	90.3±4.0	88.8±0.8
L. lactis	226.0±23.4	47.3±10.2	21.1±4.4	0.0	0.0	70.9±2.5	76.7±5.2
S. cerevisiae	0.0	349.8±16.7	2.9±3.4	0.8±1.4	7.2±4.8	93.2±11.4	97.0±1.0
Z. mobilis	0.7±0.7	373.7±17.4	16.5±15.2	0.0	0.8±0.7	94.4±0.9	95.4±3.0

SSF of 40 g L^{-1} of crystalline cellulose (Solka Floc) was carried out at a cellulase concentration of 20 FPU g^{-1} cellulose for 168 h. See "Materials and Methods" section for details. Growth temperature and culture pH for the various organisms are listed in the text. Reported average values were from three independent fermentations

[a] Total products yield was calculated as % ratio of all fermentation products listed in the table to theoretical expected yield based on the amount of cellulose consumed on a molar basis

[b] Major product fraction represents the % of major product in the total fermentation products

with *B. coagulans*, about 80% of the expected products were produced during the first 48 h of SSF at 50 °C with only about 10 FPU g^{-1} of cellulose. Increasing the cellulase concentration did not influence this productivity. With the same amount of cellulase, both yeast and *Z. mobilis*-based SSFs yielded only about 50% of the ethanol during the first 48 h of SSF. The second 50% of ethanol production required an additional 120 h of SSF due to a continual decline in volumetric productivity. Even with 30 FPU g^{-1} cellulose, these two microbial biocatalysts only yielded about 65% of the expected ethanol during the first 48 h of SSF. *L. lactis* reached the same 80% product yield as *B. coagulans* but this required slightly higher concentration of cellulase (15 FPU vs 10 FPU g^{-1} cellulose). However, it should be noted that the final lactate yield is lower for *L. lactis* compared to *B. coagulans* (Table 1). These results show that SSF with an organism that can match the optimum conditions for fungal cellulase activity, such as *B. coagulans*, is a better choice of microbial biocatalyst to reduce the cost of fungal cellulase in SSF of cellulose to low-value commodity chemicals by decreasing the amount of enzyme needed and also the fermentation time, two significant areas of cost savings.

In conclusion, the temperature optimum for *B. coagulans* more closely match the optimum for fungal cellulases used in SSF than current generation biocatalysts used by the industry for producing ethanol or lactic acid, and this match leads to higher volumetric

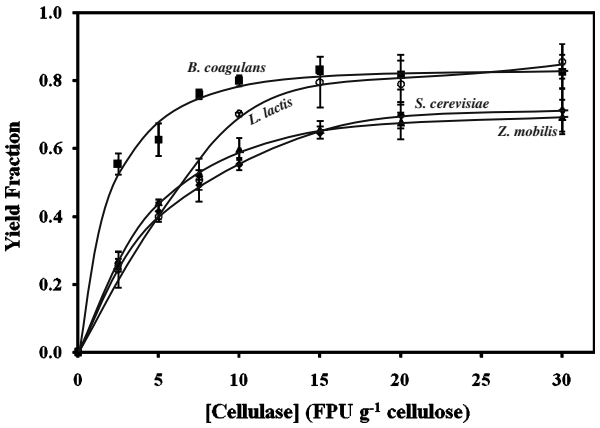

Fig. 3 Yield fraction of the major fermentation product of SSF of 40 g L^{-1} cellulose (Solka Floc) by *B. coagulans* strain 36D1, *L. lactis*, *S. cerevisiae*, and *Z. mobilis* at different fungal cellulase concentrations. Yield fraction was calculated as the ratio of major fermentation product (lactate for *B. coagulans* and *L. lactis*, ethanol for *S. cerevisiae* and *Z. mobilis*) produced at 48 h of SSF to that of the same product at the SSF endpoint of 168 h

productivity and more rapid progress to completion of SSF. This close match in temperature optima leads to a lower cellulase requirement for SSF by a factor of at least three for *B. coagulans* strain 36D1 versus the other microbial biocatalysts. The lower cellulase requirement and more rapid progress to the fermentation endpoint with *B. coagulans* in SSF is expected to lead to substantial cost savings in the amount of cellulase required for SSF. Metabolic engineering of *B. coagulans* and/or other thermotolerant microbial biocatalysts for production of ethanol as the main fermentation product should provide a new group of microbial biocatalysts that can contribute significantly in the conversion of lignocellulosic biomass to fuel ethanol in a cost-effective manner.

Acknowledgments We thank A. P. Rooney for providing some of the strains used in this study, Genencor Intl. for the cellulase preparation and International Fiber Corp. for Solka Floc. This study was supported in part by a grant from the Department of Energy (DE-FG36-04GO14019) and the State of Florida, University of Florida Agricultural Experiment Station.

References

1. Perlack, R. D., Wright, L. L., Turhollow, A. F., Graham, R. L., Stokes, B. J., & Erbach, D. C. (2005). DOE/GO-102005-2135.
2. Aden, A., Ruth, M., Ibsen, K., Jechura, J., Neeves, K., Sheehan, J., et al. (2002). NREL/TP-510-32438.
3. Duff, S. J. B., & Murray, W. D. (1996). *Bioresource Technology*, *55*, 1–33. doi:10.1016/0960-8524(95)00122-0.
4. Kheshgi, H. S., Prince, R. C., & Marland, G. (2000). *Annual Review of Energy and the Environment*, *25*, 199–244. doi:10.1146/annurev.energy.25.1.199.
5. Lynd, L. R., Laser, M. S., Bransby, D., Dale, B. E., Davison, B., Hamilton, R., et al. (2008). *Nature Biotechnology*, *26*, 169–172. doi:10.1038/nbt0208-169.
6. Wooley, R., Ruth, M., Glassner, D., & Sheehan, J. (1999). *Biotechnology Progress*, *15*, 794–803. doi:10.1021/bp990107u.
7. Wyman, C. E. (2007). *Trends in Biotechnology*, *25*, 153–157. doi:10.1016/j.tibtech.2007.02.009.
8. Zaldivar, J., Nielsen, J., & Olsson, L. (2001). *Applied Microbiology and Biotechnology*, *56*, 17–34. doi:10.1007/s002530100624.
9. Holtzapple, M., Cognata, M., Shu, Y., & Hendrickson, C. (1990). *Biotechnology and Bioengineering*, *36*, 275–287. doi:10.1002/bit.260360310.
10. Lynd, L. R., Weimer, P. J., van Zyl, W. H., & Pretorius, I. S. (2002). *Microbiology and Molecular Biology Reviews*, *66*, 506–577. doi:10.1128/MMBR.66.3.506-577.2002.
11. Gauss, W. F., Suzuki, S., & Takagi, M. (1976). Manufacture of alcohol from cellulosic materials using plural ferments. United States patent 3,990,944.
12. Patel, M. A., Ou, M., Ingram, L. O., & Shanmugam, K. T. (2005). *Biotechnology Progress*, *21*, 1453–1460. doi:10.1021/bp0400339.
13. Bothast, R. J., & Schlicher, M. A. (2005). *Applied Microbiology and Biotechnology*, *67*, 19–25. doi:10.1007/s00253-004-1819-8.
14. Carr, F. J., Chill, D., & Maida, N. (2002). *Critical Reviews in Microbiology*, *28*, 281–370. doi:10.1080/1040-840291046759.
15. Hofvendahl, K., & Hans-Hagerdal, B. (2000). *Enzyme and Microbial Technology*, *26*, 87–107. doi:10.1016/S0141-0229(99)00155-6.
16. Martin, A. M. (1996). Fermentation processes for the production of lactic acid. In T. F. Bozoglu & B. Ray (Eds.), *Lactic acid bacteria*: *Current advances in metabolism, genetics and applications*, Vol. Nato ASI Series (vol. H98, (pp. 269–301)). New York: Springer.
17. Patel, M. A., Ou, M. S., Harbrucker, R., Aldrich, H. C., Buszko, M. L., Ingram, L. O., et al. (2006). *Applied and Environmental Microbiology*, *72*, 3228–3235. doi:10.1128/AEM.72.5.3228-3235.2006.
18. Allen, M. B., & Arnon, D. I. (1955). *Plant Physiology*, *30*, 366–372. doi:10.1104/pp.30.4.366.
19. Underwood, S. A., Buszko, M. L., Shanmugam, K. T., & Ingram, L. O. (2002). *Applied and Environmental Microbiology*, *68*, 1071–1081. doi:10.1128/AEM.68.3.1071-1081.2002.

Appendix D

Biotechnology Letters **26:** 865–868, 2004.

Fermentation of sugar cane bagasse hemicellulose hydrolysate to L(+)-lactic acid by a thermotolerant acidophilic *Bacillus* sp.**

Milind Patel, Mark Ou, L.O. Ingram & K.T. Shanmugam*
Department of Microbiology and Cell Science, University of Florida, Gainesville, FL 32611, USA
**Author for correspondence (Fax: +352-392-5922; E-mail: shan@ufl.edu)*

Received 21 November 2003; Revisions requested 18 December 2003; Revisions received 16 March 2004; Accepted 17 March 2004

Key words: biocatalyst, fermentation, hemicellulose hydrolysate, lactic acid production, xylose

Abstract

Sugar cane bagasse hemicellulose, hydrolyzed by dilute H_2SO_4, supplemented with mineral salts and 0.5% corn steep liquor, was fermented to L(+)-lactic acid using a newly isolated strain of *Bacillus* sp. In batch fermentations at 50 °C and pH 5, over 5.5% (w/v) L(+)-lactic acid was produced (89% theoretical yield; 0.9 g lactate per g sugar) with an optical purity of 99.5%.

Introduction

Lactic acid is widely used in food, pharmaceutical and textile industries. It is also used as a source of lactic acid polymers which are being used as biodegradable plastics (Brown 2003, Datta *et al.* 1995). The physical properties and stability of polylactides can be controlled by adjusting the proportions of the L(+)- and D(−)-lactides (Tsuji 2002). Optically pure lactic acid is currently produced by the fermentation of glucose derived from corn starch using various lactic acid bacteria (Carr *et al.* 2002, Hofvendahl & Hahn-Hagerdal 2000). However, the fastidious lactic acid bacteria have complex nutritional requirements (Chopin 1993) and the use of corn is not favoured as the feedstock competes directly with the food and feed uses.

Lignocellulosic biomass represents a potentially inexpensive and renewable source of sugars for fermentation (Duff & Murray 1996, Parajo *et al.* 1996, Wyman 1999). The hemicellulose fraction of biomass contains up to 35% of the total carbohydrate that can be readily hydrolyzed to monomeric sugars by dilute sulfuric acid (Saha & Bothast 1999). With crop residues and hardwoods, this hemicellulose syrup contains primarily xylose. During acid hydrolysis, an assortment of microbial inhibitors are also produced which must be removed by treatment with lime (Amartey & Jeffries 1996, Clark & Mackie 1984, Martinez *et al.* 2001).

Lactobacillus spp. are used extensively in industry for starch-based lactic acid production, the majority of which lack the ability to ferment pentose sugars such as xylose and arabinose (Carr *et al.* 2002). Although, *Lactobacillus pentosus*, *Lb. brevis* and *Lactococcus lactis* ferment pentoses to lactic acid, pentoses are metabolized using the phosphoketolase pathway which is inefficient for lactic acid production (Garde *et al.* 2002, Tanaka *et al.* 2002). In the phosphoketolase pathway, xylulose 5-phosphate is cleaved to glyceraldehyde 3-phosphate and acetyl-phosphate. With this pathway, the maximum theoretical yield of lactic acid is limited to one per pentose (0.6 g lactic acid per g xylose) due to the loss of two carbons to acetic acid.

Our laboratory has recently isolated a variety of new sporogenic lactic acid bacteria that grow well at 50 °C and pH 5 and produce L(+)-lactic acid as the primary fermentation product. In this communication, we report the efficient fermentation of hemicellulose hydrolysate from sugar cane bagasse to L(+)-lactic acid by one of these isolates, *Bacillus* sp. strain 17C5.

**This paper is Florida Agricultural Experiment Station Journal Series Number R-09932.

Materials and methods

Organism, media and growth conditions

Bacillus sp. strain 17C5 was isolated from Old Faithful Geyser of California (Calistoga, CA). It was grown on *L*-broth (Lee *et al.* 1985). Sugar cane bagasse hemicellulose hydrolysate was prepared using dilute sulfuric acid under proprietary conditions and was kindly provided by BC International, Dedham, MA. This hydrolysate was treated with lime as described previously (Martinez *et al.* 2001). Total sugar content after lime treatment was 81.3 g l^{-1} (xylose, 68.6 g l^{-1}; glucose, 11.5 g l^{-1}; arabinose, 1.2 g l^{-1}). Media used in fermentation experiments contained, per liter: 50% to 90% v/v lime-treated hydrolysate; 6.25 g Na_2HPO_4, 0.75 g KH_2PO_4, 2 g NaCl, 0.2 g $MgSO_4 \cdot 7H_2O$, 1 g $(NH_4)_2\ SO_4$, 10 mg $FeSO_4 \cdot 7H_2O$, 10 mg $Na_2MoO_4 \cdot 2H_2O$, 1 ml trace mineral solution (Allen & Arnon 1955), and 5 ml corn steep liquor (50% dry solids; Grain Processing Corp., Muscatine, IO). Sterile concentrated solutions of salts and corn steep liquor were added to the lime-treated hemicellulose hydrolysate prior to pH adjustment to 5 and inoculation.

Optical purity of lactic acid

Optical purity of lactic acid was determined by HPLC using a Chiralpak MA(+) column (Chiral Technologies Inc., Exton, PA) with 2 mM $CuSO_4$ as the mobile phase at 0.4 ml per min (32 °C). Corn steep liquor used in the fermentations contained a racemic mixture of D(−)- and L(+)- lactic acids and 0.5% initial concentration used in these experiments introduced 2.6 mM D(−)-lactic acid and 3.4 mM L(+)-lactic acid into the fermentations.

Fermentation

Batch fermentations were carried out as previously described (Beall *et al.* 1991) except at 50 °C and pH of 5. Broth pH was controlled by automatic addition of 2 M KOH. Fresh overnight cultures from *L*-agar were inoculated into *L*-broth (pH 5) with glucose (1%). After incubation for 2.5 h at 50 °C with shaking (200 rpm), this mid-exponential phase culture was used to provide a 1% v/v inoculum for pH-controlled fermenters. Sugar and fermentation products were measured using HPLC (Underwood *et al.* 2002).

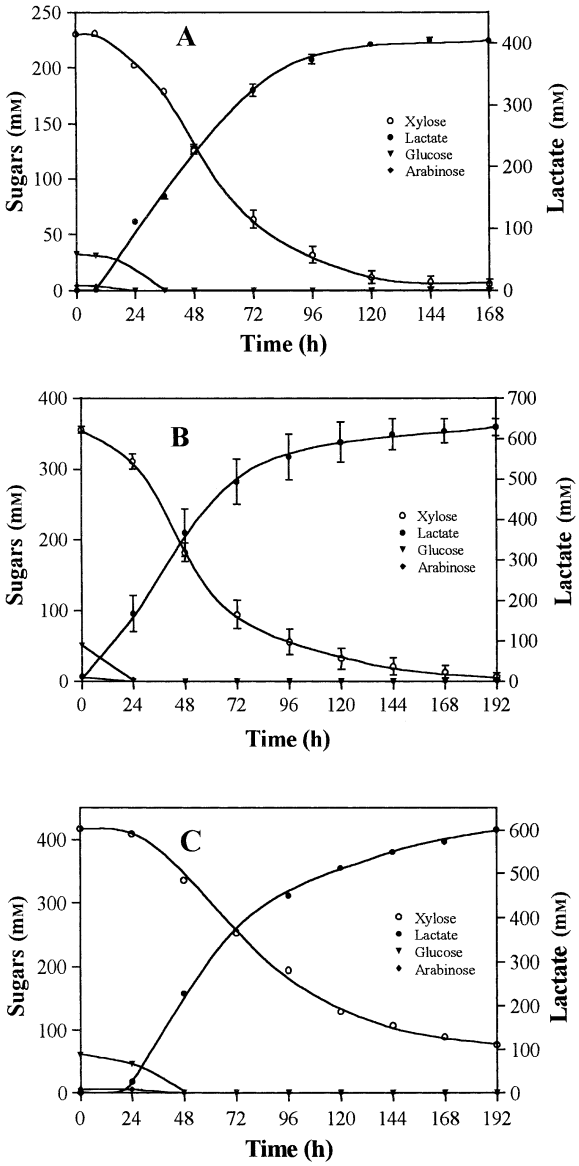

Fig. 1. Fermentation of hemicellulose hydrolysate from sugar cane bagasse by *Bacillus* sp. strain 17C5 at pH 5 and 50 °C. The initial total sugar concentrations were 256 mM (A), 412 mM (B) and 483 mM (C). In hydrolysate media, xylose represented 86% of the total sugars with glucose (12.5%) and arabinose (1.5%) as minor components. Lactate values have been corrected to reflect production by subtracting the small amount of lactate (Table 1) present in media (corn steep liquor) prior to inoculation.

Table 1. Sugar cane bagasse hemicellulose hydrolysate fermentation by *Bacillus* sp. strain 17C5[a].

Sugar[b] (mM)	Sugar consumed (mM)				Net production (mM)[c]				Lactate
	Glucose	Xylose	Arabinose	Lactate	Acetate	Ethanol	Formate	Succinate	Yield (%)[d]
256	32.5 ± 1.6	224.5 ± 9.8	4.5 ± 0.4	403.7 ± 5.6	7 ± 1.2	2.5 ± 0.5	7.8 ± 2.6	4.8 ± 0.8	90
412	50.8 ± 1.2	349.1 ± 9.9	5.5 ± 0.3	617.4 ± 18.4	0.6 ± 0.6	5.2 ± 1	9.5 ± 4.5	7.7 ± 0.4	89
483	60.3	340.4	4.7	600.2	1	3.9	11.1	9.1	86

[a]Fermentations at three concentrations of total sugar (50 °C and pH 5). Averages with standard deviations are based on three independent fermentations. A single fermentation was conducted with the highest sugar concentration, 483 mM.
[b]Sugar concentration at the beginning of fermentation (xylose, 86%; glucose, 12.5%; arabinose, 1.5%).
[c]Lime-treated sugar cane bagasse hemicellulose hydrolysate contained 66 mM acetate. Corn steep liquor at 0.5% final concentration in the fermentations contained 5.5 mM lactate, 0.2 mM acetate and 0.025 mM succinate. Appropriate amounts of these compounds were subtracted to obtain the net production by the biocatalyst. Carbon recovery as products (excluding cells) averaged 90%.
[d]Product yield was calculated as a percentage of the maximum theoretical yield assuming 2 lactates per glucose and 1.67 lactates per pentose.

Results and discussion

Fermentations were conducted at an initial sugar concentration of 256 mM (Figure 1A), 412 mM (Figure 1B) or 483 mM (Figure 1C). In lime-treated hemicellulose hydrolysate from sugar cane bagasse, xylose (86%) was the most abundant sugar with smaller amounts of glucose (12.5%) and arabinose (1.5%). In all fermentations, glucose and arabinose were metabolized first followed by xylose. Fermentation profiles were generally similar for all three levels of sugar although fermentation times increased with substrate. With 256 mM sugar (40 g l^{-1}), lactate production was measurable after 8 h and fermentation was completed within 120 h. With 412 mM sugar (60 g l^{-1}), fermentation proceeded at a constant rate until the lactate concentration reached about 0.4 M (36 g l^{-1} lactic acid). Complete fermentation of all sugars in this fermentation to 617 mM lactate (55.5 g l^{-1}) required an additional 144 h due to a progressively declining fermentation rate. With the highest level of sugar tested (483 mM; 72 g l^{-1}), 78 mM xylose remained after 192 h of incubation. These results suggest that fermentation is inhibited by lactate concentrations above 0.4 M. Even at the highest sugar concentration of 483 mM (about 72 g l^{-1}) the lactate titer did not increase beyond 0.6 M (54 g l^{-1}), consistent with 617 mM (55.8 g l^{-1}) lactate (Table 1) representing a near upper limit for strain 17C5 at pH 5 (50 °C) in this medium.

Irrespective of the initial sugar concentration, the lactic acid produced by strain 17C5 was L(+)-lactic acid at an optical purity of higher than 99%.

Protonated forms of organic acids inhibit bacterial growth (Gatje & Gottschalk 1991, Goncalves *et al.* 1997). Our selection of pH 5 for these experiments would enhance toxicity in comparison to a more neutral pH. Based on the pKa for lactic acid (pH 3.9 at 50 °C), the calculated concentration of free lactic acid in the fermentation broth would be 30 mM at a total lactate concentration of 400 mM. This concentration of undissociated acid is comparable to the 25 mM previously shown to inhibit growth of *Lactobacillus rhamnosus* (Goncalves *et al.* 1997) and consistent with the decline in fermentation rate when lactate was above 400 mM.

Lactate yields were calculated based on sugar utilized and ranged from 0.9 g lactate per g sugar for the lower two sugar concentrations to 0.86 g lactate per g sugar for the highest sugar concentration (Table 1). Maximal volumetric rates of sugar metabolism were determined to be 5.5 mM xylose l^{-1} h^{-1} (approx. 0.8 g sugar l^{-1} h^{-1}).

An analysis of products at the end of fermentation provides a quantitative basis to evaluate potential metabolic pathways for xylose metabolism in strain 17C5. Each mol glucose can be converted into 2 mol lactate by all major glycolytic pathways for hexoses. Two primary pathways are known for pentose metabolism: the transaldolase/transketolase pathway and the phosphoketolase pathway. The transaldolase/transketolase pathway quantitatively converts the pentose sugars (xylose and arabinose) into the three carbon intermediate, pyruvate, providing the potential to produce 1.67 mol lactate per mol pentose. In contrast, the phosphoketolase pathway common to most lactic acid bacteria (Garde *et al.* 2002, Tanaka *et al.* 2002), cleaves a five-carbon intermediate into glyceraldehyde 3-phosphate and acetyl-phosphate. The maximum yield from the phosphoketolase path-

way is 1 mol lactate per mol pentose accompanied by equimolar acetate. Since lactate yields from strain 17C5 (Table 1) averaged over 100-fold that of acetate, strain 17C5 can be presumed to utilize the transaldolase/transketolase pathway for pentose metabolism. Observed lactate yields were about 90% of the theoretical yield calculated with this assumption. Small amounts of succinate, formate and ethanol were also produced during fermentation. With the transaldolase/transketolase pathway, the maximum theoretical yield for lactate is the same for both pentose and hexose sugars on weight basis (1 g lactate per g sugar).

In conclusion, a new group of biocatalysts, exemplified by *Bacillus* sp. strain 17C5, fermented the sugar mixture in hemicellulose hydrolysate to L(+)-lactic acid at high yields using a simple salts medium supplemented with 0.5% corn steep liquor. The L(+)-lactate product had an optical purity of greater than 99% and comprised 90% of the sugar weight. This biocatalyst and genetically modified derivatives are potentially useful for the conversion of pentose-rich feedstocks such as corn stover, corn fiber, bagasse, rice hulls, rice straw, etc. into commodity chemicals such as lactic acid..

Acknowledgements

We thank Dr G. Luli for providing the chiral column used in this study. This study was supported by funds from the US Department of Energy (DE-FC36-01GO11073 and DEFG02-96ER20222), the US Department of Agriculture (01-35504-10669 and 00-52104-9704) and State of Florida, University of Florida Agricultural Experiment station.

References

Allen MB, Arnon DI (1955) Studies on nitrogen-fixing blue-green algae: I. Growth and nitrogen fixation by *Anabaena cylindrica* Lemm. *Plant Physiol.* **30**: 366–372.

Amartey S, Jeffries T (1996) An improvement in *Pichia stipitis* fermentation of acid-hydrolysed hemicellulose achieved by overliming (calcium hydroxide treatment) and strain adaptation. *World J. Microbiol. Biotechnol.* **12**: 281–283.

Beall DS, Ohta K, Ingram LO (1991) Parametric studies of ethanol production from xylose and other sugars by recombinant *Escherichia coli. Biotechnol. Bioeng.* **38**: 296–303.

Brown SF (2003) Bioplastic fantastic. *Fortune* **148**: 92–94.

Carr FJ, Chill D, Maida N (2002) The lactic acid bacteria: a literature survey. *Crit. Rev. Microbiol.* **28**: 281–370.

Chopin A (1993) Organization and regulation of genes for amino acid biosynthesis in lactic acid bacteria. *FEMS Microbiol. Rev.* **12**: 21–38.

Clark TA, Mackie KL (1984) Fermentation inhibitors in wood hydrolysates derived from the softwood *Pinus radiata*. *J. Chem. Technol. Biotechnol.* **34B**: 101–110.

Datta R, Tsai S, Bonsignore P, Moon S, Frank JR (1995) Technological and economic potential of poly(lactic acid) and lactic acid derivatives. *FEMS Microbiol. Rev.* **16**: 221–231.

Duff SJB, Murray WD (1996) Bioconversion of forest products industry waste cellulosics to fuel ethanol: a review. *Bioresour. Technol.* **55**: 1–33.

Garde A, Jonsson G, Schmidt AS, Ahring BK (2002) Lactic acid production from wheat straw hemicellulose hydrolysate by *Lactobacillus pentosus* and *Lactobacillus brevis. Bioresour. Technol.* **81**: 217–223.

Gatje G, Gottschalk G (1991) Limitation of growth and lactic acid production in batch and continuous cultures of *Lactobacillus helveticus. Appl. Microbiol. Biotechnol.* **34**: 446–449.

Goncalves LMD, Ramos A, Almeida JS, Xavier AMRB, Carrondo MJT (1997) Elucidation of the mechanism of lactic acid growth inhibition and production in batch cultures of *Lactobacillus rhamnosus. Appl. Microbiol. Biotechnol.* **48**: 346–350.

Hofvendahl K, Hahn-Hagerdal B (2000) Factors affecting the fermentative lactic acid production from renewable resources. *Enz. Microb. Technol.* **26**: 87–107.

Lee JH, Patel P, Sankar P, Shanmugam KT (1985) Isolation and characterization of mutant strains of *Escherichia coli* altered in H_2 metabolism. *J. Bacteriol.* **162**: 344–352.

Martinez A, Rodriguez ME, Wells ML, York SW, Preston JF, Ingram LO (2001) Detoxification of dilute acid hydrolysates of lignocellulose with lime. *Biotechnol. Prog.* **17**: 287–293.

Parajo JC, Alonso JL, Santos V (1996) Lactic acid from wood. *Process Biochem.* **31**: 271–280.

Saha B, Bothast RJ (1999) Pretreatment and enzymatic saccharification of corn fiber. *Appl. Biochem. Biotechnol.* **76**: 65–77.

Tanaka K, Komiyama A, Sonomoto K, Ishizaki A, Hall SJ, Stanbury PE (2002) Two different pathways for D-xylose metabolism and the effect of xylose concentration on the yield coefficient of L-lactate in mixed-acid fermentation by the lactic acid bacterium *Lactococcus lactis* IO-1. *Appl. Microbiol. Biotechnol.* **60**: 160–167.

Tsuji F (2002) Autocatalytic hydrolysis of amorphous-made polylactides: effects of L-lactide content, tacticity, and enantiomeric polymer blending. *Polymer* **43**: 1789–1796.

Underwood SA, Zhou S, Causey TB, Yomano LP, Shanmugam KT, Ingram LO (2002) Genetic changes to optimize carbon partitioning between ethanol and biosynthesis in ethanologenic *Escherichia coli. Appl. Environ. Microbiol.* **68**: 6263–6272.

Wyman CE (1999) Biomass ethanol: technical progress, opportunities, and commercial challenges. *Annu. Rev. Energ. Env.* **24**: 189–226.

Appendix E

APPLIED AND ENVIRONMENTAL MICROBIOLOGY, Mar. 2007, p. 1766–1771 Vol. 73, No. 6
0099-2240/07/$08.00+0 doi:10.1128/AEM.02456-06

Construction of an *Escherichia coli* K-12 Mutant for Homoethanologenic Fermentation of Glucose or Xylose without Foreign Genes▽

Youngnyun Kim, L. O. Ingram, and K. T. Shanmugam*

Department of Microbiology and Cell Science, University of Florida, Gainesville, Florida 32611

Received 19 October 2006/Accepted 13 January 2007

Conversion of lignocellulosic feedstocks to ethanol requires microorganisms that effectively ferment both hexose and pentose sugars. Towards this goal, recombinant organisms have been developed in which heterologous genes were added to platform organisms such as *Saccharomyces cerevisiae*, *Zymomonas mobilis*, and *Escherichia coli*. Using a novel approach that relies only on native enzymes, we have developed a homoethanologenic alternative, *Escherichia coli* strain SE2378. This mutant ferments glucose or xylose to ethanol with a yield of 82% under anaerobic conditions. An essential mutation in this mutant was mapped within the *pdh* operon (*pdhR aceEF lpd*), which encodes components of the pyruvate dehydrogenase complex. Anaerobic ethanol production by this mutant is apparently the result of a novel pathway that combines the activities of pyruvate dehydrogenase (typically active during aerobic, oxidative metabolism) with the fermentative alcohol dehydrogenase.

Ethanol is an important, renewable transportation fuel that currently replaces a part of our automotive fuel (12, 30). Although ethanol is currently produced in the United States by fermenting glucose from corn starch using *Saccharomyces cerevisiae* (2), expanding this process to produce a large fraction of our fuel requirement may adversely impact the food and feed industry. Cellulosic biomass is an attractive alternative feedstock that can be fermented to ethanol after appropriate pretreatment without impacting the food and feed supply (31, 32). In contrast to corn starch, biomass contains significant amount of pentose sugars that are recalcitrant to fermentation by *Saccharomyces cerevisiae*. Ethanologenic *Escherichia coli* strains containing the *pdc* and *adh* genes from *Zymomonas mobilis* ferment both hexoses and pentoses to ethanol at a high rate and yield (11). Genetic engineering of *S. cerevisiae* and *Z. mobilis* by adding genes for pentose utilization has yet to produce a biocatalyst that matches the pentose fermentation characteristics of recombinant ethanologenic *E. coli* (14, 22). However, the use of a recombinant organism for large-scale fuel production is perceived by some as a barrier to commercialization.

In this report, we describe the development of an ethanologenic *E. coli* mutant that is devoid of foreign genes. This mutant effectively ferments hexose and pentose sugars to ethanol and represents a new alternative to recombinant biocatalysts for fuel ethanol production, especially from pentoses.

MATERIALS AND METHODS

Bacterial strains. *E. coli* K-12 strain W3110 (ATCC 27325) was used as the parent for construction of the ethanologenic strain. The genotypes of the strains used in this study are listed in Table 1. Strain SE2378 is an ethanologenic mutant of strain AH242. Deletion of the genes *pflB*, *adhE*, and *aceF* was done as described by Datsenko et al. (6). An *ldhA* mutant was constructed after introduction of transposon Tn*10* into the *ldhA* gene followed by selection for fusaric acid resistance (13, 18). Construction of other strains utilized standard genetic and molecular biology techniques (19, 21).

Growth medium and fermentation. Rich medium (L broth) contained the following (per liter): Trypticase peptone, 10 g; yeast extract, 5 g; and NaCl, 5 g (16). Mineral salts medium was described previously (16). Glucose or xylose was added at the indicated concentrations. Fermentations were conducted at 37°C (10). Broth was maintained at pH 7.0 by automatic addition of KOH. Batch fermentations were conducted in 13- by 100-mm screw-cap tubes filled to the top as previously described (23).

Analytical methods. Sugars and fermentation products were determined by high-performance liquid chromatography (29). Pyruvate decarboxylase activity was measured in disrupted cell preparations as described previously (27).

Materials. Inorganic salts, organic chemicals, and medium components were obtained from either Fisher Scientific (Pittsburgh, PA) or Sigma Chemical Co. (St. Louis, MO). Corn steep liquor was purchased from the Grain Processing Corp., Muscatine, IA.

RESULTS AND DISCUSSION

Isolation of ethanologenic *E. coli* strain SE2378. Strain AH242 is incapable of anaerobic growth in rich medium containing sugars (Table 2) due to mutations in *ldhA* and *pflB*, encoding lactate dehydrogenase (LDH) and pyruvate formate-lyase (PFL), that prevent oxidation of NADH to NAD^+ (20), an essential substrate for the key glycolytic enzyme glyceraldehyde-3-phosphate dehydrogenase and associated ATP production (4). The absence of LDH eliminated NADH oxidation by the reduction of pyruvate to lactate. Due to the PFL mutation, insufficient acetyl coenzyme A (acetyl-CoA) is available for effective NADH oxidation by native aldehyde and alcohol dehydrogenase activities encoded by *adhE*. Aerobic growth of strain AH242 was unaffected (Table 2).

After mutagenesis with ethyl methane sulfonate (5), mutants of AH242 were recovered that grew anaerobically in rich medium with glucose (1%). Thirty-one independent mutants were tested for anaerobic growth and fermentation products. All mutants produced ethanol as the major fermentation product. One mutant, designated SE2378, was selected for further study. Aerobic growth of SE2378 was comparable to that of the

* Corresponding author. Mailing address: Department of Microbiology and Cell Science, Box 110700, University of Florida, Gainesville, FL 32611. Phone: (352) 392-2490. Fax: (352) 392-5922. E-mail: shan@ufl.edu.

▽ Published ahead of print on 26 January 2007.

TABLE 1. Bacterial strains used in this study

Strain	Relevant genotype	Source
W3110	Wild type	ATCC 27325
AH240	Δ(*focA-pflB*)-FRT-Km-FRT	This study
AH241	Δ(*ldhA*)	This study
AH242	Δ(*ldhA*) Δ(*focA-pflB*)-FRT-Km-FRT	This study
SE2378	AH242, anaerobic growth positive	This study
YK1	SE2378; Km^s	This study
YK29	AH242; Km^s	This study
YK87	YK1; Δ(*adhE*)-FRT-Km-FRT	This study
YK93	YK1; Δ(*aceF*)-FRT-Km-FRT	This study
YK152	YK29; Δ(*aceF*)-FRT-Km-FRT	This study
YK153	W3110; Δ(*aceF*)-FRT-Km-FRT	This study
YK157	YK152; $aceF^+$ (W3110)	YK152 × P1(W3110)
YK158	YK152; $aceF^+$ (SE2378)	YK152 × P1(SE2378)

TABLE 2. Growth characteristics of *E. coli* mutants with mutations in anaerobic pathways

Strain	Genotype	Specific growth rate (h^{-1}) in medium[a]:			
		Aerobic		Anaerobic	
		LB	Minimal	LBG	Minimal
W3110	Wild type	1.31	0.97	0.98	0.51
AH240	*pflB*	1.23	0.99	0.79	0.17
AH241	*ldhA*	1.35	0.94	0.81	0.30
AH242	*pflB ldhA*	1.21	0.97	NG	NG
SE2378	*pflB ldhA* Ana^+	1.18	0.56	0.46	(0.10; 0.16)

[a] LB, L broth; Minimal, glucose-minimal medium; LBG, LB plus glucose (1% [wt/vol]). The concentrations of glucose in minimal medium were 0.3% for aerobic growth and 1% (wt/vol) for anaerobic growth. The first value in parentheses represents the growth rate in glucose-minimal medium with acetate (1 mg ml^{-1}), and the second value is the growth rate in the same medium with glutamate added (1 mg ml^{-1}). NG, no growth.

wild type *E. coli* strain W3110 or any of the single or double mutants affected in PFL or LDH when cultured in rich medium (Table 2). In glucose-minimal medium, the aerobic growth rate of SE2378 was only about 50% of the growth rate of the parent, AH242.

Strain SE2378 grew anaerobically in rich medium, but the growth rate was only about 50% of that of AH240 and AH241 (Table 2). However, strain SE2378 did not grow anaerobically in glucose-minimal medium. In contrast to the *pflB* mutant (AH240) that grew in minimal medium with acetate, the ethanologenic derivative, SE2378, required both acetate and glutamate for comparable anaerobic growth in glucose-minimal medium. Previous studies from our laboratory have shown that ethanologenic *E. coli* strain KO11 also required glutamate for optimum fermentation of xylose (28). This glutamate requirement by KO11 in 9% xylose medium could be replaced by the addition of the protective osmolyte betaine to the medium. However, the glutamate requirement for anaerobic growth of SE2378 in minimal medium (1% sugar) was not suppressed by betaine, consistent with a biosynthetic deficiency due to limited acetyl-CoA flux to 2-ketoglutarate (precursor of glutamate) rather than an osmotic requirement. Apparently, the high rate of conversion of acetyl-CoA to ethanol by this ethanologenic mutant limited the availability of acetyl-CoA for biosynthesis. With these supplements, the growth rate of SE2378 in minimal medium was equivalent to that of the *pflB* parent, AH240. Corn steep liquor, a low-cost medium supplement, replaced glutamate for growth of SE2378 in glucose-minimal medium.

Glucose fermentation. In pH-controlled fermentations with 50 g $liter^{-1}$ glucose (278 mM), SE2378 grew with a specific growth rate of 0.46 h^{-1} after a lag of about 6 h and produced ethanol as the primary product (Fig. 1 and Tables 3 and 4). Since the immediate parent, AH242, did not grow anaerobically, the fermentation of SE2378 was compared to that of W3110. Strain W3110 completely fermented the added glucose in about 24 h, producing acetate, ethanol, lactate, formate, and succinate. The ethanologenic mutant SE2378 required about 72 h to ferment the same amount of glucose. This difference in fermentation time could be a result of cell density differences (2.5 mg dry weight ml^{-1} for the wild type versus 1.7 mg dry weight ml^{-1} for the mutant). Strain SE2378 produced about 480 mmol $liter^{-1}$ ethanol (22 g $liter^{-1}$), 88% of the total products, which included small amounts of acetate, lactate, and succinate. This is in contrast to strain W3110 fermentations, in which ethanol represented only 27% of the products. The maximum specific ethanol productivity (q_P) observed for strain SE2378 was 1.34 g h^{-1} g $cells^{-1}$ (Table 4), comparable to the value of 1.6 g h^{-1} g $cells^{-1}$ reported for batch fermentations with *S. cerevisiae* (26).

Xylose fermentation. The wild-type strain W3110 and mutant strain SE2378 grew at similar rates during anaerobic fermentation with 50 g $liter^{-1}$ xylose (333 mM), although strain SE2378 lagged by approximately 8 h (Fig. 1; Table 4). Specific growth rates on xylose were 80% of those with glucose (Table 4), consistent with previous reports (9). Surprisingly, SE2378 fermented xylose more rapidly than the prototrophic W3110 strain (Fig. 1). Approximately 88% of the fermentation products produced by SE2378 was ethanol. The maximum specific productivity of ethanol for SE2378 with xylose of 2.24 g h^{-1} g $cells^{-1}$ was higher than that with glucose, in agreement with the higher rate of fermentation of xylose than glucose (q_P; Table 4).

It is interesting to note that the specific ethanol productivities of both W3110 and SE2378 were higher with xylose than with glucose, reflecting the higher xylose consumption rate (q_S; Table 4). This may reflect the lower energy yield from xylose metabolism (10). For the wild type, the net ATP yield from xylose is only about 1.5 per xylose, compared to 3.0 per glucose due to the ATP requirement for each of the following three steps in xylose metabolism to pyruvate: xylose transport, phosphorylation of xylulose and fructose-6-phosphate. This would require that the cells utilize more xylose to produce the same amount of cell mass. However, the specific rate of xylose consumption by the wild type was only slightly higher than that of glucose (q_S, 4.93 versus 4.10 g h^{-1} g $cells^{-1}$) (Table 4) accounting for the lower growth rate, cell yield, and longer fermentation time compared to glucose fermentation (Fig. 1). In contrast, SE2378 lacks pyruvate formate-lyase, an enzyme critical for xylose fermentation in minimal medium (10). Although SE2378 produced a small amount of acetate during xylose fermentation, this acetate was produced during the nongrowth, fermentation phase and thus may not be contributing to the overall energetics of the cell. In this ethanologenic mutant, this lower ATP yield from xylose may be compen-

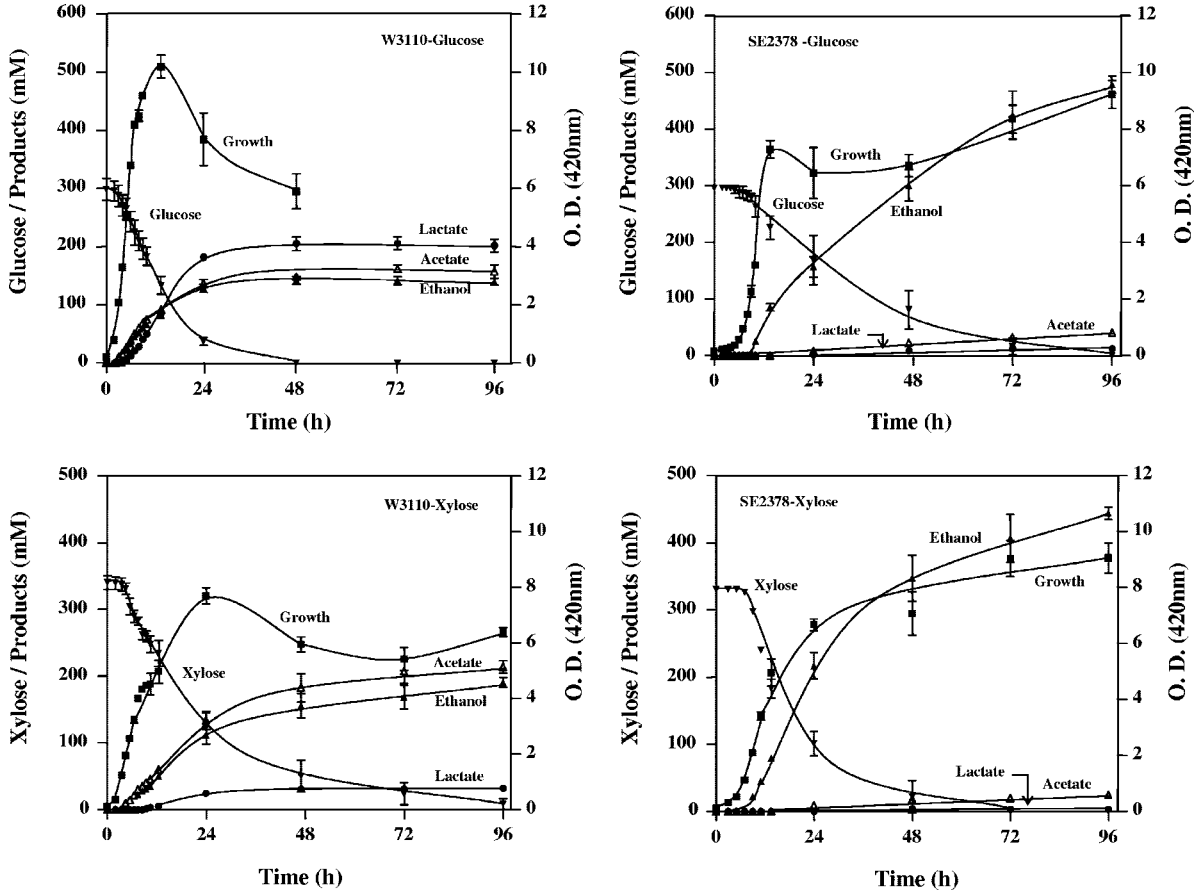

FIG. 1. Growth and fermentation characteristics of *E. coli* wild-type strain W3110 and ethanologenic mutant SE2378 in LB medium with glucose or xylose (50 g liter^{-1}) at 37°C and pH 7.0. O.D., optical density.

sated for by an increase in xylose flux. The specific productivity of ethanol from xylose of 2.24 g h^{-1} g cells^{-1} is higher than the value of 1.6 g h^{-1} g cells^{-1} reported for *S. cerevisiae* on glucose (26) and comparable to the values for glucose or xylose in the ethanologenic *E. coli* strain KO11 carrying the *Z. mobilis pdc* and *adh* genes (about 2 g h^{-1} g cells^{-1}) (unpublished data).

Pathway for homoethanologenic fermentation using native *E. coli* genes. The enzymes of glycolysis convert each mol of glucose into 2 mol of pyruvate plus 2 mol of NADH and a net of 2 mol of ATP. The production of compounds more reduced than pyruvate (ethanol, lactate, etc.) serves as a mechanism to oxidize NADH and regenerate NAD$^+$, essential for glycolysis. In the only known homoethanol pathway that evolved in yeast, plants, and bacteria (i.e., *Z. mobilis*), pyruvate is decarboxylated to yield carbon dioxide and acetaldehyde by the nonoxidative pyruvate decarboxylase. The resulting acetaldehyde serves as the electron acceptor for NADH oxidation by alcohol dehydrogenase during production of one ethanol from each pyruvate (Fig. 2A). *Z. mobilis* genes encoding these activities have been used previously to engineer homoethanol pathways in recombinant ethanologenic bacteria (11).

TABLE 3. Fermentation characteristics of *E. coli* mutant strain SE2378 and wild-type strain W3110[a]

Strain	Concn of sugar consumed (mM)	Concn of product (mM)					Ethanol yield[b]
		Ethanol	Acetate	Formate	Lactate	Succinate	
Glucose fermentation							
W3110	298 ± 19	142 ± 6	162 ± 6	206 ± 11	206 ± 11	18 ± 0.7	0.24 ± 0.01
SE2378	296 ± 4	478 ± 15	27 ± 2	0	13 ± 2	27 ± 2	0.81 ± 0.02
Xylose fermentation							
W3110	333 ± 8	191 ± 7	215 ± 10	248 ± 53	32 ± 3	57 ± 1	0.34 ± 0.00
SE2378	325 ± 2	444 ± 9	25 ± 2	0	0	33 ± 5	0.82 ± 0.01

[a] Fermentations were conducted in L broth supplemented with 50 g liter^{-1} sugar at pH 7.0 and 37°C.
[b] Ethanol yield is shown as a fraction of the theoretical maximum (0.51 g ethanol/g sugar).

TABLE 4. Growth and ethanol production by *E. coli* strain SE2378 grown on glucose or xylose[a]

Fermentation by strain	μ_{max}	$Y_{X/S}$	Q_S	Q_P	$Y_{P/S}$	q_S	q_P
W3110							
Glucose	0.44	0.04	2.94	0.50	0.12	4.10	0.49
Xylose	0.37	0.04	1.58	0.36	0.18	4.93	0.89
SE2378							
Glucose	0.46	0.04	1.29	0.61	0.41	3.26	1.34
Xylose	0.38	0.04	1.65	0.53	0.42	5.33	2.24

[a] Glucose and xylose fermentations by strains W3110 and SE2378 in L broth are presented in Table 3 and Fig. 1. The reported values are calculated maximum values. μ_{max}, specific growth rate h^{-1}; $Y_{X/S}$, g cells g substrate^{-1}; Q_S, g sugar consumed liter^{-1} h^{-1}; Q_P, g ethanol produced liter^{-1} h^{-1}; $Y_{P/S}$, g ethanol g substrate^{-1}; q_S, g sugar consumed g cell dry weight^{-1} h^{-1}; q_P, g ethanol produced g cell dry weight^{-1} h^{-1}.

A completely different ethanol pathway exists in *E. coli* in which pyruvate is converted to acetyl-CoA and formate by pyruvate formate-lyase in which reducing equivalents are contained in the formate and dissipated as hydrogen gas (and CO_2) by formate hydrogen-lyase. One acetyl-CoA is the electron acceptor for the oxidation of two NADH by *adhE*-encoded aldehyde-alcohol dehydrogenase (Fig. 2B). Due to the requirement of 2 NADH per ethanol, the second acetyl-CoA from glycolysis of glucose is converted to acetate and an additional ATP. Thus, the native *E. coli* pathway for ethanol from acetyl-CoA cannot support homoethanol fermentation due to the need for 2 NADH per ethanol produced. Redox balance is preserved by an equal amount of acetate production (Table 3).

Strain AH242 and the ethanologenic derivative SE2378 carry a deletion mutation in *pflB* and are thus incapable of producing formate and acetyl-CoA from pyruvate, blocking the native route for ethanol production. The production of ethanol as the primary fermentation product by strain SE2378 may have resulted from a mutation or mutations that activated expression of a silent unknown gene whose product has catalytic activity resembling that of pyruvate decarboxylase. However, pyruvate decarboxylase activity was not detected in the extracts of anaerobically grown SE2378. Analysis of the *E. coli* genome sequence also failed to reveal coding regions resembling pyruvate decarboxylase. A second alternative is the mutational activation of a silent pyruvate formate-lyase gene (*pflCD*) (1) restoring production of acetyl-CoA. The ethanol yield for SE2378 of 0.8 per pyruvate with an ethanol/acetate ratio of 18 to 1 and the absence of formate in the broth (Table 3) do not support the presence of pyruvate formate-lyase activity in this ethanologen.

A third alternative is the activation of pyruvate dehydrogenase (PDH), an enzyme that normally functions during aerobic growth while pyruvate formate-lyase is inactive. By metabolizing pyruvate with PDH, an additional NADH per pyruvate is made available that can be used to fully reduce each acetyl-CoA to ethanol (Fig. 2C), consistent with the observed high ethanol yield and low acetate/ethanol ratio for strain SE2378. Although genes coding for pyruvate dehydrogenase are typically expressed under both aerobic and anaerobic conditions in *E. coli*, the activity of this complex during anaerobic growth has been reported to be very low (3, 8). This lack of activity in the anaerobic cell is proposed to result from an inhibition of PDH activity by both NADH and pyruvate (7, 25). It is likely that mutations increasing the activity of this enzyme complex under anaerobic conditions have occurred to produce a homoethanol pathway in SE2378. Since 6 mol of xylose is metabolized to 10 mol of pyruvate and 10 mol of NADH, analogous arguments and yields can be directly applied to the homoethanol pathway used for pentose sugars in this mutant.

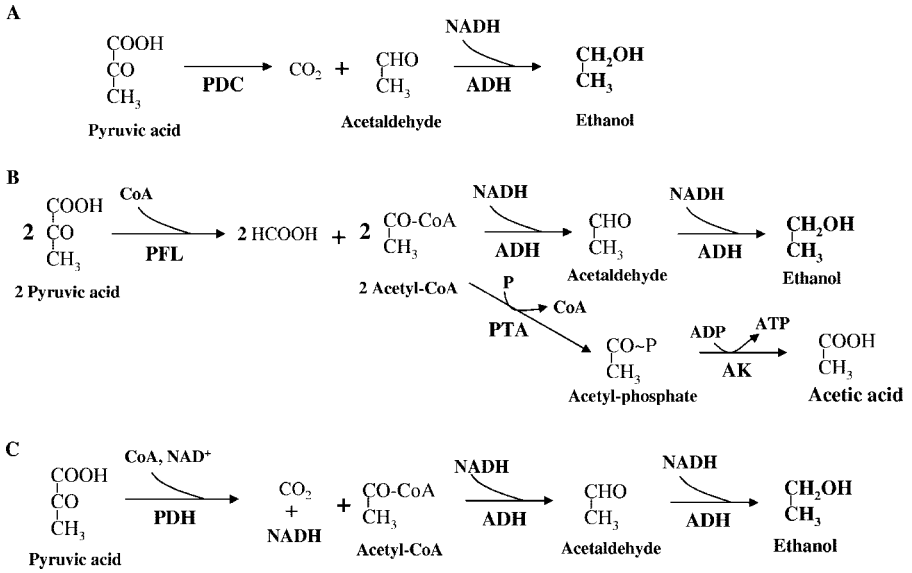

FIG. 2. Proposed pathway for ethanol production from pyruvate in *E. coli* SE2378, native *E. coli*, and other ethanologenic microorganisms. (A) Pathway for ethanologenic organisms (yeast, *Z. mobilis*, and recombinant ethanologenic *E. coli*). (B) Native pathway for ethanol production in *E. coli*. (C) Proposed pathway for ethanol production in *E. coli* strain SE2378. PDC, pyruvate decarboxylase; ADH, alcohol dehydrogenase E; PFL, pyruvate formate-lyase; PTA, phosphotransacetylase; AK, acetate kinase; PDH, pyruvate dehydrogenase.

TABLE 5. Growth characteristics of ethanologenic *E. coli* strain SE2378 with a mutation in the *pdh* locus

Strain	Genotype	Specific growth rate (h^{-1}) on medium[a]:			
		Aerobic		Anaerobic	
		LB	Minimal	LB	Minimal
W3110	Wild type	1.31	1.05	0.98	0.51
YK153	W3110; *aceF*	0.46	NG (0.55)	1.07	0.44
YK152	*pflB ldhA aceF*	0.83	NG (0.54)	NG	NG
YK157	YK152; *aceF*$^+$ (W3110)	1.32	0.96	NG	NG
YK158	YK152; *aceF*$^+$ (SE2378)	1.17	0.51	0.45	NG[b]

[a] Minimal, glucose-minimal medium. Values in parentheses represent the specific growth rate in glucose-minimal medium with acetate (1 mg ml^{-1}) under aerobic conditions. NG, no growth.

[b] The ethanologenic derivative YK158 requires acetate and glutamate for optimal anaerobic growth in glucose minimal medium as for strain SE2378 (Table 2). See Table 2 for other details.

Pyruvate dehydrogenase is essential for homoethanol production. Preliminary genetic analysis of SE2378 revealed that the mutation or mutations responsible for anaerobic growth and homoethanol production by the *ldhA pflB* double mutant are located in or near the genes coding for PDH complex (*pdh* locus: *pdhR aceEF lpd*) (24). To confirm that PDH is required for the ethanologenic phenotype of SE2378, a mutation in the *aceF* gene (dihydrolipoyl acetyltransferase; E2 enzyme of PDH) was transduced into SE2378 (strain YK152). Anaerobic growth of strain YK152 was defective in all of the media tested (Table 5). The *aceF* mutation in strain YK152 was transduced to *aceF*$^+$ by phage P1 with the gene from either W3110 (wild type) or SE2378 (ethanologen), and the transductants were selected for growth in minimal medium under aerobic conditions. Transductants that received the *aceF*$^+$ gene from the wild-type strain, W3110, grew aerobically in minimal medium but failed to grow anaerobically in any of the media tested due to the presence of *ldhA* and *pflB* mutations. On the other hand, all transductants receiving the *aceF*$^+$ gene from strain SE2378 grew anaerobically and all of the tested transductants produced ethanol as the main fermentation product. Ethanol accounted for about 90% of the total fermentation products produced by YK158 grown in L broth (LB)-glucose medium (data not presented), a value that is similar to that of SE2378 (Table 3). These results show that the ethanologenic phenotype of SE2378 requires PDH activity and are in agreement with the proposed PDH-dependent pathway (Fig. 2C) for ethanol production.

In this new pathway for homoethanol production, pyruvate is oxidatively decarboxylated to acetyl-CoA with the conservation of reductant as NADH, allowing both the reduction of acetyl-CoA to acetaldehyde and the reduction of acetaldehyde to ethanol by alcohol dehydrogenase E containing both aldehyde and alcohol dehydrogenase activities (Fig. 2C). Deletion of either *aceF* (PDH negative; YK93), required for acetyl-CoA production, or *adhE* (ADH negative; YK87), needed for ethanol production, resulted in loss of anaerobic growth, supporting the essential role of both activities for anaerobic growth of SE2378 lacking fermentative lactate dehydrogenase and pyruvate formate-lyase.

Similar conservation of reductant as NADH during pyruvate decarboxylation to acetyl-CoA has been observed in the ethanologenic anaerobes *Thermoanaerobium brockii* and *Thermoanaerobacter ethanolicus* (formerly *Clostridium thermohydrosulfuricum*). In these anaerobes, pyruvate-ferredoxin oxidoreductase produces acetyl-CoA and reduced ferredoxin from pyruvate. Reductant from the reduced ferredoxin is channeled to NAD^+ by ferredoxin-NADH oxidoreductase. Combination of these two enzyme activities produces the needed second NADH for reduction of acetyl-CoA to ethanol (15, 17).

In conclusion, an *E. coli* mutant has been developed that produces ethanol as the primary fermentation product from both glucose and xylose using only the native genetic repertoire of the *E. coli* chromosome. The rate of fermentation of xylose by the mutant was higher than that of glucose fermentation, with a specific ethanol productivity comparable to those of other ethanologenic organisms on glucose or xylose. The putative metabolic pathway for conversion of pyruvate to ethanol in this strain involves the pyruvate dehydrogenase complex and alcohol dehydrogenase E instead of pyruvate decarboxylase and alcohol dehydrogenase typical of other homoethanologenic organisms such as *S. cerevisiae*, *Z. mobilis*, and recombinant ethanologenic bacteria. Further metabolic engineering is expected to optimize this pathway towards the development of a nonrecombinant ethanologen that can ferment all of the sugars in lignocellulosic biomass. Development of this type of nonrecombinant bacterial biocatalyst may reduce one of the perceived barriers to commercial ethanol production from lignocellulosic substrates.

ACKNOWLEDGMENTS

We thank Lee Ann Blalock for performing pyruvate decarboxylase assays.

This work was supported by a grant from the Department of Energy (DE-FG36-04GO14019).

REFERENCES

1. **Blattner, F. R., G. Plunkett III, C. A. Bloch, N. T. Perna, V. Burland, M. Riley, J. Collado-Vides, J. D. Glasner, C. K. Rode, G. F. Mayhew, J. Gregor, N. W. Davis, H. A. Kirkpatrick, M. A. Goeden, D. J. Rose, B. Mau, and Y. Shao.** 1997. The complete genome sequence of *Escherichia coli* K-12. Science **277:**1453–1474.
2. **Bothast, R. J., and M. A. Schlicher.** 2005. Biotechnological processes for conversion of corn into ethanol. Appl. Microbiol. Biotechnol. **67:**19–25.
3. **Cassey, B., J. R. Guest, and M. M. Attwood.** 1998. Environmental control of pyruvate dehydrogenase complex expression in *Escherichia coli*. FEMS Microbiol. Lett. **159:**325–329.
4. **Clark, D. P.** 1989. The fermentation pathways of *Escherichia coli*. FEMS Microbiol. Rev. **5:**223–234.
5. **Close, T. J., and K. T. Shanmugam.** 1980. Genetic analysis of a pleiotropic mutant of *Klebsiella pneumoniae* affected in nitrogen metabolism. J. Gen. Microbiol. **116:**501–510.
6. **Datsenko, K. A., and B. L. Wanner.** 2000. One-step inactivation of chromosomal genes in *Escherichia coli* K-12 using PCR products. Proc. Natl. Acad. Sci. USA **97:**6640–6645.
7. **Datta, A.** 1991. Characterization of the inhibition of *Escherichia coli* pyruvate dehydrogenase complex by pyruvate. Biochem. Biophys. Res. Commun. **176:** 517–521.
8. **de Graef, M. R., S. Alexeeva, J. L. Snoep, and M. J. Teixeira de Mattos.** 1999. The steady-state internal redox state (NADH/NAD) reflects the external redox state and is correlated with catabolic adaptation in *Escherichia coli*. J. Bacteriol. **181:**2351–2357.
9. **Gonzalez, R., H. Tao, K. T. Shanmugam, S. W. York, and L. O. Ingram.** 2002. Global gene expression differences associated with changes in glycolytic flux and growth rate in *Escherichia coli* during fermentation of glucose and xylose. Biotechnol. Prog. **18:**6–20.
10. **Hasona, A., Y. Kim, F. G. Healy, L. O. Ingram, and K. T. Shanmugam.** 2004. Pyruvate formate lyase and acetate kinase are essential for anaerobic growth of *Escherichia coli* on xylose. J. Bacteriol. **186:**7593–7600.
11. **Ingram, L. O., H. C. Aldrich, A. C. Borges, T. B. Causey, A. Martinez, F. Morales, A. Saleh, S. A. Underwood, L. P. Yomano, S. W. York, J. Zaldivar, and S. Zhou.** 1999. Enteric bacterial catalysts for fuel ethanol production. Biotechnol. Prog. **15:**855–866.

12. **Kheshgi, H. S., R. C. Prince, and G. Marland.** 2000. The potential of biomass fuels in the context of global climate change: focus on transportation fuels. Annu. Rev. Energy Env. **25:**199–244.
13. **Kleckner, N., J. Bender, and S. Gottesman.** 1991. Uses of transposons with emphasis on Tn10. Methods Enzymol. **204:**139–180.
14. **Kuyper, M., M. J. Toirkens, J. A. Diderich, A. A. Winkler, J. P. van Dijken, and J. T. Pronk.** 2005. Evolutionary engineering of mixed-sugar utilization by a xylose-fermenting *Saccharomyces cerevisiae* strain. FEMS Yeast Res. **5:**925–934.
15. **Lamed, R., and J. G. Zeikus.** 1980. Ethanol production by thermophilic bacteria: relationship between fermentation product yields of and catabolic enzyme activities in *Clostridium thermocellum* and *Thermoanaerobium brockii*. J. Bacteriol. **144:**569–578.
16. **Lee, J. H., P. Patel, P. Sankar, and K. T. Shanmugam.** 1985. Isolation and characterization of mutant strains of *Escherichia coli* altered in H_2 metabolism. J. Bacteriol. **162:**344–352.
17. **Lovitt, R. W., G.-J. Shen, and J. G. Zeikus.** 1988. Ethanol production by thermophilic bacteria: biochemical basis for ethanol and hydrogen tolerance in *Clostridium thermohydrosulfuricum*. J. Bacteriol. **170:**2809–2815.
18. **Maloy, S., and W. D. Nunn.** 1981. Selection for loss of tetracycline resistance by *Escherichia coli*. J. Bacteriol. **145:**1110–1112.
19. **Maniatis, T., E. F. Fritsch, and J. Sambrook.** 1982. Molecular cloning: a laboratory manual. Cold Spring Harbor Laboratory Press, Cold Spring Harbor, NY.
20. **Mat-Jan, F., K. Y. Alam, and D. P. Clark.** 1989. Mutants of *Escherichia coli* deficient in the fermentative lactate dehydrogenase. J. Bacteriol. **171:**342–348.
21. **Miller, J. H.** 1972. Experiments in molecular genetics. Cold Spring Harbor Laboratory, Cold Spring Harbor, NY.
22. **Mohagheghi, A., N. Dowe, D. Schell, Y. Chou, C. Eddy, and M. Zhang.** 2004. Performance of a newly developed integrant of *Zymomonas mobilis* for ethanol production on corn stover hydrolysate. Biotechnol. Lett. **26:**321–325.
23. **Patel, M. A., M. S. Ou, R. Harbrucker, H. C. Aldrich, M. L. Buszko, L. O. Ingram, and K. T. Shanmugam.** 2006. Isolation and characterization of acid-tolerant, thermophilic bacteria for effective fermentation of biomass-derived sugars to lactic acid. Appl. Environ. Microbiol. **72:**3228–3235.
24. **Quail, M. A., D. J. Hayden, and J. R. Guest.** 1994. The *pdhR-aceEF-lpd* operon of *Escherichia coli* expresses the pyruvate dehydrogensae complex. Mol. Microbiol. **12:**95–104.
25. **Shen, L. C., and D. E. Atkinson.** 1970. Regulation of pyruvate dehydrogenase from *Escherichia coli*. Interactions of adenylate energy charge and other regulatory parameters. J. Biol. Chem. **245:**5974–5978.
26. **Smits, H. P., J. Hauf, S. Muller, T. J. Hobley, F. K. Zimmermann, B. Hahn-Hagerdal, J. Nielsen, and L. Olsson.** 2000. Simultaneous overexpression of enzymes of the lower part of glycolysis can enhance the fermentative capacity of *Saccharomyces cerevisiae*. Yeast **16:**1325–1334.
27. **Talarico, L. A., L. O. Ingram, and J. A. Maupin-Furlow.** 2001. Production of the Gram-positive *Sarcina ventriculi* pyruvate decarboxylase in *Escherichia coli*. Microbiology **147:**2425–2435.
28. **Underwood, S. A., M. L. Buszko, K. T. Shanmugam, and L. O. Ingram.** 2004. Lack of protective osmolytes limits final cell density and volumetric productivity of ethanologenic *Escherichia coli* KO11 during xylose fermentation. Appl. Environ. Microbiol. **70:**2734–2740.
29. **Underwood, S. A., S. Zhou, T. B. Causey, L. P. Yomano, K. T. Shanmugam, and L. O. Ingram.** 2002. Genetic changes to optimize carbon partitioning between ethanol and biosynthesis in ethanologenic *Escherichia coli*. Appl. Environ. Microbiol. **68:**6263–6272.
30. **Wooley, R., M. Ruth, D. Glassner, and J. Sheehan.** 1999. Process design and costing of bioethanol technology: a tool for determining the status and direction of research and development. Biotechnol. Prog. **15:**794–803.
31. **Wyman, C. E.** 2003. Potential synergies and challenges in refining cellulosic biomass to fuels, chemicals, and power. Biotechnol. Prog. **19:**254–262.
32. **Zaldivar, J., J. Nielsen, and L. Olsson.** 2001. Fuel ethanol production from lignocellulose: a challenge for metabolic engineering and process integration. Appl. Microbiol. Biotechnol. **56:**17–34.

Appendix F

JOURNAL OF BACTERIOLOGY, June 2008, p. 3851–3858 Vol. 190, No. 11
0021-9193/08/$08.00+0 doi:10.1128/JB.00104-08

Dihydrolipoamide Dehydrogenase Mutation Alters the NADH Sensitivity of Pyruvate Dehydrogenase Complex of *Escherichia coli* K-12[▽]

Youngnyun Kim,† L. O. Ingram, and K. T. Shanmugam*

Department of Microbiology and Cell Science, University of Florida, Gainesville, Florida 32611

Received 21 January 2008/Accepted 18 March 2008

Under anaerobic growth conditions, an active pyruvate dehydrogenase (PDH) is expected to create a redox imbalance in wild-type *Escherichia coli* due to increased production of NADH (>2 NADH molecules/glucose molecule) that could lead to growth inhibition. However, the additional NADH produced by PDH can be used for conversion of acetyl coenzyme A into reduced fermentation products, like alcohols, during metabolic engineering of the bacterium. *E. coli* mutants that produced ethanol as the main fermentation product were recently isolated as derivatives of an *ldhA pflB* double mutant. In all six mutants tested, the mutation was in the *lpd* gene encoding dihydrolipoamide dehydrogenase (LPD), a component of PDH. Three of the LPD mutants carried an H322Y mutation (*lpd102*), while the other mutants carried an E354K mutation (*lpd101*). Genetic and physiological analysis revealed that the mutation in either allele supported anaerobic growth and homoethanol fermentation in an *ldhA pflB* double mutant. Enzyme kinetic studies revealed that the LPD(E354K) enzyme was significantly less sensitive to NADH inhibition than the native LPD. This reduced NADH sensitivity of the mutated LPD was translated into lower sensitivity of the appropriate PDH complex to NADH inhibition. The mutated forms of the PDH had a 10-fold-higher K_i for NADH than the native PDH. The lower sensitivity of PDH to NADH inhibition apparently increased PDH activity in anaerobic *E. coli* cultures and created the new ethanologenic fermentation pathway in this bacterium. Analogous mutations in the LPD of other bacteria may also significantly influence the growth and physiology of the organisms in a similar fashion.

Escherichia coli, a facultative heterotroph, grows under aerobic and anaerobic conditions. During aerobic growth, this bacterium metabolizes glucose through the reactions of glycolysis, pyruvate dehydrogenase (PDH), and the tricarboxylic acid cycle. The NADH generated during these enzyme-catalyzed reactions is oxidized ultimately by oxygen. Under anaerobic conditions and in the absence of external electron acceptors, organic compounds generated from glucose during glycolysis serve as the electron acceptors to maintain the redox balance and continued growth of the bacterium. Due to the differences in electron acceptors between the two growth modes, the reported [NADH]/[NAD^+] ratio of an anaerobic cell is severalfold higher (about 0.75) than that of an aerobic cell (about 0.03) (13, 33).

The PDH complex that connects glycolysis and tricarboxylic acid cycle enzymes is composed of multiple subunits of three enzymes, pyruvate decarboxylase (dehydrogenase; enzyme 1 [E1]; EC 1.2.4.1), dihydrolipoamide acetyltransferase (enzyme 2 [E2]; EC 2.3.1.12), and dihydrolipoamide dehydrogenase (LPD) (enzyme 3 [E3]; EC 1.8.1.4) (14). NADH, a product of the PDH reaction, is a competitive inhibitor of the PDH complex (15, 30, 31). The NADH sensitivity of the PDH complex has been demonstrated to reside in LPD, the enzyme that interacts with NAD^+ as a substrate (29, 30, 38). Although PDH is critical for aerobic growth of the bacterium, this activity was also detectable in cell extracts of *E. coli* grown under anaerobic conditions (13, 32, 33). However, based on the product profile, the PDH activity in vivo in anaerobic *E. coli* cultures is either very low or undetectable (33).

In an anaerobically growing *E. coli* strain lacking PDH activity, pyruvate is metabolized by an alternative enzyme, pyruvate-formate lyase, to acetyl coenzyme A (acetyl-CoA) with conservation of the reductant as formate (9). Formate is ultimately removed as H_2 and CO_2 without influencing the [NADH]/[NAD^+] ratio of the cell (28). In order to maintain the redox balance, the NADH generated during the oxidation of glyceraldehyde-3-phosphate in the glycolysis pathway is oxidized using acetyl-CoA as the electron acceptor, with the production of ethanol (9). However, reduction of acetyl-CoA to ethanol by alcohol dehydrogenase requires two NADH molecules for each acetyl-CoA molecule, a demand that is not met by fermenting *E. coli*. Due to this constraint, the fermentation profile of a growing *E. coli* strain includes equimolar quantities of ethanol and acetate.

We recently isolated and described *E. coli* mutants that produced ethanol as the main fermentation product (19). The mutation in one of these mutants was mapped in the genes of the *pdh* locus (*pdhR*, *aceEF*, and *lpd*). Based on the phenotype and genetic analysis, it was inferred that PDH, the enzyme that is normally inactive in an anaerobic *E. coli* cell, plays a pivotal role in ethanol production by this mutant. Conversion of glucose to two acetyl-CoA molecules by the glycolytic enzymes and PDH would yield four NADH molecules per glucose molecule, and these four NADH molecules can be oxidized using

* Corresponding author. Mailing address: Department of Microbiology and Cell Science, Box 110700, University of Florida, Gainesville, FL 32611. Phone: (352) 392-2490. Fax: (352) 392-5922. E-mail: shan@ufl.edu.

† Present address: Amyris Biotechnologies, Inc., 5980 Horton Street, Ste. 450, Emeryville, CA 94608.

▽ Published ahead of print on 28 March 2008.

TABLE 1. Bacterial strains, plasmids, and phages used in this study

Strain, plasmid, or phage	Relevant genotype	Source or reference
E. coli K-12 strains		
W3110	Wild type	ATCC
AH241	W3110, Δ*ldhA*	19
AH242	W3110, Δ*ldhA* Δ(*focA-pflB*)-Km	19
BW25113	*lacI*^{q} *rrnB*$_{T14}$ Δ*lacZ*$_{W116}$ *hsdR514* Δ*araBAD*$_{AH33}$ Δ*rhaBAD*$_{LD78}$	B. Wanner
JM109(λDE3)	F′ [*traD36 proA*$^+$*B*$^+$ *lacI*^{q} Δ(*lacZ*)*M15*] Δ(*lac-proAB*) *glnV44 e14*$^-$ *gyrA96 recA1 relA1 endA1 thi hsdR17* (λDE3)	Promega
SE2377	AH242, *lpd102*(H322Y)	This study
SE2378	AH242, *lpd101*(E354K)	19
SE2382	AH242, *lpd101*(E354K)	This study
SE2383	AH242, *lpd102*(H322Y)	This study
SE2384	AH242, *lpd102*(H322Y)	This study
SE2385	AH242, *lpd101*(E354K)	This study
YK1	SE2378, Km^s	This study
YK29	AH242, Km^s	This study
YK87	YK1, Δ*adhE*-Km	This study
YK100	AH242, Δ*lpd*	This study
YK110	YK100, *lpd*$^+$	YK100 × P1(W3110)
YK111	YK100, *lpd101*	YK100 × P1(SE2378)
YK128	YK100, P*lpd*$^+$ (pKY32)	This study
YK129	YK100, P*lpd101* (pKY33)	This study
YK139	YK100, *lpd102*	YK100 × P1(SE2377)
YK141	YK100, *lpd101*	YK100 × P1(SE2382)
YK175	AH241, Δ*adhE*-Km	AH241 × P1(YK87)
YK176	YK141, Δ*adhE*-Km	YK141 × P1(YK87)
YK181	YK139, Δ*adhE*-Km	YK139 × P1(YK87)
Plasmids		
pKY10	pUC19, P*pdhR*$_{SE2378}$	This study
pKY13	pUC19, P*pdhR*$^+$	This study
pKY15	pTL61t, P*pdh*$_{SE2378}$-*lacZ*	This study
pKY17	pTL61t, P*pdh*$_{W3110}$-*lacZ*	This study
pKY32	pTrc99a, *lpd*$^+$ *bla*	This study
pKY33	pTrc99a, *lpd101 bla*	This study
pKY36	pET15b, *lpd*$^+$ *bla*	This study
pKY37	pET15b, *lpd101 bla*	This study
pKY38	pET15b, *lpd102 bla*	This study
Phages		
λYK1	λ(P*pdh*$_{W3110}$-*lacZ*)	This study
λYK2	λ(P*pdh*$_{SE2378}$-*lacZ*)	This study

the two acetyl-CoA molecules as the electron acceptors and alcohol dehydrogenase as the catalyst, with production of two equivalents of ethanol. For PDH to be active in an anaerobic cell, the LPD component of the PDH complex is expected to have lost at least part of its sensitivity to NADH inhibition.

Based on the DNA sequence, we localized the mutations in the ethanologenic *E. coli* mutants to a single change in the LPD amino acid sequence. The results presented in this paper show that the PDH from two such ethanologenic mutants, strains SE2377 and SE2378, are less sensitive to NADH inhibition. The alteration of the LPD and PDH complex to reduced sensitivity to NADH inhibition apparently allowed the enzyme to function in an anaerobic *E. coli* culture, which changed the fermentation profile of the mutant.

MATERIALS AND METHODS

Materials. Biochemicals were purchased from Sigma-Aldrich. Organic and inorganic chemicals were purchased from Fisher Scientific and were analytical grade. DNA restriction endonucleases, T4 DNA ligase, DNA polymerases, and other DNA modification enzymes and reagents were obtained from New England Biolabs Inc., Invitrogen, or Clontech Laboratories. The quantitative reverse transcription (RT)-PCR reagent was obtained from Bio-Rad Laboratories. Oligonucleotide primers were synthesized by Invitrogen or Sigma-Genosys.

Bacterial strains, bacteriophages, and plasmids. The bacterial strains, bacteriophages, and plasmids used in this study are listed in Table 1. All *E. coli* strains are derivatives of strain K-12.

Media and growth conditions. L broth (LB), used as the rich medium, and mineral salts medium were prepared as described previously (21). After the medium was autoclaved, sugars were added at final concentrations of 3 g/liter for aerobic growth and 10 g/liter for anaerobic growth. The media used for propagation of phages P1 and λ, as well as transduction, were prepared as described by Miller (25). Batch fermentation without pH control was carried out in screw-cap tubes (13 by 100 mm) filled to the top with the appropriate medium (19). The inoculum (1%, vol/vol) for the fermentations was grown aerobically for about 16 h. Antibiotics were added, as needed, at initial concentrations of 100 mg/liter of ampicillin and 50 mg/liter of kanamycin.

Genetic methods. Gene deletions in *E. coli* were constructed as described by Datsenko and Wanner (11). Appropriate genes were amplified by PCR and cloned into plasmid pCR2.1-TOPO (Invitrogen). After deletion of part of the gene, a DNA cassette containing a kanamycin resistance gene flanked by FRT sites was integrated into the deleted area. The antibiotic resistance gene with the flanking *E. coli* DNA was PCR amplified, and the PCR product was transformed into *E. coli* strain BW25113(pKD46) that was pregrown in LB containing arabinose as described previously (11). Transformants with the gene deletion were selected and verified by PCR. The deletion mutation was transduced by phage P1

to other genetic backgrounds before use. All molecular biology experiments were performed as described previously (28).

In vitro mutagenesis of *lpd*. The *lpd* gene in plasmid pKY32 was mutagenized by using either hydroxylamine or error-prone PCR. Hydroxylamine mutagenesis was performed as described by Davis et al. (12). Error-prone PCR was conducted as described previously (24) with the same primer set that was used for cloning the *lpd* gene into plasmid pET15b. In addition to the *Taq* polymerase buffer (New England Biolabs), the following ingredients were also added to increase the mutation rate: 0.8 mM dTTP, 0.8 mM dCTP, 4.8 mM $MgCl_2$, and 0.5 mM $MnCl_2$. PCR was performed using the following conditions with a Bio-Rad thermal cycler: 1 min at 95°C, followed by five cycles of 1 min at 95°C, 30 s at 45°C, and 2 min at 72°C, by 30 cycles of 1 min at 95°C, 30 s at 55°C, and 2 min at 72°C, and finally by 15 min at 72°C. The PCR product was purified, cloned into plasmid vector pTrc99a, and transformed into *E. coli* strain AH242. Transformants that grew anaerobically were selected, and the *lpd* gene in the plasmid was sequenced to identify the nature of the mutation.

Level of transcription of *pdh* operon. The *pdh* operon promoter DNA was removed from either plasmid pKY13 (W3110) or plasmid pKY10 (SE2378) after hydrolysis with BlpI and AflII. The DNA fragment was treated with the Klenow fragment of DNA polymerase and cloned into the SmaI site of plasmid pTL61t (23) upstream of a promoterless *lacZ* gene. The plasmid constructs (pKY15 for SE2378 P*pdh-lac* and pKY17 for W3110 P*pdh-lac*) were selected after transformation of *E. coli* TOP10 (Invitrogen) as blue colonies on LB containing ampicillin with X-Gal (5-bromo-4-chloro-3-indolyl-β-D-galactopyranoside) (40 μg/ml). The cloned *pdh* promoter DNA was sequenced to confirm the sequence. The P*pdh-lac* fusion was transferred to λRZ5 and transduced into *E. coli* as described previously (28).

Lysogens carrying the λP*pdh-lacZ* fusion were cultured under aerobic (LB) or anaerobic (LB containing glucose) conditions to the mid- to late exponential phase of growth. The β-galactosidase activity of the cells was determined as described by Miller (25). The specific activity of β-galactosidase was expressed in nmol · min^{-1} · mg cell $protein^{-1}$.

Quantitative RT-PCR. For isolation of total RNA, aerobic cultures were grown in 10 ml of LB in 250-ml flasks at 37°C with shaking at 200 rpm. Anaerobic cultures were grown in 9 ml of LB containing glucose in screw-cap tubes (13 by 100 mm) filled to the top. Cells were harvested at the early to mid-exponential phase of growth. Total RNA was extracted by the hot phenol method as described previously (34). Quantitative RT-PCR was performed as described previously (35).

LPD expression plasmids. Different alleles of the *lpd* gene were cloned into plasmid pTrc99a and expressed from a lactose-regulated promoter for complementation experiments. For construction of the plasmids, DNA encoding a specific *lpd* allele was amplified by PCR from appropriate *E. coli* genomic DNA. The forward primer (GCGACCATGGAGAAGGAGATATACCATGAGT ACT) contained an NcoI restriction site at the 5′ end (underlined), and the reverse primer (GCGAAAGCTTTTACTTCTTCTTCGCTTTCG) contained a HindIII restriction site at the 5′ end (underlined). A Shine-Dalgarno sequence (ribosomal binding site) was also located 7 nucleotides upstream of the start codon (ATG) in the forward primer. Both the PCR product and plasmid pTrc99A were hydrolyzed with restriction enzymes NcoI and HindIII and ligated to construct plasmids pKY32 and pKY33 containing lpd^+ and the *lpd101* allele, respectively.

For purification of LPD, the appropriate *lpd* allele was cloned into a phage T7-based expression vector. For construction of plasmids pKY36 (lpd^+), pKY37 (*lpd101*), and pKY38 (*lpd102*), the appropriate *lpd* gene was amplified by PCR with the following primers: forward primer GAGCCTCGAGATGAGTACTG AAATC and reverse primer GCGTGGATCCTTACTTCTTCTTCG. The forward primer contained an XhoI restriction site at the 5′ end (underlined), and the reverse primer had a BamHI restriction site at the 5′ end (underlined). The PCR products, digested with XhoI and BamHI, were ligated with plasmid pET-15b also digested with XhoI and BamHI. *E. coli* TOP10 cells were transformed with the ligation product, and the transformants were selected for resistance to ampicillin on LB containing ampicillin. The insert sequences in the plasmids were verified by sequencing the *lpd* gene.

Purification of LPD. For purification of LPD, the enzyme was produced in strain JM109(λDE3) transformed with plasmid pKY36, pKY37, or pKY38. A 500-ml culture in LB containing ampicillin in a 2.8-liter Fernbach flask was grown at 37°C with shaking at 250 rpm to an optical density at 420 nm of 0.6 (Beckman DU640 spectrophotometer). Arabinose (1.5%) was added to the culture to induce the T7 RNA polymerase (26). After 4 h of incubation at room temperature with shaking, cells were harvested by centrifugation (10,000 × *g*, 10 min, 4°C), washed twice with 25 ml of 50 mM potassium phosphate buffer (pH 8.0) (referred to as phosphate buffer below), and resuspended in 5 ml of the same buffer. All operations were conducted at 4°C. Cells were passed through a French pressure cell at 20,000 lb/in^2. The crude extract was clarified by centrifugation (30,000 × *g*, 45 min), and the supernatant was filtered through a 0.22-μm filter. The filtered protein solution was loaded onto a HiTrap chelating column (5 ml; General Electric) that was prewashed with 0.1 M $NiCl_2$ in the same buffer. Unadsorbed and loosely bound proteins were removed from the column by washing with 5 column volumes of phosphate buffer, followed by 5 column volumes of phosphate buffer with 50 mM imidazole. His-tagged LPD protein was eluted with a 50 mM to 0.5 M imidazole gradient in phosphate buffer. All the fractions containing LPD activity were combined. The N-terminal His tag was cleaved off the protein by incubation with thrombin (150 U; General Electric) at 4°C overnight. Thrombin and the small peptide were removed by gel filtration through a Sephacryl S-200 HR column (2.6 by 60 cm; General Electric) that was preequilibrated with phosphate buffer with 0.1 M NaCl. The protein was eluted with phosphate buffer containing 0.1 M NaCl. All the fractions with LPD activity were combined and dialyzed against phosphate buffer. The purity of the protein was verified by sodium dodecyl sulfate-polyacrylamide gel electrophoresis (SDS-PAGE). Both the native LPD protein and the mutated forms of LPD were purified by the same method. Since the purified LPD from strain SE2377, encoded by the *lpd102* allele, did not have detectable activity, purification of this LPD allele was followed by SDS-PAGE.

Purification of PDH complex. The PDH complex was purified as described by Bisswanger, with minor modifications (3), from strains YK175 (native protein), YK176 [*lpd101* allele; LPD(E354K)], and YK181 [*lpd102* allele; LPD(H322Y)]. Cells were cultured in 6 liters of glucose-mineral salts medium (1 liter per 2.8-liter Fernbach flask). When the culture reached an optical density at 420 nm of about 2.0 (Beckman DU640; late exponential phase of growth), cells were harvested by centrifugation (10,000 × *g*, 10 min, 4°C), washed with 100 ml of phosphate buffer, and resuspended in 20 ml of phosphate buffer. Cells were lysed by passage through a French pressure cell (20,000 lb/in^2) in the presence of a protease inhibitor cocktail (5 ml/20 g [wet weight] of cells; Sigma). DNase I and RNase A were each added to the extract in a centrifuge tube at a concentration of 100 μg/ml and incubated at 37°C for 1 h with gentle mixing to reduce the viscosity. All operations after this step were performed at 4°C. The cell extract was centrifuged at 12,000 × *g* for 30 min to remove cell debris. The supernatant was then centrifuged at 150,000 × *g* for 4 h to sediment the PDH complex. The supernatant was immediately decanted, and the pellet was dissolved in 6.0 ml of phosphate buffer for 2 h with gentle mixing on a rocker. The protein solution was centrifuged again at 12,000 × *g* for 15 min to remove particulates that did not dissolve. The supernatant was chromatographed through a hydroxyapatite column (1.5 by 12.0 cm; Bio-Rad) that was equilibrated with phosphate buffer. The protein was eluted from the column with a linear 50 to 500 mM phosphate gradient in phosphate buffer at pH 8.0. Fractions with PDH activity were combined, dialyzed against phosphate buffer, and concentrated. The concentrated protein solution was further purified with a gel filtration column (Sephacryl S-500HR; 2.6 by 35 cm) with phosphate buffer as the eluent. Fractions with activity were pooled and used immediately for the enzyme assay.

Enzyme activity. LPD activity was assayed as described previously (37). The standard reaction mixture (1.0 ml) for the forward reaction contained 0.1 M KH_2PO_4 (pH 8.0), 3 mM NAD^+, 3 mM DL-dihydrolipoic acid, 1.5 mM EDTA, and the appropriate amount of enzyme. One unit of enzyme activity was defined as the production of 1 μmol NADH · min^{-1} · mg $protein^{-1}$. The standard reverse reaction mixture (1.0 ml) contained 0.1 M KH_2PO_4 (pH 8.0), 0.1 mM NAD^+, 0.1 mM NADH, 3 mM DL-lipoamide, and 1.5 mM EDTA. Enzyme assays were performed at room temperature, and the rate of NADH oxidation was monitored over time. One unit of enzyme activity was defined as the oxidation of 1 μmol NADH · min^{-1} · mg $protein^{-1}$.

PDH was assayed both in crude extracts and using purified protein. A standard assay for determination of the activity of the PDH complex in crude extract was based on pyruvate-dependent reduction of NADH at 340 nm (ε = 6,220 M^{-1} cm^{-1}) at room temperature, as described by Hinman and Blass (17). Each 1-ml reaction mixture contained thiamine pyrophosphate (0.2 mM), CoA (0.1 mM), $MgCl_2 \cdot 6H_2O$ (1 mM), dithiothreitol (0.3 mM), NAD^+ (2.5 mM), bovine serum albumin (100 μg/ml), and crude extract or purified protein in 50 mM potassium phosphate buffer (pH 8.0). The reaction was started by addition of pyruvate (5 mM). Enzyme activity was expressed in μmol NADH produced · min^{-1} · mg $protein^{-1}$. The effect of NADH on enzyme activity was determined using the same reaction mixture with addition of various concentrations of NADH.

PDH activity in the crude extracts was also measured by using a partial reaction catalyzed by the pyruvate decarboxylase/dehydrogenase (E1 activity) in crude extracts (13). One milliliter of reaction mixture contained phosphate buffer (50 mM, pH 7.0), $MgCl_2 \cdot 6H_2O$ (12.5 mM), thiamine pyrophosphate (0.18 mM), CoA (0.175 mM), NAD^+ (2.0 mM), potassium ferricyanide (1.0 mM), pyruvate

TABLE 2. PDH mRNA, transcription, and protein levels in aerobically and anaerobically grown *E. coli* wild-type strain W3110 and ethanologenic mutant strain SE2378

Strain	Relative mRNA level[a]		β-Galactosidase activity[b]		PDH activity[c]	
	With O_2	Without O_2	With O_2	Without O_2	With O_2	Without O_2
W3110	1.00	0.98	600	630	370	185
SE2378	0.71	0.77	570	680	240	200

[a] Relative mRNA levels were determined by quantitative RT-PCR. The level of *aceE* mRNA in wild-type strain W3110 grown under aerobic conditions was defined as 1.0, and the relative levels of *aceE* mRNA for the other growth conditions and strain SE2378 were determined.

[b] β-Galactosidase activities of P*pdh-lacZ* fusions using λYK1 and λYK2 at λ*att* are expressed in nmol · min^{-1} · mg $protein^{-1}$.

[c] The PDH activity is the PDH (E1) activity of the PDH complex and is expressed in nmol ferricyanide reduced · min^{-1} · mg $protein^{-1}$. See Materials and Methods for other details.

(5.0 mM), and crude extract. The reaction was initiated by addition of pyruvate. The rate of reduction of ferricyanide was monitored over time at 430 nm (ε = 1,030 M^{-1} cm^{-1}). One unit of enzyme activity was defined as the reduction of 1 μmol ferricyanide · min^{-1} · mg $protein^{-1}$.

The reported results are data from a typical experiment that was repeated at least three times, and the variation in the experimental results was less than 10%. Kinetic properties of both LPD and PDH were determined as described by Cornish-Bowden (10) using the initial linear rates of the reactions.

Analytical methods. The NAD^+ concentration was determined using an Enzychrom NAD^+/NADH assay kit (Bioassay Systems, Hayward, CA). Sugars and fermentation products were analyzed by high-performance liquid chromatography as described previously (19). The nucleotide sequence of DNA was determined by the Interdisciplinary Center for Biotechnology Research DNA sequencing core facility at the University of Florida. Protein concentrations were determined using Coomassie blue G-250 as described by Bradford (5) with bovine serum albumin as the standard. SDS-PAGE was performed with 12.5% polyacrylamide gels as described by Laemmli (20).

RESULTS AND DISCUSSION

An *E. coli* mutant (strain AH242) that lacks pyruvate-formate lyase (*pflB*) and fermentative lactate dehydrogenase (*ldhA*) activities is defective for anaerobic growth (9, 19). We derived a set of mutants (e.g., strain SE2378) of strain AH242 that grew anaerobically and produced ethanol as the fermentation product (19). The mutation in strain SE2378 was mapped in or near the genes that encode the components of the PDH complex (*pdh* operon; *pdhR*, *aceE*, *aceF*, and *lpd*). Since the expected [NADH]/[NAD^+] ratio in anaerobic cells is higher than that in aerobic *E. coli* cells (13), operation of this new ethanol production pathway in strain SE2378 that includes glycolysis, PDH, and alcohol dehydrogenase suggests that the activity of the PDH complex is less sensitive or insensitive to inhibition by NADH, in addition to its optimal expression.

Expression of PDH in an anaerobic culture of *E. coli*. The results presented in Table 2 show that the relative mRNA level of the *aceE* gene (the second gene in the *pdh* operon) encoding the E1 enzyme of the PDH complex is independent of the presence of O_2 during growth of *E. coli* strain W3110. Since the *pdhR*, *aceE*, *aceF*, and *lpd* genes are transcribed as one transcript (27), it is apparent that all the genes encoding the PDH complex are transcribed under both aerobic and anaerobic growth conditions. Although the *aceE* mRNA level of strain SE2378 was also not altered by the level of O_2 during growth, this mRNA level was slightly lower than that of the wild-type strain W3110. The fact that this mRNA is further translated in cells grown under aerobic and anaerobic conditions is shown by the P*dhR-lac* fusion-based production of β-galactosidase activity and the presence of PDH activity in extracts (Table 2). In wild-type strain W3110, the level of PDH activity of anaerobic cells was about 50% of the level of activity of aerobic cells, while the levels of transcription in the two growth conditions were about the same. It is possible that the NADH-inhibited protein was subject to proteolysis in the anaerobic cells. Although the level of PDH activity in strain SE2378 grown under aerobic conditions was only about 65% of the level of activity in aerobically cultured strain W3110, this level of activity was not that dissimilar from the level in either strain grown anaerobically. These results show that both the wild-type and mutant *E. coli* strains produced PDH during anaerobic growth. The inability of strain AH242 (an *ldhA pflB* derivative of strain W3110) to grow under anaerobic conditions suggests that the PDH activity is negligible during anaerobic growth of strain W3110 due to inhibition of the enzyme complex by NADH. Similar conclusions were also reached by Snoep et al. based on the fermentation profile of *E. coli* B (33).

PDH complex is less sensitive to NADH inhibition in strain SE2378. For the PDH to be active under anaerobic growth conditions, the mutated form of the enzyme in strain SE2378 needs to be significantly less sensitive to NADH inhibition than the native enzyme. When the PDH activity of strain W3110 was assayed in crude extracts, the enzyme was completely inhibited by NADH at a concentration of about 80 μM, corresponding to an [NADH]/[NAD^+] ratio of about 0.04. At this ratio of [NADH] to [NAD^+], the PDH complex in the crude extract of strain SE2378 was fully active (Fig. 1). Increasing the NADH concentration to obtain a higher ratio did inhibit the enzyme from the mutant, indicating that the mutation did not completely mitigate the NADH inhibition. Taken together, the results presented in Table 2 and Fig. 1 show that the observed anaerobic growth phenotype of strain SE2378 is apparently due to the mutational alteration of the PDH activity.

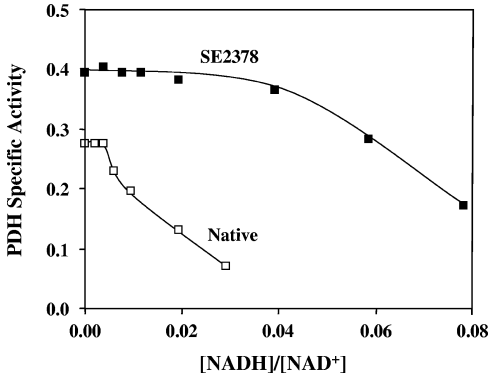

FIG. 1. NADH sensitivity of the PDH complex from *E. coli* wild-type strain W3110 (Native) and an ethanologenic mutant, strain SE2378. Crude extracts were used to assay for PDH complex activity (NADH production) as described in Materials and Methods. The NAD^+ concentration in the assay mixture (2 mM for the native enzyme and 1 mM for the enzyme from strain SE2378) was at least five times the K_m value for each enzyme. The NADH concentration was varied to obtain the indicated ratios. Specific activity is expressed in μmol min^{-1} mg $protein^{-1}$.

```
W3110 (wt)    321 AHKGVHEGHV AAEVIAGKKH YFDPKVIPSI AYTEPEVAWV
SE2377        321 .Y........ .......... .......... ..........
SE2378        321 .......... .......... .......... ...K......
SE2382        321 .......... .......... .......... ...K......
SE2383        321 .Y........ .......... .......... ..........
SE2384        321 .Y........ .......... .......... ..........
SE2385        321 .......... .......... .......... ...K......
```

FIG. 2. Amino acid sequence alignment of LPD from *E. coli* wild-type (wt) strain W3110 and various ethanologenic mutants. A period indicates that the amino acid is same as the amino acid in the wild type. All the other amino acids that are not listed are the same in the LPD from the six mutants and strain W3110.

Identification of the mutation in *lpd*. To localize the mutation that contributed to the reduced sensitivity of PDH to NADH inhibition, the genes comprising the entire *pdh* operon from six independently isolated ethanologenic *E. coli* mutants were sequenced. Based on the DNA sequence, a single mutation in *lpd* was identified in each of the six mutants (Fig. 2). Three mutants, strains SE2377, SE2383, and SE2384, had a base change from C to T at position 964 (A in the ATG codon of the LPD gene was defined as position 1; *lpd102*), resulting in a change of the histidine at position 322 to tyrosine (Fig. 2). The other three mutants, strains SE2378, SE2382, and SE2385, had a different mutation (G to A at position 1,060; *lpd101*), resulting in a change of the glutamate at position 354 to lysine (Fig. 2). Only one of the six mutants, strain SE2378, also carried two mutations in the *pdhR* gene (base change T34C leading to amino acid change S12P; insertion of a TGC sequence between positions 352 and 353, resulting in insertion of leucine between amino acids 117 and 118 in the native protein) besides the E354K change in the LPD protein. In addition, a G-to-A base change upstream of the *aceE* gene at position −59 from the translational start (A of ATG) was also observed in strain SE2378. These secondary mutations in strain SE2378 may have altered the level of expression of the PDH complex in the cell since the PdhR protein is a known regulator of the *pdh* operon (16). The mutations in LPD are in agreement with the observed lower sensitivity of the PDH complex in cell extracts to NADH inhibition since the LPD enzyme is the known site of NADH inhibition (29, 30, 38).

To confirm that the observed phenotype of anaerobic growth is due only to the *lpd* mutation and is not associated with a second mutation in an unlinked gene, the following genetic experiment was performed. In the first step, the *lpd* gene of the *ldhA pflB* double mutant strain AH242, the parent strain used in construction of the ethanologenic derivatives, was deleted (strain YK100). Strain YK100 is defective for anaerobic growth due to the *ldhA* and *pflB* mutations and defective for aerobic growth in glucose-mineral salts medium due to the absence of PDH activity (*lpd* deletion). Wild-type and *lpd101* alleles were either transduced into strain YK100 or introduced via plasmids, and the derivatives with LPD activity were selected for growth under aerobic conditions in glucose-mineral salts medium (Table 3). Only the transductants carrying the *lpd101* allele from either strain SE2378 or SE2382 grew anaerobically, while the transductants carrying the wild-type lpd^+ gene did not grow anaerobically (Table 3). Strain SE2382 is distinguished from strain SE2378 by its lack of the additional mutations found in the *pdh* operon of strain SE2378. These results show that the mutation in *lpd* is responsible for the observed phenotype. Similar results were also obtained when the Δ*lpd* mutation in strain YK100 was complemented with two alleles, lpd^+ and *lpd101* from a plasmid, expressed from a *trc* promoter with isopropyl-β-D-thiogalactopyranoside (IPTG). The complementation experiments confirmed that the mutation in the *lpd* gene alone supports anaerobic growth of an *ldhA pflB* double mutant. As expected, transductants of YK100 with the *lpd102* allele (YK139) also grew anaerobically (data not shown), confirming that the two *lpd* mutations (*lpd101* and *lpd102*) are interchangeable.

In order to isolate additional LPD mutations that also would support anaerobic growth of strain AH242 but may map at different parts of LPD, the *lpd* DNA was specifically mutagenized with hydroxylamine or by error-prone PCR. The PCR mutagenesis did not yield any *lpd* mutation that supported anaerobic growth of strain AH242 (from a total of about 4,000 transformants). Hydroxylamine treatment of *lpd* DNA did yield five additional mutants, and the mutation in all five was the same E354K mutation found in strain SE2378.

LPD activity of strain SE2378 is insensitive to NADH inhibition. Since, the *lpd* mutation in all six ethanologenic strains supported anaerobic growth in the *ldhA pflB* genetic background, the LPD protein was purified from the wild type (native enzyme) and a representative strain SE2378 (mutated enzyme; E354K), and the kinetic properties were determined (Fig. 3 and 4).

The native enzyme presented typical Michelis-Menton-type kinetics with respect to NAD^+. However, addition of NADH to the reaction mixture progressively inhibited the enzyme

TABLE 3. Anaerobic growth and fermentation profiles of *E. coli* strains with different *lpd* alleles[a]

Strain	*lpd* allele	Anaerobic growth	Concn of fermentation products (mM)				
			Ethanol	Acetate	Formate	Succinate	Lactate
W3110	lpd^+	+	7.3	9.3	2.6	4.2	18.5
SE2378	*lpd101*	+	107.3	4.7	0.0	4.1	0.8
YK110	lpd^+	−	NG	NG	NG	NG	NG
YK111	*lpd101*[b]	+	125.8	2.2	0.0	5.0	0.3
YK141	*lpd101*[b]	+	114.5	3.4	0.0	6.0	0.3
YK128	Plpd^+	−	NG	NG	NG	NG	NG
YK129	P*lpd101*	+	68.0	3.6	0.0	11.9	0.8

[a] See Table 1 for a description of strain construction. Anaerobic growth and fermentation were determined using LB containing glucose (1%) in batch fermentations without pH control. Glucose was not completely fermented by strain W3110 due to the accumulation of organic acids that lowered the culture pH to less than 5.0. See text for other details. NG, no growth.

[b] The *lpd101* allele in strains YK111 and YK141 was transduced from strains SE2378 and SE2382, respectively.

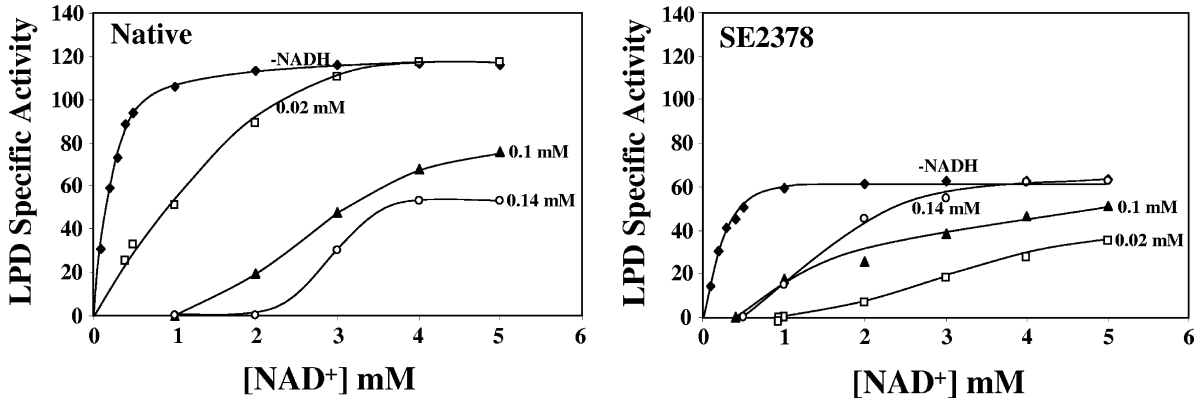

FIG. 3. NADH inhibition of LPD from *E. coli* wild-type strain W3110 (Native) and mutant strain SE2378. The rate of the forward reaction of LPD as a function of [NAD^+] was determined without NADH and with the indicated concentrations of NADH. Specific activity is expressed in μmol min^{-1} mg $protein^{-1}$.

activity (Fig. 3). The specific activity of the mutated form of the enzyme was only about 50% of that of the native enzyme, and this altered enzyme was surprisingly more sensitive to inhibition at a lower NADH concentration (0.02 mM) than at higher concentrations of NADH. At an NAD^+ concentration of 2 mM, 0.14 mM NADH completely inhibited the activity of the native enzyme, while at the same concentration of NAD^+, 0.14 mM NADH inhibited the mutated form of the enzyme only by about 25%. At 4 mM NAD^+, the mutated LPD was not inhibited by 0.14 mM NADH, while the native enzyme activity was only about 40% of the control activity without NADH. The K_m for NAD^+ (0.4 mM) was the same for both forms of the enzyme and is within the range of the reported K_m values for the *E. coli* LPD that varied as a function of pH and NADH concentration (0.09 to 1.0 mM) (29). The K_i for NADH for the native enzyme was 5.2 μM, and this value is close to the value previously reported, 9 μM (30). Due to the complexity of NADH inhibition of the mutated LPD activity (Fig. 3), K_i was not determined for the LPD(E354K) enzyme.

The reverse reaction of native LPD, lipoamide + NADH $\rightarrow$ dihydrolipoamide + NAD^+, depends on NAD^+ as an activator (38). Reversal of NADH inhibition of the enzyme activity by NAD^+ was biphasic. The first phase showed a gradual increase in activity to about 25 U when the added NAD^+ concentration matched that of the substrate, NADH. The activity of the second phase of NAD^+-dependent activation of the LPD reverse reaction was significantly higher, reaching the maximum value, about 70 U, when the NAD^+ concentration was 1.5 times the concentration of NADH (Fig. 4). The E354K form of the enzyme had about 55 U of activity in the absence of added NAD^+, which was about 75% of the maximum activity (about 75 U), which was reached with addition of a very small amount of NAD^+ (20 μM). Complete activation of the native enzyme required at least 150 μM NAD^+, an amount that was 7.5-fold larger than the amount needed for activation of the E354K form of the enzyme. These results further demonstrate that the sensitivity of LPD to inhibition by NADH is minimal in strain SE2378. An alternative possibility, the possibility that the E354K form of LPD carries a tightly bound NAD^+ that overcomes the need for external addition of NAD^+ to reverse NADH inhibition, can be ruled out due to the absence of detectable NAD^+ in the purified protein (data not shown).

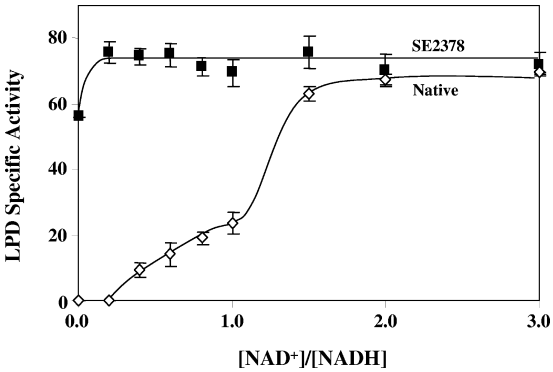

FIG. 4. Insensitivity of the LPD (reverse reaction) from mutant strain SE2378 to NADH. The reverse reaction of LPD was determined with 0.1 mM NADH and different concentrations of NAD^+ to obtain the indicated ratios. Specific activity is expressed in μmol min^{-1} mg $protein^{-1}$. Native, wild-type strain.

H322Y form of LPD is inactive upon purification. Three of the mutants isolated as derivatives of strain AH242 that could grow anaerobically carried a mutation that changed the amino acid at position 322 from histidine to tyrosine (H322Y; *lpd102*) (Fig. 2). The *lpd102* DNA was cloned into an expression vector, and the H322Y form of the LPD protein was expressed in recombinant *E. coli*. Although the cell extract had LPD activity, upon purification the protein lost the activity and associated flavin adenine dinucleotide (FAD) at the gel filtration step. Attempts to reconstitute the enzyme with added FAD as described by Lindsay et al. (22) failed to yield a protein with activity. This form of the enzyme was not studied further.

***E. coli* PDH complex with LPD mutation is less sensitive to NADH inhibition.** In order to confirm that the lower sensitivity of the LPD from strain SE2378 to NADH inhibition is translated to the entire PDH complex, the PDH complex was purified from the wild type and two mutants, strains SE2377 and SE2378, representing the two alleles. Kinetic properties of the PDH from these strains are presented in Table 4. The native form and the two mutated forms of the enzyme had similar

TABLE 4. Kinetic characteristics of the PDH complex isolated from *E. coli* wild-type strain W3110 and strains SE2377 (H322Y) and SE2378 (E354K) with a mutation in LPD[a]

PDH complex	K_m (NAD^+) (mM)	K_m (pyruvate) (mM)	K_i (NADH) (μM)	V_{max} (μmol · min^{-1} · mg $protein^{-1}$)
Native	0.07	0.40	1.00	46.64
H322Y	0.11	0.48	9.60	26.70
E354K	0.08	0.30	10.00	30.28

[a] Enzymes were purified from *E. coli* strains YK175 (native protein), YK181 [LPD(H322Y)], and YK176 [LPD(E354K)]. See Table 1 for the genotypes of the strains.

affinities for the substrates, NAD^+ and pyruvate. The K_m values for pyruvate and NAD^+ are within the range of K_m values reported for the *E. coli* PDH complex (0.2 to 0.4 mM for pyruvate and 10 μM for NAD^+) (4, 36). However, the native enzyme had a higher V_{max} than the two mutated forms of the enzyme. Apparently, the lower specific activity of the LPD than of the native enzyme (Fig. 3) is translated to lower PDH activity. It is interesting that although the LPD with the H322Y mutation (strain SE2377) lost FAD upon purification, the PDH complex with the same mutated form of the LPD was active after purification.

The two mutated forms of the PDH complex had about 10-fold-higher K_i values for NADH, in agreement with the observation that the PDH complex from the two mutants is less sensitive to inhibition by NADH (Table 4 and Fig. 5). The native PDH was completely inhibited at an NADH concentration of 0.06 mM, while the two mutated forms of PDH retained about 70 to 85% of the activity at the same NADH concentration. Even at a higher NADH concentration, the two mutated forms of PDH retained about 70% of the enzyme activity.

The intracellular [NADH]/[NAD^+] ratio of *E. coli* grown under aerobic conditions was reported to be about 0.03 to 0.05 (8, 13, 33). At this ratio, the PDH complex retained almost 90% of the maximal activity. The [NADH]/[NAD^+] ratio of an anaerobic cell is expected to be higher than that of an aerobic cell (0.7 to 0.8) (13, 33). Even at the lower reported ratio of 0.3, the PDH complex is not active in vitro (Fig. 5), supporting the inactive nature of the PDH complex in anaerobic *E. coli*. Although it is difficult to extrapolate from in vitro enzyme activity to in vivo levels, it should be noted that the PDH complex, although present, failed to support anaerobic growth of strain AH242 that lacked lactate dehydrogenase and pyruvate-formate lyase (19). The specific mutation, either H322Y or E354K, that made the LPD less sensitive to NADH inhibition also reduced the NADH sensitivity of the PDH complex and allowed the enzyme to support anaerobic growth of *E. coli* strain SE2378.

Histidine at position 322 was conserved in all LPD sequences tested, including the human LPD sequence, indicating the importance of this amino acid in the activity of LPD and PDH. Although the glutamate at position 354 was conserved in the LPD of all tested bacteria in the family *Enterobacteriaceae*, it is not conserved across bacterial families. However, a significant level of sequence identity can be found in this region; proline at position 348 is conserved in all the LPD sequences tested, including the human sequence. A glutamate is located at position 356, with few exceptions. The specific role that these amino acids play in the structure or catalysis of LPD is unclear, but these amino acids apparently are important for the normal function of the enzyme.

Although several spontaneous and induced mutations that affect the activity of LPD were reported in several organisms, none of these mutations was at the two positions reported in this study (1, 2, 6, 7, 18). In addition, none of the reported LPD mutations were reported to significantly alter the NADH sensitivity of the PDH complex. The two LPD mutations described in this study are unique in this regard in that they affect the NADH sensitivity of the protein with minimal effects on the overall activity of the protein. The inhibition of PDH (LPD) by NADH is probably caused by overreduction of the redox centers in LPD by NADH, making the enzyme inactive (14). NADH also increased the K_m for NAD^+, and there was an associated decrease in the LPD activity (29). It is possible that the two mutated forms of LPD described in this study have a higher dissociation constant (K_d) for NADH and/or a reduced rate of FAD reduction by NADH compared to the native LPD. The mechanism of this reduction in NADH sensitivity has not been determined yet.

Conclusion. The results presented here show that a mutation in LPD led to a PDH complex that is less sensitive to inhibition by NADH. The altered enzyme was active even in

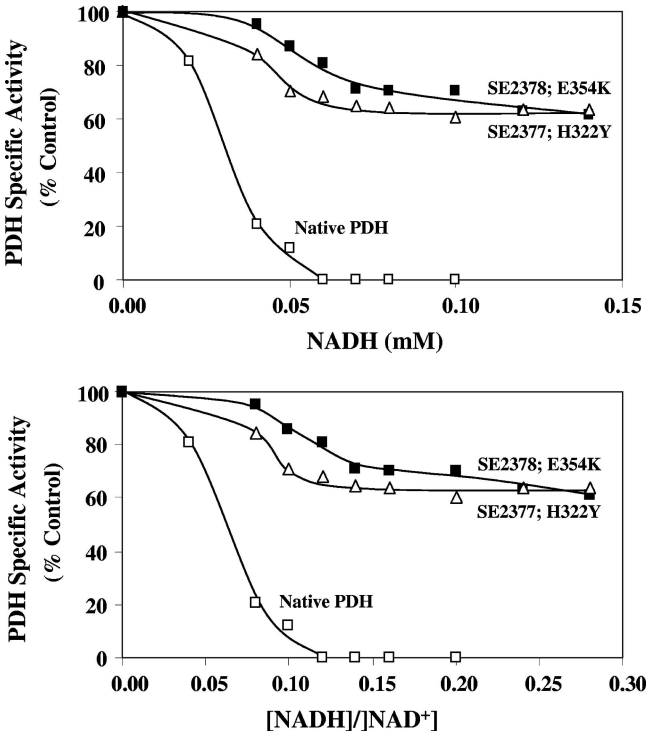

FIG. 5. Differential inhibition of the PDH complex from wild-type *E. coli* strain W3110 (Native) and the two LPD mutant derivatives by NADH. The NAD^+ concentration (0.5 mM) was at least five times the K_m value. The specific activity of the native enzyme complex without NADH was 40.16 U. The specific activities of the two PDH complexes with LPD mutations H322Y and E354K without NADH were 17.74 and 31.00 U, respectively.

the presence of a higher level of NADH in the cell and supported anaerobic growth of strains SE2378 and SE2382 and other similar mutants. The combined functions of glycolysis and the PDH complex in these mutants produced four NADH molecules during conversion of one glucose molecule to two acetyl-CoA molecules. These four NADH molecules were reoxidized by reduction of the two acetyl-CoA molecules to two ethanol molecules by the alcohol/acetaldehyde dehydrogenase (*adhE*), the observed phenotype of strain SE2378 and other mutants. These results raise an interesting possibility, that a similar alteration in the LPD of other organisms could also lead to PDH complexes that are less sensitive to NADH inhibition and active during anaerobic growth. The presence and functional activity of such an NADH-insensitive PDH may have significant unexplored physiological and biotechnological applications.

ACKNOWLEDGMENTS

This study was supported by funds from the U.S. Department of Energy (grant DE-FC36-04-GO14019) and the State of Florida University of Florida Agricultural Experiment Station.

REFERENCES

1. **Allison, N., C. H. Williams, Jr., and J. R. Guest.** 1988. Overexpression and mutagenesis of the lipoamide dehydrogenase of *Escherichia coli*. Biochem. J. **256:**741–749.
2. **Benen, J., W. van Berkel, Z. Zak, T. Visser, C. Veeger, and A. de Kok.** 1991. Lipoamide dehydrogenase from *Azotobacter vinelandii*: site-directed mutagenesis of the His450-Glu455 diad. Spectral properties of wild type and mutated enzymes. Eur. J. Biochem. **202:**863–872.
3. **Bisswanger, H.** 1981. Substrate specificity of the pyruvate dehydrogenase complex from *Escherichia coli*. J. Biol. Chem. **256:**815–822.
4. **Bisswanger, H., and U. Henning.** 1971. Regulatory properties of the pyruvate-dehydrogenase complex from *Escherichia coli*. Eur. J. Biochem. **24:**376–384.
5. **Bradford, M. M.** 1976. A rapid and sensitive method for the quantitation of microgram quantities of protein utilizing the principle of protein-dye binding. Anal. Biochem. **72:**248–254.
6. **Brautigam, C. A., J. L. Chuang, D. R. Tomchick, M. Machius, and D. T. Chuang.** 2005. Crystal structure of human dihydrolipoamide dehydrogenase: NAD^+/NADH binding and the structural basis of disease-causing mutations. J. Mol. Biol. **350:**543–552.
7. **Cameron, J. M., V. Levandovskiy, N. Mackay, J. Raiman, D. L. Renaud, J. T. Clarke, A. Feigenbaum, O. Elpeleg, and B. H. Robinson.** 2006. Novel mutations in dihydrolipoamide dehydrogenase deficiency in two cousins with borderline-normal PDH complex activity. Am. J. Med. Genet. A **140:**1542–1552.
8. **Cassey, B., J. R. Guest, and M. M. Attwood.** 1998. Environmental control of pyruvate dehydrogenase complex expression in *Escherichia coli*. FEMS Microbiol. Lett. **159:**325–329.
9. **Clark, D. P.** 1989. The fermentation pathways of *Escherichia coli*. FEMS Microbiol. Rev. **5:**223–234.
10. **Cornish-Bowden, A.** 1995. Fundamentals of enzyme kinetics. Portland Press, London, United Kingdom.
11. **Datsenko, K. A., and B. L. Wanner.** 2000. One-step inactivation of chromosomal genes in *Escherichia coli* K-12 using PCR products. Proc. Natl. Acad. Sci. USA **97:**6640–6645.
12. **Davis, R. W., D. Botstein, and J. R. Roth.** 1980. A manual for genetic engineering: advanced bacterial genetics. Cold Spring Harbor Laboratory, Cold Spring Harbor, NY.
13. **de Graef, M. R., S. Alexeeva, J. L. Snoep, and M. J. Teixeira de Mattos.** 1999. The steady-state internal redox state (NADH/NAD) reflects the external redox state and is correlated with catabolic adaptation in *Escherichia coli*. J. Bacteriol. **181:**2351–2357.
14. **de Kok, A., A. F. Hengeveld, A. Martin, and A. H. Westphal.** 1998. The pyruvate dehydrogenase multi-enzyme complex from Gram-negative bacteria. Biochim. Biophys. Acta **1385:**353–366.
15. **Hansen, H. G., and U. Henning.** 1966. Regulation of pyruvate dehydrogenase activity in *Escherichia coli* K12. Biochim. Biophys. Acta **122:**355–358.
16. **Haydon, D. J., M. A. Quail, and J. R. Guest.** 1993. A mutation causing constitutive synthesis of the pyruvate dehydrogenase complex in *Escherichia coli* is located within the *pdhR* gene. FEBS Lett. **336:**43–47.
17. **Hinman, L. M., and J. P. Blass.** 1981. An NADH-linked spectrophotometric assay for pyruvate dehydrogenase complex in crude tissue homogenates. J. Biol. Chem. **256:**6583–6586.
18. **Hopkins, N., and C. H. Williams, Jr.** 1995. Lipoamide dehydrogenase from *Escherichia coli* lacking the redox active disulfide: C44S and C49S. Redox properties of the FAD and interactions with pyridine nucleotides. Biochemistry **34:**11766–11776.
19. **Kim, Y., L. O. Ingram, and K. T. Shanmugam.** 2007. Construction of an *Escherichia coli* K-12 mutant for homoethanologenic fermentation of glucose or xylose without foreign genes. Appl. Environ. Microbiol. **73:**1766–1771.
20. **Laemmli, U. K.** 1970. Cleavage of structural proteins during the assembly of the head of bacteriophage T4. Nature **227:**680–685.
21. **Lee, J. H., P. Patel, P. Sankar, and K. T. Shanmugam.** 1985. Isolation and characterization of mutant strains of *Escherichia coli* altered in H_2 metabolism. J. Bacteriol. **162:**344–352.
22. **Lindsay, H., E. Beaumont, S. D. Richards, S. M. Kelly, S. J. Sanderson, N. C. Price, and J. G. Lindsay.** 2000. FAD insertion is essential for attaining the assembly competence of the dihydrolipoamide dehydrogenase (E3) monomer from *Escherichia coli*. J. Biol. Chem. **275:**36665–36670.
23. **Linn, T., and R. St. Pierre.** 1990. Improved vector system for constructing transcriptional fusions that ensures independent translation of *lacZ*. J. Bacteriol. **172:**1077–1084.
24. **Matsumura, I., and A. D. Ellington.** 2001. Methods in molecular biology, 2nd ed. Humana Press Inc., Totowa, NJ.
25. **Miller, J. H.** 1972. Experiments in molecular genetics. Cold Spring Harbor laboratory, Cold Spring Harbor, NY.
26. **Narayanan, N., M. Y. Hsieh, Y. Xu, and C. P. Chou.** 2006. Arabinose-induction of *lac*-derived promoter systems for penicillin acylase production in *Escherichia coli*. Biotechnol. Prog. **22:**617–625.
27. **Quail, M. A., D. J. Haydon, and J. R. Guest.** 1994. The *pdhR-aceEF-lpd* operon of *Escherichia coli* expresses the pyruvate dehydrogenase complex. Mol. Microbiol. **12:**95–104.
28. **Rosentel, J. K., F. Healy, J. A. Maupin-Furlow, J. H. Lee, and K. T. Shanmugam.** 1995. Molybdate and regulation of *mod* (molybdate transport), *fdhF*, and *hyc* (formate hydrogenlyase) operons in *Escherichia coli*. J. Bacteriol. **177:**4857–4864.
29. **Sahlman, L., and C. H. Williams, Jr.** 1989. Lipoamide dehydrogenase from *Escherichia coli*. Steady-state kinetics of the physiological reaction. J. Biol. Chem. **264:**8039–8045.
30. **Schmincke-Ott, E., and H. Bisswanger.** 1981. Dihydrolipoamide dehydrogenase component of the pyruvate dehydrogenase complex from *Escherichia coli* K12. Comparative characterization of the free and the complex-bound component. Eur. J. Biochem. **114:**413–420.
31. **Shen, L. C., and D. E. Atkinson.** 1970. Regulation of pyruvate dehydrogenase from *Escherichia coli*. Interactions of adenylate energy charge and other regulatory parameters. J. Biol. Chem. **245:**5974–5978.
32. **Smith, M. W., and F. C. Neidhardt.** 1983. 2-Oxoacid dehydrogenase complexes of *Escherichia coli*: cellular amounts and patterns of synthesis. J. Bacteriol. **156:**81–88.
33. **Snoep, J. L., M. R. de Graef, A. H. Westphal, A. de Kok, M. J. Teixeira de Mattos, and O. M. Neijssel.** 1993. Differences in sensitivity to NADH of purified pyruvate dehydrogenase complexes of *Enterococcus faecalis*, *Lactococcus lactis*, *Azotobacter vinelandii* and *Escherichia coli:* implications for their activity in vivo. FEMS Microbiol. Lett. **114:**279–283.
34. **Tao, H., R. Gonzalez, A. Martinez, M. Rodriguez, L. O. Ingram, J. F. Preston, and K. T. Shanmugam.** 2001. Engineering a homo-ethanol pathway in *Escherichia coli*: increased glycolytic flux and levels of expression of glycolytic genes during xylose fermentation. J. Bacteriol. **183:**2979–2988.
35. **Tao, H., A. Hasona, P. M. Do, L. O. Ingram, and K. T. Shanmugam.** 2005. Global gene expression analysis revealed an unsuspected deo operon under the control of molybdate sensor, ModE protein, in *Escherichia coli*. Arch. Microbiol. **184:**225–233.
36. **Visser, J., H. Kester, K. Jeyaseelan, and R. Topp.** 1982. Pyruvate dehydrogenase complex from *Bacillus*. Methods Enzymol. **89:**399–407.
37. **Wei, W., H. Li, N. Nemeria, and F. Jordan.** 2003. Expression and purification of the dihydrolipoamide acetyltransferase and dihydrolipoamide dehydrogenase subunits of the *Escherichia coli* pyruvate dehydrogenase multienzyme complex: a mass spectrometric assay for reductive acetylation of dihydrolipoamide acetyltransferase. Protein Expr. Purif. **28:**140–150.
38. **Wilkinson, K. D., and C. H. Williams, Jr.** 1981. NADH inhibition and NAD activation of *Escherichia coli* lipoamide dehydrogenase catalyzing the NADH-lipoamide reaction. J. Biol. Chem. **256:**2307–2314.

Appendix G

Available online at www.sciencedirect.com
ScienceDirect
Plasmid 58 (2007) 13–22
PLASMID
www.elsevier.com/locate/yplas

Development of plasmid vector and electroporation condition for gene transfer in sporogenic lactic acid bacterium, *Bacillus coagulans*

Mun Su Rhee, Jin-woo Kim [1], Yilei Qian [2], L.O. Ingram, K.T. Shanmugam *

Department of Microbiology and Cell Science, University of Florida, Gainesville, FL 32611, USA

Received 29 September 2006, revised 16 November 2006
Available online 9 January 2007
Communicated by C. Jeffery Smith

Abstract

Bacillus coagulans is a sporogenic lactic acid bacterium that ferments glucose and xylose, major components of plant biomass, a potential feedstock for cellulosic ethanol. The temperature and pH for optimum rate of growth of *B. coagulans* (50 to 55 °C, pH 5.0) are very similar to that of commercially developed fungal cellulases (50 °C; pH 4.8). Due to this match, simultaneous saccharification and fermentation (SSF) of cellulose to products by *B. coagulans* is expected to require less cellulase than needed if the SSF is conducted at a sub-optimal temperature, such as 30 °C, the optimum for yeast, the main biocatalyst used by the ethanol industry. To fully exploit *B. coagulans* as a platform organism, we have developed an electroporation method to transfer plasmid DNA into this genetically recalcitrant bacterium. We also constructed a *B. coagulans*/*E. coli* shuttle vector, plasmid pMSR10 that contains the *rep* region from a native plasmid (pMSR0) present in *B. coagulans* strain P4-102B. The native plasmid, pMSR0 (6823 bp), has 9 ORFs, and replicates by rolling-circle mode of replication. Plasmid pNW33N, developed for *Geobacillus stearothermophilus*, was also transformed into this host and stably maintained while several other *Bacillus*/*Escherichia coli* shuttle vector plasmids were not transformed into *B. coagulans*. The transformation efficiency of *B. coagulans* strain P4-102B using the plasmids pNW33N or pMSR10 was about 1.5×10^{16} per mole of DNA. The availability of shuttle vectors and an electroporation method is expected to aid in genetic and metabolic engineering of *B. coagulans*.

Keywords: *Bacillus coagulans*; Transformation; Electroporation; Shuttle vectors; Plasmid; Lactic acid fermentation

1. Introduction

Lactic acid is traditionally used in food, pharmaceutical and textile industries and is finding increasing use in the production of biodegradable green polymers as well as a feedstock for synthesis of other compounds such as propionic acid, acrylic acid, etc. (Datta et al., 1995; Mecking, 2004;

* Corresponding author. Fax: +1 352 392 5922.
E-mail address: shan@ufl.edu (K.T. Shanmugam).
[1] Present address: Pacific Agri-Food Research Centre, Agriculture and Agri-Food Canada, Summerland, BC, Canada V0H 1Z0.
[2] Present address: Department of Biology, Indiana University South Bend, South Bend, IN 46634, USA.

0147-619X/$ - see front matter © 2006 Elsevier Inc. All rights reserved.
doi:10.1016/j.plasmid.2006.11.006

Teusink and Smid, 2006). The industrial process for optically pure lactic acid (LA) production is the fermentation of glucose derived from corn starch by lactic acid bacteria (DOE, 2003). Corn starch is also the main feedstock for fuel ethanol production and the demand for corn starch is expected to increase exponentially to supply additional bioethanol to offset petroleum (Bothast and Schlicher, 2005). This higher demand is projected to increase the cost of corn starch and the lactic acid produced using corn starch as the feedstock. Lignocellulosics are potential sources of sugars that are non-competing with food and feed sources such as corn, sucrose, etc. and are attractive cost-effective alternate feedstocks for lactic acid production (Wooley et al., 1999; Wyman, 2003). Current pre-treatment protocols for lignocellulose release cellulose as a polymer that is further hydrolyzed to glucose by commercial fungal cellulases (Aden et al., 2002). The lactic acid bacteria used by the industry for LA production grow and ferment at temperatures that are not optimal for the activity of fungal cellulases (Hofvendahl and Hans-Hagerdal, 2000; Martin, 1996) and as a consequence increases the amount of cellulase used for depolymerization that also increases the overall production cost of LA. In addition, many of the LA bacteria lack the ability to ferment xylose, a key component of hemicellulose (Hofvendahl and Hans-Hagerdal, 2000). Xylose-fermenting LA bacteria ferment pentoses through the phosphoketolase pathway that limits the yield of LA from xylose to a maximum of 60% (Garde et al., 2002; Patel et al., 2006; Tanaka et al., 2002).

We have recently isolated and described *Bacillus coagulans* strains that grow at 50 °C and pH 5.0 and ferment both glucose and xylose to optically pure lactic acid (Patel et al., 2006). The higher growth and fermentation temperature of these strains is comparable to the optimum for fungal cellulases (Patel et al., 2005). Our previous study also showed that the amount of cellulase required for depolymerization of cellulose to glucose and fermentation to LA in a simultaneous saccharification and fermentation at 50 °C is about 1/3 of the amount required at 30 °C. These properties of *B. coagulans* make this bacterium an ideal platform for further development as an industrial biocatalyst for fermentation of biomass derived sugars to products.

Although several Gram-positive bacteria naturally develop competence for DNA uptake and can be readily transformable with both plasmid and linear DNA, *B. coagulans* is recalcitrant to genetic manipulation (De Rossi et al., 1991; Dubnau, 1991). To fully utilize the potential of this bacterium as a biocatalyst, it is important to develop a reproducible genetic system that can be used to genetically and metabolically engineer this bacterium. We have developed an electrotransformation protocol for *B. coagulans* and using this method also identified and constructed plasmids that can be used for gene transfer into *B. coagulans*. These results are presented in this communication.

2. Materials and methods

2.1. Bacterial strains and growth media

Bacillus coagulans strain P4-102B (Patel et al., 2006) was cultured in L broth (LB) at pH 5.0 and 50 °C. L broth contained, trypticase peptone (10 g), yeast extract (5 g) and NaCl (5 g) in 1 L deionized water (Lee et al., 1985). *E. coli* strain Top10 (Invitrogen) is a restriction minus derivative of *E. coli* K-12 and strain GM272 (*E. coli* Genetic Stock Center; CGSC# 6478) is defective in both adenine and cytosine methylation (*dam-3, dcm-6*). *E. coli* strains as well as *Bacillus subtilis* strain HB1000 (from Dr. F. Healy, Trinity University, San Antonio) were cultured in L broth, pH 7.0 and at 37 °C. Chloramphenicol was the antibiotic used for *Bacillus* and the concentration was 7.5 μg/ml. Ampicillin for *E. coli* medium was at 100 μg/ml. Regeneration medium (RG medium) contained in L broth, sucrose (0.5 M), glucose (55.6 mM), $MgCl_2$ (20 mM) and $CaCl_2$ (1 mM). GM1 medium was used for culturing *B. subtilis* and this medium contained in 1 L, Spizizen's minimal medium (100 ml of 10× concentrate), glucose (3.9 g), casein hydrolysate (0.2 g) and yeast extract (1.0 g) at pH 7.0 (Boylan et al., 1972). GM2 medium, used to induce competency in *B. subtilis*, was GM1 medium supplemented with $CaCl_2$ (5 mM) and $MgCl_2$ (2.5 mM) (Boylan et al., 1972). Plasmid pNW33N was obtained from late Dr. Welker (Genbank Accession number, AY237122).

2.2. Plasmid isolation

Standard molecular biology protocols (Maniatis et al., 1982) were used for plasmid isolation and DNA manipulation, unless otherwise specifically described. Plasmids from *E. coli* were isolated using alkaline lysis method or with Qiagen plasmid isolation kit as per the Manufacturer's protocol. Plasmids were also isolated using CsCl–ethidium bromide density gradient centrifugation (Maniatis et al., 1982). For isolation of plasmids from *B. subtilis* or *B. coagulans*, cells from an overnight culture grown in L broth at 37 °C with shaking (200 RPM) were collected by centrifugation (12,000*g*; 5 min; 4 °C). Cells were

resuspended in 2–4% of the original volume in SET buffer (Sucrose, 25%; EDTA, 50 mM; Tris, pH 8.0, 50 mM) with lysozyme (1 mg/ml). Cells were incubated at 37 °C for 15 min. Alkaline SDS lysis and DNA preparation method was used to isolate the plasmids from these cells (Maniatis et al., 1982). Residual proteins from the DNA preparation were removed with phenol:chloroform. After centrifugation, the aqueous phase was collected and the nucleic acids were precipitated with 2-volumes of ethanol. DNA pellet was dissolved in water.

2.3. Isolation and sequencing of native plasmid DNA from B. coagulans strain P4-102B

Bacillus coagulans strain P4-102B was cultured in L-broth with glucose (3% w/v) at 50 °C, pH 5.0 with pH control as described previously (Patel et al., 2006). Cells were harvested after 24 h (early stationary phase of growth) by centrifugation (2000*g*; 10 min; 4 °C). Native plasmids were isolated using the same protocol used for isolation of recombinant plasmids from *B. coagulans* and *B. subtilis* as described above. The plasmid preparation contained two plasmids and they were purified further by agarose gel electrophoresis and electroelution. DNA was sequenced at the University of Florida, Interdisciplinary Center for Biotechnology Research, DNA Sequencing Facility, by dideoxy chain termination method using Applied Biosystems DNA sequencers. Custom oligonucleotide primers, based on the derived DNA sequence, were synthesized by Sigma-Genosys and the sequence was extended by primer-walking to obtain the complete sequence.

2.4. Promoter-less Cm^R gene from plasmid pNW33N

The chloramphenicol resistance (Cm^R) gene in plasmid pNW33N was originally derived from plasmid pC194 from *Staphylococcus aureus* (Horinouchi and Weisblum, 1982). In preliminary transformation experiments, plasmid pNW33N was found to be transformable into *B. coagulans* strain P4-102B. For construction of plasmid vector pMSR10, the Cm^R gene from plasmid pNW33N was amplified by PCR using the following two primers: forward—CCCGGGACAAGTAAGCCTCCTAAAT; reverse—CCCGGGATTTCGAATCGTGCCAGC. The 810 bp product was cloned into TOPO vector (Invitrogen). The Cm^R gene was removed as a SmaI fragment and used in the construction of plasmid pMSR10.

2.5. Electro-transformation of B. coagulans strain P4-102B

Cells were grown overnight in 5 ml of LB in a 125 ml flask at 50 °C without shaking. This culture served as the inoculum for 100 ml of LB, in 1 L Erlenmeyer flask, at an initial cell density of about 10^7 CFU/ml (OD at 420 nm of about 0.03 using Beckman 640 spectrophotometer). Cells were incubated at 50 °C with shaking (200 RPM) for about 3–4 h until the OD 420 nm reached about 0.3–0.5 (early to mid-log phase of growth). Cells were collected by centrifugation (4 °C; 4300*g*; 10 min) and washed with ice-cold SG medium (glycerol, 10%; sucrose, 0.5 M; and $MgCl_2$, 1 mM) three times. Cells were resuspended in 0.5 ml of SG medium (about 5×10^9–10^{10} CFU/ml). These electro-competent cells were used immediately.

Seventy-five microliters of cell suspension was mixed with 100 ng of plasmid DNA and transferred to chilled electroporation cuvette (1 mm gap). The electroporation conditions using a Bio-Rad electroporator were 1.5 KV, 25 μF and 600 Ω and variations thereof, as indicated. The time constant was set between 8.5 and 10 ms. Immediately after electroporation, cells were transferred to 2 ml of pre-warmed (50 °C) RG medium. These cells were transferred to a 13 × 100 mm screw cap tube and incubated in a tube rotator for 3 h at 50 °C. Cells were collected by centrifugation (2000 × g, 10 min) at room temperature and resuspended in 0.2 ml of LB. 50–75 μl of cells or the same volume of a 10-fold dilution (in LB) was spread on L-agar with chloramphenicol (7.5 μg/ml), pH 5.0. Plates were incubated at 50 °C. Total number of transformants obtained per unit concentration of plasmid DNA was normalized per μg of plasmid DNA and this number is used as the transformation efficiency of the culture.

2.6. Transformation of B. subtilis

Bacillus subtilis was transformed according to the procedure described by Boylan et al. (1972) with minor changes. Cells from an overnight culture in stationary phase of growth in GM1 medium was inoculated (10% v/v) into 10 ml of GM2 medium in a 125 ml Erlenmeyer flask and incubated at 37 °C with shaking for 1 h. One ml of the culture was removed to a 13 × 100 mm tube and DNA was added to the cells. This culture with DNA was incubated in a rotator at 37 °C for 30 min. One ml of 2-fold concentrated L broth was added to the cells and the incubation was continued for an additional hour. Cells were collected by centrifugation at room temperature and resuspended in 0.1 ml of LB and plated on L-agar with appropriate antibiotics. Plates were incubated at 37 °C and transformants were selected next day.

2.7. Determination of plasmid stability

Plasmid stability was determined by growing *B. coagulans* strain P4-102B with plasmid pNW33N or plasmid pMSR10 in 250 ml of LB with glucose (2% w/v) in a 500 ml fleaker fermentor at 50 °C with pH control at 5.0 as described previously (Patel et al., 2005). Cultures were grown for about 24 generations by serially transferring stationary phase cultures from one fermentor to another. Samples were removed from each transfer and

serial dilutions were plated on LB-agar medium with and without chloramphenicol. The fraction of Cm^R cells in the total population was determined. At the end of the experiment, presence of plasmid DNA in appropriate cells was confirmed by isolation of plasmid DNA and transformation of *E. coli* Top10 with the isolated DNA.

2.8. Materials

All organic, inorganic chemicals and media components were from Fisher Scientific. Biochemicals were purchased from Sigma Chemical Co. Molecular biology reagents, enzymes, etc. were from new England Biolabs and Invitrogen.

3. Results and discussion

3.1. Native plasmids of B. coagulans

We tested 24 independent *B. coagulans* isolates for the presence of small plasmids that can provide a plasmid DNA replication region for shuttle vector construction. Only one strain, P4-102B, was found to carry two plasmids. Size of one of the plasmid was 6.8 kbp and the other was about 15 kbp. The small plasmid (pMSR0) was cloned into plasmid vector pUC19 using a unique *Kpn*I site and the DNA was sequenced. The plasmid size was 6823 bp (Fig. 1) with a G+C content of 36.9%, a value significantly lower than the average G+C content of several *B. coagulans* strains (45 to 48%) (De Clerck et al., 2004). This sequence was deposited into GenBank database under the Accession Number EF015591. Analysis of the sequence revealed 9 putative ORFs (Fig. 1, Table 1). Except for ORF4, all the other ORFs are read in the clockwise direction. DNA sequence analysis suggests that ORFs 1 and 2 could be transcribed as an operon and the function of the proteins encoded by these two ORFs is not known.

ORF 4 is homologous to transposon encoded protein TnpV. ORFs 5 and 8 encode proteins of unknown function. ORF 6 has the typical DNA-binding motif of the MerR family and has a homolog in *B. subtilis*. The role of this protein in

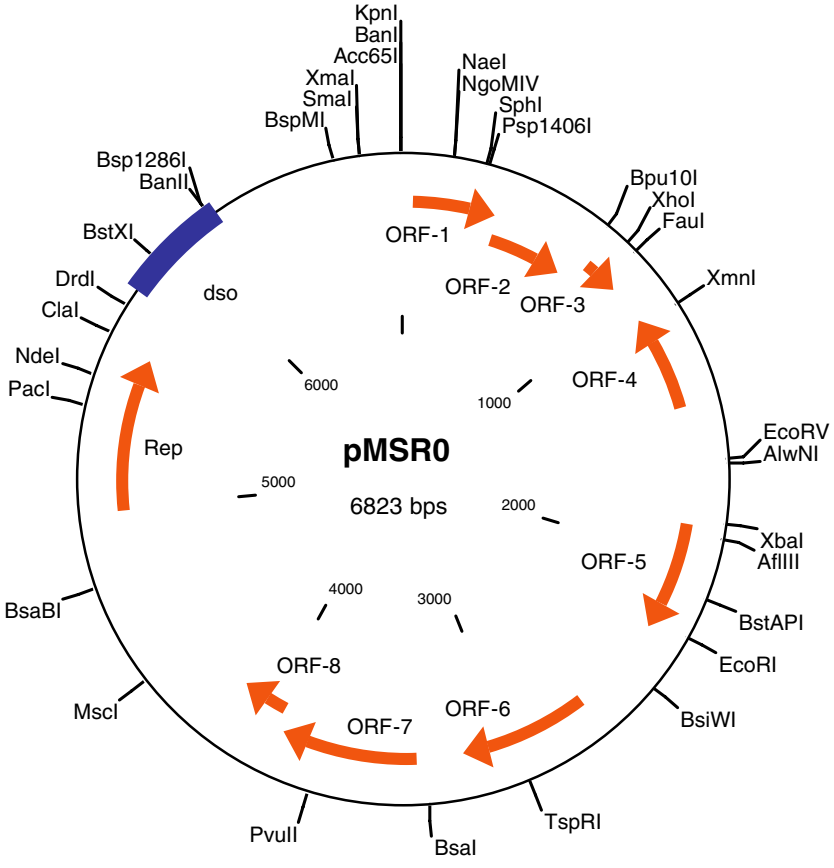

Fig. 1. Physical and genetic map of a native plasmid, pMSR0, from *B. coagulans* stain P4-102B.

Table 1
ORFs in plasmid pMSR0 and their homologs

ORF	Protein size (# amino acids)	Coordinate (bp)	Homologous proteins	Organism	Identity (similarity) (%)	Accession No.	Reference
ORF-1	121	27–392	Unnamed protein (Zn-dependent carboxypeptidase)	*Pelotomaculum thermopropionicum*	36 (58)	GAA00598	(Kosaka et al., 2006)
			Hypothetical protein	*Geobacillus kaustophilus*	39 (61)	YP 148208	(Takami et al., 2004)
ORF-2	106	376–696	Unnamed protein	*Pelotomaculum thermopropionicum*	45 (65)	GAA00598	(Kosaka et al., 2006)
			Hypothetical protein	*Geobacillus kaustophilus*	38 (68)	YP 148208	(Takami et al., 2004)
ORF-3	55	764–928	Hypothetical protein	*Bordetella bronchiseptica* RB50	29 (65)	CAE30985.1	(Parkhill et al., 2003)
ORF-4	128	1422–1036 (C)	TnpV	*Campylobacter coli* RM2228	31 (53)	ZP 00371009	
ORF-5	144	1873–2307	Hypothetical protein	*Bacillus thuringiensis*	37 (58)	ZP 00741358	
ORF-6	172	2686–3204	DNA binding Protein	*Bacillus subtilis*	27 (47)	AAC44410	
ORF-7	187	3360–3923	Site-specific recombinase, Resolvase	*Bacillus cereus*	63 (78)	ZP 00237179	(Hoffmaster et al., 2004)
			Putative resolvase	*Lactobacillus plantarum*	62 (74)	YP 133721	(Kleerebezem et al., 2003)
			Site-specific recombinase, DNA invertase	*Pediococcus pentosaceus*	61 (74)	ZP 00322971	
			Putative resolvase	*Lactobacillus salivarius*	59 (75)	YP 163746	
ORF-8	68	3923–4129	Hypothetical protein	*Bacillus halodurans*	43 (69)	BAB07265	(Takami and Horikoshi, 1999)
ORF-9	206	4988–5608	Rep14-2 in pTX14-2	*Bacillus thuringiensis*	58 (81)	AAN34374	(Andrup et al., 2003)
			Rep2 in pGI2	*Bacillus thuringiensis*	36 (62)	P10022	(Andrup et al., 2003)
			Rep14-3 in pTX14-3	*Bacillu thuringiensis*	34 (61)	ZP 00742127	(Andrup et al., 2003)
			Rep	*Bacillus mycoides*	36 (59)	YP 209644	

B. coagulans strain P4-102B is unclear. ORF 7 is a putative recombinase and this ORF appears to be co-transcribed with ORF 8 encoding a hypothetical protein.

ORF 9 is the Rep protein needed for rolling circle replication (RCR) of the plasmid with the HTH domain between amino acids 116 and 150 (Fig. 2) (Khan, 1997; Khan, 2005). Based on the similarities of the amino acid sequences and the origin of plasmid replication sequences, the Rep protein from this plasmid is a member of the RCR group VII (Database of plasmid replicons; DPR – http://www.essex.ac.uk/bs/staff/osborn/DPR_home.htm). Based on sequence similarity, the double strand origin of replication (*dso*) of plasmid pMSR0 is located 164 bp downstream of the *rep* gene. This is in agreement with the position of *dso* in plasmids with the RCR Rep protein from group VII that is generally found about 200 bp downstream of the *rep* gene (Andrup et al., 2003).

The intergenic region between ORF2 and ORF4 contains a region that is homologous to a plasmid from *B. coagulans* strain I4 encoding coagulin (Le Marrec et al., 2000). This similarity extends between 720 and 1210 bp of pMSR0 and 152 to 621 of the plasmid pI4. This region may code for a small peptide of 55 amino acids with similarity to a plasmid related protein of 77 amino acids from *Bordetella bronchiseptica* RB50 (Genbank Accession # CAE30985.1) (Parkhill et al., 2003). This sequence similarity of 65% (identity 29%) extends over a 47 amino acid region. Except for this region, no homology was detected among the two *B. coagulans* plasmids. No sequence homology was detected between plasmid pMSR0 and another *B. coagulans* plasmid pBC1 (De Rossi et al., 1992). Plasmid pMSR0 did not encode any detectable antibiotic resistance gene.

3.2. Construction of shuttle vector

A shuttle vector that can replicate in Gram-positive hosts such as *B. coagulans* and *B. subtilis* as well as in Gram-negative bacterium *E. coli* was constructed using the *rep* region from plasmid pMSR0 and ColEI region from plasmid pUC19. This plasmid, pMSR10 (6091 bp; Fig. 3), contains the DNA between the MscI and *Kpn*I from plasmid pMSR0 that includes the *rep* and *dso* (413 to 3,013 bp), pUC19 sequence (3836–413 bp) and a promoter-less chloramphenicol-resistance gene from plasmid pNW33N (bp 3,035 to 3,825). The

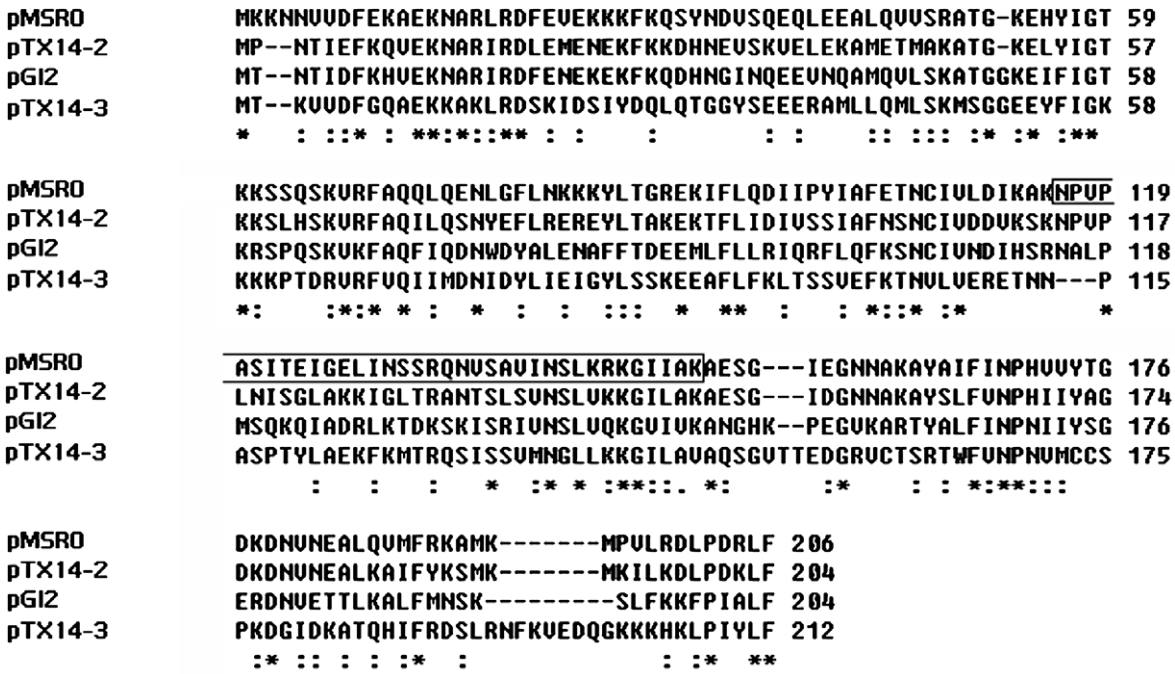

Fig. 2. Alignment of the amino acid sequence of the Rep protein from pMSR0 with homologs. Open box enclosing amino acids 116–150 represents the DNA-binding domain (HTH region). *indicates identical amino acids in all four proteins. : indicates conservative substitutions.

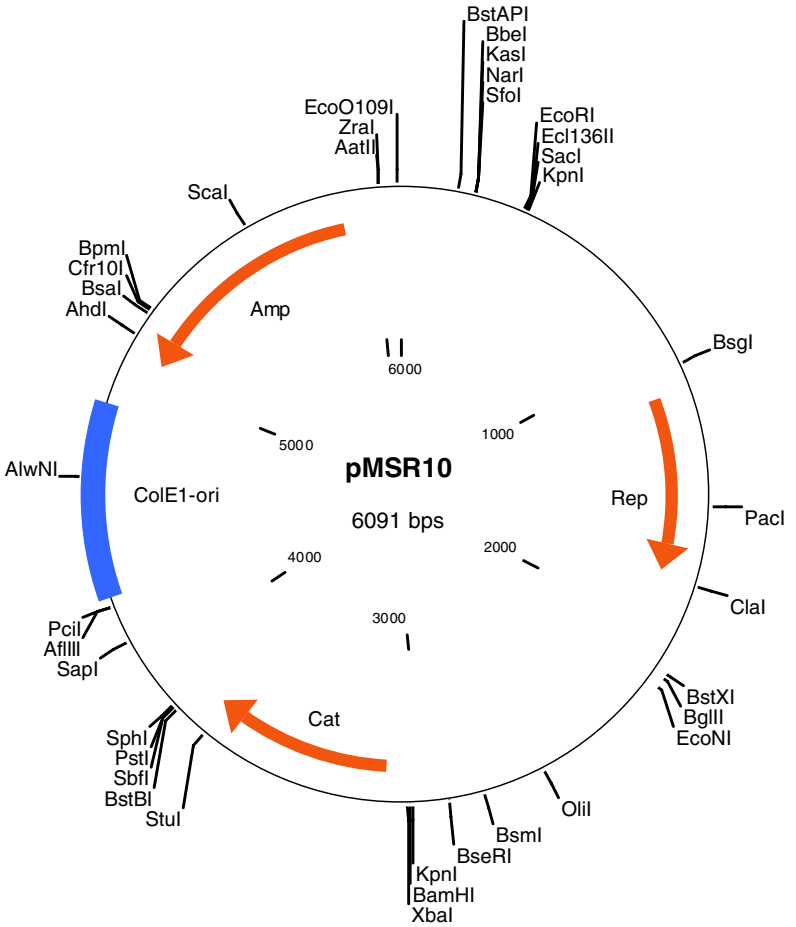

Fig. 3. Physical and genetic map of a *Bacillus*/*E. coli* shuttle vector pMSR10 carrying the *rep* region of pMSR0.

orientation of the Cm-gene in plasmid pMSR10 is such that the antibiotic resistance gene is transcribed from a promoter for ORFs 1 and 2 of plasmid pMSR0. In all three hosts, plasmid pMSR10 supported growth on LB agar with chloramphenicol at 7.5 μg/ml.

3.3. Transformation of *B. coagulans*

In order to evaluate the transformability of *B. coagulans*, we used published *E. coli*/*Bacillus* shuttle plasmid vectors that are used successfully in other Gram-positive bacteria. These include plasmids pNW33N, pDG148Stu, pMUTIN4, pMSP3535 and pMSP3535VA (Bryan et al., 2000; Joseph et al., 2001; Vagner et al., 1998). *B. coagulans* strains included strains P4-102B, 36D1, 17C5 among others (Patel et al., 2006). Preliminary electroporation experiments revealed that only the combination of *B. coagulans* strain P4-102B and plasmid pNW33N produced detectable transformants. Among these plasmids tested, only plasmid pNW33N was reported to carry the origin of replication from *Geobacillus stearothermophilus* plasmid pTHT15 (Genbank Accesion # AY237122). *B. coagulans* transformants with plasmid pNW33N replicated at 50 °C, the optimum temperature for growth of the strains of *B. coagulans* used in this study. It is possible that the inability to obtain transformants with other tested plasmids is related to the potential temperature sensitivity of the Rep proteins encoded by these plasmids designed for *B. subtilis*/*E. coli*. However, even the cells that were electroporated with DNA and incubated at 37 °C, failed to yield any transformant with these plasmids. Apparently, the antibiotic resistance encoded by these plasmids is not expressed in *B. coagulans* or the Rep protein is not functional. These plasmids were not further pursued.

Using plasmid pNW33N and pMSR10, strain P4-102B was tested for natural transformation

competence as seen with *B. subtilis*. However, cells harvested at various times during the growth cycle and exposed to DNA using the general protocol for *B. subtilis* did not yield any transformants. Chemical transformation protocol using high Ca^{2+}/Mg^{2+} during growth that was successfully used for *B. subtilis* also did not yield detectable transformants. Only electroporation of plasmid DNA into *B. coagulans* consistently provided transformants.

3.4. Electrotransformation of B. coagulans strain P4-102B

Bacillus coagulans strain P4-102B cells were harvested at an OD of 0.3 and were washed and concentrated. Various electroporation conditions were tested for optimum transformation efficiency. In initial experiments, the electroporation conditions were set as follows: voltage at 15 kV cm^{-1}; capacitance at 25 μF; resistance at 600 Ω; pulse duration (time constant) with exponential decay at 10 ms. Under these conditions, about 300 ng of plasmid pNW33N saturated the transformation producing about 1100 transformants (Fig. 4A). The highest observed transformation efficiency was about 1×10^4/μg plasmid pNW33N DNA. This required a minimum of 3 h regeneration time at 50 °C, after electroporation, and before plating on antibiotic medium. The number of transformants with plasmid pMSR10, using the same electroporation conditions was about 70% of that obtained with plasmid pNW33N. This difference between the two plasmids in the number of transformants per μg of plasmid DNA can be attributed to the differences in the sizes of the two plasmids; the sizes of the plasmids pNW33N and pMSR10 are 4217 and 6091 bp, respectively. On a molar basis, this value translates to about 1.5×10^{16} transformants per mole of either plasmid DNA. This value is about 60% of the molar transformation efficiency of *B. subtilis* transformation for plasmid pNW33N using the method described in the Methods section.

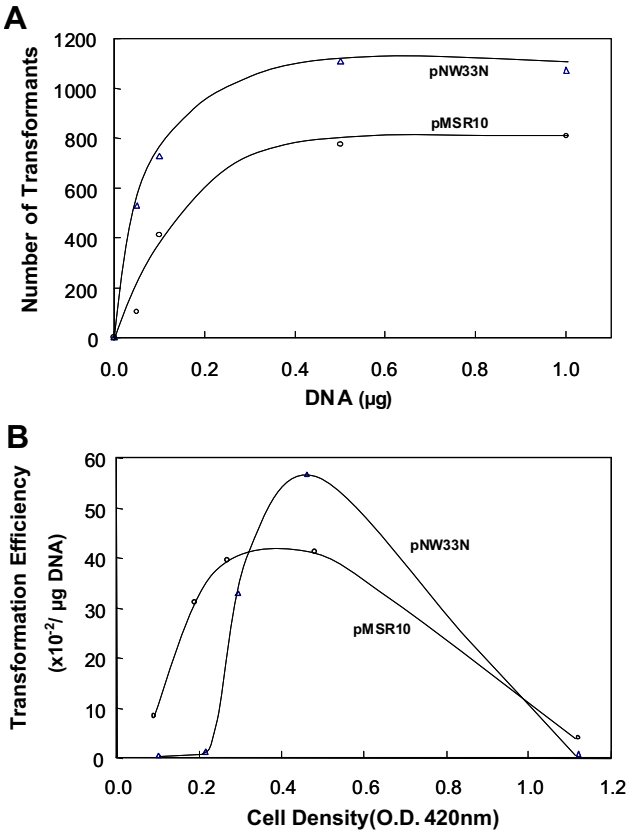

Fig. 4. (A) Plasmid concentration dependent increase in transformation of *B. coagulans* strain P4-102B (B) Influence of the age of the growing culture on transformation of *B. coagulans* strain P4-102B. Transformation efficiency represents the total number of transformants obtained per μg of plasmid DNA. See text for other details.

The number of transformants decreased by about 10-fold by decreasing the voltage from 15 kV cm^{-1} to 5 kV cm^{-1}. At 20 kV cm^{-1}, viability of cells declined very rapidly. Pulse duration of 10 ms was found to be optimal for an exponential decay wave.

Age of the culture played a significant role in the ability of the cell to be transformed by electroporation. Early to mid-exponential phase of the culture was more efficient than the cells from other phases of growth. Cells stored in glycerol at −75 °C did not yield any transformant with either plasmid necessitating the need for fresh cells. At a slightly lower voltage, such as 12.5 kV cm^{-1}, optimum transformation with the plasmids was obtained by increasing the pulse duration to 12.5–15 ms. There was an inverse relationship between the field strength and pulse duration on transformation of *B. coagulans*. The larger plasmid (pMSR10, 6091 bp) required lower voltage and longer pulse duration compared to the smaller plasmid (pNW33N, 4217 bp) for optimum transformation efficiency. These results suggest that the electroporation conditions need to be optimized for each plasmid as well as a vector plasmid with varying lengths of inserts.

Transformation efficiency of *B. coagulans* strain P4-102B was independent of the source of DNA, either from a methylation–defective *E. coli* strain GM272 or isolated from *B. coagulans* strain P4-102B. In vitro methylation of unmethylated plasmid DNA using *B. coagulans* strain P4-102B extract (Alegre et al., 2004) did not influence the electroporation efficiency of the plasmid DNA transfer. These results suggest that *B. coagulans* has an efficient methylation system for incoming DNA. DNA prepared by CsCl-method consistently yielded the highest transformation efficiency indicating that the small amount of impurities present in the DNA prepared by the alkaline lysis procedure reduced electroporation of plasmid DNA.

Both plasmid pNW33N and pMSR10 were stably maintained by *B. coagulans* strain P4-102B during growth in the absence of antibiotic selection. Although plasmids pMSR10 and the native plasmid pMSR0 contain the same *rep* region, apparently, the plasmids did not interfere with the maintenance of the other plasmid with the same replication system.

In summary, we have developed an electroporation protocol for introducing plasmid DNA into a genetically recalcitrant sporogenic lactic acid bacterium *B. coagulans* strain P4-102B. With this method, we have transformed strain P4-102B with plasmid pMSR10, a new *Bacillus*/*E. coli* shuttle vector containing a *B. coagulans* plasmid replication system and plasmid pNW33N, a *Geobacillus stearothermophilus*/*E. coli* shuttle vector.

Acknowledgments

We thank Dr. Healy for providing *B. subtilis* strain HB1000 and late Dr. Welker for plasmid pNW33N. This study was supported by funds form the US Department of Energy (DE-FC36-04-GO14019) and the State of Florida, University of Florida Agricultural Experiment Station.

Appendix A. Supplementary data

Supplementary data associated with this article can be found, in the online version, at doi:10.1016/j.plasmid.2006.11.006.

References

Aden, A., Ruth, M., Ibsen, K., Jechura, J., Neeves, K., Sheehan, J., Wallace, B., Montague, L., Slayton, A., Lukas, J., 2002. Lignocellulosic biomass to ethanol process design and economics utilizing co-current dilute acid prehydrolysis and enzymatic hydrolysis for corn stover. NREL/TP-510-32438.

Alegre, M.T., Rodriguez, M.C., Mesas, J.M., 2004. Transformation of *Lactobacillus plantarum* by electroporation with in vitro modified plasmid DNA. FEMS Microbiol. Lett. 241, 73–77.

Andrup, L., Jensen, G.B., Wilcks, A., Smidt, L., Hoflack, L., Mahillon, J., 2003. The patchwork nature of rolling-circle plasmids: comparison of six plasmids from two distinct *Bacillus thuringiensis* serotypes. Plasmid 49, 205–232.

Bothast, R.J., Schlicher, M.A., 2005. Biotechnological processes for conversion of corn into ethanol. Appl. Microbiol. Biotechnol. 67, 19–25.

Boylan, R.J., Mendelson, N.H., Brooks, D., Young, F.E., 1972. Regulation of the bacterial cell wall: analysis of a mutant of *Bacillus subtilis* defective in biosynthesis of teichoic acid. J. Bacteriol. 110, 281–290.

Bryan, E.M., Bae, T., Kleerebezem, M., Dunny, G.M., 2000. Improved vectors for nisin-controlled expression in Gram-positive bacteria. Plasmid 44, 183–190.

Datta, R., Tsai, S., Bonsignore, P., Moon, S., Frank, J.R., 1995. Technological and economic potential of poly(lactic acid) and lactic acid derivatives. FEMS Microbiol. Rev. 16, 221–231.

De Clerck, E., Rodriguez-Diaz, M., Forsyth, G., Lebbe, L., Logan, N.A., DeVos, P., 2004. Polyphasic characterization of *Bacillus coagulans* strains, illustrating heterogeneity within this species, and emended description of the species. System. Appl. Microbiol. 27, 50–60.

De Rossi, E., Brigidi, P., Rossi, M., Matteuzzi, D., Riccardi, G., 1991. Characterization of Gram-positive broad host-range plasmids carrying a thermophilic replicon. Res. Microbiol. 142, 389–396.

De Rossi, E., Milano, A., Brigidi, P., Bini, F., Riccardi, G., 1992. Structural organization of pBC1, a cryptic plasmid from *Bacillus coagulans*. J. Bacteriol. 174, 638–642.

Department of Energy, 2003. Biobased PLA polymers grow new markets for american corn products. Publication 6980, Washington, DC.

Dubnau, D., 1991. Genetic competence in *Bacillus subtilis*. Microbiol. Rev. 55, 395–424.

Garde, A., Jonsson, G., Schmidt, A.S., Ahring, B.K., 2002. Lactic acid production from wheat straw hemicellulose hydrolysate by *Lactobacillus pentosus* and *Lactobacillus brevis*. Bioresource Technol. 81, 217–223.

Hoffmaster, A.R., Ravel, J., Rasko, D.A., Chapman, G.D., Chute, M.D., Marston, C.K., De, B.K., Sacchi, C.T., Fitzgerald, C., Mayer, L.W., Maiden, M.C., Priest, F.G., Barker, M., Jiang, L., Cer, R.Z., Rilstone, J., Peterson, S.N., Weyant, R.S., Galloway, D.R., Read, T.D., Popovic, T., Fraser, C.M., 2004. Identification of anthrax toxin genes in a *Bacillus cereus* associated with an illness resembling inhalation anthrax. Proc. Natl. Acad. Sci. USA 101, 8449–8454.

Hofvendahl, K., Hans-Hagerdal, B., 2000. Factors affecting the fermentative lactic acid production from renewable resources. Enz. Microb. Technol. 26, 87–107.

Horinouchi, S., Weisblum, B., 1982. Nucleotide sequence and functional map of pC194, a plasmid that specifies inducible chloramphenicol resistance. J. Bacteriol. 150, 815–825.

Joseph, P., Fantino, J.R., Herbaud, M.L., Denizot, F., 2001. Rapid orientated cloning in a shuttle vector allowing modulated gene expression in *Bacillus subtilis*. FEMS Microbiol. Lett. 205, 91–97.

Khan, S.A., 1997. Rolling-circle replication of bacterial plasmids. Microbiol. Mol. Biol. Rev. 61, 442–455.

Khan, S.A., 2005. Plasmid rolling-circle replication: highlights of two decades of research. Plasmid 53, 126–136.

Kleerebezem, M., Boekhorst, J., van Kranenburg, R., Molenaar, D., Kuipers, O.P., Leer, R., Tarchini, R., Peters, S.A., Sandbrink, H.M., Fiers, M.W., Stiekema, W., Lankhorst, R.M., Bron, P.A., Hoffer, S.M., Groot, M.N., Kerkhoven, R., de Vries, M., Ursing, B., de Vos, W.M., Siezen, R.J., 2003. Complete genome sequence of *Lactobacillus plantarum* WCFS1. Proc. Natl. Acad. Sci. USA 100, 1990–1995.

Kosaka, T., Uchiyama, T., Ishii, S., Enoki, M., Imachi, H., Kamagata, Y., Ohashi, A., Harada, H., Ikenaga, H., Watanabe, K., 2006. Reconstruction and regulation of the central catabolic pathway in the thermophilic propionate-oxidizing syntroph *Pelotomaculum thermopropionicum*. J. Bacteriol. 188, 202–210.

Le Marrec, C., Hyronimus, B., Bressollier, P., Verneuil, B., Urdaci, M.C., 2000. Biochemical and genetic characterization of coagulin, a new antilisterial bacteriocin in the pediocin family of bacteriocins, produced by *Bacillus coagulans* I(4). Appl. Environ. Microbiol. 66, 5213–5220.

Lee, J.H., Patel, P., Sankar, P., Shanmugam, K.T., 1985. Isolation and characterization of mutant strains of *Escherichia coli* altered in H_2 metabolism. J. Bacteriol. 162, 344–352.

Maniatis, T., Fritsch, E.F., Sambrook, J., 1982. Molecular cloning: a laboratory manual. Cold Spring Harbor Laboratory Press, Cold Spring Harbor, NY.

Martin, A.M., 1996. Fermentation processes for the production of lactic acid. In: Bozoglu, T.F., Ray, B. (Ed.), Lactic acid bacteria: current advances in metabolism, genetics and applications. NATO ASI Series Vol. H98. Springer-Verlag, New York, NY. pp. 269–301.

Mecking, S., 2004. Nature or petrochemistry?—biologically degradable materials. Angew. Chem. Int. Ed. 43, 1078–1085.

Parkhill, J., Sebaihia, M., Preston, A., Murphy, L.D., Thomson, N., Harris, D.E., Holden, M.T., Churcher, C.M., Bentley, S.D., Mungall, K.L., Cerdeno-Tarraga, A.M., Temple, L., James, K., Harris, B., Quail, M.A., Achtman, M., Atkin, R., Baker, S., Basham, D., Bason, N., Cherevach, I., Chillingworth, T., Collins, M., Cronin, A., Davis, P., Doggett, J., Feltwell, T., Goble, A., Hamlin, N., Hauser, H., Holroyd, S., Jagels, K., Leather, S., Moule, S., Norberczak, H., O'Neil, S., Ormond, D., Price, C., Rabbinowitsch, E., Rutter, S., Sanders, M., Saunders, D., Seeger, K., Sharp, S., Simmonds, M., Skelton, J., Squares, R., Squares, S., Stevens, K., Unwin, L., Whitehead, S., Barrell, B.G., Maskell, D.J., 2003. Comparative analysis of the genome sequences of *Bordetella pertussis, Bordetella parapertussis* and *Bordetella bronchiseptica*. Nature Genet. 35, 32–40.

Patel, M.A., Ou, M., Ingram, L.O., Shanmugam, K.T., 2005. Simultaneous saccharification and co-fermentation of crystalline cellulose and sugar cane bagasse hemicellulose hydrolysate to lactate by a thermotolerant acidophilic *Bacillus* sp. Biotech. Prog. 21, 1453–1460.

Patel, M.A., Ou, M.S., Harbrucker, R., Aldrich, H.C., Buszko, M.L., Ingram, L.O., Shanmugam, K.T., 2006. Isolation and characterization of acid-tolerant, thermophilic bacteria for effective fermentation of biomass-derived sugars to lactic acid. Appl. Environ. Microbiol. 72, 3228–3235.

Takami, H., Horikoshi, K., 1999. Reidentification of facultatively alkaliphilic *Bacillus* sp. C-125 to *Bacillus halodurans*. Biosci. Biotechnol. Biochem. 63, 943–945.

Takami, H., Takaki, Y., Chee, G.J., Nishi, S., Shimamura, S., Suzuki, H., Matsui, S., Uchiyama, I., 2004. Thermoadaptation trait revealed by the genome sequence of thermophilic *Geobacillus kaustophilus*. Nucleic Acids Res. 32, 6292–6303.

Tanaka, K., Komiyama, A., Sonomoto, K., Ishizaki, A., Hall, S.J., Stanbury, P.E., 2002. Two different pathways for D-xylose metabolism and the effect of xylose concentration on the yield coefficient of L-lactate in mixed-acid fermentation by the lactic acid bacterium *Lactococcus lactis* IO-1. Appl. Microbiol. Biotechnol. 60, 160–167.

Teusink, B., Smid, E.J., 2006. Modelling strategies for the industrial exploitation of lactic acid bacteria. Nature Rev. Microbiol. 4, 46–56.

Vagner, V., Dervyn, E., Ehrlich, S.D., 1998. A vector for systematic gene inactivation in *Bacillus subtilis*. Microbiology 144, 3097–3104.

Wooley, R., Ruth, M., Glassner, D., Sheehan, J., 1999. Process design and costing of bioethanol technology: a tool for determining the status and direction of research and development. Biotechnol. Prog. 15, 794–803.

Wyman, C.E., 2003. Potential synergies and challenges in refining cellulosic biomass to fuels, chemicals, and power. Biotechnol. Prog. 19, 254–262.

Appendix H

Applied and Environmental Microbiology, Apr. 2010, p. 2107–2114 Vol. 76, No. 7
0099-2240/10/$12.00 doi:10.1128/AEM.02545-09

Metabolic Flux Control at the Pyruvate Node in an Anaerobic *Escherichia coli* Strain with an Active Pyruvate Dehydrogenase▽

Qingzhao Wang, Mark S. Ou, Y. Kim,† L. O. Ingram, and K. T. Shanmugam*

Department of Microbiology and Cell Science, University of Florida, Gainesville, Florida 32611

Received 20 October 2009/Accepted 16 January 2010

During anaerobic growth of *Escherichia coli*, pyruvate formate-lyase (PFL) and lactate dehydrogenase (LDH) channel pyruvate toward a mixture of fermentation products. We have introduced a third branch at the pyruvate node in a mutant of *E. coli* with a mutation in pyruvate dehydrogenase (PDH*) that renders the enzyme less sensitive to inhibition by NADH. The key starting enzymes of the three branches at the pyruvate node in such a mutant, PDH*, PFL, and LDH, have different metabolic potentials and kinetic properties. In such a mutant (strain QZ2), pyruvate flux through LDH was about 30%, with the remainder of the flux occurring through PFL, indicating that LDH is a preferred route of pyruvate conversion over PDH*. In a *pfl* mutant (strain YK167) with both PDH* and LDH activities, flux through PDH* was about 33% of the total, confirming the ability of LDH to outcompete the PDH pathway for pyruvate *in vivo*. Only in the absence of LDH (strain QZ3) was pyruvate carbon equally distributed between the PDH* and PFL pathways. A *pfl* mutant with LDH and PDH* activities, as well as a *pfl ldh* double mutant with PDH* activity, had a surprisingly low cell yield per mole of ATP (Y_{ATP}) (about 7.0 g of cells per mol of ATP) compared to 10.9 g of cells per mol of ATP for the wild type. The lower Y_{ATP} suggests the operation of a futile energy cycle in the absence of PFL in this strain. An understanding of the controls at the pyruvate node during anaerobic growth is expected to provide unique insights into rational metabolic engineering of *E. coli* and related bacteria for the production of various biobased products at high rates and yields.

In *Escherichia coli* as well as in other aerobic organisms, sugars such as glucose are metabolized in two separate steps: glycolysis, which converts glucose to pyruvate, and tricarboxylic acid (TCA) cycle enzymes, which oxidize acetyl coenzyme A (acetyl-CoA) to CO_2 (5, 9). The pyruvate dehydrogenase complex (PDH) connects the glycolytic reactions to TCA cycle enzymes by catalyzing the production of acetyl-CoA from pyruvate. Because of its unique central role in metabolism, PDH is regulated at both the genetic and the biochemical level (7, 12, 27, 33, 34). The NADH generated during the complete oxidation of sugar is reoxidized to NAD^+ by O_2 through the respiratory electron transport pathway with accompanying energy production (11). Optimum coupling of these enzyme reactions helps to maintain the internal ratios of [NADH] to [NAD^+] (redox balance) and of [ATP] to [ADP] plus [AMP] in order to support growth at the highest rate.

The absence of O_2 or another external electron acceptor during the growth of *E. coli* (anaerobic conditions) forces the bacterium to minimize the contribution of the TCA cycle enzymes to biosynthesis from catabolism (4, 14). Under these conditions, pyruvate or acetyl-CoA derived from pyruvate serves as the electron acceptor (reduced to lactate or ethanol, respectively) to maintain the redox balance. The enzymes responsible for redox balance in anaerobic *E. coli* are pyruvate formate-lyase (PFL), lactate dehydrogenase (LDH), and alcohol/aldehyde dehydrogenase (*adhE*; ADH-E). The main products of the fermentation of *E. coli* are a mixture of organic acids, such as acetate, lactate, and formate, in addition to ethanol (2, 4). Succinate, derived from phosphoenolpyruvate (PEP), is a minor product of fermentation and normally accounts for less than 5% of the total products produced from glucose by the culture.

Anaerobic growth of *E. coli*, compared to aerobic growth, is also limited by energy, leading to an increase in glycolytic flux (19). The conversion of pyruvate to acetate and ethanol yields an additional ATP per glucose, suggesting that this would be the preferred route for pyruvate oxidation during anaerobic growth. This is accomplished by the PFL-dependent production of acetyl-CoA and further conversion to acetate (Fig. 1). This preference for PFL has been demonstrated with several bacteria under carbon limitation conditions imposed either in a chemostat or in the presence of a poor carbon source (10, 20, 23). This additional ATP also elevates the ATP yield per glucose to 3, with an increase in the growth rate, and has been shown to be essential for the anaerobic growth of *E. coli* in xylose-mineral salts medium (13). The absence of this third ATP in a *pfl* mutant has been reported to increase glycolytic flux to lactate to compensate for this decrease in ATP yield per glucose (39). However, the flow of pyruvate carbon to acetate is tempered by the need to maintain redox balance, and this is achieved by the conversion of a second acetyl-CoA to ethanol by ADH-E. Under conditions of energy excess due to a declining growth rate, lactate production is expected to support redox balance maintenance without the additional ATP from the PFL–ADH-E pathway (Fig. 1). The production of this mixture of products in an appropriate ratio helps to maintain the redox balance under anaerobic conditions while also maximizing the

* Corresponding author. Mailing address: Department of Microbiology and Cell Science, Box 110700, University of Florida, Gainesville, FL 32611. Phone: (352) 392-2490. Fax: (352) 392-5922. E-mail: shan@ufl.edu.

† Present address: Amyris Biotechnologies, Inc., 5885 Hollis Street, Suite 100, Emeryville, CA 94608.

▽ Published ahead of print on 29 January 2010.

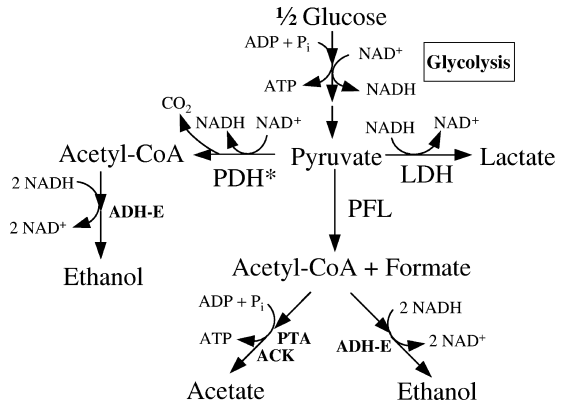

FIG. 1. Anaerobic metabolic pathways of *E. coli* carrying the *lpd101* mutation (PDH*).

ATP yield per glucose to support high growth rates and cell yields.

No PDH-based fermentation reaction to ethanol that can also help maintain cellular redox balance in an anaerobic cell has evolved in *E. coli* or other closely related bacteria. PDH activity is inhibited by NADH, normally found at higher levels in anaerobically growing cultures than in aerobic cultures (12, 18, 34, 35). Based on genome sequences available in GenBank, the genes encoding the components of PDH are not found in strictly anaerobic bacteria.

We have recently described a mutation (*lpd101*) in the dihydrolipoamide dehydrogenase (LPD) of the PDH that allowed the enzyme to function in anaerobic cells (designated PDH* here) (17, 18). With this altered PDH*, an anaerobic cell can have three different pathways for pyruvate metabolism (Fig. 1). The three main enzymes that utilize pyruvate as a substrate, PDH*, PFL, and LDH, have different apparent K_m values for pyruvate (0.4, 2.0, and 7.2 mM, respectively) (1, 18, 37, 41). PDH requires NAD^+ for activity (apparent K_m, 0.07 mM), while LDH is dependent on NADH (apparent K_m, 0.2 mM) as the second substrate (18, 37).

The PDH* serves as the first enzyme in a pathway that oxidatively decarboxylates pyruvate to acetyl-CoA and NADH, followed by reduction of the acetyl-CoA by alcohol dehydrogenase to ethanol in a two-step process using 2 NADHs (Fig. 1). The NADH produced during the conversion of ½ glucose to acetyl-CoA dictates that the acetyl-CoA generated by PDH be used for redox balance (ethanol) and not for ATP generation (acetate), unless some of the NADH is used for biosynthesis by the growing cell (17). PDH* and LDH serve essentially the same physiological role in the cell, oxidizing NADH to support continued operation of glycolysis, although it is not readily apparent with PDH*. Although PDH* contributes to an increase in NADH pool, the redox balance is still maintained by coupling PDH* to NADH-dependent reduction of acetyl-CoA to ethanol by ADH-E (Fig. 1). This potential competition between LDH and PDH has been eliminated in the wild type through inhibition of the activity of PDH by NADH (12, 18, 32). However, the *in vivo* role of PDH* in a mutant that has all three pathways has not been investigated, since the flow of pyruvate through any of the three reactions during growth and postgrowth fermentation of sugars to products is expected to be dependent on the redox state, the ATP requirement, and other physiological conditions of the anaerobic cell. Using a combination of metabolic flux analysis and mutations in one or more of the genes encoding these enzymes, we have evaluated the flow of pyruvate carbon among the three potential pathways. The results are presented in this communication.

MATERIALS AND METHODS

Bacterial strains. The bacterial strains used in this study are listed in Table 1. All strains are derived from *E. coli* K-12 strain W3110 (ATCC 27325). Strain YK1 is a kanamycin-sensitive derivative of strain SE2378 that carries the *lpd101* mutation described previously (17). Gene deletions were constructed using the method described by Datsenko and Wanner (6). Mutations were transduced using bacteriophage P1 as described previously (29).

Growth medium. L broth (LB) (29) supplemented with 20 g/liter of glucose was used for all chemostat cultivations. The glucose concentration was increased to 50 g/liter in batch fermentation experiments.

Bioreactor conditions. For metabolic flux analysis, fermentations were conducted under anaerobic chemostat conditions in a 2.5-liter Bioflo III fermenter

TABLE 1. Bacterial strains used in this study

Strain[a]	Relevant genotype[b]	Source or reference
W3110	F^- IN(*rrnD-rrnE*)*1* λ^-	ATCC 27325
AH218	BW25113 Δ(*focA-pflB*)-FRT-Km-FRT	13
AH240	Δ(*focA-pflB*)-FRT-Km-FRT	W3110 × P1 (AH218)
AH241	Δ*ldhA*	17
BW25113	*lacI*^{q} *rrnB*$_{T14}$ Δ*lacZ*$_{W116}$ *hsdR514 araBAD*$_{AH33}$ Δ*rhaBAD*$_{LD78}$	6
PMD23	Δ*hypF*-FRT-Km-FRT	15
SE2378	*lpd101* Δ*ldhA* Δ(*focA-pflB*)-FRT-Km-FRT *pdhR*	17
SE2382	*lpd101* Δ*ldhA* Δ(*focA-pflB*)-FRT-Km-FRT	18
YK1	*lpd101* Δ*ldhA* Δ(*focA-pflB*)-FRT *pdhR* Km^s	SE2378; Km^s
YK98	BW25113 Δ*lpd*-FRT-Km-FRT	This study
YK134	Δ*lpd*-FRT-Km-FRT	W3110 × P1 (YK98)
YK142	*lpd101*	YK134 × P1 (SE2382)
YK143	Δ*ldhA* Δ*lpd*-FRT-Km-FRT	AH241 × P1 (YK98)
YK167	*lpd101* Δ(*focA-pflB*)-FRT-Km-FRT	YK142 × P1 (AH240)
QZ1	Δ*ldhA lpd101*	YK143 × P1 (YK142)
QZ2	*lpd101* Δ*hypF*-FRT-Km-FRT	YK142 × P1 (PMD23)
QZ3	Δ*ldhA lpd101* Δ*hypF*-FRT-Km-FRT	QZ1 × P1 (PMD23)

[a] All strains are derivatives of *E. coli* K-12 strain W3110, a nearly wild type strain deposited by J. Lederberg, unless noted otherwise (BW25113 and YK98).
[b] FRT, FLP recombination target.

(New Brunswick Scientific, New Brunswick, NJ) with a 1.2-liter culture volume. Anaerobic conditions were established by sparging the culture with N_2 at a flow rate of 0.2 liter min^{-1}. The pH, temperature, and agitation were maintained at 7.0, 37°C, and 250 rpm, respectively. The culture pH was maintained by the addition of KOH. A dilution rate of 0.1 h^{-1} was maintained throughout the experiment by controlling the medium feed rate. The continuous culture reached steady state after 5 to 6 residence times. Samples were taken for analysis every 5 h. Three samples were taken from the steady-state culture for determination of fermentation products, and the average of the three was used for the calculation. Deviations from this mean were less than 5%, and the results from one complete representative experiment are presented. For batch fermentations, cells were cultivated with 50 g/liter glucose, starting with a 16-h-old aerobic culture as the inoculum (1%, vol/vol), as previously described (17). All fermentation experiments were repeated at least three times, and the variation among experimental results was less than 15%. Results from one representative experiment are presented in this communication.

Enzyme activity. A 250-ml culture from a batch fermentation in LB with glucose (30 g/liter) was harvested at the mid-exponential phase of growth, and the cells were collected after centrifugation (10,000 × *g*, 20 min, 4°C). Cells were washed twice with 25 ml of 50 mM potassium phosphate buffer (pH 7.5) and were then resuspended in 5 ml of the same buffer. All operations were conducted at 4°C. Cells were passed through a French pressure cell at 20,000 lb/in^2. The crude extract was centrifuged first at 10,000 × *g* for 30 min, and the supernatant was further clarified by centrifugation at 30,000 × *g* for 60 min. The supernatant was used for enzyme assays.

PDH activity was determined by monitoring pyruvate-dependent reduction of NAD^+ at 340 nm (ε, 6,220 M^{-1} cm^{-1}) at room temperature, as described previously (18). LDH activity was determined by measuring pyruvate-linked NADH oxidation at 340 nm (43). ADH-E activity was assayed by measuring the increase in absorbance at 340 nm resulting from the reduction of NAD^+ in the presence of ethanol (ADH assay; Worthington Biochemical Corporation). One unit of enzyme activity is defined as one micromole of product produced per minute.

Total RNA was extracted from the same cultures used for enzyme activity determination, and the specific mRNA level in the RNA sample was determined as described by Kim et al. (18).

Analytical methods. Sugar and fermentation products were determined by high-performance liquid chromatography using an HP1090 chromatograph (Agilent Technologies, Santa Clara, CA) fitted with an Aminex HPX-87H column (Bio-Rad Laboratories, Hercules, CA) and UV (210 nm) and refractive index detectors, in series (38). Cell density was monitored at 420 nm (DU640 spectrophotometer; Beckman Coulter, Fullerton, CA) and reported as the dry weight of cells. The dry weight of cells of a culture at 1 optical density (OD) unit at 420 nm equals 0.22 g/liter. The protein concentration was determined by the Bradford method with bovine serum albumin as the standard (3).

Metabolic flux analysis. Metabolic flux analysis was used for the calculation of *in vivo* fluxes (36). The methodology relies on the metabolite balances, biochemical constraints, and pseudo-steady-state assumption for intracellular metabolites (40). The stoichiometric reactions presented in Fig. 2 were used for the calculation of flux distributions based on experimental data. The resulting metabolic network consists of 13 reactions, 8 of which (J1, J6, J7, J8, J10, J11, J12, and J13) can be measured. All the lactate produced by the *ldhA*-plus strains was assumed to be produced by LDH (reaction J7). In *ldhA* mutants, the lactate was assumed to be from the melthylglyoxal pathway (reaction J13). In order to distinguish between the contributions of PDH* and PFL, further metabolism of formate was eliminated by introducing an *hypF* mutation to remove formate hydrogen-lyase (FHL) activity. In such an *hypF* mutant, the level of formate in the medium is a measure of PFL activity.

Materials. Inorganic salts, organic chemicals, and medium components were purchased either from Fisher Scientific (Pittsburgh, PA) or from Sigma Chemical Co. (St. Louis, MO).

RESULTS AND DISCUSSION

Preferred pathway at the pyruvate node. In strain QZ2, which carries the *lpd101* mutation, rendering the PDH* functional during anaerobic growth, pyruvate flux through PDH* in batch cultures was minimal during anaerobic growth (Fig. 3A). Strain QZ2 produced acetate, ethanol, formate, and lactate in pH-controlled batch fermentation. The specific rates of production of acetate, ethanol, and formate during the exponential phase of growth were 29.1, 27.2, and 51.5 mmol h^{-1} (g of cells [dry weight])$^{-1}$, respectively. The presence of equimolar amounts of acetate and ethanol in the medium suggests that PFL-produced acetyl-CoA is the precursor for these two products. This is also confirmed by the specific rate of production of formate, that is, the combined rates of acetate and ethanol production, a measure of the PFL pathway. The specific rate of lactate production (26.1 mmol h^{-1} [g of cells {dry weight}]$^{-1}$) during this growth phase was about 50% of the formate production rate. The presence of lactate in the fermentation broth suggests that a significant fraction of the reductant generated during glycolysis was channeled to reduce pyruvate to lactate in order to maintain redox balance. An interesting observation is the absence of PDH*-based acetyl-CoA production in this culture, since this acetyl-CoA can be converted to ethanol while also supporting optimum redox balance (17, 18). Although PDH* requires NAD^+ for activity, in contrast to LDH, a coupled PDH* and ADH pathway (pyruvate to ethanol) does oxidize 1 net NADH, as does LDH (Fig. 1). However, *in vivo*, LDH appears to be the preferred enzyme for NADH oxidation in the cell. In support of this pyruvate flux distribution, the PDH activity of strain QZ2 (0.14 U mg protein^{-1}) was found to be only about 30% of that of an isogenic "wild-type" strain, PMD23 (0.46 U mg protein^{-1}) (Table 2).

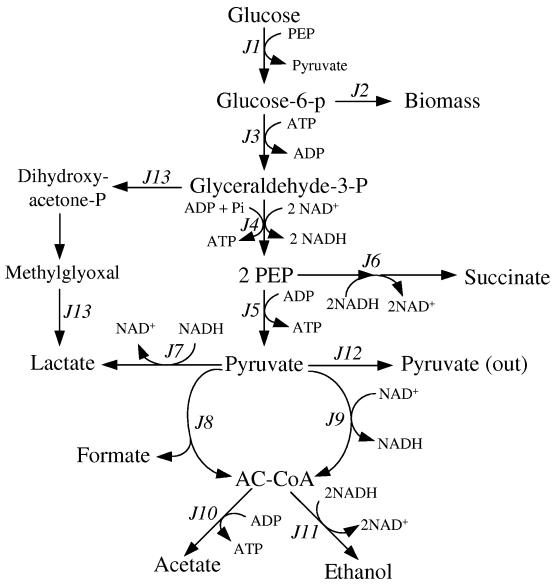

FIG. 2. Central metabolic pathways of *E. coli* used for flux analysis. Although PDH* also produces acetyl-CoA (reaction J9), due to NADH production most of this acetyl-CoA was assumed to flow only through reaction J11 to maintain redox balance.

Pyruvate flux in strain YK167, which produces only LDH and PDH*, and not PFL activity, was also directed toward LDH and not PDH* (Fig. 3B), and the PDH activity of this culture was only slightly lower than the value obtained with strain PMD23 (Table 2). However, strain YK167 extracts contained a level of LDH activity about 2.7 times higher than that of strain PMD23, and this higher LDH activity could account for the flux through LDH over PDH* at the pyruvate node. In agreement with this higher LDH activity, the *ldhA* mRNA level of strain YK167 was found to be 2.5-fold higher than that of

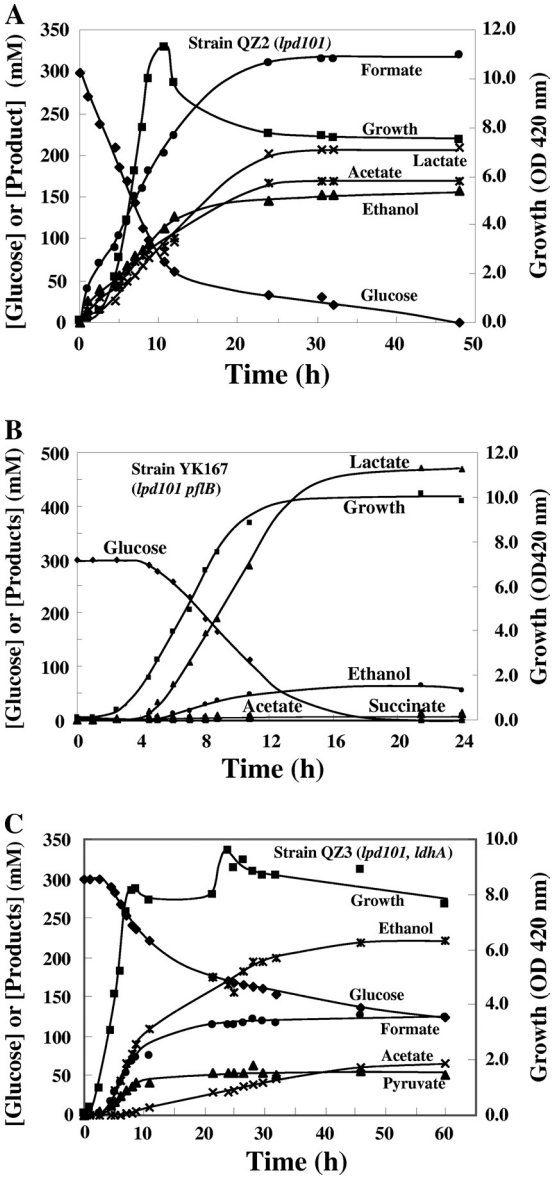

FIG. 3. Growth and fermentation characteristics of *E. coli* strains QZ2, YK167, and QZ3 with different enzyme compositions at the pyruvate node in pH-controlled batch cultures. See Materials and Methods for details. The concentrations of lactate and succinate in the strain QZ3 fermentation broth at 60 h were 19 mM and 20 mM, respectively. Formate was not detected in the broth of strain YK167.

strain PMD23. These results indicate that in the presence of both LDH and PDH*, LDH is the preferred physiological pathway of pyruvate metabolism in anaerobic *E. coli* strains for redox maintenance.

The rate of ethanol production (20.5 mmol h^{-1} [g of cells {dry weight}]$^{-1}$) by strain QZ3, lacking LDH activity, was the same as the formate production rate (20.6 mmol h^{-1} [g of cells {dry weight}]$^{-1}$) during the growth phase (Fig. 3C). Acetate production during growth was only 1.2 mmol h^{-1} (g of cells [dry weight])$^{-1}$. Strain QZ3 also produced a significant amount of pyruvate (10.6 mmol h^{-1} [g of cells {dry weight}]$^{-1}$). The reducing equivalents (NADH) generated during pyruvate production and secretion were apparently used to reduce the acetyl-CoA produced by PFL to ethanol, accounting for the equimolar amounts of ethanol and formate in the medium. These results suggest that PDH* did not contribute to pyruvate flux in strain QZ3 during this initial phase of growth. Only when the culture reached the stationary phase (after about 10 h) could a contribution of PDH to pyruvate flux be detected based on the ratios of the acetate, ethanol, and formate production rates; rates of specific productivity for acetate, ethanol, and formate were 1.1, 3.6, and 2.1 mmol h^{-1} (g of cells [dry weight])$^{-1}$.

Although the initial growth rates of all three strains were comparable, a significant amount of glucose remained in the medium of strain QZ3 even after 116 h of incubation, in contrast to levels in the other two strains with LDH activity (strains QZ2 and YK167) (Fig. 3A and B). This lower rate of glucose consumption by strain QZ3 compared to strain QZ2 suggests that PDH* and PFL are rate-limiting at the pyruvate node. This is in agreement with the observation that pyruvate was detected in the broth of strain QZ3 alone among the three strains tested (Fig. 3). However, the PDH* activity of strain QZ3 was comparable (about 0.4 U mg protein^{-1} in crude extracts) to that of the wild-type strain PMD23 (Table 2), a characteristic that may be related to a higher accumulation of pyruvate, a known activator of the *pdh* operon and of pyruvate secretion by strain QZ3.

Pyruvate distribution in a steady-state culture. Anaerobic batch cultures of *E. coli* in which the growth rate is constantly changing may not be sensitive enough to measure flux through PDH*. To overcome this limitation, various mutants lacking one or more of the enzymes at the pyruvate node were cultured in a chemostat operating at a dilution rate of 0.1 h^{-1}. In these experiments, a rich medium was used to minimize the amount of carbon that was diverted to biosynthesis.

Strains with active LDH and PFL. The biochemistry framework depicted in Fig. 2 was used to determine the flux values using a steady-state glucose-limited chemostat culture. The detailed flux distributions of these cultures are presented in Table 3. The cell mass of strain PMD23, which is wild type for fermentation except for the absence of FHL activity (*hypF*), stabilized at about 1.8 g/liter, and the specific glucose consumption rate was about 5.8 mmol h^{-1} (g of cells [dry weight])$^{-1}$. The major fermentation products of strain PMD23

TABLE 2. Enzyme activities of select mutants with alterations in the pyruvate node

Strain	Relevant genotype	Enzymes present[a]	Enzyme activity (μmol min^{-1} mg of protein^{-1})[b]		
			LDH	PDH	ADH
PMD23	Wild type	PFL, LDH	1.52	0.46	0.04
QZ2	*lpd101*	PFL, LDH, PDH*	0.41	0.14	0.05
QZ3	*lpd101 ldhA*	PFL, PDH*	0.01	0.44	0.04
YK167	*lpd101 pflB*	LDH, PDH*	4.17	0.32	0.06

[a] PFL, pyruvate formate-lyase; LDH, fermentative lactate dehydrogenase; PDH*, pyruvate dehydrogenase complex with a mutation in dihydrolipoamide dehydrogenase.

[b] Determined in extracts of cells harvested from fermenter cultures in the mid-exponential phase of growth. ADH, alcohol dehydrogenase. See Materials and Methods for assay conditions and other details.

TABLE 4. Anaerobic flux ratios at the pyruvate and acetyl-CoA branch points in select mutants with mutations in PDH, LDH, and/or PFL

Strain	Enzyme(s)[a]	Anaerobic flux ratio at the following branch point:				
		Pyruvate			Acetyl-CoA	
		PFL	PDH	LDH	Acetate	Ethanol
PMD23	PFL, LDH	0.70	0.002	0.30	0.54	0.46
QZ2	PFL, LDH, PDH*	0.66	0.01	0.33	0.55	0.45
QZ3	PFL, PDH*	0.48	0.50	0.00	0.25	0.75
YK167	LDH, PDH*	0.00	0.33	0.67	0.23	0.77
SE2382	PDH*	0.00	1.00	0.00	0.22	0.78
YK1	PDH*	0.00	1.00	0.00	0.15	0.85

[a] Enzyme(s) expected to be functional at the pyruvate node in the indicated strain based on its genotype and phenotype and on the enzyme activities in the extract.

were acetate, lactate, and ethanol, with the carbon flux ratio to these products at about 1:1:1 (J7, J10, and J11) (Tables 3 and 4). Carbon flux to formate was the sum of the fluxes to acetate and ethanol, as expected. The production of lactate indicates that this culture is apparently ATP limited and is not limited for reductant, since the rich medium provided the needed precursors for the biosynthesis of macromolecules. The additional reductant generated due to an increase in carbon flux for the production of ATP is apparently channeled to lactate to maintain redox balance. This is about 30% of the carbon flux at the pyruvate node (Table 4). The higher-than-expected flux to lactate in strain W3110 derivatives compared to the flux in a strain MC4100 derivative reported by Yang et al. (42) could reflect the significant differences between the genotypes of the two strains (25).

The introduction of an active PDH into strain PMD23 through the *lpd101* mutation (PDH*; strain QZ2) did not significantly alter the glucose flux through the three enzymes (Tables 3 and 4). This lack of carbon flux through PDH* in a strain with active LDH is in agreement with the results of the batch culture experiments (Fig. 3A) and suggests that LDH is the preferred enzyme in *E. coli* to support redox balance.

Strain QZ3, lacking LDH activity (PFL$^+$ PDH*). The deletion of the *ldhA* gene (strain QZ3) forced about 50% of the pyruvate carbon through PDH* (Tables 3 and 4). This can be seen by the higher ethanol production rate relative to that of acetate. Since the PFL-based reactions yield an acetate-to-ethanol ratio of 1.0, the additional ethanol produced by strain QZ3 is expected to come from the PDH*/ADH pathway (Fig. 1). In strain QZ3, the amount of carbon diverted to PDH* was slightly higher than the amount of carbon flux through LDH to lactate in strain QZ2 (3.9 versus 2.9 mmol h^{-1} [g of cells {dry weight}]$^{-1}$, respectively). Surprisingly, the pyruvate flux through PFL was about 35% lower in strain QZ3 than in strain QZ2, although the steady-state cell masses of the two cultures in the chemostat were comparable (about 2.0 g of cells [dry weight] liter^{-1}). The reason for this decline in pyruvate flux through PFL in a strain lacking LDH is not clear, although the lower apparent pyruvate K_m for PDH* (0.4 mM versus 2.0 mM for PFL) may be a contributing factor.

Strain QZ3 also produced pyruvate as a fermentation product, as seen with batch fermentations (Fig. 3C), suggesting that

TABLE 3. Metabolic flux distributions of different mutant strains of *E. coli* affected at the pyruvate node[a]

Strain (relevant genotype)	Metabolic flux (mmol h^{-1} [g of cells {dry wt}]$^{-1}$) for the following reaction[b]:													Y_{ATP} (g of cells [mol of ATP]$^{-1}$)
	J1 (G-6-P)	J3 (G-3-P)	J4 (PEP)	J5 (PYR)	J6 (SUCC)	J7[c] (lactate)	J8 (formate)	J9 (PDH)	J10 (acetate)	J11 (ethanol)	J12 (pyruvate)	J13[c] (lactate)	NADH formation	NADH consumption	Dry wt of cells (g/liter)	
PMD23 (*lypF*)	5.85	4.87	9.74	3.58	0.30	2.82	6.60	0.02	3.58	3.04	0.00	0.00	9.76	9.50	1.84	10.9
QZ2 (*lpd101* Δ*lypF*)	5.00	4.70	9.40	4.10	0.30	2.93	6.00	0.16	3.37	2.79	0.01	0.00	9.56	9.11	2.18	12.9
QZ3 (Δ*ldhA lpd101* Δ*lypF*)	4.45	4.29	8.44	3.79	0.20	0.00	3.81	3.91	1.93	5.78	0.52	0.15	12.34	12.12	1.93	13.6
YK167 [*lpd101* Δ(*focA-pflB*)]	7.30	7.26	14.53	6.31	0.91	8.88	0.00	4.30	1.01	3.30	0.43	0.00	18.83	17.30	1.50	6.9
SE2382 [*lpd101* Δ*ldhA* Δ(*focA-pflB*)]	3.62	3.38	6.20	2.20	0.38	0.00	0.00	4.23	0.92	3.31	1.59	0.56	10.44	7.94	0.69	7.4
YK1 [*lpd101* Δ*ldhA* Δ(*focA-pflB*) *pdhR*]	4.06	3.86	7.72	3.33	0.33	0.00	0.00	7.39	1.13	6.26	0.01	0.00	15.11	13.19	0.60	4.9

[a] All cultures were grown anaerobically in a chemostat with glucose limitation at a dilution rate of 0.1 h^{-1} as described in Materials and Methods. Reactions J1, J6, J7, J8, J10, J11, J12 and J13 were measured directly, while the other reaction rates were computed.

[b] Products of reactions are given in parentheses. G-6-P, glucose-6-phosphate; G-3-P, glyceraldehyde 3-phosphate; PEP, phosphoenolpyruvate; PYR, pyruvate; SUCC, succinate.

[c] The lactate produced by the *ldhA* deletion mutants (strains QZ3 and SE2382) is assumed to be derived from the methylglyoxal (J13) pathway; in strains with LDH activity, the amount of lactate produced by the methylglyoxal pathway (J13) was considered to be negligible.

the conversion of pyruvate to acetyl-CoA by PFL and PDH* is rate-limiting in this strain. Even with this potential limitation, the steady-state cell masses of the cultures (about 2 g/liter) and calculated yields per mole of ATP (Y_{ATP}) for strains QZ2 and QZ3 (12.9 and 13.6 g of cells, respectively) were comparable (Table 2) and similar to reported Y_{ATP} for *E. coli* (16, 22, 24, 42). These results show that PDH* effectively competes with PFL for pyruvate, even though PDH* activity requires NAD^+. This is in contrast to the inability of PDH* to compete for pyruvate when all three enzymes are present (strain QZ2) and confirms that the LDH pathway outcompetes PDH* for pyruvate, in support of maintaining the redox balance in *E. coli* strain W3110.

Strain YK167, lacking PFL activity (LDH$^+$ PDH*). A mutant that lacks PFL activity (YK167) while still retaining LDH and PDH* activities had an almost 50% increase in glucose consumption and flux over those for strains with active PFL (QZ2 and QZ3) (Table 3). Apparently, the higher glucose flux to lactate is geared to ATP production at the glycolysis step, compensating for the absence of postpyruvate ATP production. This is comparable to a similar increase in glucose flux reported for a *pfl* or *ackA pta* mutant with the native PDH over that of its corresponding parent strain (39, 42). Although PDH* was unable to compete with LDH for pyruvate in strain QZ2, in strain YK167 flux through PDH* was about 33% of the total pyruvate (Tables 3 and 4). This flux through PDH* in strain YK167 was comparable to the observed PDH* flux in strain QZ3, which lacks LDH activity (about 4 mmol h^{-1} [g of cells {dry weight}]$^{-1}$). In the absence of PFL, PDH* is the only other enzyme that can generate acetyl-CoA, which can be converted to acetate with associated ATP production. However, the NADH generated during pyruvate oxidation by PDH* is expected to limit the amount of ATP that can be produced by the PDH*, phosphotransacetylase (PTA), and acetate kinase (ACK) pathway due to the need for redox balance. The rate of PDH*-dependent acetate production may be dictated by the rate at which the growing culture can utilize NADH. Although the growth rate of strain YK167 was comparable to those of the wild-type strains in batch cultures, the Y_{ATP} for this strain in the chemostat was significantly lower, 6.9 g of cells per mol of ATP, than the values for strains with active PFL, which were higher than 10.0 g per mol of ATP (Table 3). This is unexpected and is different from the Y_{ATP} of 15.2 g per mol of ATP reported for an *ackA pta* mutant of a strain MC4100 derivative (42). This difference in Y_{ATP} between the *pfl* mutant, strain YK167, and the *ackA pta* mutant of Yang et al. (42) could result from the differences between the genotypes of the two strains of *E. coli* K-12: strain W3110, used in this study (ATCC 27325), is believed to be nearly wild type (ATCC), while strain MC4100 has multiple alterations and deletions (25), with unknown physiological consequences. Strain MC4100 is also reported to have a lower level of the anaerobic control protein FNR than another wild-type strain, MG1655 (31). The potential effect of the lower level of FNR in modulating the Y_{ATP} of an anaerobic culture is not known and needs investigation.

The Y_{ATP} calculations were based on the predicted ATP yield by the fermentation products from the chemostat cultures and do not take into account any loss of ATP through a futile cycle (21, 26, 30). It is possible that in the absence of PFL, a futile cycle is draining ATP from glycolytic reactions in strain YK167. One possible mechanism of ATP loss could be an alternate pathway for phosphoenolpyruvate conversion to pyruvate through oxaloacetate and malate catalyzed by PEP-carboxylase, malate dehydrogenase, and NAD^+-dependent malate dehydrogenase (decarboxylating). Due to the absence of PFL and the accumulation of pyruvate, the PEP-carboxylase may initiate this alternate pathway, with the loss of ATP. This pathway is redox neutral and is not expected to alter the redox balance. It is also possible that in the absence of PFL, the transport and assimilation of amino acids and other components from the medium may be limiting growth, leading to a condition of ATP excess and thus initiating a potential futile energy cycle(s).

Strain SE2382, lacking both LDH and PFL activities (PDH*). Glucose flux in strain SE2382, which lacks both PFL and LDH activities, was slightly lower than that in strain QZ3 (Δ*ldh*) but about 50% lower than that in strain YK167 (*ldh*$^+$ Δ*pflB*) (Table 2). Levels of pyruvate flux through the PDH* in strains YK167 and SE2382 were similar, suggesting that the loss of LDH activity in strain SE2382 due to mutation is the primary reason for the decrease in glucose flux. As expected, the lower rate of glycolysis in strain SE2382 led to a lower cell mass in steady-state cultures. The calculated Y_{ATP} for strains SE2382 and YK167 were comparable and were about 50% of the value for the PFL-positive strain QZ3. These results show that the absence of PFL is responsible for the lower cell yield of the *pfl* mutants in steady-state cultures, apparently due to a lower ATP yield, irrespective of the presence or absence of LDH activity.

Strain SE2382 also produced pyruvate as a product, suggesting that the rate-limiting step in glucose fermentation is PDH* activity. In addition, strain SE2382 also produced lactate, probably through the methylglyoxal pathway, indicating an accumulation of glyceraldehyde-3-phosphate and associated dihydroxyacetone-3-phosphate, the substrate for methylglyoxal synthase, which is the starting point for LDH-independent lactate production. No pyruvate or lactate was detected in the broth of strain YK1, which carries additional mutations in PdhR and the intergenic region between *pdhR* and *aceE* (Table 2) (18). These additional mutations increased the expression of the *pdh* operon by about 4-fold over that for strain SE2382 (*aceE* mRNA levels, 2.2 versus 9.4 pg μl^{-1} of total RNA for strains SE2382 and YK1, respectively) and increased flux through PDH* by about 1.75-fold. Besides the absence of lactate and pyruvate in the broth and the higher rate of ethanol production by strain YK1, there was no other significant difference between strains SE2382 and YK1 in the chemostat cultures (Tables 3 and 4). The calculated Y_{ATP} for strain YK1 (4.9 g of cells per mol of ATP) was the lowest of those for all the strains investigated.

It is known that flux through PFL would lead to ATP production, which is essential for increasing the growth rate of an anaerobic culture (13, 19, 39). Under the redox balance condition, the reactions shown in Fig. 2 can be used to maximize ATP production with linear optimization. The flux distributions in the mutant strain QZ2 were calculated to be almost the same as the calculated ATP-maximized fluxes. There was no flux to PDH. When the flux to PDH was increased, the ATP generated from glucose actually decreased. The genome-level

flux balance model also gave the same results (28) when the optimized objective was set as the maximum biomass generation. These results suggest that the cell prefers the PFL pathway over the PDH* pathway, probably due to the ATP yield.

Conclusion. Flux through LDH or PDH* alone serves to maintain redox balance in the wild type, and the low flux to PDH* (about 2%) in the "wild-type" *E. coli* strain that favors LDH is unexpected, considering the apparent pyruvate K_m values for the three competing enzymes. Although PDH requires NAD^+ for activity, the apparent NAD^+ K_m for this enzyme is 70 μM, compared to an apparent NADH K_m of 200 μm for LDH (18, 37). The reported intracellular NAD^+ concentration in *E. coli* grown anaerobically in a glucose-limited chemostat ranges from 1 to 2.5 mM depending on the strain (8), a concentration that is significantly higher than the apparent NAD^+ K_m for PDH* (18). Considering that the highest reported [NADH]/[NAD^+] ratio of an anaerobic *E. coli* strain is less than 1.0 (8), kinetically, PDH* would be the preferred enzyme at the pyruvate node. However, in the presence of LDH and PFL, flux through PDH* is negligible (strain QZ2 [Table 3]), indicating that some other factor(s) besides enzyme kinetics plays a role in distributing pyruvate among the three enzymes. In strain QZ2, the level of PDH in cell extracts was about 0.14 U mg protein^{-1}, a reduction in activity of about 70% from those of strain QZ3 and "wild-type" strain PMD23 (about 0.4 U mg protein^{-1}). Although strain QZ2 had a lower PDH activity than strain PMD23, the ratios of LDH to PDH* activities in the extracts of these two strains were about 3.0 and may not account for the significant difference in pyruvate flux through PDH*. However, it should be noted that besides the kinetic constants, the intracellular enzyme concentration, the levels of various regulatory metabolites, and substrate and product concentrations, etc., do play significant roles in the flux through a specific enzyme, and a combination of these factors may divert pyruvate carbon to LDH. It is noteworthy that the high glucose flux in strain YK167, lacking PFL activity, was supported by elevating the LDH activity and not by increasing flux through PDH* (Tables 2 and 3), although PDH* can support redox balance. These results suggest a complex physiological interaction among the three pathways at the pyruvate node that includes control at the genetic level.

PDH is highly regulated by various metabolic intermediates, including pyruvate (7, 12, 33, 34), and accumulation of some of the effectors in the cell may have a negative effect on the activity of PDH*. Although this is possible, flux through PDH* in mutant strains lacking either PFL or LDH, or both, argues against complete inhibition of PDH activity by metabolic inhibitors. Apparently, there are other, unknown intricate physiological factor(s) that regulate flux at the pyruvate node toward lactate production for redox balance. One possibility is that ADH is rate-limiting and the accumulation of acetyl-CoA is inhibitory to PDH* activity (33). In strains PMD23, QZ2, YK167, and SE2382, the overall flux through ADH (step J11) (Table 3 and Fig. 2) is an almost constant value of about 3 mmol · h^{-1} · (g of cells [dry weight])$^{-1}$. Although flux through reaction J11 (Fig. 2) increased to 5.8 mmol · h^{-1} · (g of cells [dry weight])$^{-1}$ in strain QZ3 (Δ*ldh lpd101*), the level of ADH activity in the extract of this strain was only slightly higher (0.05 U mg protein^{-1}) than those for strains PMD23 and QZ2 (0.04 U mg protein^{-1}). These physiological and biochemical results suggest that ADH activity may not be limiting flux through PDH* in strain QZ2. This is further confirmed by the absence of increased flux through PDH* even after an increase in the expression of the *adhE* gene, from a plasmid, in strain QZ2 (data not presented).

Pyruvate is reported to function as an allosteric activator of LDH, and this may favor pyruvate flux through LDH (37). Pyruvate is also a known activator of *pdh* operon expression (27), and thus, pyruvate may not provide a unique advantage for flux through one enzyme complex or the other.

The results presented above suggest that the mechanism that splits pyruvate among the three available pathways (PFL, LDH, and PDH*) is apparently determined by energy requirement and redox balance constraints. Under anaerobic conditions, the cell prefers PFL due to the energy supply and LDH for redox balance maintenance, even in the presence of an active PDH. The lack of flux through PDH* in a strain with all three enzymes could result from a reluctance of the cell to elevate the level of NADH and further increase the [NADH]/[NAD^+] ratio, although this NADH can be reoxidized in subsequent ADH-dependent reactions. An understanding of the controls at the pyruvate node, as well as the potential function of a futile cycle(s) in the absence of PFL, can provide unique insights toward rational metabolic engineering of *E. coli* and related bacteria for the production of various biobased products, including ethanol, at high rates and yields.

ACKNOWLEDGMENTS

We thank Phi M. Do for providing strain PMD23 with the Δ*hypF* mutation.

This study was supported in part by a grant from the Department of Energy (DE-FG36-04GO14019) and the State of Florida, University of Florida Agricultural Experiment Station.

REFERENCES

1. **Bisswanger, H., and U. Henning.** 1971. Regulatory properties of the pyruvate-dehydrogenase complex from *Escherichia coli*. Positive and negative cooperativity. Eur. J. Biochem. **24:**376–384.
2. **Bock, A., and G. Sawers.** 1996. Fermentation, p. 262–282. *In* F. C. Neidhardt, R. Curtiss III, J. L. Ingraham, E. C. C. Lin, K. B. Low, B. Magasanik, W. S. Reznikoff, M. Riley, M. Schaechter, and H. E. Umbarger (ed.), *Escherichia coli* and *Salmonella*: cellular and molecular biology. ASM Press, Washington, DC.
3. **Bradford, M. M.** 1976. A rapid and sensitive method for the quantitation of microgram quantities of protein utilizing the principle of protein-dye binding. Anal. Biochem. **72:**248–254.
4. **Clark, D. P.** 1989. The fermentation pathways of *Escherichia coli*. FEMS Microbiol. Rev. **5:**223–234.
5. **Cronan, J. E., Jr., and D. LaPorte.** 1996. Tricarboxylic acid cycle and glyoxalate bypass, p. 206–216. *In* F. C. Neidhardt, R. Curtiss III, J. L. Ingraham, E. C. C. Lin, K. B. Low, B. Magasanik, W. S. Reznikoff, M. Riley, M. Schaechter, and H. E. Umbarger (ed.), *Escherichia coli* and *Salmonella*: cellular and molecular biology. ASM Press, Washington, DC.
6. **Datsenko, K. A., and B. L. Wanner.** 2000. One-step inactivation of chromosomal genes in *Escherichia coli* K-12 using PCR products. Proc. Natl. Acad. Sci. U. S. A. **97:**6640–6645.
7. **Datta, A.** 1991. Characterization of the inhibition of *Escherichia coli* pyruvate dehydrogenase complex by pyruvate. Biochem. Biophys. Res. Commun. **176:** 517–521.
8. **de Graef, M. R., S. Alexeeva, J. L. Snoep, and M. J. Teixeira de Mattos.** 1999. The steady-state internal redox state (NADH/NAD) reflects the external redox state and is correlated with catabolic adaptation in *Escherichia coli*. J. Bacteriol. **181:**2351–2357.
9. **Fraenkel, D. G.** 1996. Glycolysis, p. 189–198. *In* F. C. Neidhardt, R. Curtiss III, J. L. Ingraham, E. C. C. Lin, K. B. Low, B. Magasanik, W. S. Reznikoff, M. Riley, M. Schaechter, and H. E. Umbarger (ed.), *Escherichia coli* and *Salmonella*: cellular and molecular biology. ASM Press, Washington, DC.
10. **Garrigues, C., P. Loubiere, N. D. Lindley, and M. Cocaign-Bousquet.** 1997. Control of the shift from homolactic acid to mixed-acid fermentation in *Lactococcus lactis*: predominant role of the NADH/NAD^+ ratio. J. Bacteriol. **179:**5282–5287.

11. **Gennis, R. B., and V. Stewart.** 1996. Respiration, p. 217–261. *In* F. C. Neidhardt, R. Curtiss III, J. L. Ingraham, E. C. C. Lin, K. B. Low, B. Magasanik, W. S. Reznikoff, M. Riley, M. Schaechter, and H. E. Umbarger (ed.), *Escherichia coli* and *Salmonella*: cellular and molecular biology. ASM Press, Washington, DC.
12. **Hansen, H. G., and U. Henning.** 1966. Regulation of pyruvate dehydrogenase activity in *Escherichia coli* K12. Biochim. Biophys. Acta **122:**355–358.
13. **Hasona, A., Y. Kim, F. G. Healy, L. O. Ingram, and K. T. Shanmugam.** 2004. Pyruvate formate lyase and acetate kinase are essential for anaerobic growth of *Escherichia coli* on xylose. J. Bacteriol. **186:**7593–7600.
14. **Iuchi, S., and E. C. Lin.** 1993. Adaptation of *Escherichia coli* to redox environments by gene expression. Mol. Microbiol. **9:**9–15.
15. **Kajiya, M., K. Sato, M. J. Silva, K. Ouhara, P. M. Do, K. T. Shanmugam, and T. Kawai.** 2009. Hydrogen from intestinal bacteria is protective for concanavalin A-induced hepatitis. Biochem. Biophys. Res. Commun. **386:** 316–321.
16. **Kayser, A., J. Weber, V. Hecht, and U. Rinas.** 2005. Metabolic flux analysis of *Escherichia coli* in glucose-limited continuous culture. I. Growth-rate-dependent metabolic efficiency at steady state. Microbiology **151:**693–706.
17. **Kim, Y., L. O. Ingram, and K. T. Shanmugam.** 2007. Construction of an *Escherichia coli* K-12 mutant for homoethanologenic fermentation of glucose or xylose without foreign genes. Appl. Environ. Microbiol. **73:**1766–1771.
18. **Kim, Y., L. O. Ingram, and K. T. Shanmugam.** 2008. Dihydrolipoamide dehydrogenase mutation alters the NADH sensitivity of pyruvate dehydrogenase complex of *Escherichia coli* K-12. J. Bacteriol. **190:**3851–3858.
19. **Koebmann, B. J., H. V. Westerhoff, J. L. Snoep, D. Nilsson, and P. R. Jensen.** 2002. The glycolytic flux in *Escherichia coli* is controlled by the demand for ATP. J. Bacteriol. **184:**3909–3916.
20. **Lawford, H. G., and J. D. Rousseau.** 1995. Comparative energetics of glucose and xylose metabolism in ethanologenic recombinant *Escherichia coli* B. Appl. Biochem. Biotechnol. **51–52:**179–195.
21. **Liao, J. C., Y. P. Chao, and R. Patnaik.** 1994. Alteration of the biochemical valves in the central metabolism of *Escherichia coli*. Ann. N. Y. Acad. Sci. **745:**21–34.
22. **Mainzer, S. E., and W. P. Hempfling.** 1976. Effects of growth temperature on yield and maintenance during glucose-limited continuous culture of *Escherichia coli*. J. Bacteriol. **126:**251–256.
23. **Melchiorsen, C. R., K. V. Jokumsen, J. Villadsen, H. Israelsen, and J. Arnau.** 2002. The level of pyruvate-formate lyase controls the shift from homolactic to mixed-acid product formation in *Lactococcus lactis*. Appl. Microbiol. Biotechnol. **58:**338–344.
24. **Paalme, T., R. Elken, A. Kahru, K. Vanatalu, and R. Vilu.** 1997. The growth rate control in *Escherichia coli* at near to maximum growth rates: the A-stat approach. Antonie Van Leeuwenhoek **71:**217–230.
25. **Peters, J. E., T. E. Thate, and N. L. Craig.** 2003. Definition of the *Escherichia coli* MC4100 genome by use of a DNA array. J. Bacteriol. **185:**2017–2021.
26. **Qian, H., and D. A. Beard.** 2006. Metabolic futile cycles and their functions: a systems analysis of energy and control. Syst. Biol. **153:**192–200.
27. **Quail, M. A., and J. R. Guest.** 1995. Purification, characterization and mode of action of PdhR, the transcriptional repressor of the *pdhR-aceEF-lpd* operon of *Escherichia coli*. Mol. Microbiol. **15:**519–529.
28. **Reed, J. L., T. D. Vo, C. H. Schilling, and B. O. Palsson.** 2003. An expanded genome-scale model of *Escherichia coli* K-12 (iJR904 GSM/GPR). Genome Biol. **4:**R54.
29. **Rosentel, J. K., F. Healy, J. A. Maupin-Furlow, J. H. Lee, and K. T. Shanmugam.** 1995. Molybdate and regulation of *mod* (molybdate transport), *fdhF*, and *hyc* (formate hydrogenlyase) operons in *Escherichia coli*. J. Bacteriol. **177:**4857–4864.
30. **Russell, J. B.** 2007. The energy spilling reactions of bacteria and other organisms. J. Mol. Microbiol. Biotechnol. **13:**1–11.
31. **Sawers, R. G.** 2005. Expression of *fnr* is constrained by an upstream IS*5* insertion in certain *Escherichia coli* K-12 strains. J. Bacteriol. **187:**2609–2617.
32. **Schmincke-Ott, E., and H. Bisswanger.** 1981. Dihydrolipoamide dehydrogenase component of the pyruvate dehydrogenase complex from *Escherichia coli* K12. Comparative characterization of the free and the complex-bound component. Eur. J. Biochem. **114:**413–420.
33. **Schwartz, E. R., and L. J. Reed.** 1970. Regulation of the activity of the pyruvate dehydrogenase complex of *Escherichia coli*. Biochemistry **9:**1434–1439.
34. **Shen, L. C., and D. E. Atkinson.** 1970. Regulation of pyruvate dehydrogenase from *Escherichia coli*. Interactions of adenylate energy charge and other regulatory parameters. J. Biol. Chem. **245:**5974–5978.
35. **Snoep, J. L., M. R. de Graef, A. H. Westphal, A. de Kok, M. J. Teixeira de Mattos, and O. M. Neijssel.** 1993. Differences in sensitivity to NADH of purified pyruvate dehydrogenase complexes of *Enterococcus faecalis*, *Lactococcus lactis*, *Azotobacter vinelandii* and *Escherichia coli*: implications for their activity in vivo. FEMS Microbiol. Lett. **114:**279–283.
36. **Stephanopoulos, G. N., A. A. Aristidou, and J. Nielsen.** 1998. Metabolic engineering: principles and methodologies. Academic Press, Burlington, MA.
37. **Tarmy, E. M., and N. O. Kaplan.** 1968. Kinetics of *Escherichia coli* B D-lactate dehydrogenase and evidence for pyruvate-controlled change in conformation. J. Biol. Chem. **243:**2587–2596.
38. **Underwood, S. A., S. Zhou, T. B. Causey, L. P. Yomano, K. T. Shanmugam, and L. O. Ingram.** 2002. Genetic changes to optimize carbon partitioning between ethanol and biosynthesis in ethanologenic *Escherichia coli*. Appl. Environ. Microbiol. **68:**6263–6272.
39. **Utrilla, J., G. Gosset, and A. Martinez.** 2009. ATP limitation in a pyruvate formate lyase mutant of *Escherichia coli* MG1655 increases glycolytic flux to D-lactate. J. Ind. Microbiol. Biotechnol. **36:**1057–1062.
40. **Wang, Q., X. Chen, Y. Yang, and X. Zhao.** 2006. Genome-scale in silico aided metabolic analysis and flux comparisons of *Escherichia coli* to improve succinate production. Appl. Microbiol. Biotechnol. **73:**887–894.
41. **Yang, Y. T., G. N. Bennett, and K. Y. San.** 2001. The effects of feed and intracellular pyruvate levels on the redistribution of metabolic fluxes in *Escherichia coli*. Metab. Eng. **3:**115–123.
42. **Yang, Y. T., K. Y. San, and G. N. Bennett.** 1999. Redistribution of metabolic fluxes in *Escherichia coli* with fermentative lactate dehydrogenase overexpression and deletion. Metab. Eng. **1:**141–152.
43. **Zhou, S., K. T. Shanmugam, and L. O. Ingram.** 2003. Functional replacement of the *Escherichia coli* D-(−)-lactate dehydrogenase gene (*ldhA*) with the L-(+)-lactate dehydrogenase gene (*ldhL*) from *Pediococcus acidilactici*. Appl. Environ. Microbiol. **69:**2237–2244.

Appendix I

Appl Biochem Biotechnol (2009) 155:379–385
DOI 10.1007/s12010-008-8509-4

Thermophilic *Bacillus coagulans* Requires Less Cellulases for Simultaneous Saccharification and Fermentation of Cellulose to Products than Mesophilic Microbial Biocatalysts

Mark S. Ou · Nazimuddin Mohammed · L. O. Ingram · K. T. Shanmugam

Received: 21 May 2008 / Accepted: 22 December 2008 /
Published online: 21 January 2009

Abstract Ethanol production from lignocellulosic biomass depends on simultaneous saccharification of cellulose to glucose by fungal cellulases and fermentation of glucose to ethanol by microbial biocatalysts (SSF). The cost of cellulase enzymes represents a significant challenge for the commercial conversion of lignocellulosic biomass into renewable chemicals such as ethanol and monomers for plastics. The cellulase concentration for optimum SSF of crystalline cellulose with fungal enzymes and a moderate thermophile, *Bacillus coagulans*, was determined to be about 7.5 FPU g^{-1} cellulose. This is about three times lower than the amount of cellulase required for SSF with *Saccharomyces cerevisiae*, *Zymomonas mobilis*, or *Lactococcus lactis* subsp. *lactis* whose growth and fermentation temperature optimum is significantly lower than that of the fungal cellulase activity. In addition, *B. coagulans* also converted about 80% of the theoretical yield of products from 40 g/L of crystalline cellulose in about 48 h of SSF with 10 FPU g^{-1} cellulose while yeast, during the same period, only produced about 50% of the highest yield produced at end of 7 days of SSF. These results show that a match in the temperature optima for cellulase activity and fermentation is essential for decreasing the cost of cellulase in cellulosic ethanol production.

Keywords Cellulase · Cellulose SSF · *Bacillus coagulans* · *Saccharomyces* · *Zymomonas* · Lactic acid bacteria

Introduction

The limited nature and rising costs of fossil fuels have provided the needed impetus to the use of sustainable and renewable sources of fuels and chemicals. Lignocellulosic biomass from plants is the only promising sustainable feedstock that can be converted to both fuels

M. S. Ou · N. Mohammed · L. O. Ingram · K. T. Shanmugam (✉)
Department of Microbiology and Cell Science, University of Florida, Box 110700,
Gainesville, FL 32611, USA
e-mail: shan@ufl.edu

and chemicals without increasing greenhouse gas emissions [1]. Although the hemicellulose in the biomass can be readily hydrolyzed to fermentable sugars by mild acid treatment, bioconversion of cellulose in the biomass to glucose requires hydrolysis by cellulases before fermentation by microbial biocatalysts [2–7].

Fungal cellulases, such as those from *Trichoderma reesei*, dominate the industrial applications of cellulases and are one of the significant cost components of deriving sugars from cellulose for fermentation to ethanol and other chemicals [5–7]. One processing strategy in the production of cellulose-based fuels and chemicals involves separate hydrolysis of cellulose by enzymes followed by fermentation by microbial biocatalysts (SHF) [8]. Due to the low yield of glucose in the SHF process, a result of inhibition of cellulases by the hydrolysis products cellobiose and glucose [9], combined with inherent low specific activity of the fungal cellulases [10], the amount of cellulases required for optimal conversion of cellulose to ethanol is higher than desired for economical production of ethanol and other commodity chemicals. To overcome the product inhibition of cellulases, a strategy of simultaneous saccharification and fermentation (SSF) has been developed in which hydrolysis of cellulose is coupled with fermentation of the released sugars in the same reaction vessel [11]. In the SSF process, the fungal enzymes hydrolyzed the cellulose to sugars that were immediately fermented by the microbial biocatalyst to ethanol and/or chemicals. Because of this combination, hydrolysis of cellulose by the enzymes could not be optimized separately and the growth and fermentation optimum of the microbial biocatalyst also need to be considered in selecting an optimum temperature and pH for SSF of cellulose to products.

Although the SSF process minimized the product inhibition of cellulase activity, the relatively low specific activity of fungal cellulases in relation to bacterial-cell-associated cellulases is yet to be overcome [1, 8]. This is further magnified by the SSF process at a lower-than-optimum temperature for the enzyme activity (optimum of 50 °C and pH 5.0) [10, 12] due to the need for a lower temperature (30–35 °C) that is the growth and fermentation optimum for the current industrial biocatalysts, such as *Saccharomyces cerevisiae* [13] and *Zymomonas mobilis*. Lactic acid bacteria used by the industry for production of optically pure lactic acid, a potential renewable source of plastics, also suffers from the low temperature optimum (35–40 °C) for growth and fermentation compared to that of the fungal cellulase activity optimum [10, 12, 14–16]. Using these microbial biocatalysts in SSF of cellulose to products is expected to result in a mismatch in optima leading to either a higher requirement of fungal cellulases or an increase in the time required for SSF, both of which significantly increase the cost of bioconversion of cellulose to fuels and chemicals.

Our laboratory has described Gram-positive bacterial isolates that have growth and fermentation temperature optima which closely match those of fungal cellulases being developed for use in SSF of cellulose [12, 17]. These isolates, such as *Bacillus coagulans* strain 36D1, grow and ferment hexoses and pentoses at 50–55 °C and pH 5.0 producing L (+)-lactic acid as the primary fermentation product. Use of *B. coagulans* for optically pure lactic acid production for plastics industry or an engineered *B. coagulans* derivative for ethanol production at 50–55 °C is expected to reduce the amount of fungal cellulases required for optimum conversion of cellulose to products in the SSF process. However, no comparative experimental evidence exists establishing this possibility. In this communication, evidence is presented that coupling the microbial biocatalyst in the SSF process to the optimum temperature for fungal cellulases significantly reduces the amount of enzyme required for conversion of cellulose to products in comparison with yeast or lactic acid bacteria currently used by the industry as microbial biocatalysts. This reduction in the

amount of cellulase in SSF of cellulose to products is expected to reduce the cost of the process and final product.

Materials and Methods

Organisms, Media, and Growth Conditions

B. coagulans strain 36D1 was described previously [12, 17]. Media used in experiments with *B. coagulans* strain 36D1 contained, per liter: 6.25 g Na_2HPO_4, 0.75 g KH_2PO_4, 2 g NaCl, 0.2 g $MgSO_4 \cdot 7H_2O$, 1 g $(NH_4)_2SO_4$, 10 mg $FeSO_4 \cdot 7H_2O$, 10 mg $Na_2MoO_4 \cdot H_2O$, 1 ml trace mineral solution [18], and 5 ml corn steep liquor (50% dry solids; Grain Processing Corp., Muscatine, IO), adjusted to pH 5.0 with H_2SO_4. Media used for *Lactococcus lactis* subsp. *lactis* (NRRL B-4449) SSF contained, per liter: 10 g yeast extract, 2 g K_2HPO_4, 0.2 g $MgSO_4 \cdot 7H_2O$, 0.05 g $MnSO_4 \cdot H_2O$, 2 g $(NH_4)_2SO_4$, adjusted to pH 5.5 with H_2SO_4. Media used for *S. cerevisiae* (NRRL Y-12632) SSF contained, per liter: 10 g yeast extract, 2 g KH_2PO_4, 1 g $MgSO_4 \cdot 7H_2O$, 1 g $(NH_4)_2SO_4$, adjusted to pH 5.5 with H_2SO_4. Media used for *Z. mobilis* (ATCC 1050) SSF contained, per liter: 10 g yeast extract and 0.3 g KH_2PO_4, adjusted to pH 5 with H_2SO_4. These media were supplemented with glucose at 1% (*w*/*v*) for growth and fermentation without pH control and with 2% (*w*/*v*) in fermentations with pH control for preparation of inoculum for SSF experiments. Optimum temperature and pH for the growth of organisms were determined in batch fermentations without pH control as described previously [17], at various temperatures and initial culture pH.

SSF of Cellulose

SSF of crystalline cellulose (Solka Floc) was carried out in the media described above containing 40 g L^{-1} Solka Floc (International Fiber Corp., North Tonawanda, NY) and varying amounts of cellulase (GC220; Genencor International, Palo Alto, CA). Specific activity of the cellulase preparation as FPU/ml was determined before use as described previously [12]. SSF of crystalline cellulose was carried out at the temperature and pH that were found to be optimal for growth of the specific microbial biocatalyst (*B. coagulans* strain 36D1 at 50 °C and pH 5.0; *L. lactis* at 40 °C and pH 5.5; *S. cerevisiae* at 35 °C and pH 5.5; *Z. mobilis* at 35 °C and pH 5.0). Fermentation pH was maintained by automatic addition of 2 N KOH for strain 36D1 and *L. lactis* or 0.5 N KOH for *S. cerevisiae* and *Z. mobilis*. Sugar and fermentation products were determined using HPLC as described previously [19]. Inoculum for SSF experiments with crystalline cellulose was derived from pH-controlled fermentations in the same media but with 2% (*w*/*v*) glucose. Cells were collected by centrifugation at room temperature and resuspended in appropriate growth media before inoculation in the SSF medium at an initial O.D. at 420 nm of 0.2.

Results and Discussion

In order to obtain the highest volumetric productivity for each organism, optimal temperature and pH for anaerobic growth and fermentation of glucose was determined for each of the four microbial biocatalysts in batch fermentations without pH control. Based on the results of these experiments, the optimal conditions for *B. coagulans* strain 36D1, *L.*

lactis, *S. cerevisiae*, and *Z. mobilis* were determined to be 50 °C and pH 5.0, 40 °C and pH 5.5, 35 °C and pH 5.5, 35 °C and pH 5.0, respectively. These conditions were subsequently used for SSF of cellulose by each organism such that growth and fermentation conditions of the microbial biocatalyst would not be limiting the rate of conversion of cellulose-derived glucose to products. Although industrial yeast fermentations of corn starch to ethanol are conducted at temperatures below 35 °C, this temperature was used in this study since the growth rate of *S. cerevisiae* NRRL Y-12632 at 35 °C was slightly higher than at 30 °C.

SSF of crystalline cellulose was carried out with varying concentrations of cellulase. For each organism, the fermentation profile was dominated by one major fermentation product: lactate produced by *B. coagulans* and *L. lactis* or ethanol produced by *S. cerevisiae* and *Z. mobilis*. The rate of product formation was linear with time and also the highest during the first 18 h; after this period, the rate of product formation continually declined, irrespective of the microbial biocatalyst or the cellulase concentration. Representative SSF profiles for *B. coagulans* and yeast are presented in Fig. 1. With *B. coagulans* as the microbial biocatalyst and the SSF at 50 °C, the initial rate of product formation was not significantly altered by increasing the cellulase concentration from 5 FPU to 20 FPU g^{-1} of cellulose (Fig. 1a). Contrasting this observation, with yeast as the biocatalyst and SSF at 35 °C, the initial rate of ethanol production doubled with every twofold increase in cellulase concentration from 5–20 FPU g^{-1} cellulose (Fig. 1b).

Using the initial high rate of product formation, maximum volumetric productivity for each cellulase concentration and microbial biocatalyst was calculated and presented in

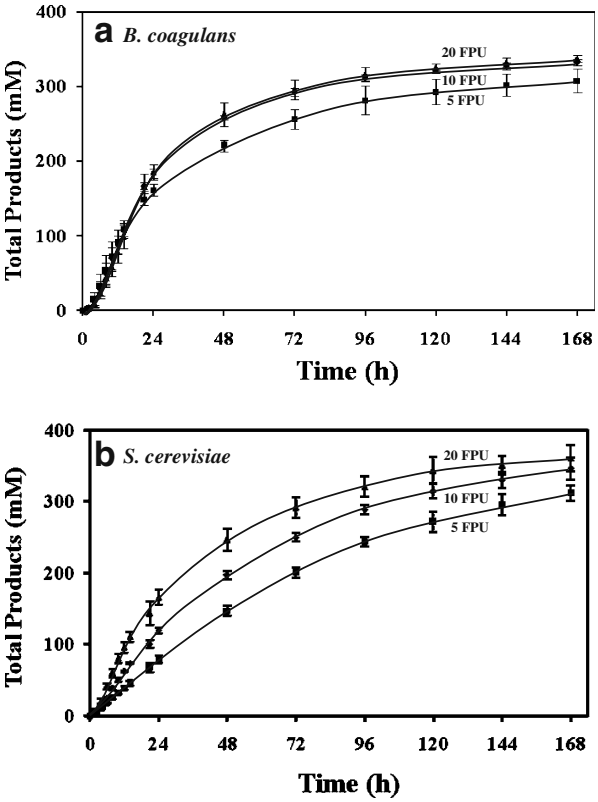

Fig. 1 Time course of SSF of 40 g L^{-1} crystalline cellulose (Solka Floc) with different concentrations of fungal cellulase (GC220; Genencor) **a** *B. coagulans* strain 36D1 at 50 °C and pH 5.0; **b** *S. cerevisiae* at 35 °C and pH 5.5

Fig. 2. Except for *L. lactis*, the volumetric productivity of the other three organisms increased with increasing cellulase concentration until the maximum value was reached. For *B. coagulans*, SSF at 50 °C, the cellulase concentration required for the highest volumetric productivity was between 5 and 7.5 FPU g^{-1} cellulose. With yeast or *Z. mobilis* as the microbial biocatalyst, volumetric productivity continued to increase up to a cellulase concentration of 30 FPU g^{-1} cellulose and, at this concentration of cellulase, the volumetric productivities of the ethanologens and *B. coagulans* at 50 °C were about the same. These results show that SSF at 50 °C can reduce the cellulase requirement by at least threefold without affecting volumetric productivity.

Increasing the SSF temperature to 55 °C with *B. coagulans* as the microbial biocatalyst, increased the volumetric productivity by about 40% without affecting the cellulase requirement (Fig. 2). *L. lactis*-based SSF also reached the same high volumetric productivity observed with *B. coagulans* at 55 °C but this required higher than 20 FPU g^{-1} cellulose in contrast to *B. coagulans* at 55 °C that required only about 5 to 7.5 FPU g^{-1} cellulose, a three- to fourfold reduction in cellulase requirement. At a cellulase concentration of 5 FPU g^{-1} cellulose, the volumetric productivity with *B. coagulans* SSF at 55 °C was at least 2.5-fold higher than that of any of the other three microbial biocatalysts. This difference is apparently due to the higher activity of the enzyme at 55 °C [12] compared to by the optimum temperature for growth of the microbial biocatalysts.

Although the maximum volumetric productivity of yeast and *Z. mobilis* was lower in the presence of lower cellulase concentrations (7.5 FPU g^{-1} cellulose) as compared to *B. coagulans*, all three fermentations produced about the same final yield of products at the end of 168 h of SSF (Table 1). At the end of 168 h of SSF and with 20 FPU g^{-1} cellulose, all three microbial biocatalysts (except *L. lactis*) converted about 90–95% of the glucose equivalents of cellulose. For *B. coagulans*, the time required to reach this product yield was about 96 h while the other three microbial biocatalysts required at least 168 h to reach the same product yield. These results are in agreement that SSF with *B. coagulans* at 50 °C is more effective in converting cellulose to products than with yeast as the microbial biocatalyst even at its optimal growth and fermentation temperature.

The amount of product produced by the various microbial biocatalysts in the SSF of cellulose at the end of 48 h was determined to further evaluate the efficiency of the process. The results presented in Fig. 3 are the fraction of the major product of fermentation at 48 h as compared to the maximum yield obtained at the end of fermentation at 168 h. In an SSF

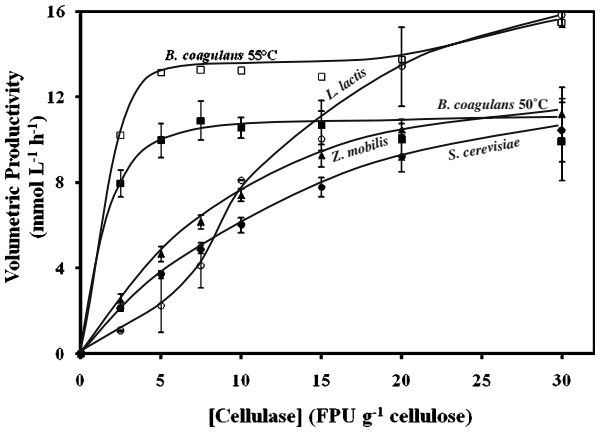

Fig. 2 Maximum volumetric productivity of SSF of 40 g L^{-1} cellulose (Solka Floc) by *B. coagulans* strain 36D1 (50 or 55 °C; pH 5.0), *L. lactis* (40 °C; pH 5.5), *S. cerevisiae* (35 °C; pH 5.5), and *Z. mobilis* (35 °C; pH 5.0) as a function of fungal cellulase concentration. Volumetric productivity was calculated as lactate produced by *B. coagulans* strain 36D1 and *L. lactis* and as ethanol produced by *S. cerevisiae* and *Z. mobilis*. See text for other details

Table 1 Profile of SSF of crystalline cellulose by *B. coagulans*, *L. lactis*, *S. cerevisiae*, and *Z. mobilis*.

Organism	Net production (mM)					Total product	Major product
	Lactate	Ethanol	Acetate	Succinate	Glycerol	Yield (%)[a]	Fraction (%)[b]
B. coagulans	299.9±0.8	17.6±2.4	17.9±1.0	2.2±1.9	0.0	90.3±4.0	88.8±0.8
L. lactis	226.0±23.4	47.3±10.2	21.1±4.4	0.0	0.0	70.9±2.5	76.7±5.2
S. cerevisiae	0.0	349.8±16.7	2.9±3.4	0.8±1.4	7.2±4.8	93.2±11.4	97.0±1.0
Z. mobilis	0.7±0.7	373.7±17.4	16.5±15.2	0.0	0.8±0.7	94.4±0.9	95.4±3.0

SSF of 40 g L^{-1} of crystalline cellulose (Solka Floc) was carried out at a cellulase concentration of 20 FPU g^{-1} cellulose for 168 h. See "Materials and Methods" section for details. Growth temperature and culture pH for the various organisms are listed in the text. Reported average values were from three independent fermentations

[a] Total products yield was calculated as % ratio of all fermentation products listed in the table to theoretical expected yield based on the amount of cellulose consumed on a molar basis

[b] Major product fraction represents the % of major product in the total fermentation products

with *B. coagulans*, about 80% of the expected products were produced during the first 48 h of SSF at 50 °C with only about 10 FPU g^{-1} of cellulose. Increasing the cellulase concentration did not influence this productivity. With the same amount of cellulase, both yeast and *Z. mobilis*-based SSFs yielded only about 50% of the ethanol during the first 48 h of SSF. The second 50% of ethanol production required an additional 120 h of SSF due to a continual decline in volumetric productivity. Even with 30 FPU g^{-1} cellulose, these two microbial biocatalysts only yielded about 65% of the expected ethanol during the first 48 h of SSF. *L. lactis* reached the same 80% product yield as *B. coagulans* but this required slightly higher concentration of cellulase (15 FPU vs 10 FPU g^{-1} cellulose). However, it should be noted that the final lactate yield is lower for *L. lactis* compared to *B. coagulans* (Table 1). These results show that SSF with an organism that can match the optimum conditions for fungal cellulase activity, such as *B. coagulans*, is a better choice of microbial biocatalyst to reduce the cost of fungal cellulase in SSF of cellulose to low-value commodity chemicals by decreasing the amount of enzyme needed and also the fermentation time, two significant areas of cost savings.

In conclusion, the temperature optimum for *B. coagulans* more closely match the optimum for fungal cellulases used in SSF than current generation biocatalysts used by the industry for producing ethanol or lactic acid, and this match leads to higher volumetric

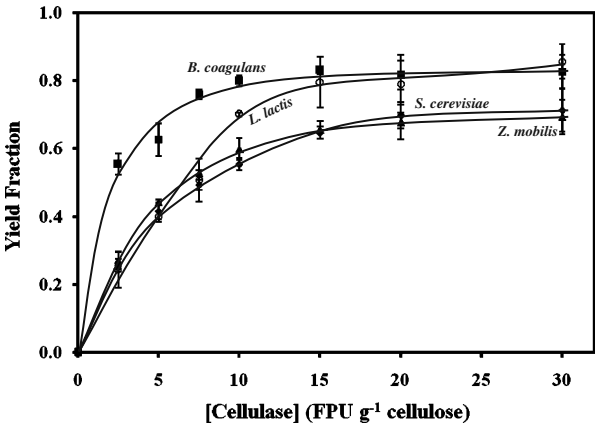

Fig. 3 Yield fraction of the major fermentation product of SSF of 40 g L^{-1} cellulose (Solka Floc) by *B. coagulans* strain 36D1, *L. lactis*, *S. cerevisiae*, and *Z. mobilis* at different fungal cellulase concentrations. Yield fraction was calculated as the ratio of major fermentation product (lactate for *B. coagulans* and *L. lactis*, ethanol for *S. cerevisiae* and *Z. mobilis*) produced at 48 h of SSF to that of the same product at the SSF endpoint of 168 h

productivity and more rapid progress to completion of SSF. This close match in temperature optima leads to a lower cellulase requirement for SSF by a factor of at least three for *B. coagulans* strain 36D1 versus the other microbial biocatalysts. The lower cellulase requirement and more rapid progress to the fermentation endpoint with *B. coagulans* in SSF is expected to lead to substantial cost savings in the amount of cellulase required for SSF. Metabolic engineering of *B. coagulans* and/or other thermotolerant microbial biocatalysts for production of ethanol as the main fermentation product should provide a new group of microbial biocatalysts that can contribute significantly in the conversion of lignocellulosic biomass to fuel ethanol in a cost-effective manner.

Acknowledgments We thank A. P. Rooney for providing some of the strains used in this study, Genencor Intl. for the cellulase preparation and International Fiber Corp. for Solka Floc. This study was supported in part by a grant from the Department of Energy (DE-FG36-04GO14019) and the State of Florida, University of Florida Agricultural Experiment Station.

References

1. Perlack, R. D., Wright, L. L., Turhollow, A. F., Graham, R. L., Stokes, B. J., & Erbach, D. C. (2005). DOE/GO-102005-2135.
2. Aden, A., Ruth, M., Ibsen, K., Jechura, J., Neeves, K., Sheehan, J., et al. (2002). NREL/TP-510-32438.
3. Duff, S. J. B., & Murray, W. D. (1996). *Bioresource Technology*, *55*, 1–33. doi:10.1016/0960-8524(95)00122-0.
4. Kheshgi, H. S., Prince, R. C., & Marland, G. (2000). *Annual Review of Energy and the Environment*, *25*, 199–244. doi:10.1146/annurev.energy.25.1.199.
5. Lynd, L. R., Laser, M. S., Bransby, D., Dale, B. E., Davison, B., Hamilton, R., et al. (2008). *Nature Biotechnology*, *26*, 169–172. doi:10.1038/nbt0208-169.
6. Wooley, R., Ruth, M., Glassner, D., & Sheehan, J. (1999). *Biotechnology Progress*, *15*, 794–803. doi:10.1021/bp990107u.
7. Wyman, C. E. (2007). *Trends in Biotechnology*, *25*, 153–157. doi:10.1016/j.tibtech.2007.02.009.
8. Zaldivar, J., Nielsen, J., & Olsson, L. (2001). *Applied Microbiology and Biotechnology*, *56*, 17–34. doi:10.1007/s002530100624.
9. Holtzapple, M., Cognata, M., Shu, Y., & Hendrickson, C. (1990). *Biotechnology and Bioengineering*, *36*, 275–287. doi:10.1002/bit.260360310.
10. Lynd, L. R., Weimer, P. J., van Zyl, W. H., & Pretorius, I. S. (2002). *Microbiology and Molecular Biology Reviews*, *66*, 506–577. doi:10.1128/MMBR.66.3.506-577.2002.
11. Gauss, W. F., Suzuki, S., & Takagi, M. (1976). Manufacture of alcohol from cellulosic materials using plural ferments. United States patent 3,990,944.
12. Patel, M. A., Ou, M., Ingram, L. O., & Shanmugam, K. T. (2005). *Biotechnology Progress*, *21*, 1453–1460. doi:10.1021/bp0400339.
13. Bothast, R. J., & Schlicher, M. A. (2005). *Applied Microbiology and Biotechnology*, *67*, 19–25. doi:10.1007/s00253-004-1819-8.
14. Carr, F. J., Chill, D., & Maida, N. (2002). *Critical Reviews in Microbiology*, *28*, 281–370. doi:10.1080/1040-840291046759.
15. Hofvendahl, K., & Hans-Hagerdal, B. (2000). *Enzyme and Microbial Technology*, *26*, 87–107. doi:10.1016/S0141-0229(99)00155-6.
16. Martin, A. M. (1996). Fermentation processes for the production of lactic acid. In T. F. Bozoglu & B. Ray (Eds.), *Lactic acid bacteria*: *Current advances in metabolism, genetics and applications*, Vol. Nato ASI Series (vol. H98, (pp. 269–301)). New York: Springer.
17. Patel, M. A., Ou, M. S., Harbrucker, R., Aldrich, H. C., Buszko, M. L., Ingram, L. O., et al. (2006). *Applied and Environmental Microbiology*, *72*, 3228–3235. doi:10.1128/AEM.72.5.3228-3235.2006.
18. Allen, M. B., & Arnon, D. I. (1955). *Plant Physiology*, *30*, 366–372. doi:10.1104/pp.30.4.366.
19. Underwood, S. A., Buszko, M. L., Shanmugam, K. T., & Ingram, L. O. (2002). *Applied and Environmental Microbiology*, *68*, 1071–1081. doi:10.1128/AEM.68.3.1071-1081.2002.

Appendix J

Appl Biochem Biotechnol (2009) 153:21–33
DOI 10.1007/s12010-008-8508-5

Engineering *Escherichia coli* for Fermentative Dihydrogen Production: Potential Role of NADH-Ferredoxin Oxidoreductase from the Hydrogenosome of Anaerobic Protozoa

Phi Minh Do · Alexander Angerhofer · Ivan Hrdy · Lucie Bardonova · Lonnie O. Ingram · K. T. Shanmugam

Received: 30 April 2008 / Accepted: 22 December 2008 /
Published online: 27 January 2009

Abstract *Trichomonas vaginalis* generates reduced ferredoxin within a unique subcellular organelle, hydrogenosome that is used as a reductant for H_2 production. Pyruvate ferredoxin oxidoreductase and NADH dehydrogenase (NADH-DH) are the two enzymes catalyzing the production of reduced ferredoxin. The genes encoding the two subunits of NADH-DH were cloned and expressed in *Escherichia coli*. Kinetic properties of the recombinant heterodimer were similar to that of the native enzyme from the hydrogenosome. The recombinant holoenzyme contained 2.15 non-heme iron and 1.95 acid-labile sulfur atoms per heterodimer. The EPR spectrum of the dithionite-reduced protein revealed a [2Fe–2S] cluster with a rhombic symmetry of g_{xyz}=1.917, 1.951, and 2.009 corresponding to cluster N1a of the respiratory complex I. Based on the Fe content, absorption spectrum, and the EPR spectrum of the purified small subunit, the [2Fe–2S] cluster was located in the small subunit of the holoenzyme. This recombinant NADH-DH oxidized NADH and reduced low redox potential electron carriers, such as viologen dyes as well as *Clostridium* ferredoxin that can couple to hydrogenase for H_2 production from NADH. These results show that this unique hydrogenosome NADH dehydrogenase with a critical role in H_2 evolution in the hydrogenosome can be produced with near-native properties in *E. coli* for metabolic engineering of the bacterium towards developing a dark fermentation process for conversion of biomass-derived sugars to H_2 as an energy source.

Electronic supplementary material The online version of this article (doi:10.1007/s12010-008-8508-5) contains supplementary material, which is available to authorized users.

P. M. Do · L. O. Ingram · K. T. Shanmugam (✉)
Department of Microbiology and Cell Science, University of Florida, P.O. Box 110700, Gainesville, FL 32611, USA
e-mail: shan@ufl.edu

A. Angerhofer
Department of Chemistry, University of Florida, Gainesville, FL 32611, USA

I. Hrdy · L. Bardonova
Department of Parasitology, Faculty of Science, Charles University, Prague, Czech Republic

Keywords Trichomonas · Hydrogenosome · NADH dehydrogenase · Fermentation · H_2 production

Introduction

Nonrenewable nature of fossil fuels combined with an increase in atmospheric CO_2 has prompted a search for alternate sources of energy to support human endeavors. Among the various energy sources that are being explored, H_2 is attractive due to its higher energy density. The product of combustion of dihydrogen is water and does not contribute to environmental pollution and global warming. Dihydrogen is an energy carrier and can be produced by several methods [1]. Biologically, H_2 can be produced by photosynthetic microorganisms from water along with O_2 and also by fermentation of sugars using microbial biocatalysts [2–5].

Photosynthetic microorganisms are known to produce H_2 from water using sunlight as the energy source [6–8]. Gaffron demonstrated H_2 production by green algae over 60 years ago [9], and this process is sensitive to evolved O_2, produced by photosynthesis, that limited the yield and rate of H_2 production from water. This O_2 sensitivity of the algal hydrogenase has been overcome recently by separating O_2 evolving photosynthesis from H_2 production phase by manipulating the S-content of the medium [7]. In the first photosynthetic phase, carbohydrates were synthesized from CO_2 and water using light energy, and the accumulated carbohydrates were fermented to H_2 in the second S-limitation phase that minimizes O_2 evolution. Similar separation of photosynthesis and H_2 evolution was also reported for cyanobacteria [10]. We have previously reported fermentation of sugars by cyanobacteria in a photoheterotrophic mode under N-limitation reaching a H_2 to fructose ratio as high as 15 [11].

Dihydrogen produced by light-dependent microbial biocatalysts may not be cost-competitive with other sources of energy, and strictly from an economic point of view, a dark fermentation process to H_2 could be a viable option [2]. In such a dark fermentation process, sugars derived from photosynthetic processes, such as stored carbohydrates or lignocellulosic biomass, can be fermented by anaerobic and facultative microbial biocatalysts to H_2 and CO_2. Microorganisms are well known for their ability to produce copious amounts of dihydrogen during fermentation of sugars [3]. Although the dark fermentation proceeds at high rate, the net yield of H_2 per glucose is usually less than two (Fig. 1). Either formate or reduced ferredoxin produced by appropriate bacteria is the main electron donor for H_2 production and in most cases the only source of H_2 produced by fermenting bacteria. The NADH produced by the glycolytic pathway is normally not used as a source of H_2 and instead is reoxidized to maintain redox balance by reduction of organic molecules such as pyruvate or acetyl-CoA leading to characteristic end products of fermentation of the organism. There are reports of bacteria that produce H_2 yield of higher than 2.0 but never reaching the expected maximum of 4.0 H_2/glucose [12–14]. For hydrogen to be a viable energy source, the yield needs to reach at least 10 H_2/glucose [15]. To reach this high H_2 to hexose ratio, microbial biocatalysts need to be metabolically engineered to divert all the NADH produced during glycolysis and TCA cycle to H_2. This requires a unique set of enzymes that can couple oxidation of NADH to reduction of electron carriers such as ferredoxin that can transfer the electrons to hydrogenase and ultimately released as H_2 (Fig. 1). In their pioneering work, Greenbaum and his colleagues demonstrated a biochemical pathway using a combination of enzymes that can catalyze the conversion of hexose to H_2 at a yield per hexose that is close to the theoretical maximum [16]. This was further extended to include starch [17].

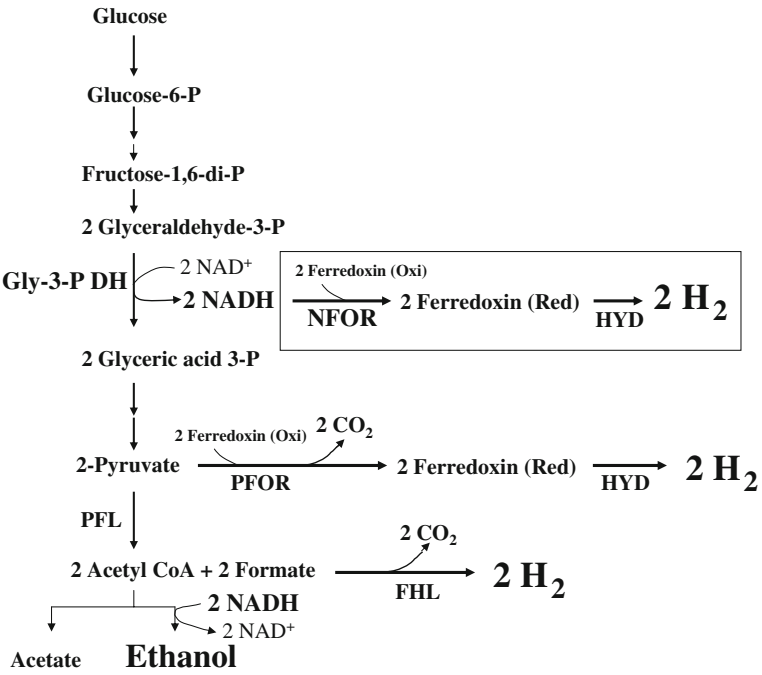

Fig. 1 Fermentative pathways in microorganisms that lead to H_2 production. The reactions within the rectangular box are found in the hydrogenosome of anaerobic protozoa. pyruvate ferredoxin oxidoreductase (*PFOR*) dependent reactions are found in Clostridia and the pyruvate formate-lyase (*PFL*) based reactions are normally seen in facultative bacteria. *FHL*, formate hydrogen-lyase; *HYD*, hydrogenase

The biochemical reaction presented in Fig. 1 (within the box) is an alternate pathway for H_2 production that has been reported in the hydrogenosomes of anaerobic protozoan, such as *Trichomonas vaginalis* [18]. Trichomonads lack mitochondria but contain unique subcellular organelles, the hydrogenosomes [19]. This organelle is critical for anaerobic energy metabolism of the protozoan and likely share evolutionary ancestry with the mitochondrion [19–21]. A NADH-dehydrogenase (NADH-DH) was purified from *T. vaginalis* hydrogenosomes and this enzyme reduced *Trichomonas* ferredoxin in vitro [22]. This ferredoxin is likely the in vivo electron acceptor of NADH-DH [22]. Once reduced, the electrons are transferred from ferredoxin to hydrogenase for H_2 evolution. The *Trichomonas* NADH-DH consists of two subunits (51 and 24 kDa subunits, designated Tvh-47 and Tvh-22 [22]; this nomenclature is maintained here for the proteins) that are similar to the core NADH-oxidizing subunits of the NADH:ubiquinone oxidoreductase of mitochondrial or bacterial complex I (complex I; NDH; EC 1.6.5.3). The ability of the hydrogenosome NADH-DH to reduce electron acceptors at the midpoint redox potential of ferredoxin (−0.36 V; [23]) or to more electronegative electron acceptors such as methyl viologen (E_0' of −0.44 V) has not been reported in any of its homologs that constitute the respiratory complex of aerobic organisms. This raises an interesting possibility that a metabolically engineered *Escherichia coli* that produces the unique hydrogenosome NADH-DH, ferredoxin, and hydrogenase could couple NADH oxidation to H_2 production in *E. coli* also. As a first step towards constructing such a NADH to H_2 pathway, we have cloned and expressed the corresponding genes from *T. vaginalis* in *E. coli* and biochemically characterized this critical component of the pathway, the recombinant NADH-DH. Since

the heterodimer is expected to have cofactors, FMN and Fe/S, it is important that the recombinant protein is endowed with these cofactors for full activity. The results presented in this communication show that the *T. vaginalis* NADH-DH produced by *E. coli* is fully active and catalyzes the reduction of methyl viologen with midpoint redox potential close to that of H_2 and can serve as a starting point for the construction of microbial biocatalysts for fermentative H_2 production at high yield.

Experimental Procedures

Materials

All organic and inorganic chemicals were from Fisher Scientific and were analytical grade. Biochemicals were from Sigma Chemical Co. Reagents, enzymes and supplies for molecular biology experiments were from New England Biolabs unless specified otherwise.

Medium and Culture Condition

E. coli cultures were grown in rich medium (L-broth) as described previously [24]. *E. coli* strains with plasmids were selected and maintained in rich medium with ampicillin (100 mg/L). *E. coli* strain Rosetta (Novagen) carries lambda DE3 with T7 gene *1* encoding RNA polymerase under *lac* promoter at the λ*att* site and a plasmid pRARE (Novagen) encoding a set of less-abundant tRNAs of *E. coli*. *E. coli* strain JM109(DE3) was from Promega.

E. coli Expression Plasmid with *nuoE* and *nuoF* Genes

Plasmids containing *T. vaginalis nuoE* (Tvh-22) and *nuoF* (Tvh-47) genes encoding the two subunits of the NADH-DH were described previously [22, 25]. Using predicted signal peptide cleavage site [22], two sets of primers were synthesized for polymerase chain reaction (PCR) amplification of the two genes and cloning into expression plasmid, pET15b (Novagen; Electronic Supplementary Material).

Plasmid, pPMD40, in which both genes are expressed from independent T7-gene *10* promoters, was constructed to produce approximately equimolar quantities of both subunits in the same cell towards production of an active NADH-DH. Plasmid pPMD40 was constructed after PCR amplification of the entire *nuoF* gene along with the phage T7-promoter (forward primer: CGGCAAGCTTCCACGATGCGTCCGGCGTAG; reverse primer: GCCGAAGCTTTTGGTTATGCCGGTACTGCC) and inserting this DNA into a HindIII site in plasmid pPMD38 (Electronic Supplementary Material). Plasmid pPMD40 contains tandem T7-gene *10* promoters each expressing *nuoE* or *nuoF* gene.

Expression of *nuoE* and *nuoF* Genes in *E. coli*

NADH dehydrogenase was produced in *E. coli* strain JM109(λDE3, pRARE) after inducing the *nuo* genes with arabinose since the protein produced after IPTG induction was inactive. The level of expression from T7 gene *10* promoter found in T7 expression plasmids was lower with arabinose as the inducer compared to IPTG, the traditional *lac* inducer. For these experiments, a freshly transformed *E. coli* JM109(λDE3, pRARE) with plasmid pPMD40 (or plasmid pPMD38 or pPMD39; Electronic Supplementary Material)

was cultured in 1 L LB medium in a shaker at 200 RPM. When the OD420nm of the culture reached about 0.6 (Beckman DU640 spectrophotometer), arabinose (1.5% *w*/*v*) was added to the medium and incubation continued at 28 °C for additional 4 h. Ferrous sulfate was also added at the same time ($FeSO_4$ $7H_2O$, 20 mg/L) to support production and incorporation of Fe/S clusters into the amplified proteins. Cells were harvested by centrifugation (10,000×*g*, 10 min, 4 °C), washed once with ice-cold Buffer A (K-phosphate, 50 mM, pH 7.5; NaCl, 0.1 M) and stored at −20 °C until use.

Purification of NADH-DH

Cells from a 500-mL (or 1 L) culture were suspended in 10 mL (or 20 mL) of Buffer A and broken by passage through a French pressure cell (20,000 psi). The extract was clarified by centrifugation (30,000×*g*; 45 min) and the supernatant was filtered through a 0.22-μm filter. The filtered extract was loaded on a Hi Trap chelating column (5 mL; General Electric) in Buffer A that was prewashed with $NiCl_2$ (0.1 M) in Buffer A. Unadsorbed and loosely bound proteins were washed off the column with five volumes of Buffer A followed by five volumes of Buffer A with imidazole (50 mM). Proteins were eluted with a linear imidazole gradient of 50 to 300 mM imidazole in Buffer A. The NADH-DH eluted at about 80 mM imidazole as determined by sodium dodecyl sulfate polyacrylamide gel electrophoresis (SDS-PAGE) and activity. Fractions with highest purity of the protein, as determined by SDS-PAGE, were pooled and the N-terminal His-tags from both proteins (Tvh-22 and Tvh-47) were removed by thrombin (75 units; General Electric) treatment for 16 h at 4 °C during dialysis of the protein against Buffer A with DTT (0.5 mM). The protein was further purified by gel filtration on a Hi Prep Sephacryl S-200 HR column (2.6/60 cm; General Electric) in Buffer A with DTT (0.5 mM). Fractions with NADH-DH activity were pooled and dialyzed overnight against 4 L of K-phosphate buffer (50 mM, pH 7.5) with DTT (0.5 mM). To one half of the total protein, glycerol was added to a final concentration of 20% and stored at −75 °C. This protein was stable for several months at −75 °C. The other half of the protein was maintained on ice and used for biochemical assays.

Individual subunits of NADH dehydrogenase were also purified essentially as described for the holoenzyme. Since the subunits lack enzyme activity, purification was followed by SDS-PAGE.

Enzyme Activity

NADH-DH activity was determined spectrophotometrically using NADH as the electron donor and various artificial electron acceptors. Standard reaction mixture consisted of K-phosphate buffer (50 mM, pH 7.5), NADH (1 mM), and benzyl viologen (BV) (1 mM). Reaction mixture in a 13×100-mm tube was sealed with a serum stopper, and the gas phase was replaced by evacuation and refill with N_2. Enough sodium dithionite was added to the reaction mixture to titrate out the residual O_2. Reaction was initiated by the addition of enzyme, and BV reduction was monitored continuously at 600 nm at room temperature. Although the small amount of added dithionite will reduce both the Fe–S cluster and flavin in the protein, the presence of excess BV in the reaction mixture is expected to reoxidize these cofactors and not interfere with the assay. Under these conditions, the small amount of added dithionite did not affect the kinetics of BV reduction. With ferricyanide as electron acceptor, assays were under aerobic condition. Concentrations of BV, methyl viologen (MV), and K-ferricyanide were 1.00 mM in the experiments leading to determination of *K*m of NADH. Molar extinction coefficients used for BV and MV are 7,800 and 6,300,

respectively, at 600 nm with 1.00 cm path length. Ferricyanide-dependent NADH-DH activity was determined in the same buffer as the BV assay (410 nm; extinction coefficient of 1,020 M^{-1} cm^{-1}). Ferredoxin-dependent NADH-DH activity was determined in the same buffer with 0.10 mM NADH and 40 μM *Clostridium acetobutylicum* ferredoxin by following the oxidation of reduced NADH at 340 nm. One unit of enzyme activity is defined as 1 μmol substrate reduced min^{-1} mg $protein^{-1}$.

Clostridium Ferredoxin Purification

C. acetobutylicum strain 824 (NRRL B-23491) obtained from USDA-ARS (Peoria, IL, USA) was cultured in Reinforced Clostridial Medium (Oxoid) without the agar. Ferredoxin was isolated from the cells as described previously [26, 27]. Protein concentration was determined from the molar extinction coefficient of 30,600 cm^{-1} at 390 nm.

Non-heme iron and sulfur determination—Non-heme iron was determined as described by Harvey et al. [28] and sulfur was determined using the method described by Cline [29].

EPR Measurements

Cw-EPR spectra of the NADH-DH complex at cryogenic temperatures were determined using a commercial EPR spectrometer (Bruker Elexsys E580) equipped with an Oxford Instruments ESR900 helium-flow cryostat and the standard TE_{102} mode rectangular cavity (Bruker ER4102ST). EPR samples were placed in a Wilmad 3×4 (ID×OD)-mm quartz tubes (CFQ), prefrozen in liquid nitrogen, before insertion into the precooled cryostat.

Analytical Methods

Protein concentration was determined using Coomassie blue (Bradford reagent) or BCA assay [30, 31] with bovine serum albumin as standard. SDS-PAGE utilized 12.5% gel as per Laemmli [32]. The protein standards used in SDS-PAGE (Bio-Rad Laboratories, Hercules, CA, USA) were aprotinin (6,500 Da), lysozyme (14,400 Da), trypsin inhibitor (21,500 Da), carbonic anhydrase (31,000 Da), ovalbumin (45,000 Da), serum albumin (66,200 Da), phosphorylase b (97,400 Da), β-galactosidase (116,250 Da), and myosin (200,000 Da). Protein standards used to calibrate Hi Prep Sephacryl S-200 HR column used for gel filtration (Sigma Chemical Co., St. Louis, MO, USA) were bovine carbonic anhydrase (29,000 Da), ovalbumin (45,000 Da), bovine serum albumin (66,000 Da), and yeast alcohol dehydrogenase (150,000 Da).

Results

Purification of the Recombinant NADH-DH

T. vaginalis hydrogenosome NADH dehydrogenase is a heterodimer comprising two subunits with anhydrous molecular weights of 20,706 and 45,723, respectively [22, 25]. Optimal expression of the two proteins in *E. coli* required plasmid pRARE (Novagen) expressing *E. coli* less-abundant tRNAs. The two subunits of the protein were expressed separately in *E. coli* host BL21(DE3)(pRARE) and attempts to reconstitute an active enzyme either from crude extracts or from purified subunit components were unsuccessful. Similar results were also obtained when the two genes were expressed from the same

promoter in the cytoplasm. An active protein was only detected when both proteins were expressed from tandem promoters in plasmid pPMD40 in the same cell. Although induction of gene expression with IPTG (as low as 50 μM) supported significant amount of NADH-DH protein synthesis, the activity of the recombinant protein was very low. In order to alleviate this, arabinose was used as an inducer for production of T7-polymerase from the *lac* promoter in λDE3. Arabinose is not a known inducer of *lac* promoter; however, a metabolic product of arabinose appears to induce the *lac* promoter at a lower level [33]. The specific activity of NADH-DH after arabinose induction and purification increased to about 600 units with ferricyanide as electron acceptor (Table 1), an activity that is similar to that of the native enzyme [22].

This protein migrated through the gel filtration column as a heterodimer with a molecular mass of 69,100 and SDS-PAGE revealed the two subunits corresponding to Tvh-47 and Tvh-22. The specific activity of the recombinant enzyme was highest with ferricyanide as electron acceptor (Table 1) as seen with the native enzyme. The specific activity of the enzyme with benzyl viologen as electron acceptor was comparable to that of the values with ferricyanide. The recombinant protein also reduced methyl viologen (about 65% of the ferricyanide value). The activity of the recombinant protein with methyl viologen as electron acceptor was significantly higher than that of the enzyme purified directly from the hydrogenosome. In addition, the enzyme also reduced Clostridial ferredoxin. These results show that the recombinant NADH-DH reduces low-potential electron acceptors such as methyl viologen (E_0' of −0.44 V) readily.

Apparent *K*m for NADH for the recombinant enzyme was dependent on the electron acceptor and varied between 0.10 mM with BV and 0.31 mM with ferricyanide (Table 2). These values were significantly higher than the 0.021 mM reported for the native enzyme with ferricyanide as the electron acceptor [22]. The affinity of the recombinant protein to ferricyanide was significantly higher than that of the native protein purified from the hydrogenosome (*K*m of 0.06 vs 0.29 mM). The *K*m for BV was about threefold higher than that of ferricyanide and the electron acceptor with the highest *K*m was methyl viologen. The reaction rate was also highest with ferricyanide as the electron acceptor although the Vmax with the other two acceptors was not that dissimilar. These results show that the *T. vaginalis* hydrogenosome NADH-DH produced in *E. coli* is capable of reducing electron acceptors

Table 1 Specific activities of recombinant *T. vaginalis* hydrogenosome NADH-DH produced in *E. coli* with arabinose as inducer.

Electron acceptor	Specific activity (μmol min^{-1} mg $protein^{-1}$)	
	Arabinose-induced[a]	Native[b]
Ferricyanide	604±24	690
Benzyl viologen	582±44	ND
Methyl viologen	392±19	262
Ferredoxin	24±0.2[c]	48[d]

[a] Values are the mean of 3–5 replicates with standard deviation

[b] These values for the native enzyme isolated from *Trichomonas vaginalis* hydrogenosomes were from Hrdy et al. [22]

[c] *Clostridium acetobutylicum* ferredoxin

[d] *T. vaginalis* ferredoxin

ND not determined

Table 2 Kinetic properties of recombinant *T. vaginalis* hydrogenosome NADH-DH (arabinose-induced) purified from *E. coli*.

Acceptor	*K*m (NADH) (mM)	*K*m (acceptor) (mM)	Vmax[a]	*K*cat (s^{-1})
Ferricyanide	0.31	0.06	870	1,170
Benzyl viologen	0.10	0.17	645	725
Methyl viologen	0.22	0.44	570	650

*K*m for NADH was determined in an assay mixture containing 50 mM phosphate buffer, pH 7.5 with 5 mM benzyl viologen, 20 mM methyl viologen, or 1 mM potassium ferricyanide. *K*m for electron acceptors was determined in a reaction mixture containing 50 mM phosphate buffer, pH 7.5, 1 mM NADH and the electron acceptor at various concentrations. The reaction was followed by the reduction of electron acceptor (ε_{600nm} BV=7,800 M^{-1} cm^{-1} ; ε_{600nm} MV=6,300 M^{-1} cm^{-1} ; ε_{410nm} ferricyanide=1,020 M^{-1} cm^{-1}). All assays with viologen dyes were preformed under anaerobic conditions at room temperature using $S_2O_4^{-2}$ to titrate out residual oxygen in the assay mixture

[a] Vmax—μmoles min^{-1} (mg protein)$^{-1}$

with standard redox potentials that are significantly lower than that of NADH such as methyl viologen.

Absorbance Spectrum and Iron/Sulfur Content

The holoenzyme had a spectrum typical of Fe–S proteins with absorbance peaks at 326, 420, 463, and 551 nm (Fig. 2). Upon reduction with dithionite, the peaks at 420 and 463 nm disappeared, and the absorbance at 551 nm was lower than the protein as purified. Oxidation of the reduced protein by air restored the original spectrum. A spectrum similar to that of the holoenzyme was also obtained with the small subunit (Tvh-22) alone that was purified separately (Fig. 2). These spectra resemble the spectra of the corresponding flavoprotein subcomplex of respiratory NADH dehydrogenase complex I and the 25 KDa subunit of the same complex from *Paracoccus denitrificans* [34, 35] and also a [2Fe–2S] clostridial hydrogenase N-terminal domain [36].

The active NADH-DH had 2.15 non-heme iron and 1.95 acid-labile sulfur atoms per heterodimer. The Tvh-22 protein expressed and purified separately also had Fe and acid-labile sulfur at the same level. These results show that the holoenzyme only contains a [2Fe–2S] cluster that is located in the small subunit.

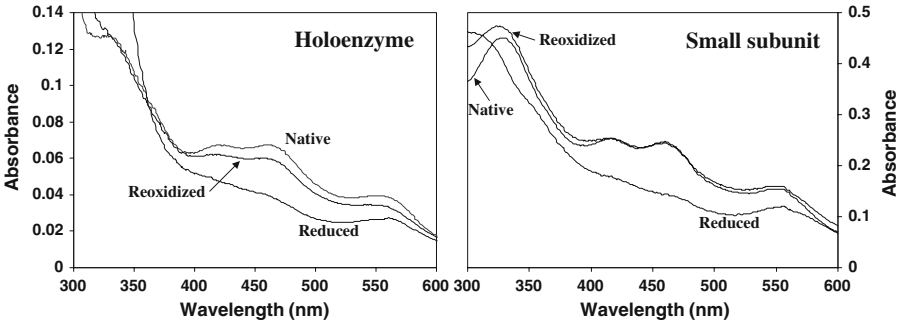

Fig. 2 Absorption spectrum of recombinant *T. vaginalis* hydrogenosome NADH-DH. Native spectrum represents the protein as purified. Reduced spectrum was obtained after titrating the protein with sodium dithionite. Reoxidized spectrum was obtained after gently mixing the reduced protein with air

The absence of Fe/S in the large subunit of NADH-DH is unique since the Tvh-47 homologs from respiratory chain complex I contain a [4Fe–4S] cluster [34, 37] and the cysteines implicated in liganding the tetranuclear Fe–S cluster in these proteins are conserved in the *Trichomonas* protein. The presence of only [2Fe–2S] cluster in the recombinant holoenzyme indicates that the Tvh-47 component lacks the anticipated tetranuclear N3 cluster. In agreement with this, the Tvh-47 protein expressed and purified separately also did not have any detectable Fe and labile S.

EPR Measurements of the Recombinant NADH-DH

In order to confirm the presence of only the binuclear Fe–S cluster in the purified NADH-DH, EPR spectra of the protein were obtained. The purified protein did not show an EPR spectrum but reduction with dithionite generated a spectrum that was rhombic in symmetry with g_{xyz} values corresponding to 1.917, 1.951, and 2.009 (Fig. 3). Although NADH was a substrate for the enzyme, NADH failed to reduce it to an EPR-active form. An EPR signal corresponding to a tetranuclear Fe–S cluster N3 (g_{xyz}=1.87, 1.94, and 2.04) found in homologous 54 KDa proteins of the respiratory complex I [34] was not detected in this *Trichomonas* NADH-DH purified from *E. coli*. The Tvh-22 protein by itself also produced an EPR spectrum that was similar to the holoenzyme upon reduction by dithionite (g_{xyz}= 1.92, 1.953, and 2.008; Fig. 4). These EPR studies support the conclusion that the protein contains only the binuclear Fe–S cluster corresponding to N1a in the small subunit. It is unlikely that an additional Fe–S cluster is present in the holoenzyme that is not reduced by dithionite to a paramagnetic state for detection by EPR since the spectrum of the holoenzyme in the 400–500 nm range was completely bleached by dithionite, indicating complete reduction of the Fe–S clusters in the protein (Fig. 2). In addition, the Fe content of the purified protein was only 2/heterodimer.

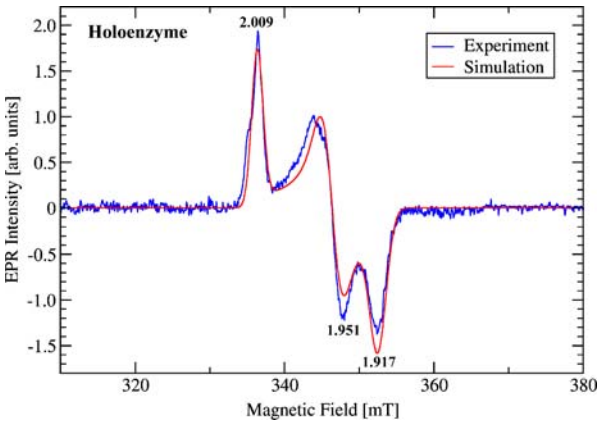

Fig. 3 EPR spectrum of the recombinant *T. vaginalis* hydrogenosome NADH-DH holoenzyme produced in *E. coli*. Spectrum of the holoenzyme (123.3 μM) was recorded at a microwave power of 2.0 mW after reducing the protein with sodium dithionite. EPR conditions: sample temperature, 25°K; microwave frequency, 9.45801 GHz; modulation amplitude, 5 G; modulation frequency, 100 kHz; time constant, 80 ms; scan rate, 160 ms/data point for 4.9 G/s, 0.78 G/data point, receiver gain 60 dB. Wavy lines represent the experimental data and the smooth line is the simulation of the spectrum

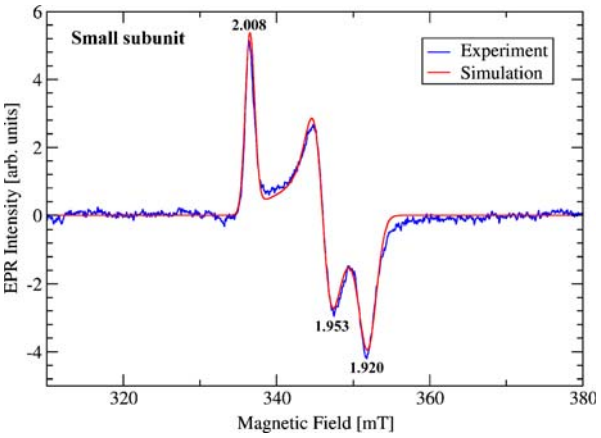

Fig. 4 EPR spectrum of Tvh-22 of the *T. vaginalis* NADH-DH produced in *E. coli*. Spectrum of the small subunit (121.0 μM) was obtained after reducing the protein with sodium dithionite. Other conditions were as listed for Fig. 3

Discussion

The hydrogenosomal NADH dehydrogenase is the only known enzyme with a predicted physiological role of coupling NADH oxidation to H_2 evolution that has been purified and biochemically characterized. As a first step in our attempt to engineer *E. coli* for production of H_2 at a higher yield, we have developed methods for optimum expression of the protein in an active form in *E. coli*. The purified protein reduced ferredoxin, and it is likely that the NADH-DH reduces ferredoxin in vivo also as an intermediate in H_2 evolution pathway (Fig. 1). In metabolic engineering of *E. coli* for H_2 production, the other components of the hydrogenosome pathway, ferredoxin, and hydrogenase need to be cloned and expressed in *E. coli*. In the interim, the ability of the NADH-DH to reduce viologen dyes leads to the possibility of using these intermediate electron carriers to couple the recombinant NADH-DH with the native hydrogenase 3 isoenzyme for H_2 evolution. *E. coli* whole cells as well as isolated membranes are well known for their ability to utilize BV or MV as an intermediate electron carrier in coupling dithionite to HYD-3 for H_2 evolution and this reaction could replace the need for ferredoxin and hydrogenase from the hydrogenosome. The [NADH]/[NAD^+] ratio of anaerobic *E. coli* is also significantly higher than that of an aerobically growing *E. coli* [38] and this could lead to a reduction in the in vivo midpoint redox potential of the NADH/NAD^+ couple (less than the Eo' of −0.32 V) to facilitate reduction of viologen dyes by NADH-DH in vivo. However, this requires complete removal of O_2 from the fermenting *E. coli* since the reduced viologen dyes react with O_2 to generate superoxide radicals that are detrimental to the cell. An alternate possibility is to engineer the bacterium to be less sensitive to superoxide.

The tetranuclear N3 cluster that plays a critical role in electron transport to ubiquinone [37, 39, 40] in all homologs of the respiratory complex I is absent in the recombinant *T. vaginalis* NADH-DH produced in *E. coli*. This is similar to the observed lack of the tetranuclear N3 cluster in the recombinant *Paracoccus denitrificans* NADH-DH produced in *E. coli* [34]. In contrast to the recombinant *T. vaginalis* protein of this study, the recombinant *P. denitrificans* protein also lacked FMN and NADH-dependent enzyme activity. Reconstitution of the recombinant *P. denitrificans* protein with FMN alone (without the N3 cluster but with N1a cluster) only produced about 25% of the NADH-dependent ferricyanide reduction activity of a complex that was reconstituted with FMN, iron, and S_2^-. This raises the possibility that a specific chaperone may be needed for

insertion of the N3 cluster in heterologous NADH-DH produced in *E. coli*. The absence of the N3 cluster in the recombinant NADH-DH is not due to high level of expression of the protein in *E. coli* is shown by the presence of N3 cluster in recombinant NuoF subunit of *E. coli* [41]. However, it should be noted that the *T. vaginalis* protein produced in *E. coli*, although lacking the N3 cluster, did reduce several electron acceptors at rates that are comparable to the native enzyme isolated from the hydrogenosome (Table 1).

The reported midpoint redox potential of FMN (−340 mV) in the respiratory complex I [37] may not suggest efficient electron flow from $FMNH_2$ to the N1a cluster of the recombinant *T. vaginalis* NADH-DH. However, the higher $[NADH]/[NAD]^+$ ratio of the anaerobic cell coupled with an increase in the ratio of $[FMNH_2]/[FMN]$ may lower the redox potential sufficiently to facilitate transfer of electrons to the [2Fe–2S] cluster at a midpoint potential of about −0.37 V. With the anticipated physiological role in NADH oxidation to H_2 production in a microbial biocatalyst such as recombinant *E. coli*, the tetranuclear cluster N3, if present in the flavoprotein of the NADH-DH, would drain electrons from NADH to a more oxidized form (−0.25 V) that is not energetically favorable to H_2 production.

In summary, we have taken the first step towards constructing a recombinant *E. coli* that can potentially oxidize glucose to at least 10 H_2 by cloning and expressing an active NADH-DH that can readily reduce low-potential electron carriers such as viologen dyes and ferredoxin. Further metabolic engineering of the bacterium with appropriate ferredoxin and hydrogenase genes could introduce an active pathway for release of the reductant in NADH as H_2 towards developing a microbial biocatalyst for production of H_2 as an energy source by dark fermentation of biomass derived sugars.

Acknowledgements We thank Dr. A. Rooney, USDA-ARS, for providing *C. acetobutylicum* strain. This work was supported in part by US Department of Energy grant DE-FG36-04GO14019 and funds from the Florida Agricultural Experiment Station. This work was also supported in part by the In-House Research Program of the National High Magnetic Field Laboratory (AA) and by a grant by the Grant Agency of the Czech Republic no. 204/06/0944 (IH). L.B. was supported by grant MSM0021620858.

References

1. Edwards, P. P., Kuznetsov, V. L., & David, W. I. (2007). Hydrogen energy. *Phil. Trans. Royal Soc. A*, *365*, 1043–1056.
2. Benemann, J. (1996). Hydrogen biotechnology: Progress and prospects. *Nature Biotechnology*, *14*, 1101–1103. doi:10.1038/nbt0996-1101.
3. Nandi, R., & Sengupta, S. (1998). Microbial production of hydrogen: An overview. *Critical Reviews in Microbiology*, *24*, 61–84. doi:10.1080/10408419891294181.
4. Prince, R. C., & Kheshgi, H. S. (2005). The photobiological production of hydrogen: Potential efficiency and effectiveness as a renewable fuel. *Critical Reviews in Microbiology*, *31*, 19–31. doi:10.1080/10408410590912961.
5. Sakurai, H., & Masukawa, H. (2007). Promoting R & D in photobiological hydrogen production utilizing mariculture-raised cyanobacteria. *Marine Biotechnology (New York, N.Y.)*, *9*, 128–145. doi:10.1007/s10126-006-6073-x.
6. Dutta, D., De, D., Chaudhuri, S., & Bhattacharya, S. K. (2005). Hydrogen production by Cyanobacteria. *Microbial Cell Factories*, *4*, 36. doi:10.1186/1475-2859-4-36.
7. Melis, A. (2007). Photosynthetic H_2 metabolism in *Chlamydomonas reinhardtii* (unicellular green algae). *Planta*, *226*, 1075–1086. doi:10.1007/s00425-007-0609-9.
8. Melis, A., Seibert, M., & Ghirardi, M. L. (2007). Hydrogen fuel production by transgenic microalgae. *Advances in Experimental Medicine and Biology*, *616*, 110–121. doi:10.1007/978-0-387-75532-8_10.
9. Gaffron, H., & Rubin, J. (1942). Fermentative and phochemical production of hydrogen in algae. *The Journal of General Physiology*, *26*, 219–240. doi:10.1085/jgp.26.2.219.

10. Mitsui, A., Kumizawa, S., Takahashi, A., Ikemoto, H., & Cao, S. A. T. (1986). Strategy by which nitrogen-fixing unicellular cyanobacteria grow photoheterotrophically. *Nature*, *323*, 720–722. doi:10.1038/323720a0.
11. Reddy, P. M., Spiller, H., Albrecht, S. L., & Shanmugam, K. T. (1996). Photodissimilation of fructose to H_2 and CO_2 by a dinitrogen-fixing cyanobacterium, *Anabaena variabilis*. *Applied and Environmental Microbiology*, *62*, 1220–1226.
12. Eriksen, N. T., Nielsen, T. M., & Iversen, N. (2008). Hydrogen produciton in anaerobic and microaerobic *Thermatoga neapolitana*. *Biotechnology Letters*, *30*, 103–109. doi:10.1007/s10529-007-9520-5.
13. Maeda, T., Sanchez-Torres, V., & Wood, T. K. (2007). Enhanced hydrogen production from glucose by metabolically engineered *Escherichia coli*. *Applied Microbiology and Biotechnology*, *77*, 879–890. doi:10.1007/s00253-007-1217-0.
14. Yoshida, A., Nishimura, T., Kawaguchi, H., Inui, M., & Yukawa, H. (2005). Enhanced hydrogen production from formic acid by formate hydrogen lyase-overexpressing *Escherichia coli* strains. *Applied and Environmental Microbiology*, *71*, 6762–6768. doi:10.1128/AEM.71.11.6762-6768.2005.
15. Eggeman, T. (2005). Boundary analysis for H_2 production by fermentation. NREL/SR-560-36129.
16. Woodward, J., Orr, M., Cordray, K., & Greenbaum, E. (2000). Enzymatic production of biohydrogen. *Nature*, *405*, 1014–1015. doi:10.1038/35016633.
17. Zhang, Y. H., Evans, B. R., Mielenz, J. R., Hopkins, R. C., & Adams, M. W. (2007). High-yield hydrogen production from starch and water by a synthetic enzymatic pathway. *PLoS ONE*, *2*, e456. doi:10.1371/journal.pone.0000456.
18. Hrdy, I., Cammack, R., Stopka, P., Kulda, J., & Tachezy, J. (2005). Alternative pathway of metronidazole activation in *Trichomonas vaginalis* hydrogenosomes. *Antimicrobial Agents and Chemotherapy*, *49*, 5033–5036. doi:10.1128/AAC.49.12.5033-5036.2005.
19. Embley, T. M., Horner, D. A., & Hirt, R. P. (1997). Anaerobic eukaryote evolution: Hydrogenosomes as biochemically modified mitochondria? *Trends in Ecology & Evolution*, *12*, 437–441. doi:10.1016/S0169-5347(97)01208-1.
20. Lindmark, D. G., & Muller, M. (1973). Hydrogenosome, a cytoplasmic organelle of the anaerobic flagellate *Tritrichomonas foetus*, and its role in pyruvate metabolism. *The Journal of Biological Chemistry*, *248*, 7724–7728.
21. Martin, W. (2005). The missing link between hydrogenosomes and mitochondria. *Trends in Microbiology*, *13*, 457–459. doi:10.1016/j.tim.2005.08.005.
22. Hrdy, I., Hirt, R. P., Dolezal, P., Bardonova, L., Foster, P. G., Tachezy, J., et al. (2004). *Trichomonas* hydrogenosomes contain the NADH dehydrogenase module of mitochondrial complex I. *Nature*, *432*, 618–622. doi:10.1038/nature03149.
23. Vidakovic, M. S., Fraczkiewicz, G., & Germanas, J. P. (1996). Expression and spectroscopic characterization of the hydrogenosomal [2Fe-2S] ferredoxin from the protozoan *Trichomonas vaginalis*. *The Journal of Biological Chemistry*, *271*, 14734–14739. doi:10.1074/jbc.271.25.14734.
24. Lee, J. H., Patel, P., Sankar, P., & Shanmugam, K. T. (1985). Isolation and characterization of mutant strains of *Escherichia coli* altered in H_2 metabolism. *Journal of Bacteriology*, *162*, 344–352.
25. Dyall, S. D., Yan, W., Delgadillo-Correa, M. G., Lunceford, A., Loo, J. A., Clarke, C. F., et al. (2004). Non-mitochondrial complex I proteins in a hydrogenosomal oxidoreductase complex. *Nature*, *431*, 1103–1107. doi:10.1038/nature02990.
26. Rabinowitz, J. (1972). Preparation and properties of clostridial ferredoxins. *Methods in Enzymology*, *24*, 431–446. doi:10.1016/0076-6879(72)24089-7.
27. Shanmugam, K. T., Buchanan, B. B., & Arnon, D. I. (1972). Ferredoxins in light- and dark-grown photosynthetic cells with special reference to *Rhodospirillum rubrum*. *Biochimica et Biophysica Acta*, *256*, 477–486. doi:10.1016/0005-2728(72)90076-X.
28. Harvey Jr, A. E., Smart, J. A., & Amis, E. S. (1955). Simultaneous spectrophotometric determination of iron(II) and total iron with 1,10-phenanthroline. *Analytical Chemistry*, *27*, 26–29. doi:10.1021/ac60097a009.
29. Cline, J. D. (1969). Spectrophotometric determination of hydrogen sulfide in natural waters. *Limnology and Oceanography*, *14*, 454–458.
30. Bradford, M. M. (1976). A rapid and sensitive method for the quantitation of microgram quantities of protein utilizing the principle of protein-dye binding. *Analytical Biochemistry*, *72*, 248–254. doi:10.1016/0003-2697(76)90527-3.
31. Smith, P. K., Krohn, R. I., Hermanson, G. T., Mallia, A. K., Gartner, F. H., Provenzano, M. D., et al. (1985). Measurement of protein using bicinchoninic acid. *Analytical Biochemistry*, *150*, 76–85. doi:10.1016/0003-2697(85)90442-7.
32. Laemmli, U. K. (1970). Cleavage of structural proteins during the assembly of the head of bacteriophage T4. *Nature*, *227*, 680–685. doi:10.1038/227680a0.

33. Narayanan, N., Hsieh, M. Y., Xu, Y., & Chou, C. P. (2006). Arabinose-induction of lac-derived promoter systems for penicillin acylase production in *Escherichia coli*. *Biotechnology Progress*, *22*, 617–625. doi:10.1021/bp050367d.
34. Yano, T., Sled, V. D., Ohnishi, T., & Yagi, T. (1996). Expression and characterization of the flavoprotein subcomplex composed of 50-kDa (NQO1) and 25-kDa (NQO2) subunits of the proton-translocating NADH-quinone oxidoreductase of *Paracoccus denitrificans*. *The Journal of Biological Chemistry*, *271*, 5907–5913. doi:10.1074/jbc.271.4.1849.
35. Yano, T., Sled, V. D., Ohnishi, T., & Yagi, T. (1994). Expression of the 25-kilodalton iron-sulfur subunit of the energy-transducing NADH-ubiquinone oxidoreductase of *Paracoccus denitrificans*. *Biochemistry*, *33*, 494–499. doi:10.1021/bi00168a014.
36. Atta, M., Lafferty, M. E., Johnson, M. K., Gaillard, J., & Meyer, J. (1998). Heterologous biosynthesis and characterization of the [2Fe-2S]-containing N-terminal domain of *Clostridium pasteurianum* hydrogenase. *Biochemistry*, *37*, 15974–15980. doi:10.1021/bi9812928.
37. Ohnishi, T. (1998). Iron-sulfur clusters/semiquinones in complex I. *Biochimica et Biophysica Acta*, *1364*, 186–206. doi:10.1016/S0005-2728(98)00027-9.
38. de Graef, M. R., Alexeeva, S., Snoep, J. L., & Teixeira de Mattos, M. J. (1999). The steady-state internal redox state (NADH/NAD) reflects the external redox state and is correlated with catabolic adaptation in *Escherichia coli*. *Journal of Bacteriology*, *181*, 2351–2357.
39. Brandt, U. (2006). Energy converting NADH:quinone oxidoreductase (complex I). *Annual Review of Biochemistry*, *75*, 69–92. doi:10.1146/annurev.biochem.75.103004.142539.
40. Sazanov, L. A. (2007). Respiratory complex I: Mechanistic and structural insights provided by the crystal structure of the hydrophilic domain. *Biochemistry*, *46*, 2275–2288. doi:10.1021/bi602508x.
41. Velazquez, I., Nakamaru-Ogiso, E., Yano, T., Ohnishi, T., & Yagi, T. (2005). Amino acid residues associated with cluster N3 in the NuoF subunit of the protontranslocating NADH-quinone oxidoreductase from *Escherichia coli*. *FEBS Letters*, *579*, 3164–3168.

Supplementary Material

Cloning the genes encoding the two subunits of Trichomonas vaginalis NADH-DH

The PCR primers used for cloning the two subunits of *Trichomonas vaginalis* NADH-DH had the following sequences; NuoE forward, GGAGCCTCGAGATGAACAAGAAGTCTGTTCTTAT; NuoE reverse, CGGCGGATCCTTATGGGAGTGGTCTTGGTG; NuoF forward, GCCGCTCGAGATGCAGACAAAATTCCTTGA; NuoF reverse, CGGCGGATCCTTACTCAGCGACGCAAGCCT. The 5'-end of the forward primers has the recognition sequence for XhoI and the 5'-end of the reverse primers carry recognition sequence for BamHI. The *nuoE* and *nuoF* genes were independently amplified by PCR using previously cloned DNA as the template. The PCR product was hydrolyzed by the enzymes XhoI and BamHI and cloned into appropriately hydrolyzed *E. coli* expression plasmid pET15b (Novagen). Plasmid pPMD38 contains a *nuoE* gene insert of 596 bp encoding a protein of 20,366 Da. Plasmid pPMD39 includes the *nuoF* gene (1.292 kb DNA coding for the 45,723 Da protein). In *E. coli* strain Rosetta, these two plasmids produced the two subunits of NADH-DH as N-terminal His-tagged proteins with IPTG as inducer. The Tvh-22 protein, after expression, purification and thrombin cleavage, is expected to have an N-terminal extension of GSHMLEM compared to the native protein processed at the predicted site. This predicted site was recently found to differ from the actual processing site by three amino acids (Hrdy, unpublished data). Thus, the final protein produced by this construct is missing the first three amino acids of the processed native protein, ARL, and will have seven extra amino acids at the N-terminus derived from the plasmid vector sequence. The predicted and actual processing site for NuoF is the same and the protein produced by the recombinant *E. coli* will have an extension of the same seven amino acids as in Tvh-22. The Tvh-47 sequence starts from QTKF.